

FTD-MT- 64-318

628788
766-60640

TRANSLATION

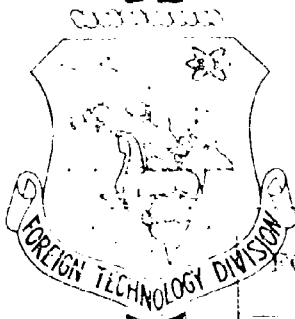
NEWS OF INSTITUTIONS OF HIGHER LEARNING.
AERONAUTICAL ENGINEERING

(COLLECTION OF ARTICLES)

FOREIGN TECHNOLOGY DIVISION

AIR FORCE SYSTEMS COMMAND

WRIGHT-PATTERSON AIR FORCE BASE



CLEARINGHOUSE FOR FEDERAL SCIENTIFIC AND TECHNICAL INFORMATION	
Hardcopy	Microfiche
\$2340	\$1.25
238 PP 40	
ARCHIVE COPY	

Co-cc-1

MAR 9 1966

LIBRARY
TOM F.

This document is a machine translation of Russian text which has been processed by the AN/GSQ-16(XW-2) Machine Translator, owned and operated by the United States Air Force. The machine output has been post-edited to correct for major ambiguities of meaning, words missing from the machine's dictionary, and words out of the context of meaning. The sentence word order has been partially rearranged for readability. The content of this translation does not indicate editorial accuracy, nor does it indicate USAF approval or disapproval of the material translated.

EDITED MACHINE TRANSLATION

NEWS OF INSTITUTIONS OF HIGHER LEARNING. AERONAUTICAL
ENGINEERING (COLLECTION OF ARTICLES)

English Pages: 231

S/0147-064-000-002

THIS TRANSLATION IS A RENDITION OF THE ORIGINAL FOREIGN TEXT WITHOUT ANY ANALYTICAL OR EDITORIAL COMMENT. STATEMENTS OR THEORIES ADVOCATED OR IMPLIED ARE THOSE OF THE SOURCE AND DO NOT NECESSARILY REFLECT THE POSITION OR OPINION OF THE FOREIGN TECHNOLOGY DIVISION.

PREPARED BY:

TRANSLATION DIVISION
FOREIGN TECHNOLOGY DIVISION
WP-AFB, OHIO.

Ministerstvo Vysshego i Srednego
Spetsial'nogo Obrazovaniya SSSR

IZVESTIYA
Vysshikh Uchebnykh Zavedeniy

AVIATIONNAYA TEKHNIKA

No. 2

1964

Kazan'

Pages 1-163

BLANK PAGE

TABLE OF CONTENTS

U. S. Board on Geographic Names Transliteration System.....	iii
Designations of the Trigonometric Functions.....	iv
Analysis of Weight Characteristics of Fuel Tanks of Flight Vehicles with Liquid-Propellant Engines, by V. N. Novikov.....	1
The Solution of Problems of Bending of Three-Layered Plates and Shells by Means of a Displacement Function, by A. M. Gol'denstein.....	16
Calculation of the Nonaxially Symmetric State of Strain of Cylindrical Shells Taking into Account the Elasticity of the Reinforcing Frames, by Yu. I. Kaplan.....	26
Vibrations of an Anisotropic Plate Under a Continuously Moving Distributed Load, by A. P. Kovrevskiy.....	35
Edge Effect During the Joint Action of Axial and Radial Pressure for Anisotropic Circular Cylindrical Shells, by D. Ye. Lipovskiy.....	45
Application of the Method of Asymptotic Integration to Problems of Vibrations of Shells of Revolution Which are Similar in Form to Spherical Shells, by R. L. Malkina.....	61
Calculation of Closed Cylindrical and Slightly Conical Shells with Arbitrary Contour of Cross Section, by N. A. Shelomov.....	76
Experimental Investigation of the Propagation of Fan and Paired Plane Jets in a Transverse Flow, by Ye. V. Rzhevskiy and V. A. Kosterin.....	91
Method of Supersonic Analogy for Calculation of One-Dimen- sional Non-Stationary Gas Flows, by A. P. Pudoveyev.....	110
Optimum Compression in the Compressor of a Ducted-Fan Turbojet Engine with an Afterburner, by Ye. D. Sten'kin.....	121
An Approximate Method of Estimating Gas-Dynamic Influence on a Supersonic Flow, by Z. G. Shaykhutdinov.....	142
The Influence of a Sequential Decrease in Thickness of a Metal on the Curvature of Shaped Components, by M. N. Lysov and Yu. P. Katayev.....	153

TECHNICAL NOTES

Approximate Calculation of Speed of Flight in a Slanted Dive and Determination of Loss in Altitude and Range on the Dive Entry Section on a Program for a Pilotless Aircraft with Turbojet Engine (TJE), by Ye. A. Kuklev.....	175
Speed of Propagation of a Flame in an Open and Limited Flow of Uniform Mixture, by V. M. Yermolayev and A. V. Talantov.....	188
Investigation of an Ultrasonic Generator of a Liquid Fuel, by N. S. Lamekin.....	199
Investigation of a Partial Turbine, by V. N. Zanadvorova and V. A. Podgornov.....	209
Heating of a Limited Volume of Liquid Through Plates, by M. D. Mikhaylov.....	219
Application of the Principle of Minimum Dissipation of Mechanical Energy to the Equalizing Action of Lattices, by Yu. V. Stepanov.....	223

U. S. BOARD ON GEOGRAPHIC NAMES TRANSLITERATION SYSTEM

Block	Italic	Transliteration	Block	Italic	Transliteration
А а	<i>А а</i>	A, a	Р р	<i>Р р</i>	R, r
Б б	<i>Б б</i>	B, b	С с	<i>С с</i>	S, s
В в	<i>В в</i>	V, v	Т т	<i>Т т</i>	T, t
Г г	<i>Г г</i>	G, g	У у	<i>У у</i>	U, u
Д д	<i>Д д</i>	D, d	Ф ф	<i>Ф ф</i>	F, f
Е е	<i>Е е</i>	Ye, ye; E, e*	Х х	<i>Х х</i>	Kh, kh
Ж ж	<i>Ж ж</i>	Zh, zh	Ц ц	<i>Ц ц</i>	Ts, ts
З з	<i>З з</i>	Z, z	Ч ч	<i>Ч ч</i>	Ch, ch
И и	<i>И и</i>	I, i	Ш ш	<i>Ш ш</i>	Sh, sh
Й й	<i>Й й</i>	Y, y	Щ щ	<i>Щ щ</i>	Shch, shch
К к	<i>К к</i>	K, k	Ъ ъ	<i>Ъ ъ</i>	"
Л л	<i>Л л</i>	L, l	Ы ы	<i>Ы ы</i>	Y, y
М м	<i>М м</i>	M, m	Ь ь	<i>Ь ь</i>	'
Н н	<i>Н н</i>	N, n	Э э	<i>Э э</i>	E, e
О о	<i>О о</i>	O, o	Ю ю	<i>Ю ю</i>	Yu, yu
П п	<i>П п</i>	P, p	Я я	<i>Я я</i>	Ya, ya

* ye initially, after vowels, and after ъ, ь; e elsewhere.
 When written as ѣ in Russian, transliterate as yě or ѣ.
 The use of diacritical marks is preferred, but such marks
 may be omitted when expediency dictates.

FOLLOWING ARE THE CORRESPONDING RUSSIAN AND ENGLISH
DESIGNATIONS OF THE TRIGONOMETRIC FUNCTIONS

Russian	English
sin	sin
cos	cos
tg	tan
ctg	cot
sec	sec
cosec	csc
sh	sinh
ch	cosh
th	tanh
cth	coth
sch	sech
csch	csch
arc sin	\sin^{-1}
arc cos	\cos^{-1}
arc tg	\tan^{-1}
arc ctg	\cot^{-1}
arc sec	\sec^{-1}
arc cosec	\csc^{-1}
arc sh	\sinh^{-1}
arc ch	\cosh^{-1}
arc th	\tanh^{-1}
arc cth	\coth^{-1}
arc sch	sech^{-1}
arc csch	csch^{-1}
<hr/>	
rot	curl
lg	log

SEVENTH PUBLICATION EDITOR-IN-CHIEF G. S. Zhiritskiy

E D I T O R I A L S T A F F:

M. B. Vakhimov, A. F. Gurov (assistant editor-in-chief), A. V. Kvasnikov, L. A. Kolesnikov, G. I. Kosmychev (assistant editor-in-chief), N. V. Kurshev, M. I. Lysov, I. V. Ostoslavskiy, A. V. Talantov (assistant editor-in-chief), A. F. Feofanov, and A. S. Shevelev.

EXECUTIVE SECRETARY M. KH. VOZDVIZHENSKAYA

BLANK PAGE

MT-64-318

News of Higher Educational Institutions. Ministry of Higher and Intermediate Special Education, USSR. Kazan'. Aeronautical Engineering. No. 2, 1964.

Pages: Cover-163

ANALYSIS OF WEIGHT CHARACTERISTICS OF FUEL
TANKS OF FLIGHT VEHICLES WITH LIQUID-
PROPELLANT ENGINES

V. N. Novikov

Definitions of Cyrillic Items

изг = bend = bending
б = tank = fuel tank
экв = eq = equivalent
т = t (arbitrary designation)
р = r (arbitrary designation)
кр = crit = critical
бо = tc = tank compartment
ц = cy = cylindrical
т = f = fuel
мбо = itc = intertank compartment
вн = in = internal
н = ex = external
дн = bot = bottom
об = sh = shell
ср = av = average
в = h = high
н = low = low pressure
ла = fv = flight vehicle
 $\frac{кг}{см} = \frac{kg}{cm}$
подкр = reinf = reinforced
стр = str = stringer
пр = red = reduced
обш = sk = skin

The ideal design weight of flight vehicles with liquid-propellant rocket engines in many respects is determined by the perfection of the propulsion systems, whose weight can constitute up to 50-80% of the total design weight of the vehicle.

Therefore, in the designing of assemblies of propulsion systems, including fuel tanks, it is necessary to correctly select their main parameters, which affect the flight, weight, and economic characteristics of the flight vehicle.

Fuel tanks serve for distribution of components of liquid fuel; they are usually a structural part of flight vehicle bodies, and are subjected to the influence of external forces, and also forces caused by the pressure feed of the tanks, whose magnitude is determined by the operating conditions of the system of fuel feed from the tanks to the engine.

1. Analysis of the State of Strain of Cylindrical Tank Shells

The complex influence of all forces on tanks can lead to a different character of loss of the carrying capacity of tank shells (walls). These cases are characterized either by conditions of strength of the shell, or by losses in stability, which leads to an essential distinction in the methods of strength analysis of a tank and the methods which ensure it.

We shall determine the stresses existing in the shell of a cylindrical tank which is loaded simultaneously by axial forces (N), bending moment (M_{bend}), and internal pressure (p_{tank}), using the membrane theory of shells.

Meridional stresses with small relative thickness of shell are

$$\sigma_m = \frac{p_{\text{tank}} D}{4\delta} \pm \frac{4M_{\text{bend}}}{\pi D^2 \delta} \pm \frac{N}{\pi D \delta}, \quad (1)$$

and annular stresses are

$$\sigma_r = \frac{p_i D}{2s} \quad (2)$$

Annular stresses in a shell, which is loaded by excess internal pressure, are always positive, i.e., $\sigma_r > 0$, and the meridional stresses, depending upon the magnitude and sign of bending moment, axial force, and internal pressure, can be both positive and negative.

A. If $\sigma_m < 0$, the main stresses will be

$$\sigma_1 = \sigma_r, \quad \sigma_2 = 0, \quad \sigma_3 = \sigma_m.$$

Then the equivalent stress, according to the theory of the largest tangential stresses, is determined:

$$\sigma_{\text{eqv}} = \frac{4M_{\text{axr}}}{\pi D^3} + \frac{N}{\pi D^2} + \frac{p_i D}{4s} \quad (3)$$

Equating this rated stress to a limited value, equal to σ_t

($\sigma_{0.2}$ or $\sigma_{0.3}$), or to a permissible value $\frac{\sigma_t}{f}$ (where f is the safety factor), which is selected according to certain considerations, and designating it conditionally as σ_p , we find the relative thickness of the shell:

$$\delta = \frac{s}{D} > \frac{1}{\sigma_p} \left(\frac{4M_{\text{axr}} + ND}{\pi D^2} + \frac{p_i}{4} \right) \quad (4)$$

Introducing the parameter of loading, which characterizes the necessary relative thickness of the shell, and is determined by the external loads,

$$\Delta_1 = \frac{1}{\sigma_p} \frac{4M_{\text{axr}} + ND}{\pi D^2} \quad (5)$$

we obtain:

$$\delta > \Delta_1 + \frac{p_i}{4\sigma_p} \quad (6)$$

The maximum permissible pressure in the tank, with the selected relative shell thickness and given loads, is

$$p_6(\text{max}) = 4\sigma_p(\bar{\delta} - \Delta_1). \quad (7)$$

The conditions of shell stability are determined by the limiting critical compression stresses (σ_{crit})

$$\sigma_{\text{crit}} < k_1 E \frac{\delta}{D}, \quad (8)$$

where k_1 is the critical compression stress factor;

E is the elastic modulus [$\frac{\text{kg}}{\text{cm}^2}$].

Then, by equating (8) to meridional stress (1), we obtain

$$k_1 E \frac{\delta}{D} > \frac{4M_{\text{ext}}}{\pi D^3} + \frac{N}{\pi D \delta} - \frac{p_6 D}{4\delta}, \quad (9)$$

whence the necessary relative thickness of the tank shell, from the conditions of stability, is determined by the following expression:

$$\bar{\delta} > \sqrt{\frac{\sigma_p}{k_1 E} \left(\Delta_1 - \frac{p_6}{4\sigma_p} \right)}. \quad (10)$$

We shall introduce a stability parameter which expresses the relation of ultimate strength of the design material to the characteristic of stability of the shell:

$$\Delta_2 = \frac{\sigma_p}{k_1 E}. \quad (11)$$

Without calculation of the influence of internal pressure in the tank on the critical stability factor k_1 , the stability parameter undergoes a relatively small change ($\Delta_2 = 0.006-0.008$). By putting (11) in (10), we obtain:

$$\bar{\delta} = \sqrt{\Delta_2 \left(\Delta_1 - \frac{p_6}{4\sigma_p} \right)}. \quad (12)$$

By replacing the values of permissible tank pressure here with the given shell thickness, according to (7), and solving the quadratic equation, we find the minimum-permissible relative shell thickness, which satisfies the conditions of strength and stability:

$$\bar{\delta}^I = \frac{\Delta_1}{2} \left(\sqrt{1 + 8 \frac{\Delta_1}{\Delta_2}} - 1 \right). \quad (13)$$

Optimum pressure in the tank p_{tank}^I , which ensures minimum shell thickness, may be found after substitution of (13) into (7):

$$p_0^I = 2\sigma_y \left[\Delta_2 \left(\sqrt{1 + 8 \frac{\Delta_1}{\Delta_2}} - 1 \right) - 2\Delta_1 \right]. \quad (14)$$

B. If $\sigma_m > 0$, the main stresses will be

$$\sigma_1 = \sigma_t, \quad \sigma_2 = \sigma_m, \quad \sigma_3 = 0.$$

Equivalent stress is

$$\sigma_{\text{eqv}} = \frac{p_0 D}{2s} < \sigma_y,$$

whence, the necessary relative thickness will be:

$$\bar{\delta} > \frac{p_0}{2\sigma_y}. \quad (15)$$

Between the calculated cases of A and B there exists a boundary which corresponds to the equality to zero of meridional stresses:

$$\sigma_m = \frac{p_0 D}{4s} - \left(\frac{4M_{\text{ext}}}{\pi D^3} + \frac{N}{\pi D^2} \right) = 0.$$

From this condition we may find the limiting pressure in the tank, above which the tank shell analysis is conducted from the conditions of tensile strength:

$$p_0^{II} = 4\sigma_y \Delta_1. \quad (16)$$

Analysis of the obtained expressions for determination of relative shell thickness, depending upon the magnitude of loading by external forces and the internal pressure, makes it possible to divide all tanks into three groups (Fig. 1).

1) The first group (zone I) includes tanks whose shell analysis is conducted from conditions of stability, while the necessary relative shell thickness is determined by expression (12). Such tanks, which are conditionally called tanks of "low" pressure, have the

relationships of parameters of loading and stability $\frac{\Delta_1}{\Delta_2} < 1$, and

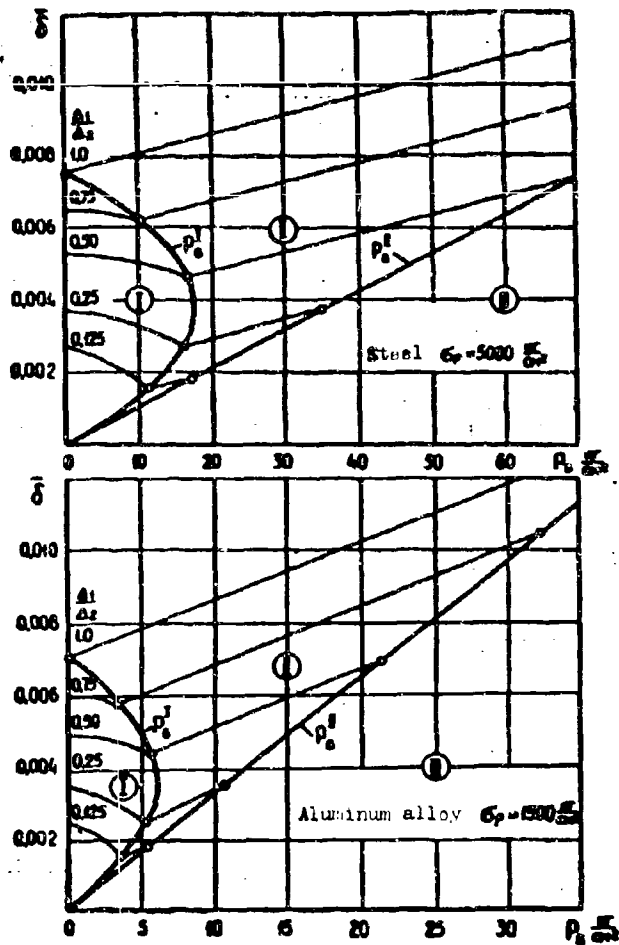


Fig. 1.

shell thickness is determined by expression (6) from conditions of tensile strength. Tanks pertaining to zone II will be conditionally called tanks of "medium" pressure.

3) For all tanks whose pressure exceeds $p_{\text{tank}}^{\text{II}}$ (zone III), the calculation of relative shell thickness is produced with equation (15) from conditions of tensile strength. This group includes tanks of "high" pressures, which usually operate with gas-displacement supply systems with a pressure feed of $p_{\text{tank}} > 25 \text{ atm(abs)}$.

pressure in the tank is less than $p_{\text{tank}}^{\text{I}}$. Since for the majority of tanks of maneuvering flight vehicles, the relationship of parameters of loading and stability is within the limits of $0.1 < \frac{\Delta_1}{\Delta_2} < 0.5$, then practically all tanks of power plants with turbo-pump supply systems, for which the pressure feed is $p_{\text{tank}} < 5 \text{ atm(abs)}$, pertain to tanks of "low" pressure.

2) At tank pressures $p_{\text{tank}}^{\text{I}} < p_{\text{tank}} < p_{\text{tank}}^{\text{II}}$, the relative

2. Determination of Weight Dependences for Cylindrical Fuel Tanks

The weight of fuel tanks depends on the volume of the fuel placed in them, the external and internal loads, and also on the

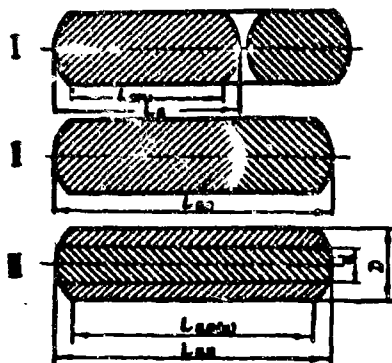


Fig. 2.

geometric and design features of the tank.

For liquid-propellant rocket engines, operating on bi-propellants, they usually employ cylindrical tanks, which are arranged according to one of the diagrams represented in Fig. 2.

The volume of a tank compartment with elliptic bottoms, for which the values of the semiaxes of an ellipsoid are taken $a = \frac{D}{4}$, $b = c = \frac{D}{2}$, will be equal to

$$V_{tc} = \frac{\pi D^3}{12} (1 + 3\lambda_{tc}). \quad (17)$$

where $\lambda_{tc} = \frac{L_{tc}(cy)}{D}$ is the elongation of the cylindrical part of the tank compartment (or tank).

We shall express the volume of the tank compartment by the weight of the fuel placed in it

$$V_{tc} = \beta_{tc} \frac{G_f}{\gamma_f}, \quad (18)$$

where

γ_f is the average specific gravity of fuel;

$\beta_{tc} = \frac{V_{tc}}{V_f}$ is the coefficient which considers the free volumes in the tanks and the volume of the intertank compartment;

$$\beta_{tc} = \beta_s \cdot \beta_{int}. \quad (19)$$

$\beta_{tank} = \frac{V_{tank}}{V_f}$ characterizes the volume of the air cushion in the tank ($\beta_{tank} = 1.03-1.08$);

$\beta_{1tc} = \frac{V_{tc}}{V_{\text{tank}}}$ expresses the volume of the tank compartment with respect to the volume of the tanks (Fig. 2).

For diagram I we have: $\beta_{1tc} = 1 + \frac{1}{3\lambda_{tc}}$.

For diagram II and III: $\beta_{1tc} = 1.0$.

The surface area of a tank compartment with elliptic bottoms is determined by the surfaces of the shells, the bottoms, and the inter-tank compartment

$$S = \pi D^2 (0.8\xi_{tc} + \lambda_{tc}). \quad (20)$$

where ξ_{tc} is the coefficient which considers the number of bottoms and the diagram of the tank compartment.

For a single tank: $\xi_{tc} = 1.0$.

For tank compartments of diagrams I and II: $\xi_{tc} = 2.0$.

For diagram III: $\xi_{tc} = 1 + \frac{d}{D} (1 + \lambda_{tc})$,

where d is the diameter of the internal tank

$$d = D \sqrt{\frac{\gamma_{f(in)}}{\gamma_{f(in)} + K_f \cdot \gamma_{f(ex)}}}$$

$\gamma_{f(in)}$ and $\gamma_{f(ex)}$ are the specific gravities of components in the internal and external tanks;

$K_f = \frac{G_{f(ex)}}{G_{f(in)}}$ is the weight ratio of fuel components.

The weight of the fittings of tank compartment may be taken as proportional to the weights of the bottoms and shells

$$G_{fo} = a_{sh} G_{sh} + a_{bot} G_{bot}. \quad (21)$$

where a_{bot} and a_{sh} are the design factors of tank fittings, $a_{bot} = 1.6-2.0$ and $a_{sh} = 1.15-1.25$.

By expressing the surface of the tank compartment by its volume, and substituting the specific gravity of the tank material (γ_{tank}), we shall determine the weight of the tank compartment according to the

following expression:

$$Q_{\infty} = 12 Q_{\infty} \beta_{\infty} \frac{\gamma_0}{\gamma_r} \frac{0.8 \xi_{\infty} a_{\infty} \bar{\gamma}_{\infty} + \lambda_{\infty} a_{\infty} \bar{\gamma}_{\infty}}{1 + 3 \lambda_{\infty}}. \quad (22)$$

The relative weight of the tank compartment α_{tc} , which is defined as the ratio of the weight of the tank compartment to the weight of the fuel in it, can be found from this expression:

$$\alpha_{tc} = \frac{Q_{\infty}}{Q_0} = 12 \beta_{\infty} \frac{\gamma_0}{\gamma_r} \frac{0.8 \xi_{\infty} a_{\infty} \bar{\gamma}_{\infty} + \lambda_{\infty} a_{\infty} \bar{\gamma}_{\infty}}{1 + 3 \lambda_{\infty}}. \quad (23)$$

Tanks that are used in vehicles with liquid-fuel rocket engines usually can carry either tanks of "low" pressure, for which the relative shell thickness is determined from (12), or tanks of "high" pressure, for which the relative shell thickness is found through expression (15).

Total pressure in the tank p_{tank} is determined by the pressure feed p_{tc} and by the additional pressure Δp_{tank} that is created by the liquid column in the tank in the presence of longitudinal overloads n_x ,

$$p_0 = p_{tc} + \Delta p_0. \quad (24)$$

where

$$\Delta p_0 = n_x \gamma L_x.$$

L_x is the distance from the free surface of liquid in the tank.

The mean value of additional pressure in the tank, considering that one of the bottoms is subjected to the influence of the liquid column, will be:

$$\Delta p_{0 \text{ (cp)}} = 0.5 n_x \gamma \lambda_0 D.$$

The relative thickness of the elliptic bottoms, depending upon the magnitude of internal pressure p_{tank} , is found by the formula:

$$\bar{\gamma}_m = \frac{p_0}{2 \gamma_0}. \quad (25)$$

For determination of the relative weight of tanks of "high"

pressure, upon substitution of the characteristic values of coefficients and thicknesses, we shall obtain the following expression:

$$\sigma_{\theta}^{(a)} = 9\beta_{\text{acc}} \frac{\gamma_0}{\gamma_1} \frac{p_0}{c_p} \frac{\delta_{\text{acc}} + 0.84 \lambda_{\text{acc}}}{1 + 3\lambda_{\text{acc}}} \quad (26)$$

The relative weight of tanks of "low" pressure, when the magnitudes of bending moments and axial forces are unknown, may be found by the approximate dependences which are used in design calculations.

Disregarding the influence of internal pressure on the magnitude of meridional stresses of tanks of "low" pressure, for highly maneuverable vehicles it is possible to consider that the parameter of external loading (5) basically depends on the magnitude of bending moment M_{bend} , which in turn depends on the lateral overload $M_{\text{bend}} = f(n_y)$. Then the approximate value of the loading parameter will be

$$\Delta_1 = k_2 \frac{n_y}{c_p} \quad (27)$$

where coefficient k_2 , with central location of tanks and with body elongation of $\lambda_k = 10-14$, it is possible to take $k_2 = 0.35-0.45$, and the relative shell thickness is

$$\delta_{\text{acc}}^{(a)} = \sqrt{\frac{k_2}{k_1} \frac{n_y}{E}} \quad (28)$$

For tanks of "low" pressure of rarely maneuvering vehicles, the parameter of external loading basically depends on the axial compressing force N , which is characterized by the magnitude of longitudinal overload $N = f(n_x)$, i.e.,

$$\Delta_1 = k_3 \frac{n_x}{c_p} \quad (29)$$

where coefficient k_3 depends on the body length L_{k_1} to the location of tanks in the body and the average specific gravity of the vehicle γ_{fv} :

$$k_3 = \gamma_{fv} L_{k_1}$$

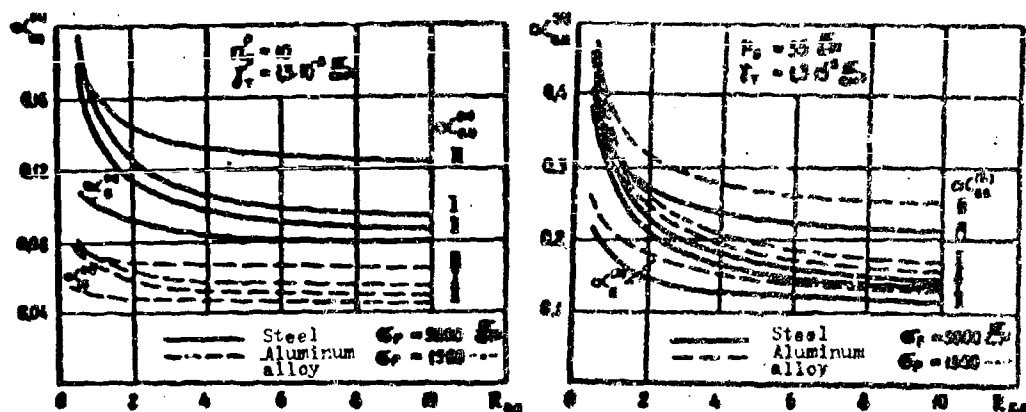


Fig. 3a, b.

With the middle location of tanks in the body, body elongation of $\lambda_k = 10^{-4}$, and average specific gravity of the vehicle $\gamma_{fv} = 1.5 \cdot 10^{-3} \frac{\text{kg}}{\text{cm}^3}$, we may take $k_2 = 0.01 D$, while the relative shell thickness will be:

$$t_{k2} = \sqrt{\frac{k_2 \cdot \sigma_x}{\sigma_y \cdot E}} \quad (30)$$

The relative thickness of bottoms of tanks of "low" pressure is usually determined not by strength specifications, but by design and fabrication factors, which allows us to take the following dependence:

$$\bar{t}_{k2} = 1.5 \cdot 10^{-3} \quad (31)$$

Then it is possible to write approximate formulas for determination of relative weights of tank compartments of "low" pressure:

a) for high-maneuvering aircraft —

$$\sigma_{k2}^{(a)} = 0.027 \bar{p}_{\text{max}} \frac{t_0}{r_1} \frac{t_{k2} + 0.64 \cdot 10^3 t_0 \sqrt{\frac{\sigma_x}{E}}}{1 + 3t_{k2}} \quad (32)$$

b) for low-maneuvering aircraft —

$$\sigma_{k2}^{(b)} = 0.027 \bar{p}_{\text{max}} \frac{t_0}{r_1} \frac{t_{k2} + 10^3 t_0 \sqrt{\frac{\sigma_x}{E}}}{1 + 3t_{k2}} \quad (32')$$

The dependences represented in Fig. 3 show that the relative weights

of tank compartments weakly depend on elongations, whereby the most profitable in the weight respect are tank diagrams I and II.

3. Analysis of the Application of Reinforced Shells in Tanks of Flight Vehicles

The operating conditions of tanks of "low" pressure show that the stability of shells may be increased either by the corresponding excess pressure in the tank, by reinforcing the shell with special profiles of the longitudinal structural assembly.

In the investigation of the stability of a cylindrical shell with a sufficiently closely-spaced structural assembly, it is possible to replace the reinforced shell with a smooth orthotropic shell whose relative thickness is

$$\bar{\delta}_{\text{экв}} = \Delta_1. \quad (33)$$

The thickness of the unreinforced shell, in the presence of internal pressure, will be determined by formula (13). By equating the expressions of necessary shell thicknesses, we shall find the boundary condition which characterizes the equivalence of reinforced (orthotropic) and unreinforced shells;

$$\frac{\Delta_1}{\Delta_2} = 1. \quad (34)$$

Thus, if $\frac{\Delta_1}{\Delta_2} < 1$, in the weight respect it would be more profitable

to use the reinforced shell; if $\frac{\Delta_1}{\Delta_2} > 1$, the unreinforced shell. For determination of the expediency of application of reinforced and unreinforced shells with respect to the magnitude of necessary areas of body sections, for each of them we shall find the destroying moments (M_{bend}) in given sections of the body in the presence of axial forces (N).

During the calculation of reinforced shells we can consider two cases: the first one corresponds to the limiting moment at which stability is lost by the most extreme stringer, and all others work within the limits of elasticity; the second case occurs when in the extreme stringer the stresses reach their limiting-permissible values.

If one considers that the skin is reinforced by stringers in the calculations it is joined to n stringers, then the total area of the reinforced shell will be

$$F_{\text{ср}} = n(F_{\text{стр}} + b_{\text{сп}}\delta) = nF_1, \quad (35)$$

where $b_{\text{ред}}$ is the reduced skin width

$$b_{\text{сп}} = \delta \sqrt{\frac{\sigma_{\text{сп}}(\text{сбм})}{\sigma_{\text{стр}}} \frac{E_{\text{сбм}}}{E_{\text{стр}}}}.$$

For the first calculating case we shall obtain the expression which characterizes the limit moment:

$$M_{\text{лр}} = 0,25D(\sigma_{\text{сп}} nF_1 - N). \quad (36)$$

If we introduce the relative parameters Δ_1 and Δ_2 and take the distance between stringers $b_0 = \frac{\pi D}{n}$, and also $\sigma_{\text{стр}} = \sigma_r$, we shall obtain the condition of existence of a stable reinforced design within the limits of elastic deformations

$$\Delta_2 = \frac{5}{4\Delta_1} \left(\frac{F_{\text{стр}}}{D} + b_{\text{сп}}\delta \right), \quad (37)$$

from which we can find the required thickness of the reinforced shell.

For the second case of calculation of a tank according to limiting carrying capacity, we shall determine the expression for total limit moment perceived by the reinforced skin

$$M_{\text{лр}} = 0,25D \{ n[(F_{\text{стр}} + b_{\text{сп}}\delta)\sigma_{\text{стр}} + (b_0 - b_{\text{сп}})\sigma_{\text{сп}}] - N \} \quad (38)$$

or, by expressing through the relative parameters, we shall obtain the

condition of existence of a reinforced design according to limiting carrying capacity:

$$\Delta_1 = \frac{1}{\Delta_2} \left[\frac{F_{cr}}{D} + b_{sp} \bar{\delta} + \frac{\bar{\delta}^2}{\Delta_2} (b_0 - b_{sp}) \right]. \quad (39)$$

As can be seen from these equations, the total carrying capacity of a reinforced cylindrical shell depends not only on the relation of parameters, but also on the distribution of the shell material between the skin and the stringer assembly.

Gravimetric analysis of reinforced shells shows:

a) that a gain in weight from the application of reinforced cylindrical shells, as opposed to unreinforced shells, may be only when $\frac{\Delta_1}{\Delta_2} < 1$. Thus, for small-loaded designs of tanks $\left(\frac{\Delta_1}{\Delta_2} < 0.25\right)$, the maximum gain will constitute 25-30%. Figures 4 and 5 show the

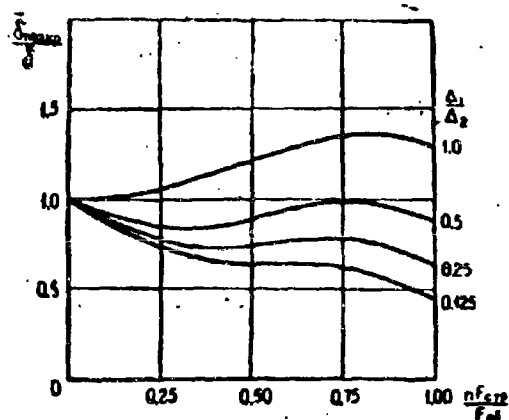


Fig. 4.

relation of the necessary thickness of a reinforced shell to an unreinforced one, according to limiting carrying capacity, whereby with the decrease of the specific load $\left(\frac{\Delta_1}{\Delta_2}\right)$, the portion of the stringer assembly, which together with the skin makes up the necessary area of cross

section of the shell, should be increased;

b) that a gain in weight of the reinforced shell can also be obtained in the presence of excess pressures in the tanks. For instance, when $\frac{\Delta_1}{\Delta_2} = 0.25$ (Fig. 5), theoretically up to pressures of

$P_{\text{tank}} = 40 \left[\frac{\text{kg}}{\text{cm}^2} \right]$ there is a gain in weight of reinforced designs.

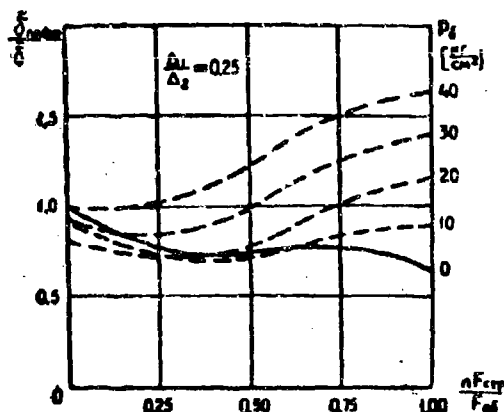


Fig. 5.

However, it is practically impossible to ensure uniform loading of profiles of the structural assembly and skin. Moreover, during intense wave formation, the skin itself additionally loads the profiles of the structural assembly and promotes their destruction, which causes a premature local loss of stability.

The obtained conclusions on the application of different diagrams and designs of tank compartments are not final, since exact recommendations can be made only with the calculation of the design, fabrication, and economic factors. But this analysis allows the designer to conduct a weight appraisal of tank compartments taking into account the conditions of their work on a vehicle, to outline the means by which it would be expedient to investigate the designs of tanks, and to make a number of practical recommendations for the designing of tank compartments and the determination of weight dependences for them.

Literature

1. M. I. Shevelyuk. Theoretical fundamentals and design of liquid-propellant rocket engines. Oborongiz, 1960.
2. S. P. Timoshenko. Strength of materials. Volume I, State United Publishing Houses, 1945; Volume II, State United Publishing Houses, 1946.

Submitted
23 December 1963

PROBLEMS OF BENDING OF
THREE-LAYERED PLATES AND SHELLS BY
MEANS OF A DISPLACEMENT FUNCTION

A. M. Gol'denshteyn

Definitions of Cyrillic Items

$\kappa = f$ - filler

Our work shows that for analyzing three-layered (sandwich-type) structures of symmetrical structure with isotropic layers and filler it is possible to introduce a displacement function φ , with whose help the equations of moments (1.3), (1.4) are automatically satisfied.

As a solution to the problems of bending of three-layered sandwich plates under the action of a lateral load, we obtain a solving equation for function φ . By disregarding the flexural rigidity of the carrying layers, the solving equation of bending of a three-layered plate with light filler coincides in form with the equation of bending of a single-layer plate. We shall show the analogy of function φ in the solving equation of three-layered plates with deflection w in the theory of single-layer plates, as a consequence of which, the formulas for calculation of shearing stresses and moments of three-layered plates have the same form as the respective formulas for single-layer plates.

Thus, the introduction of function φ reduces the calculation of a three-layer plate to the calculation of a single-layer plate. The solution for deflection w of a three-layer plate is obtained in the form of the sum of two parts, one of which expresses bending of the carrying layers, and the second one expresses bending of the filler. The following problems are solved as examples: bending of a freely supported rectangular plate with light filler and a circular plate with stiffener under the action of a transverse load. The proposed method allows us to solve those problems whose boundary conditions can be satisfied by the introduction of function φ . When the problem is not symmetric, usually its solution is difficult. Function φ will make it possible to significantly decrease the volume of calculations and reduce the solution to calculating formulas. Finally, we shall note that if the total thickness of a three-layer plate with carrier layers of constant thickness changes according to the law $H = k\varphi$, where k is the proportionality factor, then in this case it is also possible to automatically satisfy the equation of moments, express deflection through φ , and obtain a solving equation for φ .

Designations

α, β — curvilinear coordinates of the middle surface of the filler,

A_1, A_2 — Lamé parameters,

R_1, R_2 — main radii of curvature of middle surface of filler,

u', v', u'', v'' — movement of point of middle surface correspondingly of the upper and lower carrier layers,

w — deflection, not depending on coordinate z ,

$$\sigma_1 = \frac{1}{A_1} \frac{\partial w}{\partial \alpha}, \quad \sigma_2 = \frac{1}{A_2} \frac{\partial w}{\partial \beta}, \quad \tau = \frac{1}{A_1 A_2} \left[\frac{\partial}{\partial \alpha} \left(\frac{A_2}{A_1} \frac{\partial \varphi}{\partial \alpha} \right) + \frac{\partial}{\partial \beta} \left(\frac{A_1}{A_2} \frac{\partial \varphi}{\partial \beta} \right) \right].$$

h, t — thicknesses of filler and carrier layer,

$$\xi = \frac{\sigma' - \sigma''}{h + t}, \quad \eta = \frac{\sigma'' - \sigma''}{h + t}.$$

$T'_1, T'_2, T'_{12}, T''_1, T''_2, T''_{12}$ — membrane forces correspondingly for the upper and lower carrier layers,

m_1, m_2, m_{12} — bending and twisting moments with respect to the middle surface of filler,

E, E' — elastic moduli of filler and carrier layer,

ν, ν_1 — Poisson coefficients for filler and carrier layer,

G', G_3 — shear moduli of carrier layer and filler,

$$\begin{aligned} B_1 &= \frac{Ek}{1-\nu}, \quad D = \frac{Ek^3}{12(1-\nu^2)}, \quad C_1 = \frac{E't(h+t)^2}{2(1-\nu_1^2)}, \\ B' &= -\frac{E't}{1-\nu_1}, \quad D' = \frac{E't^3}{12(1-\nu_1^2)}, \quad C'_3 = G't(h+t), \\ B_3 &= G_3 h, \quad D_3 = \frac{G_3 h^3}{6}. \end{aligned} \quad (3)$$

$\overrightarrow{1,2}$ signifies cyclic permutation.

1. Introduction of the Displacement Function for a Three-Layer Shell with Light Filler

The system of differential equations of equilibrium of a three-layer shell with light filler of symmetric structure has the following form [1], [2], [3]:

$$L_1(T) = 0, \quad L_2(T) = 0, \quad (1.1)$$

$$\begin{aligned} 2D'A_1A_2\nabla^2 w + \frac{A_1A_2}{R_1}T_1 + \frac{A_1A_2}{R_2}T_2 - G_3 \frac{(h+t)^2}{h} \left\{ \frac{\partial}{\partial x} [A_1(\xi - \omega_1)] + \right. \\ \left. + \frac{\partial}{\partial y} [A_1(\eta - \omega_2)] \right\} - pA_1A_2 = 0, \end{aligned} \quad (1.2)$$

$$\frac{1}{A_1A_2} L_1(m) - \frac{(h+t)^2}{h} G_3 (\xi - \omega_1) = 0, \quad (1.3)$$

$$\frac{1}{A_1A_2} L_2(m) - \frac{(h+t)^2}{h} G_3 (\eta - \omega_2) = 0, \quad (1.4)$$

$$T_1 = T'_1 + T''_1, \quad T_2 = T'_2 + T''_2, \quad T_{12} = T'_{12} + T''_{12},$$

where

$$L_1(T) = \frac{\partial}{\partial x} (T_1 A_2) - T_2 \frac{\partial A_2}{\partial x} + \frac{\partial}{\partial y} (T_{12} A_1) + T_{12} \frac{\partial A_1}{\partial y}, \quad (\overrightarrow{1,2}).$$

(1.1) is the equation of equilibrium for membrane forces, (1.2) is the equation of bending, (1.3) and (1.4) are the equations of moments.

Assuming that the deflection w does not depend on z , according to Hooke's law, we obtain

$$m_1 = \frac{B'(h+t)^2}{2} \left[\frac{1}{A_1} \frac{\partial \xi}{\partial z} + \frac{1}{A_1 A_2} \frac{\partial A_1}{\partial \varphi} \eta + \nu_1 \left(\frac{1}{A_2} \frac{\partial \eta}{\partial \varphi} + \frac{1}{A_1 A_2} \frac{\partial A_2}{\partial z} \xi \right) \right], \quad [1, 2]$$

$$m_{12} = \frac{B'(h+t)^2(1-\nu_1)}{4} \left[\frac{1}{A_1} \frac{\partial \xi}{\partial z} + \frac{1}{A_2} \frac{\partial \eta}{\partial \varphi} - \frac{2A_1}{A_1 A_2 \partial \varphi} - \frac{\eta}{A_1 A_2} \frac{\partial A_2}{\partial z} \right].$$

consequently,

$$L_1(m) = L_1(\xi, \eta), \quad L_2(m) = L_2(\xi, \eta).$$

We shall try to satisfy the equations of moments with the help of function φ , considering that

$$\xi = \frac{1}{A_1} \frac{\partial \varphi}{\partial z}, \quad \eta = \frac{1}{A_2} \frac{\partial \varphi}{\partial \varphi}. \quad (1.5)$$

After transformations, equations (1.3) and (1.4) are reduced to the form of

$$\frac{1}{2} B' \left\{ \frac{\partial}{\partial z} (\nabla^2 \varphi) + \frac{\nu_1}{A_1 A_2} \frac{\partial \varphi}{\partial z} \left[\frac{\partial}{\partial z} \left(\frac{1}{A_1} \frac{\partial A_2}{\partial z} \right) + \frac{\partial}{\partial \varphi} \left(\frac{1}{A_2} \frac{\partial A_1}{\partial \varphi} \right) \right] \right\} - \frac{G_2}{h} \left(\frac{\partial \varphi}{\partial z} - \frac{\partial w}{\partial z} \right) = 0, \quad (1.6)$$

$$\frac{1}{2} B' \left\{ \frac{\partial}{\partial \varphi} (\nabla^2 \varphi) + \frac{\nu_1}{A_1 A_2} \frac{\partial \varphi}{\partial \varphi} \left[\frac{\partial}{\partial \varphi} \left(\frac{1}{A_1} \frac{\partial A_2}{\partial \varphi} \right) + \frac{\partial}{\partial z} \left(\frac{1}{A_2} \frac{\partial A_1}{\partial z} \right) \right] \right\} - \frac{G_2}{h} \left(\frac{\partial \varphi}{\partial \varphi} - \frac{\partial w}{\partial \varphi} \right) = 0. \quad (1.7)$$

According to [4], the expression in the brackets constitutes a Gaussian curvature of surface; therefore, equations (1.6) and (1.7) will contain the main curvatures

$$\begin{aligned} \frac{\partial w}{\partial z} &= \frac{-B'}{2G_2} \frac{\partial}{\partial z} (\nabla^2 \varphi) + \frac{\partial \varphi}{\partial z} (1-f), \\ \frac{\partial w}{\partial \varphi} &= \frac{-B'}{2G_2} \frac{\partial}{\partial \varphi} (\nabla^2 \varphi) + \frac{\partial \varphi}{\partial \varphi} (1-f), \end{aligned} \quad (1.8)$$

where $f = \frac{\nu_1 B' h}{2G_2 R_1 R_2}$.

Thus, if the main curvatures of the shell is constant, then, by integrating (1.8), for deflection w , we shall obtain:

$$w = (1-f) \varphi - \frac{B' h}{2G_2} \nabla^2 \varphi. \quad (1.9)$$

Formula (1.9) will be valid for cylindrical, conical, and spherical sloping shells.

Let us consider the general case of a sloping shell, for which $\left(\frac{L}{R}\right)^2 \sim \varepsilon \ll 1$, where L is a characteristic dimension of the shell, R is the smallest radius of curvature, and ε is the error allowed, as compared to unity.

Formula (1.9) will also take place in this case, if $f \ll 1$.

2. Bending of Three-Layer Plates with Light Filler

Let us consider small deflections of three-layer plates with a light filler. If we disregard the flexural rigidity of the carrier layers D' , then with the help of (1.9) the equation of bending (1.2) is biharmonic with the right side:

$$\nabla^4 \varphi = \frac{2p}{B'(k+t)^2}. \quad (2.1)$$

The formulas for shear stresses and moments of a three-layer plate coincide in form with the corresponding formulas of a single-layer plate:

$$m_{11} = C_1 \left(\frac{\partial^2 \varphi}{\partial x^2} + \nu_1 \frac{\partial^2 \varphi}{\partial y^2} \right), \quad m_{12} = C_1 \frac{\partial^2 \varphi}{\partial x \partial y},$$

$$N_x = C_1 \frac{\partial}{\partial x} (\nabla^2 \varphi), \quad \overline{1, 2}.$$

We shall write the boundary conditions which should be satisfied by function φ :

a) if edge $x = a$ is secured, then

$$\varphi = \frac{B'h}{2G_s} \nabla^2 \varphi \Big|_{x=a} = 0, \quad \frac{\partial \varphi}{\partial x} \Big|_{x=a} = 0, \quad \frac{\partial \varphi}{\partial y} \Big|_{x=a} = 0,$$

b) a freely supported edge will be

$$\varphi = \frac{B'h}{2G_s} \nabla^2 \varphi \Big|_{x=a} = 0, \quad \frac{\partial^2 \varphi}{\partial x^2} + \nu_1 \frac{\partial^2 \varphi}{\partial y^2} \Big|_{x=a} = 0, \quad \frac{\partial \varphi}{\partial y} \Big|_{x=a} = 0,$$

c) a free edge will be

$$\frac{\partial^2 \varphi}{\partial x^2} + \nu_1 \frac{\partial^2 \varphi}{\partial y^2} \Big|_{x=a} = 0, \quad \frac{\partial}{\partial x} (\nabla^2 \varphi) \Big|_{x=a} = 0, \quad \frac{\partial \varphi}{\partial x \partial y} \Big|_{x=a} = 0.$$

As an example we shall consider the bending of a freely supported rectangular plate under the action of a lateral load. The boundary conditions will be satisfied if function φ is taken in the form of

$$\varphi = \sum_{m,n=1,2,3} a_{mn} \sin \alpha_m x \cdot \sin \beta_n y,$$

where

$$\alpha_m = \frac{m\pi}{a}, \quad \beta_n = \frac{n\pi}{b}.$$

Let us assume that the load p is constant. Then, expanding one in a double Fourier series

$$1 = \frac{16}{\pi^2} \sum_{m,n=1,2,3} \frac{\sin \alpha_m x \sin \beta_n y}{mn}$$

and using equation (2.1), we find:

$$a_{mn} = \frac{32p}{\pi^2 B' (k + 1)^2 mn (\alpha_m^2 + \beta_n^2)}$$

According to formula (1.9), deflection w will be written as

$$w = \sum_{m,n=1,2,3} A_{mn} \sin \alpha_m x \cdot \sin \beta_n y,$$

where

$$A_{mn} = \frac{16 p a^4}{C_1 \pi^2 mn (\alpha_m^2 + \beta_n^2)^3} [1 + k (m^2 + n^2 \lambda^2)], \quad (2.2)$$

$$k = \frac{\pi^2 B' h}{2 G_2 a^3}, \quad \lambda = \frac{a}{b}.$$

Equation (2.2) and the corresponding formula of [5] was performed for $\lambda = 0.5$. The results of calculations turned out to be very close.

3. Bending of Three-Layer Plates of Variable Thickness

Let us consider a three-layer plate with carrier layers of constant thickness t . If the equation of moments (1.3), which was written for such a plate, is differentiated with respect to y , and equation (1.4), with respect to x , and it is subtracted, we will obtain:

$$v^2 \left[\frac{\partial}{\partial y} (k\epsilon) - \frac{\partial}{\partial x} (k\gamma) \right] = \frac{4G_2}{B' (1 - \nu_1)} \left[\frac{\partial \epsilon}{\partial y} - \frac{\partial \gamma}{\partial x} \right]. \quad (3.1)$$

If the total thickness of the plate changes according to the law $H = k\varphi$, where k is the proportionality factor, equation (3.1) will be

satisfied with the help of function φ , by considering that

$$\xi = \frac{\partial \varphi}{\partial x}, \quad \eta = \frac{\partial \varphi}{\partial y}.$$

Instead of (1.9), for deflection w we will have:

$$w = \varphi - \frac{B'k}{2G_s} \left[\varphi \nabla^2 \varphi + \left(\frac{\partial \varphi}{\partial x} \right)^2 + \left(\frac{\partial \varphi}{\partial y} \right)^2 \right]. \quad (3.2)$$

For simplicity we shall consider cylindrical bending of a plate, so that $\varphi = \varphi(x)$. The equation of bending takes on the form of

$$\varphi^2 \varphi_{xxxx} + 3\varphi \varphi_x^2 + 5\varphi \varphi_x \varphi_{xxx} + 3\varphi_x^2 \varphi_{xx} = \frac{2p}{B'k^2}, \quad (3.3)$$

where

$$\varphi_x = \frac{\partial \varphi}{\partial x}.$$

Let us assume that the edges of the plates are secured, i.e.,

$$w|_{x=\pm a} = 0, \quad \xi|_{x=\pm a} = 0.$$

The boundary conditions will be satisfied if function φ is taken in the form of

$$\varphi = a_0 \left[1 - \left(\frac{x}{a} \right)^2 \right]^2.$$

Consequently, in this case the plate thickness changes according to the following law:

$$H = ka_0 \left[1 - \left(\frac{x}{a} \right)^2 \right]^2.$$

By calculating coefficient a_0 according to Galerkin's method, we shall determine the deflection from formula (3.2)

$$w = -\frac{pa^4}{40B'k_0^2} \left[1 - \left(\frac{x}{a} \right)^2 \right]^2 + \frac{pa^2}{20k_0G_s} [(1-x^2)^2 - 4x^2(1-x^2)],$$

where h_0 is the maximum thickness of the plate. Consequently, the values of maximum deflection will be:

$$w_{\max} = -\frac{pa^4}{40B'k_0^2} + \frac{pa^2}{20k_0G_s}.$$

4. Introduction of the Displacement Function for a Three-Layer Plate with a Stiffener

In this case the dependence between the deflection and the displacement function φ is the following:

$$(a_1 \nabla^2 - a_2 G_2) \varphi - (a_3 \nabla^2 + a_4 G_2) w + C = 0. \quad (4.1)$$

Here

$$a_1 = C_1 + \frac{(k+t)^2}{k^2} D, \quad a_2 = \frac{(k+t)^2}{k}, \quad a_3 = \frac{(k+t)t}{k^2} D.$$

In formula (4.1) C is an arbitrary constant. If the deflections are small, the equation of bending [3], which is expressed by φ and w , will have the form of

$$\nabla^2 [a_1 \nabla^2 \varphi + a_3 \nabla^2 w + X] = 0, \quad (4.2)$$

where

$$\begin{aligned} \nabla^2 X &= p, \\ a_4 &= C_1 + \frac{k+t}{t} D, \quad a_5 = 2D' - \frac{t}{k} D. \end{aligned} \quad (4.3)$$

From (4.2), we find

$$\nabla^2 (a_1 \varphi + a_3 w) + X = f(x, y), \quad (4.2')$$

where $f(x, y)$ is a harmonic function.

Function X satisfies Poisson equation (4.3), and the boundary conditions for it are established in the course of solution of the problem.

Consequently, for the solution of problems of bending, we have two equations (4.1) and (4.2') with respect to unknowns w and φ , from which we obtain:

$$w = -\varphi + \frac{a_1 a_2 + a_3 a_4}{a_2 a_4 G_2} \nabla^2 \varphi + \frac{a_2 X}{a_2 a_4 G_2} - \frac{a_2 f}{a_2 a_4 G_2} + C a_2. \quad (4.4)$$

Constant C characterizes rigid movement, and therefore it can be rejected. Putting (4.4) in the equation of bending, we arrive at the equation for determination of φ :

$$\frac{a_1 a_2 + a_3 a_4}{a_2 G_2} \nabla^4 \varphi + (a_1 - a_3) \nabla^2 \varphi + p + \nabla^2 p = 0. \quad (4.5)$$

5. Bending of a Three-Layer Circular Plate with a Stiffener

Below we shall solve the problem of bending of a circular plate with a stiffener under action of constant external pressure with the help of equations (4.4) and (4.5). If the plate is secured all over its contour, the boundary condition for φ will be:

$$-\varphi + \frac{a_1 a_2 + a_2 a_1}{a_2 a_3 G_3} \nabla^2 \varphi \Big|_{r=a} = 0, \quad \frac{dw}{dr} \Big|_{r=a} = 0, \quad \frac{d\varphi}{dr} \Big|_{r=a} = 0. \quad (5.1)$$

From formulas (4.3) and (4.4) and the given boundary conditions, we find:

$$f = 0, \quad X = \frac{p}{4} (r^2 - a^2).$$

Introducing a system of substitutions,

$$s_1 = \frac{a_1 a_2 + a_2 a_1}{a_2 G_3}, \quad s_2 = a_1 - a_3,$$

$$\psi = \nabla^4 \varphi, \quad A = \sqrt{\frac{s_2}{s_1}} r,$$

we reduce (4.5) to a Bessel equation:

$$\frac{d^2 \psi}{dA^2} + \frac{1}{A} \frac{d\psi}{dA} + \psi \frac{p}{s_2} = 0. \quad (5.2)$$

The solution for φ will be obtained in the form of

$$\varphi = \frac{C_1 a^4}{k_0^4} I_0(k_0 p) - \frac{p a^4 p^4}{64 s_2} + \frac{C_2 a^2 p^2}{4} + C_3, \quad (5.3)$$

where I_0 is a Bessel function of the first kind,

$$k_0 = a \sqrt{\frac{s_2}{s_1}}, \quad p = \frac{r}{a}.$$

C_1, C_2, C_3 are arbitrary integration constants.

By determining C_1, C_2, C_3 from conditions (5.1), we find the value of maximum plate deflection from equation (4.4)

$$w_{r=a} = \frac{p a^4}{s_2} \left\{ \frac{(1-\nu)}{2} \left(\frac{1}{k_0^2} + \frac{s_1}{a_2 a^4} \right) \left[\frac{1}{2} + \frac{k_0 - 1}{k_0 I_1} \right] + \frac{1}{64} \right\} \quad (5.4)$$

$$I_0 = \frac{s_2 a_2}{G_3 a_2 s_1}, \quad I_0 = I_0(k_0), \quad I_1 = I_1(k_0).$$

Literature

1. Kh. M. Mushtari. The general theory of three-layer shells with a stiffener. Academy of Sciences USSR, OTN, No. 2, 1961.
2. E. I. Grigolyuk. Equation of three-layer shells with light filler. Academy of Sciences USSR, OTN, No. 1, 1957.
3. E. I. Grigolyuk. Finite deflections of three-layer shells with a stiffener. Academy of Sciences USSR, OTN, No. 1, 1958.
4. Kh. M. Mushtari and K. Z. Galimov. Nonlinear theory of elastic shells. Tatknigoizdat, 1957.
5. A. Ya. Aleksandrov et al. Analysis of three-layer panels. Moscow, Oborongiz, 1960.
6. A. S. Vol'mir. Flexible plates and shells. State Press for Technical and Theoretical Literature, 1956.
7. Ye. Yanke and F. Emde. Tables and functions. Fizmatgiz, 1959.

Submitted
26 September 1963

CALCULATION OF THE NONAXIALLY SYMMETRIC STATE OF STRAIN OF CYLINDRICAL SHELLS TAKING INTO ACCOUNT THE ELASTICITY OF THE REINFORCING FRAMES

Yu. I. Kaplan

Definitions of Cyrillic Items

дон = sec = secondary

ш = f = frame

кр = crit = critical

In this article, by the methods of [1], we obtain analogous results for nonaxially symmetric strain. All assumptions concerning the work of frames and the approach to the solution of problems are presented in the mentioned article. The basic designations are also taken from it.

As a functional unknown in the solution of the problem, we take the total moments in longitudinal sections by the energetic method:

$$M_{\varphi} = \sum_{n=0}^{\infty} \psi_n(x) \cos n\varphi. \quad (1)$$

Then, under certain assumptions ($\varepsilon_{\varphi} = 0$, $\varepsilon_{\varphi x} = 0$, i.e., with inextensibility of the outline of the cross section and the absence of shear strain in the middle surface), all internal forces can be expressed through the introduced unknowns. The stresses in cross

sections are

$$q_{n, \text{tot}} = -\frac{ER^3}{D_n} \sum_{n=1}^{\infty} \frac{\psi_n'(x)}{n^2(n^2-1)} \cos n\varphi = - \sum_{n=1}^{\infty} \psi_n'(x) f_n(s), \quad (2)$$

where

$$f_n(s) = \frac{ER^3}{D_n} \cdot \frac{\cos n\varphi}{n^2(n^2-1)}, \quad (3)$$

D_f is the cylindrical rigidity of the shell wall. The remaining internal forces are easily expressed through ψ_n and their derivatives, but they do not make an essential contribution to strain energy, which for a section of the shell has the following form:

$$U = \int_{x_1}^L \left\{ \oint \left[\frac{m_{\varphi, \text{tot}}^2}{2D_n} + \frac{q_{\varphi, \text{tot}}^2}{2E} + A_p \right] ds \right\} dx + \Gamma_{\text{tot}}. \quad (4)$$

Intermediate frames are loaded by the drop of tangent forces that are acting in a given section of the shell:

$$\Delta q_{n, \text{tot}} = q_{n, \text{tot}}(x, -0) - q_{n, \text{tot}}(x, +0) = \\ = [\psi_n'(x, +0) - \psi_n'(x, -0)] \int_0^L \delta_s f_n(s) ds. \quad (5)$$

These forces produce bending of the frame by a load

$$\Delta M_{n, s} = [\psi_n'(x, +0) - \psi_n'(x, -0)] \cdot m_n(s), \quad (6)$$

where the moments from the tangent flow

$$f_n(s) = \int_0^L \delta_s f_n(s) ds = \frac{ER^3}{D_n n^2(n^2-1)} \sin n\varphi \quad (7)$$

will be:

$$m_n(s) = \frac{ER^3}{D_n n^2(n^2-1)^2} \cos n\varphi = \frac{\cos n\varphi}{4h_n^4}. \quad (8)$$

In (8) we designate:

$$h_n^4 = \frac{D_n n^2(n^2-1)^2}{4ER^3}. \quad (9)$$

Consequently, formula (4) takes on the form:

$$U = \int_{x_1}^L \left\{ \oint \left[\frac{1}{2D_n} \left[\sum_{n=1}^{\infty} \psi_n(x) \cos n\varphi \right]^2 + \frac{1}{2E} \left[\sum_{n=1}^{\infty} \psi_n'(x) f_n(s) \right]^2 + A_p \right] ds dx + \right. \\ \left. + \frac{1}{2EJ_{\text{tot}}} \oint \left[\sum_{n=1}^{\infty} [\psi_n'(x, +0) - \psi_n'(x, -0)] \frac{\cos n\varphi}{4h_n^4} \right]^2 ds = \right. \\ \left. - \int_{x_1}^L \Gamma(\psi_n, \psi_n', \psi_n'') dx + \Gamma_{\text{tot}}[\psi_n'(x=x_1)] \right\}. \quad (10)$$

Here I_{fr} is the moment of inertia of the frame with coordinate $x = x_r$.

Since (10) in general notation coincides with (6)*,¹⁾ the natural boundary conditions of the mixed variational problem will also be the same as (8)*:

$$\frac{\partial \Gamma}{\partial \psi_n^{IV}} - \frac{\partial \Gamma}{\partial \psi_n''} = 0 \quad (x = x_r). \quad (11)$$

The Euler equation in this case reduces to a differential equation

$$\psi_n^{IV} + \frac{D_n \pi^4 (\pi^2 - 1)^2}{ER^3} \psi_n + B_r = 0, \quad (12)$$

or

$$\psi_n^{IV} + 4k_n^4 \psi_n + B_r = 0. \quad (13)$$

The solution of the last equation is (12)*.

In case of rigid intermediate frames, the constants D_r are determined from these conditions:

$$\psi_n(x = a_{r-1}) = 0. \quad (14)$$

With elastic frames, these constants are found from condition (11).

For determination of $\frac{\partial \Gamma}{\partial \psi_n^{IV}}$ we express ψ_n , by analogy with [1], in the

formula for energy (10) through ψ_n^{IV} from the equation of equilibrium of moments in the longitudinal section of the shell in its additional state (m_φ are balanced by the moments which appear due to the tangent forces)

$$\psi_n(x) \cos \pi \varphi + \psi_n^{IV}(x) m_\pi(z) = 0 \quad (15)$$

or, using (8),

$$\psi_n^{IV}(x) + 4k_n^4 \psi_n(x) = 0, \quad (16)$$

whence

$$\psi_n(x) = -\frac{1}{4k_n^4} \psi_n^{IV}(x). \quad (17)$$

Putting (17) in (10), and calculating $\frac{\partial \Gamma}{\partial \psi_n^{IV}}$, we have:

¹⁾ Asterisks note formulas of [1].

$$\frac{\partial \pi}{\partial \psi_{\pm}^{IV}} = -\frac{1}{D_{\pm}} \cdot \frac{1}{4k_{\pm}^4} \psi_{\pm}(x) \cdot \pi R. \quad (18)$$

The second term in (11) will be

$$\frac{\partial \pi}{\partial \psi_{\pm}^{IV}} = \frac{1}{EI_{\pm r}} \left(\frac{1}{4k_{\pm}^4} \right)^2 [\psi_{\pm}''(x_r + 0) - \psi_{\pm}''(x_r - 0)] \cdot \pi R. \quad (19)$$

so that the boundary condition finally takes on the form:

$$\psi_{\pm}''(x_r - 0) = \psi_{\pm}''(x_r + 0) + \frac{EI_{\pm r}}{D_{\pm}} 4k_{\pm}^4 \psi_{\pm}(x - x_r). \quad (20)$$

Using now (12)*, (11)*, and (20), we obtain the sought constant

$$D_{\pm} = -\frac{1}{\psi_{\pm}''(x=0)} \cdot \frac{EI_{\pm r}}{D_{\pm}} 4k_{\pm}^4 \psi_{\pm}(x - x_r) \quad (21)$$

and the general solution of (12)*:

$$\begin{aligned} \psi_{\pm}(x) = & A_1 \Phi_0(x) + B_1 \Phi_1(x) + C_1 \Phi_2(x) + D_1 \Phi_3(x) + \Phi^*(x) \{ - \\ & - \frac{1}{\psi_{\pm}''(x=0)} 4k_{\pm}^4 \sum_{r=1}^n \frac{EI_{\pm r}}{D_{\pm}} \psi_{\pm}(x - a_{r-1}) \Phi_3(x - a_{r-1}). \end{aligned} \quad (22)$$

Further solution depends on the character of the considered problem, which is expressed by equation (13).

The system of equations for the determination of the constants completely coincides with (21)* and (22)*,¹⁾ only, naturally, formula (23)* looks otherwise:

$$G_r = \frac{1}{\psi_{\pm}''(x=0)} 4k_{\pm}^4 \frac{EI_{\pm r}}{D_{\pm}}. \quad (23)$$

1. Transverse Bending of Cylindrical Shells

In case of transverse bending, the energy of the unit of length of the shell in its secondary state is

¹⁾In formula (22)* one term is left out and there is an error within the limits of summation. The corrected formula has the form:

$$M = \Phi_3(L) - \sum_{r=1}^n G_{r-1} \Phi_3(a_{r-1}) \Phi_3(L - a_{r-1}) + \sum_{r=1}^{n-1} (...).$$

$$r = \oint \left\{ \frac{1}{2D_m} \left[\sum_{n=1}^{\infty} (\psi_n(x) - A_n(x)) \cos n\varphi \right]^2 + \frac{1}{2E} \left[\sum_{n=1}^{\infty} \psi_n'(x) f_n(s) \right]^2 \right\} ds, \quad (24)$$

where $A_n(x)$ are the coefficients of expansion in a series of the moments acting in the base system. Therefore, in equation (13)

$$B_p = -4k_n^4 A_n(x), \quad (25)$$

and it takes on the form:

$$\psi_n^{IV} + 4k_n^4 \psi_n = 4k_n^4 A_n(x). \quad (26)$$

$\Phi_1(x)$ in this case constitute Krylov functions for the calculation of beams on an elastic support. The particular solution will be:

$$\Phi^*(x) = 4k_n \int_0^x A_n(\tau) \Phi_3(x - \tau) d\tau. \quad (27)$$

Therefore, general solution (22) will be written:

$$\begin{aligned} \psi_n(x) = & A_1 \Phi_0(x) + B_1 \Phi_1(x) + C_1 \Phi_2(x) + D_1 \Phi_3(x) + \\ & + 4k_n \int_0^x A_n(\tau) \Phi_3(x - \tau) d\tau - 4k_n \sum_{r=2}^n \frac{El_{mr}}{D_m} \psi_n(x = a_{r-1}) \Phi_3(x - a_{r-1}). \end{aligned} \quad (28)$$

2. The Asymmetric Form of Stability Loss Under the Action of Axial Forces

In this case,

$$\begin{aligned} A_p = & -\frac{\sigma_{sp}^2}{2} \left[\frac{dV}{dx} \frac{w_n^2 + v_n^2}{n^2} \right]^2 = \\ = & -\frac{\sigma_{sp}^2}{2} \cdot \frac{R^4}{D_m^2 (n^2 - 1)^2} \left(1 + \frac{1}{n^2} \right) \left(\frac{d\psi_n(x)}{dx} \right)^2, \end{aligned} \quad (29)$$

where w_n and v_n correspondingly are the normal and tangent shifts in the plane of cross section.

Then

$$B_p = \sigma_{sp} \frac{n^2(n^2 + 1)}{ER^3} \psi_n'(x), \quad (30)$$

and equation (13) takes on the form of

$$\psi_n^{IV} + 2v_n^2 \psi_n'' + 4k_n^4 \psi_n = 0, \quad (31)$$

where

$$v_n^2 = c_{sp} \frac{n^2(n^2 + 1)}{2ER^3}. \quad (32)$$

It completely coincides in structure with (33)* and is therefore solved in the same functions as the latter. These functions and their properties are shown in formulas (34)* and (38)*, and Table 1 [1], only, naturally, instead of γ_1 and γ_2 , there will appear γ_{1n} and γ_{2n} :

$$\gamma_{1n} = \sqrt{v_n^2 - \sqrt{v_n^4 - 4k_n^4}}, \quad (33)$$

$$\gamma_{2n} = \sqrt{v_n^2 + \sqrt{v_n^4 - 4k_n^4}}, \quad (34)$$

$$x_n^2 = \gamma_{1n}\gamma_{2n} = 2k_n^2. \quad (35)$$

As a result, general solution (22) is thus written:

$$\begin{aligned} \phi_n(x) = & A_1\Phi_0(x) + B_1\Phi_1(x) + C_1\Phi_2(x) + D_1\Phi_3(x) \parallel - \\ & - \frac{1}{x_n(\gamma_{2n}^2 - \gamma_{1n}^2)} 4k_n^4 \sum_{r=2}^n \frac{EI_{nr}}{D_n} \phi_n(x - a_{r-1}) \Phi_3(x - a_{r-1}). \end{aligned} \quad (36)$$

3. Stability Under the Action of Uniform Transverse Pressure

In this case

$$\Delta p = -\frac{\Delta p w_n}{2}, \quad (37)$$

where

$$\Delta p = -\frac{p_{sp}}{R^3} \left(w_n + \frac{\partial^2 w_n}{\partial \varphi^2} \right) = p_{sp} \frac{R}{D_n} \psi_n(x) \cos n\varphi. \quad (38)$$

Here p_{crit} is radial pressure, under whose action the shell loses its stability.

Then

$$B_p = -\frac{n^2(n^2 - 1)}{4ER^3} p_{sp} \psi_n(x) \quad (39)$$

and equation (13) can be represented as

$$\psi_n^{IV} - x_n^2 \psi_n = 0, \quad (40)$$

where

$$\chi_n^2 = \frac{D_m \pi^4 (n^2 - 1)^2}{E I_m R^2} \left[P_{cr} \frac{R^2}{D_m (n^2 - 1)} - 1 \right]. \quad (41)$$

Equation (40) coincides in structure with the equation that describes free oscillations of rods, and it is solved in Krylov functions $\Phi_1(x)$ of the first kind. The general expression of (22) will be:

$$\begin{aligned} \psi_n(x) = & A_1 \Phi_0(x) + B_1 \Phi_1(x) + C_1 \Phi_2(x) + D_1 \Phi_3(x) - \\ & - \frac{4k_n^4}{\chi_n^4} \sum_{r=2}^n \frac{EI_{mr}}{D_m} \psi_n(x - a_{r-1}) \Phi_3(x - a_{r-1}). \end{aligned} \quad (42)$$

4. Stability During the Joint Action of Uniform Transverse Pressure and Axial Compression

This problem essentially is a combination of the preceding solutions. Here, besides (37), it is necessary to also add the potential of external forces, which is expressed by (29). Thus, B_p also will be represented by the sum of (39) and (30), as a result of which equation (13) takes on the form of

$$\psi_n^{IV} + 2\nu_n^2 \psi_n'' - \chi_n^4 \psi_n = 0, \quad (43)$$

where

$$\nu_n^2 = \sigma_{cr} \frac{\pi^2 (n^2 + 1)}{2ER^2} \quad (44)$$

and

$$\chi_n^2 = \frac{D_m \pi^4 (n^2 - 1)^2}{E I_m R^2} \left[P_{cr} \frac{R^2}{D_m (n^2 - 1)} - 1 \right]. \quad (45)$$

Function $\Phi_1(x)$ in this case will be written as

$$\begin{aligned} \Phi_0(x) &= \frac{1}{\lambda_n^2} (\beta_{1n}^2 \cos \beta_{2n} x + \beta_{2n}^2 \operatorname{ch} \beta_{1n} x), \\ \Phi_1(x) &= \frac{1}{\lambda_n^2} (\beta_{1n}^2 \sin \beta_{2n} x + \beta_{2n}^2 \operatorname{sh} \beta_{1n} x), \\ \Phi_2(x) &= \cos \beta_{2n} x - \operatorname{ch} \beta_{1n} x, \\ \Phi_3(x) &= \frac{1}{\lambda_n^2} (\beta_{1n} \sin \beta_{2n} x - \beta_{2n} \operatorname{sh} \beta_{1n} x). \end{aligned} \quad (46)$$

Here

$$\beta_{1n} = \sqrt{-\nu_n^2 + \sqrt{\nu_n^4 + \chi_n^2}}, \quad (47)$$

$$\beta_{2n} = \sqrt{\nu_n^2 + \sqrt{\nu_n^4 + \chi_n^2}}, \quad (48)$$

$$\lambda_n^2 = \beta_{1n}\beta_{2n} = \chi_n^2. \quad (49)$$

The derivatives from functions (46) are shown in the table, where the following designations are introduced:

$$\begin{aligned} \bar{\Phi}_0(x) &= \lambda_n^2 \left(-\frac{1}{\beta_{1n}^2} \cos \beta_{2n}x - \frac{1}{\beta_{2n}^2} \operatorname{ch} \beta_{1n}x \right), \\ \bar{\Phi}_1(x) &= \lambda_n \left(-\frac{1}{\beta_{1n}} \sin \beta_{2n}x - \frac{1}{\beta_{2n}} \operatorname{sh} \beta_{1n}x \right), \\ \bar{\Phi}_2(x) &= \lambda_n^2 \left(-\frac{1}{\beta_{1n}^2} \sin \beta_{2n}x + \frac{1}{\beta_{2n}^2} \operatorname{sh} \beta_{1n}x \right). \end{aligned} \quad (50)$$

Table

$\Phi_i(x) \backslash \Phi_j^{(n)}(x)$	$\Phi_0(x)$	$\Phi_1(x)$	$\Phi_2(x)$	$\Phi_3(x)$
$\Phi_0(x)$	$-\lambda_n \Phi_3(x)$	$-\lambda_n^2 \Phi_2(x)$	$-\lambda_n^3 \bar{\Phi}_1(x)$	
$\Phi_1(x)$	$\lambda_n \Phi_0(x)$	$-\lambda_n^2 \Phi_3(x)$	$-\lambda_n^3 \bar{\Phi}_2(x)$	
$\Phi_2(x)$	$\lambda_n \bar{\Phi}_1(x)$	$\lambda_n^2 \bar{\Phi}_0(x)$	$-\lambda_n^3 \bar{\Phi}_3(x)$	
$\Phi_3(x)$	$\lambda_n \bar{\Phi}_2(x)$	$\lambda_n^2 \bar{\Phi}_3(x)$	$\lambda_n^3 \bar{\Phi}_0(x)$	

The general expression of (22) will be:

$$\begin{aligned} \varphi_n(x) &= A_0 \Phi_0(x) + B_1 \Phi_1(x) + C_1 \Phi_2(x) + D_1 \Phi_3(x) + \\ &+ \frac{4k_n^4}{\lambda_n(\beta_{1n}^2 + \beta_{2n}^2)} \sum_{r=2}^n \frac{EI_{nr}}{D_n} \varphi_r(x - a_{r-1}) \Phi_3(x - a_{r-1}). \end{aligned} \quad (51)$$

Conclusion

With any number of elastic intermediate frames, the problem is reduced to no more than four constants, and practically, to two (since the extreme frames are almost always sufficiently powerful), for which the system of equations is written in general form. In

the example of different problems we show the application of the presented method for obtaining a general solution.

Literature

1. Yu. I. Kaplan. Calculation of the axially symmetric state of strain of cylindrical shells in the presence of discretely located elastic frames. IVUZ, "Aeronautical Engineering," No. 4, 1963.

Submitted
9 December 1963

VIBRATIONS OF AN ANISOTROPIC PLATE UNDER A CONTINUOUSLY MOVING DISTRIBUTED LOAD

A. P. Kovrevskiy

Definition of Cyrillic Item

pa3M = dim = dimensionless

The problem of vibrations of elastic bodies during the movement of a flow of mass through their surface arises in the study of different radiator systems, and also in examining the vibrations of bodies of liquid-fuel rocket engines taking into account the liquid coolant between walls.

Here we study the free vibrations of orthotropic plates which carry a mass flow evenly distributed along their surface. We consider that there are no frictional forces between the flow and the plate. The trajectory of flow repeats the bending mode of vibrations of the plate.

Structurally, such a system may be accomplished by passing a fluid flow between the layers of a three-layer plate with a corrugation filler. In a certain range of frequencies, the three-layer plate may be replaced by a one-layer orthotropic plate, which is equivalent to it in the sense of flexural rigidity; however, questions of such reduction are not considered here.

This work is an extension of the known problem of free vibrations of pipelines to vibrations of plates.

A similar problem concerning the free vibrations of an isotropic plate under the action of an evenly distributed moving load was set up by I. I. Gol'denblat [1]; however, the author did not give its solution, as he limited himself to general instructions about the method of solution.

§ 1. The equation of free vibrations of an orthotropic rectangular plate of constant thickness is written in the form [2]:

$$D_1 \frac{\partial^2 \zeta}{\partial \xi^2} + 2D_2 \frac{\partial^2 \zeta}{\partial \xi \partial \eta} + D_3 \frac{\partial^2 \zeta}{\partial \eta^2} = m_1 \frac{\partial^2 \zeta}{\partial \tau^2}. \quad (1)$$

Here we designate:

$\zeta = \zeta(\xi, \eta, \tau)$ is the deflection of the middle layer of the plate,

ξ, η, τ are the coordinates and measured time,

m_1 is the density of the plate material per unit of surface,

$$D_1 = \frac{E_x h^3}{12(1-\nu_x^2)}, \quad D_2 = \frac{E_y h^3}{12(1-\nu_x^2)}, \quad D_3 = \frac{E_x h^3 \nu_y}{12(1-\nu_x^2)} + 2 \frac{G_{xy} h^3}{12}.$$

G_{xy}, E_x, E_y is the shear modulus in plane $\xi\eta$ and the elastic moduli in the direction of axes ξ and η , correspondingly,

ν_x, ν_y are the Poisson ratios of the plate material,

l_x, l_y are the dimensions of the plate in the plan along axes ξ and η ,

h is the thickness of the plate.

Let us assume that the flow moves in the direction of axis ξ with constant speed v (Fig. 1). Flow density per unit of surface is

designated as ρ .

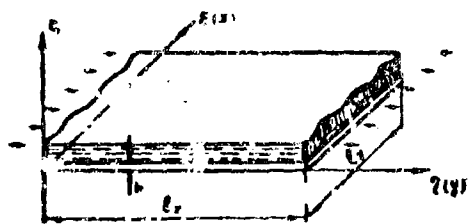


Fig. 1.

During vibrations of the plate the trajectory of flow is distorted. In the direction of flow on the plate there will act two additional inertial forces:

centrifugal $\rho v^2 \frac{\partial^2 \zeta}{\partial \xi^2}$ and Coriolis $2\rho v \frac{\partial^2 \zeta}{\partial \xi \partial \tau}$.

Furthermore, in the expression of the d'Alembert force of inertia, the mass of the plate m_1 must be increased by $\rho(m_1 + \rho)$.

Now the equation of free vibrations of the plate, taking into

account the flowing mass, will be written by the following form:

$$D_1 \frac{\partial^4 \zeta}{\partial x^4} + 2D_2 \frac{\partial^4 \zeta}{\partial x^2 \partial y^2} + D_3 \frac{\partial^4 \zeta}{\partial y^4} + 2\rho v \frac{\partial \zeta}{\partial t} + \rho v^2 \frac{\partial^2 \zeta}{\partial x^2} + m \frac{\partial^2 \zeta}{\partial t^2} = 0. \quad (2)$$

We shall introduce dimensionless magnitudes:

$$x = \frac{\xi}{l_x}, \quad y = \frac{\eta}{l_y}, \quad w = \frac{\zeta}{l_x}, \quad t = \frac{t_y}{l_x}, \\ t = \tau \sqrt{\frac{D_1}{m l_x^4}}, \quad d_3 = 2 \frac{D_2}{D_1}, \quad d_2 = \frac{D_3}{D_1}, \\ \mu = \frac{2\rho v l_x}{\sqrt{D_1 m}}, \quad \sigma = \frac{\rho v^2 l_x^2}{D_1}.$$

From the last two relationships, we find:

$$\sigma = \mu^2 k, \text{ where } k = \frac{m}{4\rho}.$$

In the shown designations, equation (2) takes on the form:

$$L[w] = \frac{\partial^4 w}{\partial x^4} + d_3 \frac{\partial^4 w}{\partial x^2 \partial y^2} + d_2 \frac{\partial^4 w}{\partial y^4} + \mu \frac{\partial^2 w}{\partial x \partial t} + \sigma \frac{\partial^2 w}{\partial x^2} + \frac{\partial^2 w}{\partial t^2} = 0. \quad (3)$$

The system described by the given equation is nonconservative. If the Coriolis force is small, as compared to the remaining terms, then equation (3) coincides with the equation of vibrations of a plate that is compressed by a longitudinal force. In systems of such type, unstable conditions are possible.

Finding of an exact solution of equation (3) is hampered; therefore, we shall use Galerkin's method. The problem consists of finding the function $w(x, y, t)$, which satisfies the variational equation:

$$\int_0^1 \int_0^1 L[w] \delta w \, dx \, dy = 0. \quad (4)$$

The sought solution is presented in the form of a double series

$$w(x, y, t) = \sum_{m=1}^{\infty} \sum_{n=1}^{\infty} X_m(x) \cdot Y_n(y) a_m(t), \quad (5)$$

where $a_m(t)$ are variable parameters. In such a form, Galerkin's method was applied in the solution of certain problems concerning the flutter

of panels [5]. As the basic functions $X_m(x)$ and $Y_n(y)$, it is convenient to take beam functions, since they immediately satisfy the boundary conditions. Substitution of (5) in (4) gives:

$$\int_0^1 \int_0^l \sum_{m=1}^{\infty} \sum_{n=1}^{\infty} \left[\left(Y_n \frac{d^4 X_m}{dx^4} + d_3 \frac{d^3 X_m}{dx^3} \cdot \frac{d^3 Y_n}{dy^3} + d_2 X_m \frac{d^4 Y_n}{dy^4} + d_1 Y_n \frac{d^2 X_m}{dx^2} \right) a_m + \right. \\ \left. + \mu Y_n \frac{d X_m}{dx} \cdot \frac{da_m}{dt} + X_m Y_n \frac{d^2 a_m}{dt^2} \right] \cdot \sum_{i=1}^{\infty} \sum_{j=1}^{\infty} X_i Y_j \delta u_i dx dy = 0. \quad (6)$$

The property of orthogonality of beam functions with respect to derivatives of the zero and fourth orders is well known. Subsequently, we shall consider only plates that are freely supported on their edges $y = 0$ and $y = l$. For such cases, functions $Y_n(y)$ are orthogonal also with respect to derivatives of the second order.

From the properties of the beam functions, it also follows that

$$\frac{d^4 X_m}{dx^4} = \alpha_m^4 X_m, \quad \frac{d^4 Y_n}{dy^4} = \beta_n^4 Y_n,$$

where α_m , β_n are eigenvalues of the boundary value problem of vibrations of beams with boundary conditions that correspond to the conditions of supporting the plate on its edges $x = 0$, $x = 1$ and $y = 0$, $y = l$.

Inasmuch as the edges $y = 0$ and $y = l$ of the considered plates are freely supported, functions $Y_n(y)$ must be taken in the form:

$$Y_n(y) = \sin \beta_n y, \quad \beta_n = \frac{n\pi}{l}. \quad (7)$$

Considering the shown properties of beam functions, from (6) we will have:

$$\sum_{m=1}^{\infty} \sum_{n=1}^{\infty} \left[\left((\alpha_m^4 + d_2 \beta_n^4) \int_0^1 X_m X_i dx \int_0^l Y_n^2 dy + \left(d_3 \int_0^1 \sum_{n=1}^{\infty} \frac{d^3 Y_n}{dy^3} Y_n dy + \right. \right. \right. \\ \left. \left. + d_1 \int_0^l \sum_{n=1}^{\infty} Y_n^2 dy \right) \int_0^1 \frac{d^2 X_m}{dx^2} X_i dx \right] a_m + \frac{da_m}{dt} \mu \int_0^1 \frac{d X_m}{dx} X_i dx \int_0^l Y_n^2 dy + \\ \left. + \frac{d^2 a_m}{dt^2} \int_0^1 X_m X_i dx \int_0^l Y_n^2 dy \right] \delta u_i = 0. \quad (8)$$

During free vibrations of a plate, along axis y exactly n half-waves are set. Therefore, instead of the entire sum $\sum_{n=1}^{\infty} y_n^2$, it is possible to consider only one n -th term. If we still consider that δa_1 are arbitrary, then from (8) we obtain finally a system of ordinary differential equations with constant coefficients for the determination of $a_m(t)$:

$$\sum_{m=1}^{\infty} \left(A_{mi} u_m + B_{mi} \frac{du_m}{dt} + C_{mi} \frac{d^2 u_m}{dt^2} \right) = 0, \quad i = 1, 2, 3, \dots \quad (9)$$

Here

$$A_{mi} = \frac{1}{2} (\alpha_m^4 + \beta_m^4 d_2) \int_0^1 X_m X_i dx + \frac{d}{2} \int_0^1 \frac{d^2 X_m}{dx^2} X_i dx - \frac{d^2 \beta_m^2 d}{3} \int_0^1 \frac{d^2 X_m}{dx^2} X_i dx, \quad (10)$$

$$B_{mi} = \frac{r d}{2} \int_0^1 \frac{d X_m}{dx} X_i dx, \quad (11)$$

$$C_{mi} = \frac{1}{2} \int_0^1 X_m X_i dx. \quad (12)$$

Obviously, in virtue of the orthogonality of beam functions, $C_{m1} = 0$ when $m \neq 1$. The solution of system (9) reduces to the determination of the roots of the determinant:

$$\begin{vmatrix} A_{11} + r B_{11} + r^2 C_{11} & A_{21} + r B_{21} & \dots \\ A_{12} + r B_{12} & A_{22} + r B_{22} + r^2 C_{22} & \dots \\ \dots & \dots & \dots \end{vmatrix} = 0. \quad (13)$$

The roots of the determinant in general are complex, i.e., $r = \delta + i\omega$. The imaginary part of the roots corresponds to the dimensionless frequency of vibrations; the negative real part constitutes the logarithmic damping decrement. If the real part of either root is positive, the vibrations are unstable. The dimensional frequencies and the logarithmic damping decrement are connected with corresponding dimensionless magnitudes by means of the following relationships:

$$\sigma_{\text{max}} = \sigma \sqrt{\frac{D_1}{m l_x^3}}, \quad (14)$$

$$\tau_{\text{max}} = \tau \sqrt{\frac{D_1}{m l_x^3}}.$$

§ 2. We shall now define coefficients A_{mi} , B_{mi} , and C_{mi} for certain simple forms of edge fastenings.

A. A plate which is freely supported around its entire outline:

$$A_{mi} = \begin{cases} 0 & i \neq m, \\ (a_m^4 + d_3 \beta_m^4) \frac{l}{4} - (a - d_3 \beta_m^2) \frac{\pi^2 l m^2}{4} & i = m, \end{cases} \quad (15)$$

$$B_{mi} = \begin{cases} 0 & i = m, \\ \frac{\pi l m}{4(l^2 - m^2)} [2i - (i - m) \cos(m + i)\pi - (i + m) \cos(i - m)\pi], & i \neq m, \end{cases} \quad (16)$$

$$C_{mi} = \begin{cases} 0, & i \neq m, \\ \frac{l}{4}, & i = m. \end{cases} \quad (17)$$

B. The plate edges $y = 0$, $y = l$ are freely supported, edge $x = 0$ is fixed, edge $x = 1$ is free:

$$A_{mi} = (a_m^4 + d_3 \beta_m^4) C_{mi} + (a - d_3 \beta_m^2) \frac{l}{2} \int_0^1 \frac{d^2 X_m}{dx^2} X_i dx, \quad (18)$$

$$B_{mi} = \frac{\pi l}{2} \int_0^1 \frac{d X_m}{dx} X_i dx, \quad (19)$$

$$C_{mi} = \frac{l}{2} \int_0^1 X_m X_i dx. \quad (20)$$

The values of the integrals in expressions (18) and (19) are given in [3]. We shall write out some of their values.

Table

mi	11	22	12	21
$\int_0^1 \frac{d X_m}{dx} X_i dx$	8.711	1.928	-6.364	1.016
$\int_0^1 \frac{d^2 X_m}{dx^2} X_i dx$	1.523	-12.815	2.982	2.982

The value of integral (20) when $m = 1$ will be determined by the value of function X_m on edge $x = 1$, and will be:

$$\int_0^1 X_m^2 dx = \frac{X_m^2}{4} \Big|_{x=0}^1 = \begin{cases} 1.855, & m=1. \\ 0.964, & m=2. \end{cases} \quad (21)$$

The last two values are taken from the book by V. Z. Vlasov [4].

§ 3. We shall perform certain calculations for an illustration of the influence of the rate of flow on the natural frequencies of a plate.

The calculations will be conducted in second approximation. From determinant (13) we obtain in this case the following characteristic equation:

$$C_{11}C_{22}r^4 + (C_{22}B_{11} + C_{11}B_{22})r^3 + (C_{22}A_{11} + C_{11}A_{22} + B_{22}B_{11} - B_{12}B_{21})r^2 + (A_{11}B_{22} + A_{22}B_{11} - A_{12}B_{21} - A_{21}B_{12})r + A_{11}A_{22} - A_{12}A_{21} = 0. \quad (22)$$

By examining the coefficients of equation (22), it is possible to note that case A equation (22) will be biquadratic, and in case B it constitutes a full polynomial of the fourth degree.

A more attentive study of the following approximations allows us to conclude that in cases when the edges of the plate $x = 0$, $x = 1$ are secured from transverse shifts, the characteristic equation will have only even powers of r . In the range of parameters μ and k , which present practical interest, the squares of the roots of this equation are real numbers. The power of equation is equal to $2p$, where p is the selected number of approximations. If, however, the plate has a free edge in a direction transverse to the flow, the characteristic equation is a full polynomial of the power $2p$.

In the first case the roots of the equation are either purely imaginary, or real, i.e., there occur vibrations without damping or the plate will lose its stability by exponential law.

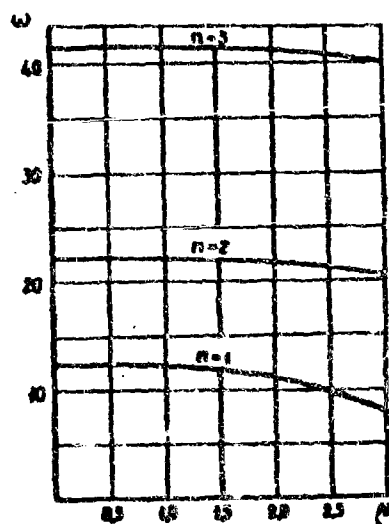


Fig. 2.

Figures 2 and 3 show the dependences of the lowest roots of equation (22) on the parameter of speed μ for cases A and B, correspondingly.

The calculations were conducted

with the following values of parameters:

$$d_2 = 0.01, d_3 = 0.1, l = 0.5, k = 1.$$

Let us note that the results of calculations in third approximation insignificantly improve the results of second approximation. For instance, for a plate that is freely supported around its entire outline, when $n = 1$ and $\mu = 3$, from the second approximation we have: $\omega = 7.88$. The third approximation gives: $\omega = 7.59$. The divergence constitutes a total of 3.9%

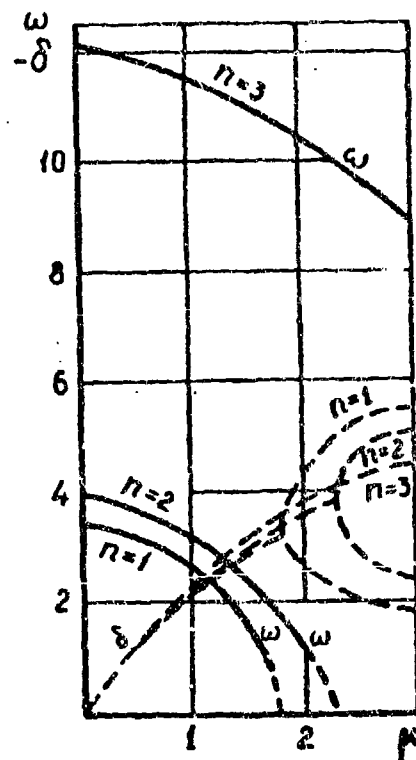


Fig. 3.

§ 4. On the basis of what has been

said, we can make the following conclusions.

1. The influence of a mass flow on the dimensionless natural frequencies of a plate is determined by two parameters μ and k .

Inasmuch as k depends on the mass ratio of the fluid and plate, i.e., for the given structure it is a constant factor, then all further conclusions will pertain only to the change of parameter μ .

2. The natural frequency of plates, which do not have free edges in a direction transverse to the flow, decreases with the increase of parameter μ .

With respect to plates having a free edge, it is necessary to note the following. Experiments in the study of free vibrations of pipelines allowed us to establish that the natural frequency of cantilever pipelines do not change (within the limits of accuracy of the experiment) upon increasing the speed of the fluid flowing from them, in spite of the predicted drop of natural frequency as calculated. Therefore, also for plates with a free edge it is not necessary to expect a noticeable change of natural frequency with the increase of the speed of flow. In any case this conclusion needs an experimental check.

Let us note also that in pipelines with both secured edges, the change of natural frequency found in the experiments, with the increase of the speed of flow, well agreed with the calculation data.

3. The mass flow renders a damping action on the vibration of plates with a free edge in a direction transverse to the flow. The magnitude of damping increases with the increase of parameter μ . Upon the achievement of a certain value μ , the damping increases so much that the free vibrations become impossible (the frequency becomes equal to zero). As shown by experiments with cantilever-secured pipelines, the transition from the periodic motion of a pipe to aperiodic (motion at zero frequency) with the increase of speed of flow occurs at a constant natural frequency of vibrations of the system. Evidently, an analogous phenomenon also occurs in plates.

If there is no free edge in the plate, there will be no damping of vibrations.

4. A constant mass flow may cause a loss in the stability of a plate. Using the terminology of V. V. Bolotin [4], this type of loss of stability for plates with a free edge pertains to the "vibratory" type. In the remaining plates there will occur a loss of stability of the "static" type. The boundaries of the regions of stability are established by means of the application of the Hurwitz method to a characteristic equation of the form (22).

In view of the limited volume of this article, this part of the work is not represented.

Literature

1. I. I. Gol'denblat. Dynamic stability of structures. Stroyizdat, 1948.
2. S. G. Lekhnitskiy. Anisotropic plates. State United Publishing Houses, Gostekhizdat, 1947.
3. R. D. Stepanov. Certain quadratures of fundamental beam functions. Engineering Collection, Vol. XXVI, 1958.
4. V. Z. Vlasov. Thin-walled spatial systems. Gosstroyizdat, 1958.
5. V. V. Bolotin. Nonconservative problems of the theory of elastic stability. Fizmatgiz, 1961.
6. R. H. Long. Experimental and Theoretical Study of Transverse Vibration of a Tube Containing Flowing Fluid. Journ. Appl. Mech., Vol. 22, No. 1, 1955.

Submitted
30 November 1963

EDGE EFFECT DURING THE JOINT ACTION OF AXIAL AND RADIAL
PRESSURE FOR ANISOTROPIC CIRCULAR CYLINDRICAL SHELLS

D. Ye. Lipovskiy

Definitions of Cyrillic Items

H = init = initial

r = r = radial

E = e = elastic

KP = crit = critical

B = up = upper

OPT = ort = orthotropic

MP = fr = frame

KP/CM = kg/cm

This article considers the case of axially symmetric loading of anisotropic circular cylindrical shells by transverse pressure and axial forces.

As it is known, the state of strain for such type of loading carries the character of an edge effect, since it quickly becomes momentless with the removal from the place of perturbation (sites of transverse ribs, intermittent change of cross section of shell, and others).

The edge effect in the case of the action of radial pressure is the subject of extensive literature (for instance, [1], [5], and others). In [2] the edge effect is examined by taking into account the axial forces, which, as will be shown, essentially affect the character of the state of strain. This work is a development of [2].

1. Differential Equation of the Problem and its Solution

Let us consider an anisotropic shell that is loaded uniformly on its perimeter by axial forces σ_x and transverse pressure p (Fig. 1). We shall consider extension for σ_x and internal pressure for p as positive.

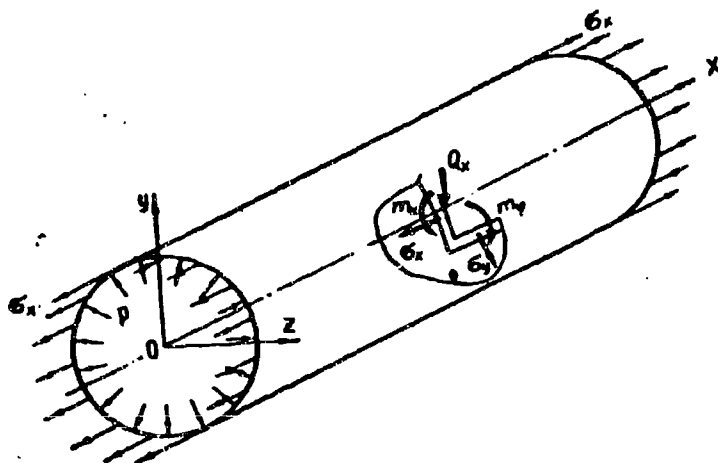


Fig. 1.

The character of anisotropy depends on the angle ψ between directions of fibers, from which the shell is made, and its generatrices. For multilayer shells with crossing layers, we assume the equality of angles ψ with respect to absolute value for different layers and symmetry with respect to the middle surface.

Angle ψ affects the magnitude of the constants a_{ij} in the generalized equations of elasticity

$$\begin{aligned} \epsilon_x &= a_{11}\sigma_x + a_{12}\sigma_y + a_{13}\tau_{xy}, \\ \epsilon_y &= a_{12}\sigma_x + a_{22}\sigma_y + a_{23}\tau_{xy}, \\ \gamma &= a_{13}\sigma_x + a_{23}\sigma_y + a_{33}\tau_{xy}. \end{aligned} \quad (1)$$

where ε_x and σ_x are the relative strain and normal stress in cross sections of the shell,

ε_φ and σ_φ are the same magnitudes for longitudinal sections,

γ and $\tau_{x\varphi}$ are the relative shear strain and tangential stress.

Inasmuch as under an axially symmetric load $\tau_{x\varphi} = 0$, we shall write out only the expression for a_{11} , a_{12} , and a_{22} [4]:

$$\begin{aligned} a_{11} &= \frac{\cos^2 \psi}{E_1} + \left(\frac{1}{G} - \frac{2\mu_1}{E_1} \right) \sin^2 \psi \cdot \cos^2 \psi + \frac{\sin^4 \psi}{E_2}, \\ a_{12} &= - \left[\frac{\mu_1}{E_1} - \frac{1}{4} \left(\frac{1+\mu_1}{E_1} + \frac{1+\mu_2}{E_2} - \frac{1}{G} \right) \sin^2 2\psi \right], \\ a_{22} &= \frac{\sin^4 \psi}{E_1} + \left(\frac{1}{G} - \frac{2\mu_1}{E_1} \right) \sin^2 \psi \cdot \cos^2 \psi + \frac{\cos^4 \psi}{E_2}. \end{aligned} \quad (2)$$

In equation (2) E_1 and μ_1 , E_2 and μ_2 correspondingly are the elastic moduli and Poisson ratios in the direction of the fibers and perpendicular to them, and G is the shear modulus.

A differential equation of the problem will be obtained by the variational method. We shall use this relationship:

$$\begin{aligned} \varepsilon_\varphi &= \frac{w_\varphi}{R}, \\ \varepsilon_\varphi &= \frac{1}{a_{22}} \left(\frac{w_\varphi}{R} - a_{12} \varepsilon_x \right), \\ \varepsilon_x &= \left(a_{11} - \frac{a_{12}^2}{a_{22}} \right) \varepsilon_\varphi + \frac{a_{12}}{a_{22}} \frac{w_\varphi}{R}. \end{aligned}$$

We shall write the expression for potential energy of a unit of length of a shell that has initial deflection $w_{init,0}$ and radial displacement w_0

$$\Gamma = \oint \left\{ \frac{1}{2} \left(\frac{D_{xx}}{2} + \varepsilon_\varphi \varepsilon_x \right) + \frac{D_{xx}}{2} - \varepsilon_x \left[\frac{1}{2} (w_{\alpha x} w_{\alpha x} - w_{\alpha 0} w_{\alpha 0}) + \right. \right. \quad (3)$$

$$\left. \left. + \varepsilon_x \right] - p w_0 \right\} R d\varphi,$$

where $x_x = -w_0''$ is the change of curvature of the shell in the direction of axis x ,

$D_x = \frac{C_{118}^3}{12}$ is the cylindrical rigidity,

$$\begin{aligned} c_{11} &= \frac{1}{1-\mu_1\mu_2} \{ E_1 \cos^4 \psi + E_2 \sin^4 \psi + 2[E_1\mu_2 + 2G(1-\mu_1\mu_2)] \sin^2 \psi \cdot \cos^2 \psi \}, \\ w_{\alpha x} &= w_\alpha + w_{\alpha 0}. \end{aligned}$$

In (3), the first three terms represent the energy of internal stresses, and the second two, the potential of the external load.

In the brackets, the first term expresses the work of axial forces $\sigma_x \delta$ on the change of curvature w_0'' in the presence of the initial deflection.

Placing the expressions of the magnitudes in (3) through w_0 , and applying an Euler equation of a variational problem, we will obtain:

$$w_0^{IV} - \frac{\sigma_x \delta}{D_x} w_0'' + \frac{\delta}{a_{22} R^2 D_x} w_0 = \frac{1}{D_x} \left[p + \frac{a_{12} \delta}{a_{22} R} + \frac{\sigma_x \delta}{2} w_{n,0}'' \right]. \quad (4)$$

The roots of the characteristic equation for (4) are generally complex

$$\lambda = \pm (\alpha \pm \beta i),$$

where

$$\alpha = \sqrt{\frac{1}{2} \left(\sqrt{\frac{\delta}{a_{22} R^2 D_x}} + \frac{\sigma_x \delta}{2 D_x} \right)}, \quad (5)$$

$$\beta = \sqrt{\frac{1}{2} \left(\sqrt{\frac{\delta}{a_{22} R^2 D_x}} - \frac{\sigma_x \delta}{2 D_x} \right)}.$$

The solution of equation (4) can be presented in the form of

$$w_0 = w_0^r + w_0^e,$$

where w_0^r is the radial displacement for shell which does not have deflection,

w_0^e is the elastic radial displacement caused by the initial deflection.

When $p = \text{const}$ or with the linear dependence of p on x , we have:

$$w_0^r = c_1 \operatorname{sh} \alpha x \cdot \cos \beta x + c_2 \operatorname{ch} \alpha x \cdot \cos \beta x + c_3 \operatorname{ch} \alpha x \cdot \sin \beta x + \\ + c_4 \operatorname{sh} \alpha x \cdot \sin \beta x + \frac{R^2 a_{22}}{\delta} \left(p + \frac{a_{12} \sigma_x \delta}{a_{22} R} \right). \quad (6)$$

In particular, if

$$w_{n,0} = \sum_{m=1}^{\infty} f_{n,m} \sin \frac{m\pi x}{L},$$

where $f_{\text{init},m}$ is the peak value of the initial deflection for the m -th harmonic,

under boundary conditions

$$w_0 \Big|_{x=0} = 0, \quad w_0' \Big|_{x=L} = 0,$$

then

$$\sigma_0^2 = - \sum_{n=1}^{\infty} \frac{\bar{\sigma}_x}{1 + \bar{\sigma}_x} f_{n,m} \sin \frac{m\pi}{L} x, \quad (7)$$

where

$$\begin{aligned} \bar{\sigma}_x &= \frac{\sigma_x}{\sigma_{xp}}, \\ \sigma_{xp} &= \frac{D_x}{8} \left(\frac{m\pi}{L} \right)^2 + \frac{1}{a_{22} R^2} \left(\frac{L}{m\pi} \right)^2. \end{aligned} \quad (8)$$

The minimum value of (8) is the upper critical stress during axial compression:

$$\sigma_{xp}^2 = \sqrt{\frac{4D_x}{a_{22} R^2}} = \sqrt{\frac{c_{11}}{3a_{22}}} \frac{8}{R}. \quad (9)$$

It takes place when

$$\bar{m}^2 = \left(\frac{m\pi R}{L} \right)^2 = \sqrt{\frac{4R^2}{a_{22} D_x}} = \frac{3.46}{\sqrt{a_{22} c_{11}}} \frac{R}{8}. \quad (10)$$

In the particular case of an orthotropic shell, when $\psi = 0$, and

$$a_{22} = \frac{1}{E_y} \text{ and } D_x = \frac{E_x R^3}{12(1 - \nu_x \nu_y)},$$

instead of (9) and (10), we obtain

$$\sigma_{xp}^2 = \sqrt{\frac{E_x E_y}{3(1 - \nu_x \nu_y)}} \frac{8}{R} \quad (9')$$

and

$$\bar{m}^2 = \sqrt{12(1 - \nu_x \nu_y)} \frac{E_y}{E_x} \left(\frac{R}{8} \right)^2, \quad (10')$$

where the x subscripts pertain to cross sections, and the y subscripts refer to longitudinal sections.

Formula (9) can be reduced to the form of

$$\sigma_{xp}^2 = \sigma_{xp \text{ opt}}^2 F(\varphi),$$

where

$$\begin{aligned} F(\varphi) &= \sqrt{\frac{\cos^4 \varphi + \eta \sin^4 \varphi + 2[\mu_2 + 2\zeta\eta(1 - \nu_1 \nu_2)] \sin^2 \varphi \cdot \cos^2 \varphi}{\cos^4 \varphi + \eta \sin^4 \varphi + \left(\frac{1}{\zeta} - 2\nu_1 \nu_2 \right) \sin^2 \varphi \cdot \cos^2 \varphi}}, \\ \eta &= \frac{E_2}{E_1}, \\ \zeta &= \frac{G}{E_2}. \end{aligned}$$

Figure 2 shows the construction of a graph of $F(\psi)$ for certain values of η and ξ , from which it is clear that in a wide range of values of elasticity parameters (E_2 , E_1 , G), the values of $F(\psi)$ are greater than one when $\psi \neq 0$ and $\psi \neq 90^\circ$. Thus, the critical stresses of the axially symmetric form of stability loss in anisotropic shells are always lower than in orthotropic shells. They approximate $\sigma_{crit\ orth}^{up}$ with the growth of the ratios of elastic moduli η and ξ .

After obtaining the dependence of the elastic radial displacement on x , it is possible by known relationships to find the stresses in the transverse and longitudinal sections.

2. Certain Solutions for Edge Effect near Elastic and Rigid Frames

The solutions of (4) are simplified for strain that is symmetric with respect to the middle of a shell and for shells of comparatively great length.

In the first case, after selecting the origin of coordinates in the plane of symmetry of the shell, the solution can be written:

$$w_0 = c_1 \operatorname{sh} \alpha x \sin \beta x + c_2 \operatorname{ch} \alpha x \cos \beta x + w_p \quad (11)$$

In the second case, considering the shell as being semi-infinite, we will obtain

$$w_0 = e^{-\alpha x} (c_1 \sin \beta x + c_2 \cos \beta x) + w_p \quad (12)$$

where w_p is the particular solution of equation (4).

The constants of integration c_1 and c_2 are determined from the boundary conditions. In the case of placing elastic frames, one of the conditions is the equality of radial displacements of the shell and frame

$$w_0 = w_{fn} \quad (13)$$

where $w_{fr} = \frac{R^2}{Ef_{fr}} Q_{fr}$ is the radial displacement of the frame,

$Q_{fr} = \frac{dm_x}{dx} + \sigma_x \delta w'_0$ is the transverse force in the region of the frame (its radial load),

f_{fr} is the area of cross section of the frame.

Condition (13), after substitution of w_{fr} , obtains the form of

$$w_0 + \bar{w}_{mn} \left(w_0' - \frac{\sigma_x \delta}{D_s} w_0' \right) = 0, \quad (13')$$

where

$$\bar{w}_{mn} = \frac{D_s R^2}{(Ef)_{mn}}.$$

The expressions for the constants of integration, which correspond to solutions (11) and (12) when $w_r = \text{const}$, are given in Tables 1 and 2, where we designate:

$$\begin{aligned} S_{11} L/2 &= \text{sh } \alpha L/2 \cdot \sin \beta L/2, & S_{12} L/2 &= \text{sh } \alpha L/2 \cdot \cos \beta L/2, \\ S_{21} L/2 &= \text{ch } \alpha L/2 \cdot \cos \beta L/2, & S_{22} L/2 &= \text{ch } \alpha L/2 \cdot \sin \beta L/2. \end{aligned}$$

The case of support on rigid frames corresponds to

$$f_{mn} \rightarrow \infty \text{ or } \bar{w}_{mn} = 0.$$

As an example of edge effect, we shall consider the determination of additional force factors near an elastic frame for a sufficiently long closed shell that is loaded by manifold pressure p . After mentally dismembering the shell (Fig. 3), it is possible, by disregarding the torsional rigidity of the frame, to obtain, from the conditions of compatibility of strains,

$$\begin{aligned} w_{0,1}|_{x=0} - w_{0,2}|_{x=0} - w_{mn} &= \frac{Q_1 - Q_2}{Ef_{mn}} R^2, \\ w_{0,1}'|_{x=0} &= -w_{0,2}'|_{x=0} \end{aligned}$$

expressions for linear bending moment m_x and transverse forces Q_1 and Q_2 in a section on the frame:

$$m_x = -0.3pR^2 \frac{\sqrt{\frac{c_{11}}{c_{22}} \left(c_{22} + \frac{c_{12}^2}{2} \right)}}{1 + 1.19 \frac{\alpha R^2}{(Ef)_{mn}} \sqrt{\frac{c_{11}}{c_{22}}}}, \quad (14)$$

$$Q_1 = -Q_2 = -2am. \quad (15)$$

Table 1. Expressions of Integration Constants for Solution [11]

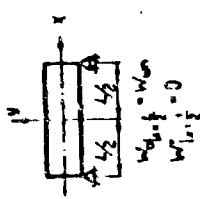
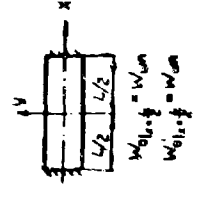
Character of support and boundary conditions	C_1	C_2
 <p> $w_{0,L/2} = w_{0,L}$ $w'_{0,L/2} = 0$ </p>	$C_1 = \frac{w_4}{\varphi_1(\alpha, \beta)} \left[(\alpha^2 - \beta^2) S_{22} \frac{L}{2} - 2\alpha\beta S_{11} \frac{L}{2} \right],$ <p>where</p> $\varphi_1(\alpha, \beta) = 2\alpha\beta (\operatorname{ch} \alpha L + \cos \beta L) - w_{\max} (\alpha^2 + \beta^2) \left[(\alpha^2 + \beta^2) (\alpha \sin \beta L + \beta \operatorname{sh} \alpha L) + \frac{\alpha^2 \beta}{D_x} (\beta \operatorname{sh} \alpha L - \alpha \sin \beta L) \right].$	$C_2 = -\frac{w_4}{\varphi_1(\alpha, \beta)} \left[(\alpha^2 - \beta^2) S_{11} \frac{L}{2} - 2\alpha\beta S_{22} \frac{L}{2} \right].$
 <p> $w_{0,L/2} = w_{0,L}$ $w'_{0,L/2} = w'_{0,L}$ </p>	$C_1 = \frac{w_4}{\varphi_2(\alpha, \beta)} \left(\alpha S_{12} \frac{L}{2} - \beta S_{21} \frac{L}{2} \right),$ <p>where</p> $\varphi_2(\alpha, \beta) = \frac{1}{2} (\alpha \sin \beta L + \beta \operatorname{sh} \alpha L) - w_{\max} \alpha^2 (\alpha^2 + \beta^2) (\operatorname{ch} \alpha L - \cos \beta L).$	$C_2 = -\frac{w_4}{\varphi_2(\alpha, \beta)} \left(\alpha S_{21} \frac{L}{2} + \beta S_{12} \frac{L}{2} \right).$

Table 1 continued

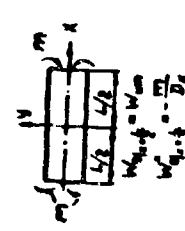
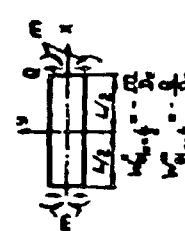
Character of support and boundary conditions	C_1	C_2
III 	$C_1 = F_m^{(C)} + F_{w_1}^{(C)},$ <p>where</p> $F_m^{(C)} = \frac{1}{D_2 \varphi_2(\alpha, \beta)} \left\{ S_m \frac{L}{2} + \bar{w}_{mn} \left[\alpha (\alpha^2 - 3\beta^2) S_m \frac{L}{2} - \beta (3\alpha^2 - \beta^2) S_m \frac{L}{2} - \frac{\alpha^2}{D_2} \left(\alpha S_m \frac{L}{2} - \beta S_m \frac{L}{2} \right) \right] \right\},$ $F_{w_1}^{(C)} = - \frac{w_1}{\varphi_2(\alpha, \beta)} \left[(\alpha^2 - \beta^2) S_m \frac{L}{2} - 2\alpha\beta S_m \frac{L}{2} \right],$ $\varphi_2(\alpha, \beta) = -\alpha\beta (\operatorname{ch} \alpha L + \cos \beta L) + \frac{\bar{w}_{mn}}{2} (\alpha^2 + \beta^2) \left[\alpha \sin \beta L + \beta \operatorname{sh} \alpha L + \frac{\alpha^2 \beta}{D_2 (\alpha^2 + \beta^2)} (3 \operatorname{sh} \alpha L - \alpha \sin \beta L) \right].$	$C_2 = F_m^{(C)} + F_{w_1}^{(C)},$ <p>where</p> $F_m^{(C)} = \frac{1}{D_2 \varphi_2(\alpha, \beta)} \left\{ S_m \frac{L}{2} + \bar{w}_{mn} \left[\alpha (\alpha^2 - 3\beta^2) S_m \frac{L}{2} + \beta (3\alpha^2 - \beta^2) S_m \frac{L}{2} - \frac{\alpha^2}{D_2} \left(\alpha S_m \frac{L}{2} - \beta S_m \frac{L}{2} \right) \right] \right\},$ $F_{w_1}^{(C)} = \frac{w_1}{\varphi_2(\alpha, \beta)} \left[(\alpha^2 - \beta^2) S_m \frac{L}{2} - 2\alpha\beta S_m \frac{L}{2} \right].$
IV 	$C_1 = F_m^{(C)} + F_Q^{(C)} Q,$ <p>where</p> $F_m^{(C)} = - \frac{1}{D_2 \varphi_2(\alpha, \beta)} \left[\alpha (\alpha^2 - 3\beta^2) S_m \frac{L}{2} - \beta (3\alpha^2 - \beta^2) S_m \frac{L}{2} \right],$ $F_Q^{(C)} = \frac{1}{D_2 \varphi_2(\alpha, \beta)} \left[(\alpha^2 - \beta^2) S_m \frac{L}{2} - 2\alpha\beta S_m \frac{L}{2} \right],$ $\varphi_2(\alpha, \beta) = \beta (\alpha^2 + \beta^2) \left[S_m \frac{L}{2} \left(\frac{\alpha}{\beta} S_{12} \frac{L}{2} - S_m \frac{L}{2} \right) - S_m \frac{L}{2} \right].$	$C_2 = F_m^{(C)} + F_Q^{(C)} Q,$ <p>where</p> $F_m^{(C)} = \frac{1}{D_2 \varphi_2(\alpha, \beta)} \left[\alpha (\alpha^2 - 3\beta^2) S_m \frac{L}{2} + 2\alpha\beta S_m \frac{L}{2} \right],$ $F_Q^{(C)} = - \frac{1}{D_2 \varphi_2(\alpha, \beta)} \left[(\alpha^2 - \beta^2) S_m \frac{L}{2} + 2\alpha\beta S_m \frac{L}{2} \right].$

Table 2. Expressions of Integration Constants for Solution [12]

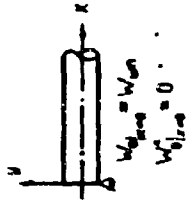
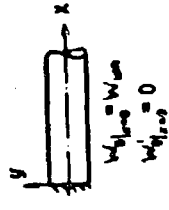
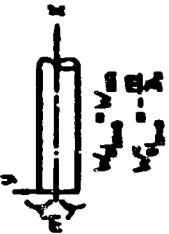

Character of support and boundary conditions	C_1	C_2
 <p> $w_{y,l/2,0} = w_{y,l/2,l}$ $w'_{y,l/2,0} = 0$ </p>	$C_1 = - \frac{(\alpha^2 - \beta^2) w_0}{2\alpha\beta + \beta(\alpha^2 + \beta^2) \frac{l}{2} w_{max}} \left[1 + \frac{\alpha^2 \beta^2}{D_x(\alpha^2 + \beta^2)} \right]$	$C_2 = - \frac{w_0}{1 + \frac{(\alpha^2 + \beta^2)}{2\alpha} \frac{l}{2} w_{max}} \left[1 + \frac{\alpha^2 \beta^2}{D_x(\alpha^2 + \beta^2)} \right]$
 <p> $w_{y,0,0} = w_{y,l,0}$ $w'_{y,0,0} = 0$ </p>	$C_1 = - \frac{w_0}{\beta/a + 2\alpha \frac{l}{2} (\alpha^2 + \beta^2)}$	$C_2 = - \frac{w_0}{1 + 2\alpha \frac{l}{2} (\alpha^2 + \beta^2)}$

Table 2 continued

Character of sup- port and boundary conditions	C_1	C_2
 <p>III</p>	<p>where</p> $C_1 = f_m^{(C)} + f_{m_0}^{(C)},$ $f_m^{(C)} = \frac{1}{2\beta D_x} \times$ $\left[1 - \frac{\bar{w}_{mm}}{2\alpha + \bar{w}_{mm}} \frac{(a^2 - \beta^2) \left(a^2 - \beta^2 \right)}{\left[1 + \frac{a^2 \beta^2}{D_x (a^2 + \beta^2)} \right]} \right],$ $f_{m_0}^{(C)} = - \frac{a^2 - \beta^2}{2\beta} \cdot \frac{v_{m_0}}{1 + \frac{\bar{w}_{mm}}{2\alpha} \frac{(a^2 - \beta^2)}{D_x} \left[1 + \frac{a^2 \beta^2}{D_x (a^2 + \beta^2)} \right]}.$	$C_2 = f_m^{(C)} + f_{m_0}^{(C)},$ $f_m^{(C)} = - \frac{\bar{w}_{mm}}{D_x} \frac{2a^2 - \beta^2 - \frac{a^2 \beta^2}{D_x}}{2\alpha + \bar{w}_{mm} (a^2 + \beta^2) \left[1 + \frac{a^2 \beta^2}{D_x (a^2 + \beta^2)} \right]},$ $f_{m_0}^{(C)} = - \frac{w_{m_0}}{1 + \frac{\bar{w}_{mm}}{2\alpha} \frac{(a^2 + \beta^2)}{D_x} \left[1 + \frac{a^2 \beta^2}{D_x (a^2 + \beta^2)} \right]}.$
 <p>IV</p>	<p>where</p> $C_1 = f_m^{(C)} + f_{m_0}^{(C)} Q,$ $f_m^{(C)} = - \frac{1}{D_x} \frac{a(a^2 - 3\beta^2)}{\beta(a^2 + \beta^2)},$ $f_{m_0}^{(C)} = - \frac{1}{D_x} \frac{a^3 - \beta^3}{\beta(a^2 + \beta^2)}.$	<p>where</p> $C_2 = f_m^{(C)} + f_{m_0}^{(C)} Q,$ $f_m^{(C)} = - \frac{1}{D_x} \frac{2a^2 - \beta^2}{(a^2 + \beta^2)},$ $f_{m_0}^{(C)} = - \frac{1}{D_x} \frac{2a}{(a^2 + \beta^2)}.$

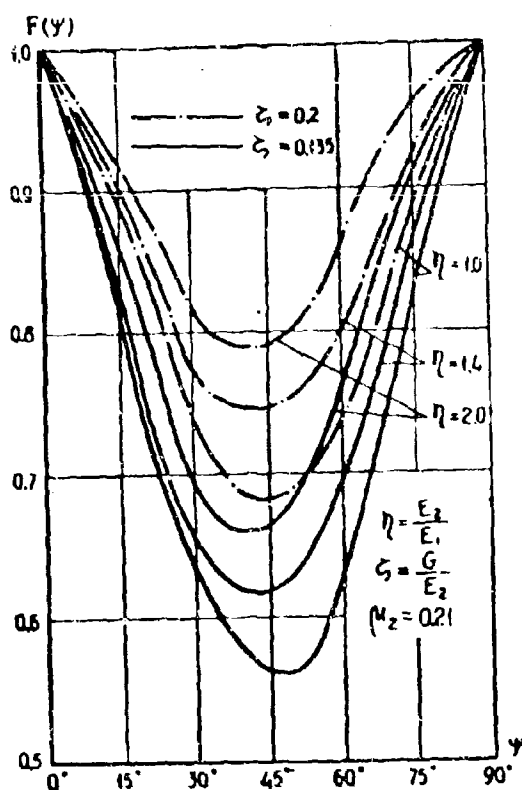


Fig. 2.

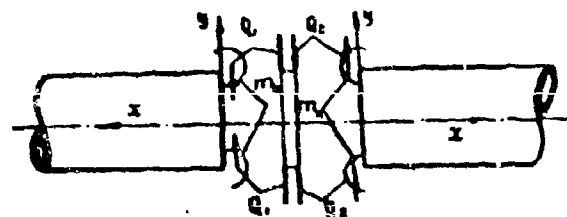


Fig. 3.

With them, it is easy to express the total stresses in the extreme fibers of the shell

$$\sigma_{xz} = \frac{PR}{2\delta} + \frac{6m_x}{\delta^2}$$

and

$$\sigma_{yz} = \frac{1}{\delta_{22}} \left(\frac{w_0}{R} - a_{12} \sigma_x \right) + \frac{D_x}{D_{xy}} \frac{6m_x}{\delta^2},$$

where

$$c_{12} = \frac{E_1}{1 - \mu_1 \mu_2} \{ \mu_2 + [1 +$$

$$+ \eta - 2(\mu_2 + 2\eta^2(1 - \mu_1 \mu_2))] \sin^2 \psi \cos^2 \psi.$$

Considering the shell as being semi-infinite with origin of coordinates on the frame, it is possible to use solution (12).

Here

$$w_r = R \left(a_{22} \frac{PR}{\delta} + a_{12} \sigma_x \right),$$

$$\sigma_x = \frac{PR}{2\delta}.$$

When $x \approx 0$

$$w_0 = c_2 + \frac{PR^2}{\delta} \left(a_{22} + \frac{a_{12}}{2} \right),$$

where, according to Table 2

$$c_2 = - \frac{1}{D_x (\alpha^2 + \beta^2)} [(3\alpha^2 - \beta^2)m + 2\alpha Q]$$

or taking into account (15)

$$c_2 = \frac{m}{D_x (\alpha^2 + \beta^2)}.$$

Figure 4 shows the construction of graphs of relative stresses

$$\bar{\sigma}_{xz} = \frac{\sigma_{xz}}{PR/2\delta}$$

and

$$\bar{\sigma}_{x\varphi} = \frac{\sigma_{x\varphi}}{PR/\delta}$$

At two values of pressure: $p = 1.962 \cdot 10^5 \text{ N/m}^2$ and

$$p = -1.962 \cdot 10^5 \text{ N/m}^2.$$

In the calculation we took:

$$E_1 = 1.81 \cdot 10^{10} \text{ N/m}^2, E_{\text{lin}} = 2.55 \cdot 10^{10} \text{ N/m}^2, \\ \eta = \frac{E_2}{E_1} = 1.41, \zeta = \frac{G}{E_2} = 0.135, \mu_1 = 0.15, \mu_2 = 0.21.$$

The geometric dimensions of the shell are shown in Fig. 4.

As can be seen from the graph, the edge effect essentially changes the state of strain, as compared to the momentless effect.

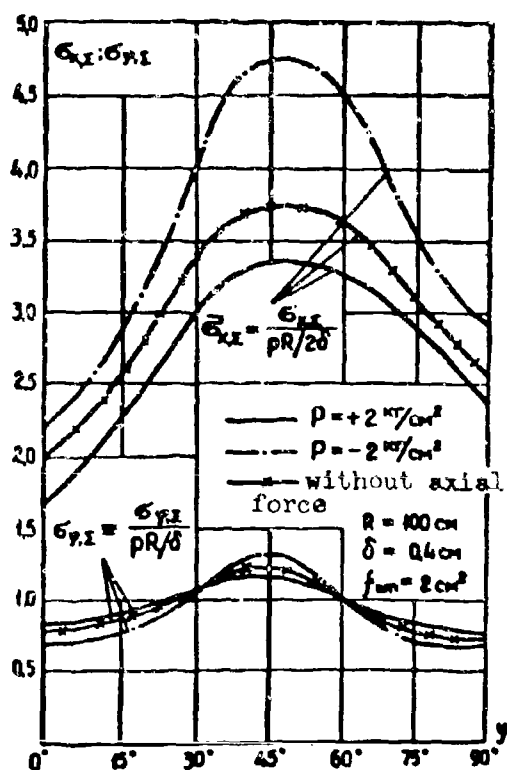


Fig. 4.

This change is especially significant during the action of external pressure for angles ψ in the range of $20-70^\circ$. At these angles, the lowering of annular stresses, due to the decrease of radial displacements w_0 in the frame, is overlapped by secondary stresses caused by the moment

$$m_\varphi = \frac{D_x}{D_{x\varphi}} m_x.$$

For the purpose of comparison, Fig. 4 shows graphs of $\bar{\sigma}_{x\Sigma}$ and $\bar{\sigma}_{\varphi\Sigma}$ in the absence of axial force,

i.e., when there is only radial pressure. From them it follows that an axial force, especially during compression, introduces an essential change into the state of strain of cross sections of a shell and does not have a great effect on the annular stresses.

The conducted investigation shows that from the point of view of the edge effect and the axially symmetric form of stability loss, orthotropic shells are more appropriate, where the directions of the principal curvatures coincide with the principal axes of elasticity.

3. Damping of Edge Effect

Reference [5] gives the wavelength

$$l = 4.9\sqrt{R\delta}$$

for the case of axially symmetric transverse loading of a shell and makes the conclusion that for sufficiently thin shells the state of strain, caused by edge effect, quickly disappears with the removal from places of perturbation. Analogous conclusions are made in [1] on the basis of the analysis of roots of characteristic equations.

However, in the case of joint action of transverse pressure and axial forces, the above-indicated length l does not characterize the propagation distance of the edge effect. Here, both the wavelength along the generatrices, and also the degree of damping, essentially depend on the magnitudes and directions of the action of axial forces and the character of anisotropy of the shell.

Actually, in accordance with (5), the wavelength is

$$l_0 = \frac{2\pi}{\beta} = \frac{2\pi}{\sqrt{\frac{1}{2}\left(\sqrt{\frac{\delta}{a_x R^3 D_x}} - \frac{\sigma_x \delta}{2D_x}\right)}} = \frac{2\pi}{\sqrt{\frac{1}{2}\sqrt{\frac{\delta}{a_x R^3 D_x}}\left(1 - \frac{\sigma_x \delta}{\sigma_{xp} \delta}\right)}} \quad (16)$$

For orthotropic shells —

$$l_0 = \frac{2\pi}{\sqrt{\frac{1}{\delta R} \sqrt{3(1 - \mu_x \mu_y)} \frac{E_y}{E_x} \left(1 - \frac{\sigma_x \delta}{\sigma_{xp} \delta}\right)}} \quad (17)$$

In a particular case of an isotropic shell, from (16) and (17) it follows for $\mu = 0.3$:

$$l_0 = 4.9 \sqrt{\frac{R^3}{1 - \frac{\sigma_x}{\sigma_{cr}^b}}} \quad (18)$$

As can be seen from the given formulas, the wavelength is increased with the growth of positive values of σ_x and when $\sigma_x \rightarrow \sigma_{crit}^b$ it envelopes the entire shell.

Damping of perturbations, as may be seen from (12), depends on coefficient α . For instance, length $l_{1.0}$, where w_0 constitutes 0.01 of the value at the edge, can be determined from the condition

$$l^{-\alpha} = 0.01,$$

from which we obtain:

for anisotropic shells —

$$l_{1.0} = \frac{4.6}{\sqrt{\frac{1}{2} \sqrt{\frac{8}{\alpha R^3 D_x}} \left(1 + \frac{\sigma_x}{\sigma_{cr}^b}\right)}} \quad (19)$$

for orthotropic —

$$l_{1.0} = \frac{4.6}{\sqrt{\frac{1}{3R} \sqrt{3(1 - \mu_x \mu_y)} \frac{E_y}{E_x} \left(1 + \frac{\sigma_x}{\sigma_{cr}^b}\right)}} \quad (20)$$

In a particular case of isotropic shells when $\mu = 0.3$,

$$l_{1.0} = 3.6 \sqrt{\frac{R^3}{1 + \frac{\sigma_x}{\sigma_{cr}^b}}} \quad (21)$$

Length $l_{1.0}$ grows with the increase of negative (i.e., compressing) values of σ_x and when $\sigma_x \rightarrow \sigma_{crit}^b$ the perturbation from the edge effect practically does not attenuate.

Thus, during the action of significant tensile forces, strains from edge effect are obtained with a great wavelength, but with quickly attenuating amplitude. And, conversely, in the case of essential compressing axial loads along the shell, there are obtained

short, but slowly attenuating waves of strain. The mutual merging of frames during the calculation of edge effect can be disregarded, if the distance between them is greater than $2l_{1,0}$. In this case the edge effect at every frame can be considered as for a semi-infinite shell.

Literature

1. A. L. Gol'denveyzer. Theory of thin elastic shells. State Press for Technical and Theoretical Literature, 1953.
2. S. N. Kan and D. Ye. Lipovskiy. Longitudinal-transverse bending of reinforced circular cylindrical shells. IVUZ, "Aeronautical Engineering," No. 1, 1963.
3. S. N. Kan and P. Ye. Lipovskiy. Stability of reinforced circular cylindrical shells during the action of axial compression and transverse pressure. IVUZ, "Aeronautical Engineering," No. 4, 1962.
4. S. G. Lekhnitskiy. Anisotropic plates. State Technical Press, 1957.
5. S. P. Timoshenko. Plates and shells. State Technical Press, 1948.

Submitted
30 November 1963

APPLICATION OF THE METHOD OF ASYMPTOTIC INTEGRATION TO PROBLEMS OF VIBRATIONS OF SHELLS OF REVOLUTION WHICH ARE SIMILAR IN FORM TO SPHERICAL SHELLS

R. L. Malkina

The solution of certain problems of free vibrations of shells of revolution of positive curvature is expounded; the asymptotic method of integration of differential equations, developed by A. L. Gol'denveyzer [1], [2], [3], is used.

§ 1. Equations of Free Vibrations of an Arbitrary Shell with a Large Index of Variability

Experience shows that the free vibrations of shells correspond to the multiwave character of strains. Due to this, the equation of frequencies and the approximate form of vibrations can be found by means of integration of the equations offered by V. Z. Vlasov [4] for sloping shells:

$$\Delta \Delta \varphi - E h \Delta_k w = 0, \quad \Delta_k \varphi + D \Delta w + \frac{\gamma h}{E} \frac{\partial^2 w}{\partial t^2} = 0,$$

$$\Delta = \frac{1}{AB} \left[\frac{\partial}{\partial \alpha} \left(\frac{B}{A} \frac{\partial}{\partial \alpha} \right) + \frac{\partial}{\partial \beta} \left(\frac{A}{B} \frac{\partial}{\partial \beta} \right) \right], \quad (1.1)$$

$$\Delta_k = \frac{1}{AB} \left[\frac{\partial}{\partial \alpha} \left(\frac{B}{A} \frac{1}{R_2} \frac{\partial}{\partial \alpha} \right) + \frac{\partial}{\partial \beta} \left(\frac{A}{B} \frac{1}{R_1} \frac{\partial}{\partial \beta} \right) \right].$$

Here w is the radial displacement,

φ is the function of stresses,

h is the thickness of the shell,

D is the cylindrical rigidity,

γ/g is the density of the material,

α and β are the curvilinear coordinates of the middle surface,

A and B are the Lamé parameters,

R_1 and R_2 are the main radii of curvature.

The equations (1.1) can, under certain circumstances, be obtained from the general theory of shells without the assumption that the shell is sloping. In [1], [2], and [3] it is shown that with the help of equations (1.1) it is possible to approximately construct the state of strain of shells when their variability is sufficiently great. Therefore, following A. L. Gol'denveyzer, we shall subsequently call (1.1) equations with a large index of variability.

In the case of an arbitrary shell of revolution, referred to geographic coordinates (Fig. 1), in equations (1.1) it is necessary to put $A = R_1$, $B = R_2 \sin \alpha$. They they will take on the form:

$$\begin{aligned} \Delta \Delta \varphi - Eh \Delta_s w &= 0, \quad \Delta_s \varphi + D \Delta \Delta w + \frac{\gamma h}{g} \frac{\partial^2 w}{\partial \alpha^2} = 0, \\ \Delta &= \frac{1}{R_1 R_2} \sin^{-1} \alpha \left[\frac{\partial}{\partial \alpha} \left(\frac{R_2 \sin \alpha}{R_1} \frac{\partial}{\partial \alpha} \right) + \frac{\partial}{\partial \beta} \left(\frac{R_1}{R_2 \sin \alpha} \frac{\partial}{\partial \beta} \right) \right], \\ \Delta_s &= \frac{1}{R_1 R_2 \sin \alpha} \left[\frac{\partial}{\partial \alpha} \left(\frac{\sin \alpha}{R_1} \frac{\partial}{\partial \alpha} \right) + \frac{\partial}{\partial \beta} \left(\frac{1}{R_2 \sin \alpha} \frac{\partial}{\partial \beta} \right) \right]. \end{aligned} \quad (1.2)$$

Equations (1.2) are correct when the index of variability is positive. If $t = \frac{1}{2}$, then they are correct with an accuracy up to terms of the order h^* , as compared to unity. h^* designates the small parameter:

$$h^* = \frac{h}{2V3(1-\nu)R_1}.$$

The points that are close to $\alpha = 0$, where the equations have peculiarities, will be excluded from consideration.

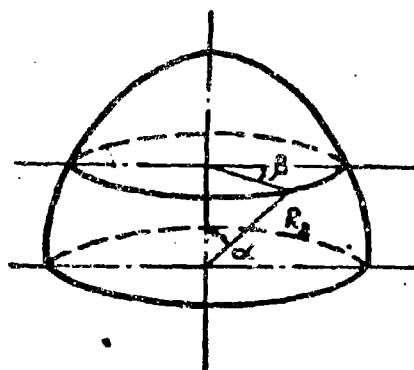


Fig. 1.

§ 2. Vibrations of a Spherical Shell

We shall present the function of stresses φ and radial displacement w in the form:

$$\varphi(\alpha, \beta, t) = \varphi(\alpha, \beta) \cos \omega t, \quad w(\alpha, \beta, t) = w(\alpha, \beta) \cos \omega t. \quad (2.1)$$

Here ω is the frequency of natural vibrations.

Considering $R_1 = R_2 = R$ in (1.2), and excluding function φ , we will obtain the equation of vibrations of a spherical shell:

$$D \Delta \Delta \Delta w + \left(\frac{Eh}{R^3} - p^2 \right) \Delta w = 0,$$

where

$$p^2 = \frac{\gamma \omega^2 h}{g},$$

$$\Delta = \frac{1}{R^2 \sin \alpha} \left[\frac{\partial}{\partial \alpha} \left(\sin \alpha \frac{\partial}{\partial \alpha} \right) + \frac{1}{\sin \alpha} \left(\frac{\partial^2}{\partial \beta^2} \right) \right]. \quad (2.2)$$

Let us consider a section of a spherical shell, which is limited by parallels $\alpha = \alpha_1$ and $\alpha = \alpha_2$. In this case, all displacements will be functions of angle β of period 2π . The solution of (2.2) will be found in the form of

$$w(\alpha, \beta) = \sum_{m=0,1,2}^{\infty} w_m(\alpha) \cos m\beta. \quad (2.3)$$

Placing (2.3) in (2.2), we will obtain:

$$\Delta\Delta w_m(\alpha) - b^4 w_m(\alpha) = 0, \left(\Delta = \frac{d^2}{d\alpha^2} + \operatorname{ctg} \alpha \frac{d}{d\alpha} - \frac{m^2}{\sin^2 \alpha} \right), \quad (2.4)$$

$$(m = 0, 1, 2, \dots),$$

$$b^4 = h^2 R^2 \left(\frac{Y^2 R^2}{gE} - 1 \right), \quad h^2 = \frac{h^2}{12(1-\nu^2)R^2}. \quad (2.5)$$

Here and subsequently we shall consider $b^2 \gg 1$, i.e., we shall exclude from consideration the vibrations whose frequency exactly or approximately satisfies this equation:

$$\frac{Y^2 R^2}{gE} - 1 = 0. \quad (2.6)$$

We shall designate $\Delta w = w^*$. Then (2.4) will be reduced to the following:

$$\Delta\Delta w_m^*(\alpha) - b^4 w_m^*(\alpha) = 0, \quad \left(\Delta = \frac{d^2}{d\alpha^2} + \operatorname{ctg} \alpha \frac{d}{d\alpha} - \frac{m^2}{\sin^2 \alpha} \right). \quad (2.7)$$

For the given value of m equation (2.7) is broken up into two, each which can be presented in the form of

$$w^{*''} + w^* \operatorname{ctg} \alpha - \frac{m^2}{\sin^2 \alpha} w^* + (n+1) n w^* = 0. \quad (2.8)$$

In order to obtain the first or second equation, it is necessary to put accordingly $n = n_1$ or $n = n_2$:

$$n_1(n_1+1) = b^2, \quad n_2(n_2+1) = -b^2. \quad (2.9)$$

Parameter b^2 is great as compared to unity; therefore, with the same degree of accuracy with which the calculations are conducted, it is possible to take:

$$n_1 + \frac{1}{2} = b, \quad n_2 + \frac{1}{2} = ib. \quad (2.10)$$

The general solution of (2.8) is expressed by this formula:

$$w_m^* = c_{1m} P_n^m(\cos \alpha) + c_{2m} Q_n^m(\cos \alpha). \quad (2.11)$$

Here $P_n^m(\cos \alpha)$, $Q_n^m(\cos \alpha)$ are generalized associated Legendre functions of the first and second kind [5],

c_{1m} and c_{2m} are integration constants.

Consequently, the general solution of equation (2.6) for a certain specifically given m has the form of

$$w_m^*(\alpha) = c_{1m} P_{n1}^m(\cos \alpha) + c_{2m} Q_{n1}^m(\cos \alpha) + c_{3m} P_{n2}^m(\cos \alpha) + c_{4m} Q_{n2}^m(\cos \alpha). \quad (2.12)$$

Let us consider vibrations of a shell, in which there will form more waves along the meridian than along the parallel, i.e.,

$$n \gg m.$$

As it is known [5], functions P_n^m , Q_n^m can be expanded in series with respect to parameters m and n . Under the conditions

$$n \gg m, \quad \alpha < \pi < (\pi - \alpha), \quad 0 < \epsilon < \frac{\pi}{6}, \quad (2.13)$$

retaining the main terms in these series, we will obtain asymptotic formulas:

$$P_{n1}^m(\cos \alpha) = (b - 0.5)^m \left(\frac{2}{\pi(b - 0.5) \sin \alpha} \right)^{\frac{1}{2}} \sin \left(\frac{\pi}{4} + b\alpha + \frac{m\pi}{2} \right), \quad (2.14)$$

$$Q_{n1}^m(\cos \alpha) = (b - 0.5)^m \left(\frac{\pi}{2(b - 0.5) \sin \alpha} \right)^{\frac{1}{2}} \cos \left(\frac{\pi}{4} + b\alpha + \frac{m\pi}{2} \right),$$

$$P_{n2}^m(\cos \alpha) = (0.5 - ib)^m \left(\frac{2}{\pi(ib - 0.5) \sin \alpha} \right)^{\frac{1}{2}} \sin \left(\frac{\pi}{4} + ib\alpha + \frac{m\pi}{2} \right), \quad (2.15)$$

$$Q_{n2}^m(\cos \alpha) = (0.5 - ib)^m \left(\frac{\pi}{2(ib - 0.5) \sin \alpha} \right)^{\frac{1}{2}} \cos \left(\frac{\pi}{4} + ib\alpha + \frac{m\pi}{2} \right).$$

We shall put (2.14) and (2.15) in (2.12). Taking into account that w^* is real, after certain transformations we obtain:

$$w_m^* = (\sin \alpha)^{-\frac{1}{2}} [c_{1m} \sin b\alpha + c_{2m} \cos b\alpha + c_{3m} \operatorname{sh} b\alpha + c_{4m} \operatorname{ch} b\alpha] \quad (2.16)$$

($m = 0, 1, 2, \dots$).

Let us consider the case of axially symmetric vibrations in which waves are formed only along the meridians. Considering $m = 0$, or in the operator of (2.2) $\frac{\partial}{\partial \beta} = 0$, instead of (2.4) and (2.7) we have following the initial equations

$$\Delta \Delta \Delta w(\alpha) - b^4 \Delta w(\alpha) = 0, \quad (2.17)$$

$$\Delta \Delta w^*(\alpha) - b^4 w^*(\alpha) = 0, \quad (2.18)$$

where

$$\Delta = \frac{d^2}{d\alpha^2} + \operatorname{ctg} \alpha \frac{d}{d\alpha}, \quad w^* = \Delta w.$$

The asymptotic solution of equation (2.18) will be:

$$\varpi^*(a) = (\sin a)^{-\frac{1}{2}} (c_1 \sin ba + c_2 \cos ba + c_3 \operatorname{sh} ba + c_4 \operatorname{ch} ba). \quad (2.19)$$

In the following paragraph we shall show that solutions (2.16) and (2.19) can be obtained by the general method of asymptotic integration, whose advantages consist in its comparative simplicity and universality.

§ 3. Application of the Method of Asymptotic Integration to the Problem of Vibrations of a Spherical Shell

The essence of the method of asymptotic integration will be considered in an example of integration of equation (2.2), which, if we introduce the designation $\Delta w = w^*$, can be presented in the following manner:

$$(1 - p^2) w^* + h^2 L(w^*) = 0,$$

where

$$p^2 = \frac{\gamma w^2 R^2}{gE}, \quad L = \Delta \Delta, \quad \Delta = \frac{1}{\sin \alpha} \left[\frac{\partial}{\partial \alpha} \left(\sin \alpha \frac{\partial}{\partial \alpha} \right) + \frac{1}{\sin^2 \alpha} \frac{\partial^2}{\partial \beta^2} \right]. \quad (3.1)$$

The solution of (3.1) will be found in the form of

$$w^*(\alpha, \beta) = e^{f(\alpha, \beta)} W^*(\alpha, \beta). \quad (3.2)$$

Here $f(\alpha, \beta)$, $W^*(\alpha, \beta)$ are the sought functions, whereby $f(\alpha, \beta)$ is called the function of variability, and $W^*(\alpha, \beta)$ is the function of intensity: k is a constant which is connected with h^* by the relationship

$$k = h^{*2\tau}, \quad h^* = \frac{h}{2R \sqrt[3]{3(1-\nu^2)}}, \quad (3.3)$$

where τ is the index of variability of the sought integral selected by us. We shall consider $\tau > 0$, and consequently, k is a large number.

The function of intensity $W^*(\alpha, \beta)$ and the sought frequency will be expanded in asymptotic series in diminishing powers of k . Then the sought solution (3.2) will be presented in the form of

$$w^* = e^{f(\alpha, \beta)} (W_0^* + k^{-1} W_1^* + k^{-2} W_2^* + \dots), \quad p^2 = p_0^2 + k^{-1} p_1^2 + \dots, \quad (3.4)$$

where $W_j^*(j = 0, 1, 2, \dots)$ are functions of α and β , and do not depend on parameter k . Placing (3.4) in (3.1) and considering (3.3), we will obtain:

$$\begin{aligned} & [1 - (p_0^2 + k^{-1} p_1^2 + \dots)] (W_0^* + k^{-1} W_1^* + \dots) + k^{4 - \frac{2}{\tau}} L_0 W_0^* + \\ & + k^{2 - \frac{2}{\tau}} [L_0 W_1^* + L_1(W_0^*)] + k^{2 - \frac{2}{\tau}} [L_0 W_2^* + L_1(W_1^*) + \\ & + L_2(W_0^*)] + \dots = 0. \end{aligned} \quad (3.5)$$

Here $L_j(j = 1, 2, \dots)$ are linear differential operators, and

$$L_0 = \left[\left(\frac{\partial f}{\partial x} \right)^2 + \frac{1}{\sin^2 \alpha} \left(\frac{\partial f}{\partial \beta} \right)^2 \right]. \quad (3.6)$$

We shall assign the index of variability τ . On the selection of τ depends the density of the nodal lines and the frequency of natural vibrations.

Reference [3] shows that for shells of positive curvature the frequency of natural vibrations with the growth of τ is not increased, while $\tau < 0.5$ and increases when $\tau > 0.5$.

We shall find the frequencies of vibrations corresponding to the index of variability $\tau = 0.5$, which is called the characteristic frequency in [3].

Considering $\tau = 0.5$ in (3.5), we will require that in the left part of the equations the coefficients become equal to zero at all powers of k . We shall obtain an infinite system of equations. Finding of functions $f(\alpha, \beta)$, $W_j^*(\alpha, \beta)$ ($j = 0, 1, 2, \dots$) will be reduced to a certain recurrent process. The function of variability $f(\alpha, \beta)$ is always determined from the first equation, which is obtained by equating the coefficients to zero at the highest power of k in the given equation. From the remaining equations we shall consecutively determine $W_j^*(j = 0, 1, 2, \dots)$.

Preserving the degree of accuracy of the initial equations in all calculations, we shall limit ourselves in series (3.4) to the

first two terms and to the value of the frequency of free vibrations in zero approximation. Then, by equating the coefficients in equation (3.5) to zero at the highest powers of k (k^0 and k^{-1}), we obtain:

$$1 - p_0^2 + \left[\left(\frac{\partial f}{\partial \alpha} \right)^2 + \frac{1}{\sin^2 \alpha} \left(\frac{\partial f}{\partial \beta} \right)^2 \right] = 0, \quad (3.7)$$

$$L_1(W_0^*) = 0, \quad \left(p_0^2 = \frac{1 R^2 \omega_0^2}{g E} \right).$$

Integration of (3.7) makes it possible to express $f(\alpha, \beta)$ through an unknown frequency ω . Putting $f(\alpha, \beta)$ and $W_0(\alpha, \beta)$ in (3.4), and satisfying the boundary conditions of the problem, we can obtain the equation of frequencies.

We shall show the application of the method of asymptotic integration in an example of vibrations of a section of a spherical shell that is limited by parallels $\alpha = \alpha_1$, $\alpha = \alpha_2$ (§ 2).

Let us first consider axially symmetric vibrations in which the index of variability is great in the meridional direction and is equal to zero in the direction of parallel circles.

The solution of equation (2.18) will be found in the form of

$$w^*(\alpha) = e^{k f(\alpha)} [W_0^*(\alpha) + k^{-1} W_1^*(\alpha)], \quad p^2 \approx p_0^2. \quad (3.8)$$

Substitution of (3.8) in (2.18) under the condition of $\tau = 0.5$ leads to this equation:

$$(1 - p_0^2) (W_0^* + k^{-1} W_1^*) + k^0 f'^2 W_0^* + k^{-1} [f''^2 W_1^* + (6f' f'' + 2f'^3 \operatorname{ctg} \alpha) W_0^* + 4f'^3 W_0^{*'}] = 0. \quad (3.9)$$

Equating the coefficients to zero at k^0 and k^{-1} , for determination of functions $f(\alpha)$ and $W_0^*(\alpha)$, we have

$$1 - p_0^2 + f'^2 = 0, \quad (3.10)$$

or

$$(6f'^2 f'' + 2f'^3 \operatorname{ctg} \alpha) W_0^* + 4f'^3 W_0^{*'} = 0$$

$$f(\alpha) = \int_{\alpha_1}^{\alpha} \sqrt{p_0^2 - 1} d\alpha, \quad w_0 = f'^{-\frac{1}{2}} (\sin \alpha)^{-\frac{1}{2}}.$$

Taking into account that

$$kf_1 = -kf_2 = b(\alpha - \alpha_0), \quad kf_3 = -kf_4 = ib(\alpha - \alpha_0),$$

we will obtain:

$$w^* = (\sin \alpha)^{-\frac{1}{3}} [c_1 \sin b(\alpha - \alpha_0) + c_2 \cos b(\alpha - \alpha_0) + c_3 \operatorname{sh} b(\alpha - \alpha_0) + c_4 \operatorname{ch} b(\alpha - \alpha_0)]. \quad (3.11)$$

Solution (3.11) coincides with (2.19), which was obtained earlier. By substituting (3.11) in formula $\Delta w = w^*$, we find the general solution to equation (2.18)

$$w = w_0 (A_1 \sin kf + A_2 \cos kf + A_3 \operatorname{sh} kf + A_4 \operatorname{ch} kf) + A_5 \alpha + A_6, \quad (3.12)$$

where A_j ($j = 1, 2, \dots$) are integration constants. The last two terms in (3.12) correspond to two multiple zero roots of the characteristic equation. It is easy to show that one of the multiple zero roots must be rejected, otherwise the obtained solution will not satisfy the equations of axially symmetric vibrations of a spherical shell:

$$\frac{d}{d\alpha} (u' + u \operatorname{ctg} \alpha + 2w) - (1 - \nu) w' = 0, \\ (1 + \nu) (u' + u \operatorname{ctg} \alpha + 2w) + \frac{k^2}{12R^3} w^{IV} - \frac{7R^2 w^3 (1 - \nu)}{8E} w = 0. \quad (3.13)$$

Equations (3.13) directly ensue from the general theory of shells with an accuracy up to terms of the order h^* , if we consider that the index of variability is equal to half.

Excluding displacement u from (3.13), which is directed along the meridian, we obtain an equation of the fifth order for w . Thus, w will be expressed in five, and u in six constants of integration, which corresponds to the number of boundary conditions and is equal to six with axially symmetric strain.

By comparing (3.13) and (2.2), in which it is necessary to take $\partial/\partial\beta = 0$, we notice that inasmuch as in the considered case of $\Delta p = Eh/R(1 - \nu) \times (u' + u \cot \alpha + 2w)$, the second equation of (2.2) accurately coincides with the second equation of (3.13), and the first equation of (2.2) is one order above the first equation of (3.13). This explains the appearance of the extraneous root, and

after rejecting it we will obtain:

$$w(\alpha) = (\sin \alpha)^{-\frac{1}{2}} (c_1 \sin b\alpha + c_2 \cos b\alpha + c_3 \operatorname{sh} b\alpha + c_4 \operatorname{ch} b\alpha) + c_5. \quad (3.14)$$

We shall introduce a new variable $\theta = \frac{\pi}{2} - \alpha$. Then expression (3.14) can be presented in the form of

$$w(\alpha) = (\cos \alpha)^{-\frac{1}{2}} (A_1 \sin b\theta + A_2 \cos b\theta + A_3 \operatorname{sh} b\theta + A_4 \operatorname{ch} b\theta) + A_5. \quad (3.15)$$

For tangential displacement we find the following asymptotic solution:

$$u = -(\cos \theta)^{-\frac{1}{2}} (1 + \nu) \left\{ \frac{1}{b} [-A_1 \cos b\theta + A_2 \sin b\theta + A_3 \operatorname{ch} b\theta + A_4 \operatorname{sh} b\theta] + \frac{A_5}{1 + \nu} [2 - \rho^2 (1 - \nu)] \theta \right\} + A_6. \quad (3.16)$$

Let us turn to consideration of the case when, during vibrations, waves are formed both along the meridians, and also along the parallel circles. We shall find the solution of equation (2.7) in the form of

$$w_m^*(\alpha) = e^{k f(\alpha)} [W_{m0}^*(\alpha) + k^{-1} W_{m1}^*(\alpha)]. \quad (3.17)$$

After substitution of (3.15) in (2.7), and equating the coefficients to zero with k^0 and k^{-1} , we will obtain:

$$\begin{aligned} 1 - \rho_0^2 + \left(f'^2 - \frac{\eta^2}{\sin^2 \alpha} \right)^2 &= 0, & \rho_0^2 &= \frac{\gamma \omega^2 R^2}{gE}, & \eta &= \frac{m}{k}, \\ \left(6f'^2 f'' - \frac{2\eta^2}{\sin^2 \alpha} f'' + 2f'^3 \operatorname{ctg} \alpha - \frac{2\eta^2 f'}{\sin^3 \alpha} \operatorname{ctg} \alpha \right) w_0^* &+ \\ + 4f'' \left(f'^2 - \frac{\eta^2}{\sin^2 \alpha} \right) w_0^{*'} &= 0. \end{aligned} \quad (3.18)$$

From the first equation of (3.18) we find the expression for the variability function

$$f(\alpha) = \int_{\alpha_0}^{\alpha} \left(\frac{\eta^2}{\sin^2 \alpha} \pm \frac{b^2}{k^2} \right)^{\frac{1}{2}} d\alpha, \quad b^2 = k^2 \left(\frac{\gamma \omega^2 R^2}{gE} - 1 \right), \quad (3.19)$$

and from the second we determine the function of intensity of zero approximation.

However, the expression for the $f(\alpha)$, calculated according to (3.19), and the corresponding equation of frequencies, are excessively

awkward. When $b^2 \gg m^2$ and angle α satisfies conditions (2.13), solution (3.17) will be:

$$kf_1 = -kf_2 = b(\alpha - \alpha_0), \quad kf_3 = -kf_4 = ib(\alpha - \alpha_0).$$

§ 4. Examples of Composition of a Frequency Equation for a Spherical Shell

Let us assume that a shell is bounded by angles $\theta = \pm\theta_1$ and both edges are secured equally. Let us consider the case of axially symmetric vibrations. They are broken up into symmetric and antisymmetric with respect to $\theta = 0$. In the case of symmetric vibrations, in formulas (3.15) and (3.16) it is necessary to put $A_1 = A_3 = A_6 = 0$, and in the case of antisymmetric, $A_2 = A_4 = A_5 = 0$. Let us assume that both edges of the shell are rigidly fixed, i.e., the following conditions must be fulfilled:

$$u = w = w' = 0 \text{ when } \theta = \pm\theta_1.$$

Satisfying these conditions with the help of (3.15) and (3.16), we will obtain a frequency equation for symmetric vibrations:

$$\frac{a_1 \theta_1}{1 + \nu} (1 + \operatorname{tg} \theta_1 b \operatorname{cth} \theta_1 b) - 2 \operatorname{tg} \theta_1 b \operatorname{th} \theta_1 b, \\ (a_1 = [2 - p^2(1 - \nu)]b, \quad b = k^{-\frac{1}{2}}(p^2 - 1)^{\frac{1}{4}}). \quad (4.1)$$

Inasmuch as $b \gg 1$, argument $\theta_1 b$ in many cases can be so large that

$$\operatorname{cth} \theta_1 b \approx \operatorname{th} \theta_1 b \approx 1.$$

Then (4.1) will take on the form of

$$\operatorname{ctg} \theta_1 b = \frac{2(1 + \nu)b^{\frac{1}{2}} + (p^2 - 1)^{\frac{1}{4}}(p^2(1 - \nu) - 2)\theta_1}{[2 - p^2(1 - \nu)](p^2 - 1)^{\frac{1}{4}}\theta_1} \\ \left(n = 0, 1, 2, \dots, p^2 = \frac{10^3 R^3}{kE} \right). \quad (4.2)$$

The frequency of natural vibrations ω is determined from equation (4.2) by the method of series approximations. For

sufficiently thin shells, the first term in the numerator is small as compared to the second. In this case the frequency equation is simplified:

$$\operatorname{ctg} \theta_1 b = -1, \quad \theta_1 b = \left(n - \frac{1}{4}\right) \pi \quad (n = 0, 1, 2, \dots)$$

or

$$\frac{12(1-\nu^2)R^3}{h^3} \left(\frac{\gamma \omega^2 R^2}{gE} - 1 \right) \theta_1^4 = \left(n - \frac{1}{4}\right)^4 \pi^4. \quad (4.3)$$

In the case of hinged support on the edges, the radial displacement w , bending moment M_1 , and normal force N_1 must become equal to zero. With the same degree of accuracy with which we obtained the final formulas, these conditions can be represented in the following way:

$$w = w' = u' = 0 \quad \text{when } \theta = \pm \theta_1. \quad (4.4)$$

Satisfying conditions (4.4) with the help of (3.15) and (3.16), we will obtain the frequency equation:

$$\frac{12(1-\nu^2)R^3}{h^3} \left(\frac{\gamma \omega^2 R^2}{gE} - 1 \right) \theta_1^4 = \left(\frac{n}{2}\right)^4 \pi^4 \quad (n = 0, 1, 2, \dots). \quad (4.5)$$

§ 5. Free Vibrations of Shells that Differ Very Little from Spherical Shells

Let us consider free vibrations of an arbitrary shell of revolution of positive curvature. Let us assume that the shell is closed with respect to the axis of symmetry. Then all displacements and forces will be functions of angle β of period 2π , and the solution of equations (1.2) can be found in the form of

$$\begin{aligned} w(\alpha, \beta, t) &= w(\alpha) \cos m\beta \cos \omega t, \\ \varphi(\alpha, \beta, t) &= \varphi(\alpha) \cos m\beta \cos \omega t. \end{aligned} \quad (5.1)$$

Under this condition, operators Δ and Δ_k , which were determined by expressions (1.2), will take on the form of

$$\Delta = \frac{1}{R_1^2 \rho \sin \alpha} \left[\frac{d}{d\alpha} \left(\rho \sin \alpha \frac{d}{d\alpha} \right) - \frac{m^2}{\rho \sin \alpha} \right],$$

$$\Delta_2 = \frac{1}{R_1^2 \rho \sin \alpha} \left[R_1 \frac{d}{d\alpha} \left(\frac{\sin \alpha}{R_1} \frac{d}{d\alpha} \right) - \frac{m^2}{\rho \sin \alpha} \right] \left(\rho - \frac{R_2}{R_1} \right). \quad (5.2)$$

Let us assume that radii R_1 and R_2 change so smoothly that in formulas (5.2) it is possible to disregard the terms containing factors ρ^1/ρ and R_1/R_1^1 . Then the formulas of (5.2) give:

$$\Delta = \frac{1}{R_1^2} \left(\frac{d^2}{d\alpha^2} + \operatorname{ctg} \alpha \frac{d}{d\alpha} - \frac{m^2}{\rho^2 \sin^2 \alpha} \right), \quad (5.3)$$

$$\Delta_2 = \frac{1}{R_1^2 \rho} \left(\frac{d^2}{d\alpha^2} + \operatorname{ctg} \alpha \frac{d}{d\alpha} - \frac{m^2}{\rho \sin^2 \alpha} \right) \left(\rho - \frac{R_2}{R_1} \right).$$

Hence, in the case of axially symmetric vibrations, it follows that

$$\Delta = R_2^{-1} \Delta_2. \quad (5.4)$$

When $m \neq 0$, condition (5.4) is fulfilled only approximately due to the distinction of the last terms in the formulas of (5.3). Under conditions (5.1) and (5.4), system (1.2) is reduced to an equation for w :

$$\Delta \Delta w - k^{*-2} \left(\rho^2 - \frac{1}{\rho^2} \right) \Delta w = 0,$$

$$\rho^2 = \frac{7R_1^2 \omega^2}{gE}, \quad k^{*-2} = \frac{12(1-\nu)R_1^2}{h^3}. \quad (5.5)$$

In comparing equations (2.4) and (5.5), let us note that the latter differs only by the factor in front of Δw , which contains variable $1/\rho^2$.

Equation (5.5), just as (2.4), is easily solved by the method of asymptotic integration, an account of which is contained in § 3. We find the solution of equation (5.5) again in the form of (3.8). In the case, for instance, of axially symmetric vibrations, i.e., when $m = 0$, we obtain for the function of variability f :

$$f^2 \left[f^4 - \left(\frac{7\omega^2 R_1^2}{gE} - \frac{R_1^2}{R_2^2} \right) \right] = 0. \quad (5.6)$$

Rejecting one of the multiple zero roots of this equation, as also for a spherical shell, we will obtain the following solutions to (5.6):

$$f = \int_{\alpha_0}^{\alpha} \left(\frac{10^2 R_1^2}{8E} - \frac{R_1^2}{R_2^2} \right)^{\frac{1}{4}} d\alpha, \quad f_0 = c_3 = \text{const.} \quad (5.7)$$

For calculation of the obtained integral it is necessary to be given the form of the shell, i.e., the functions $R_1(\alpha)$ and $R_2(\alpha)$. Let us assume that for a certain shell the problem may be approximately solved by replacement of R_1 and R_2 and angle α by certain of their mean values. Let us assume that the subradical expression in formula (5.7) is positive. Then for radial displacement w we will find:

$$w(\alpha) = (\sin \alpha)^{-\frac{1}{2}} (c_1 \sin kf + c_2 \cos kf + c_3 \operatorname{sh} kf + c_4 \operatorname{ch} kf) + c_5, \quad (5.8)$$

$$f = \left(\frac{10^2 R_1^2}{8E} - \frac{R_1^2}{R_2^2} \right)^{\frac{1}{4}} (\alpha - \alpha_0).$$

When $R_1 = R_2 = R$, solution (5.8) coincides with the one earlier obtained (3.11) for a spherical shell. Thus, we simply determine w also when $m \neq 0$. After $w(\alpha)$ is found, by formula (5.8) we determine u :

$$u' + \frac{\alpha}{p} \operatorname{ctg} \alpha = (1 - \nu) \rho [p^2 w - h^2 \Delta \Delta w] + \left(1 + \frac{1}{p} \right) w. \quad (5.9)$$

Formulas (5.8) and (5.9) allow us to formulate a frequency equation by the same method as for a spherical shell.

Literature

1. A. L. Gol'denveyzer. Theory of thin elastic shells. State Technical Press, 1953.
2. A. L. Gol'denveyzer. Certain mathematical problems of the theory of thin elastic shells. "Progress of mathematical sciences," Vol. 5, No. 5 [95], State Technical Press, 1960.
3. A. L. Gol'denveyzer. Asymptotic properties eigenvalues in problems of the theory of thin elastic shells. "Applied mathematics and mechanics," Vol. XXV, No. 4, 1961.

4. V. Z. Vlasov. General theory of shells and its application in engineering. Gostekhizdat, 1949.

5. E. V. Hobson. Theory of spherical and ellipsoidal functions. IL, Moscow, 1952.

Submitted
2 November 1963

CALCULATION OF CLOSED CYLINDRICAL AND SLIGHTLY CONICAL SHELLS WITH ARBITRARY CONTOUR OF CROSS SECTION

N. A. Shelomov

Definitions of Cyrillic Items

III = f = frame

III = f = frame

§ 1. Formulation of Problem

Let us consider a structurally-orthotropic semimomentless shell under the action of an arbitrary surface load. (In places of application of concentrated forces the shell is reinforced by additional structural frames.)

The problem concerning the state of strain of such a shell will be solved by the method of forces in the form of Castigliano's variational principle. In this case the calculating diagram of the shell may be based on the following assumptions [1], [4], [5], and [6].

1. The Kirchhoff - Love hypothesis concerning straight normals is valid.

2. Moments (Fig. 1) are

$$O_1 = H_1 = H_2 = 0. \quad (1.1)$$

3. The expression for specific strain energy of the shell is taken in the form of

$$W = \frac{1}{2E_1} \cdot T_1^2 + \frac{12}{2E_2} \cdot S_2^2 \quad (1.2)$$

Here δ_1 and δ_2 are the given skin thicknesses of a structurally-orthotropic shell in transverse and longitudinal sections, according to [1].

For a conical shell, we additionally take $\cos \theta \approx 1$ (Fig. 2).

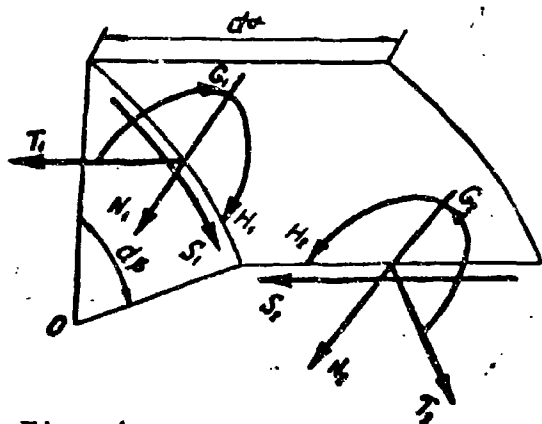


Fig. 1.

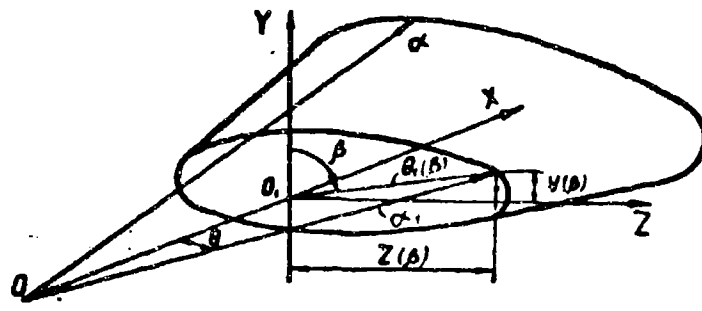


Fig. 2.

Considering (1.1), the differential and integral conditions of equilibrium of the shell can be presented in the form of

$$\begin{aligned} \frac{\partial B T_1}{\partial \alpha} + \frac{\partial S_1}{\partial \beta} \cdot A - \left[\frac{\partial B}{\partial \alpha} \cdot T_2 \right] + AB \cdot X &= 0, \\ \frac{1}{B} \frac{\partial B^2 S_1}{\partial \alpha} + A \cdot \frac{\partial T_1}{\partial \beta} - \frac{A}{R} \frac{\partial G_1}{\partial \beta} + ABY &= 0, \\ A \cdot B \frac{T_1}{R} + A \frac{\partial}{\partial \beta} \left(\frac{1}{B} \frac{\partial G_1}{\partial \beta} \right) - \left[\frac{\partial B}{\partial \alpha} \cdot \frac{\partial G_1}{\partial \alpha} \right] + ABZ &= 0, \\ \oint (T_1 + S_1) \cdot B d\beta + P &= 0, \\ \oint [(T_1 + S_1) \times r] B d\beta + M &= 0. \end{aligned} \quad (1.3)$$

$$(1.4)$$

Here α and β are the orthogonal curvilinear coordinates of the middle surface of the shell,

$$A = 1, B = f_1(\alpha) B_1(\beta),$$

$\frac{1}{R} = \frac{1}{f_1(\alpha)} \cdot \frac{1}{R_1(\beta)}$ are coefficients of first quadratic form and the curvature of the middle surface of the shell (Fig. 2),

$$B_1 = [\theta_1^2(\beta) + \theta_1'^2(\beta)]^{\frac{1}{2}}, \quad \frac{1}{R_1} = \frac{\theta_1^2(\beta) + 2\theta_1'(\beta)\theta_1''(\beta) - \theta_1(\beta)\theta_1'''(\beta)}{B_1^3}, \quad (1.5)$$

$$f_1(\alpha) = 1 - \text{for a cylinder}, \quad (1.6)$$

$$f_1(\alpha) = \frac{\alpha}{\alpha_1} - \text{for a cone},$$

X, Y, Z are the component of the external surface of the load,

T₁, T₂, S₁, G₂ are the forces in the semimomentless shell,

P, M and T₁, S₁ are the main vector and moment of external forces and vectors of internal forces of the shell in section $\alpha = \text{const}$,

r is the vector radius of points of the middle surface of the shell in section $\alpha = \text{const}$.

In virtue of (1.6), in equations (1.3) for a cylinder, the members in brackets become equal to zero. They, being small, as compared with the other terms of these equations, will be disregarded subsequently also for the cone.

Following P. F. Papkovich, we shall break down the state of strain of the shell into main (equilibrium) and secondary (self-balanced).

The main state of strain of the shell will be considered found by one of the methods presented in [1], [7], and [8]. Specifically, it can be represented in the form of

1) forces in the shell

$$\begin{aligned} T_1^* &= T_1^* + T_1^{(0)}, \\ S_1^* &= S_1^* + S_1^{(0)}, \\ T_2^* &= T_2^*, \end{aligned} \quad (1.7)$$

where T₁^{*}, S₁^{*}, T₂^{*} is a particular solution of system (1.3) when G₂ = 0 [5],

$$\begin{aligned} T_1^* &= - \int_{\alpha_1}^{\alpha} \frac{\partial}{\partial \beta} \left[\frac{1}{B} \int_{\alpha_1}^{\alpha} B \frac{\partial}{\partial \beta} (RZ) d\alpha - \frac{1}{B^2} \int_{\alpha_1}^{\alpha} B^2 Y d\alpha \right] d\alpha - \frac{1}{B} \int_{\alpha_1}^{\alpha} B X d\alpha, \\ S_1^* &= \frac{1}{B^2} \left[\int_{\alpha_1}^{\alpha} B \frac{\partial}{\partial \beta} (RZ) d\alpha - \int_{\alpha_1}^{\alpha} B^2 Y d\alpha \right], \\ T_2^* &= -RZ, \end{aligned} \quad (1.8)$$

and forces $T_1^{(1)}$ and $S_1^{(1)}$ are found from (1.3) and (1.4) when $G_2 = 0$ after substitution there of (1.7) and (1.8);

2) forces in the q -th structural frame

$$M_{q1m}^0, M_{q2m}^0, M_{q3m}^0, \quad Q_{q1m}^0, Q_{q2m}^0, Q_{q3m}^0 \quad (1.9)$$

(M_{qif}^0 and Q_{qif}^0 are the bending and twisting moments, the axial and transverse forces, respectively) are determined by methods of structural mechanics in considering the frame as a static indefinite frame under the action of external concentrated loads P_{qx} , P_{qy} , P_{qz} and reactions on the part of the shell

$$\Delta T_{iq}^0 = T_{iq}^0(\alpha_q + 0, \beta) - T_{iq}^0(\alpha_q - 0, \beta), \quad \Delta S_{iq}^0 = S_{iq}^0(\alpha_q + 0, \beta) - S_{iq}^0(\alpha_q - 0, \beta),$$

where α_q is the coordinate of the q -th frame.

The secondary state of strain of the shell should be the solution of uniform systems (1.3) and (1.4).

System (1.3) consists of three equations for four unknown functions T_1^0 , S_1^0 , T_2^0 , G_2^0 . Thus, in every point of the middle surface the semimomentless shell is statically indefinite one. We take the functional unknown as extraneous:

$$G_2 = \sum_{i=1}^n \varphi_i(\beta) \left[f_i(\alpha) \cdot \frac{d^2 a_i(\alpha)}{d\alpha^2} \right], \quad (1.10)$$

where $a_1(\alpha)$ are the sought functions,

$f_1(\alpha)$ are determined by formulas (1.6),

$\varphi_1(\beta)$ play the role of given functions that satisfy uniform conditions (1.4) and the conditions of periodicity.

In §§ 2 and 3 we shall show the method of obtaining these functions.

After placing (1.10) in (1.3) when $X = Y = Z = 0$, we will obtain:

$$\begin{aligned}
T_1^0 &= - \sum_{i=1}^n \psi_i(\beta) \cdot \frac{a_i(\alpha)}{f_1'(\alpha)}, \\
\psi_i(\beta) &= \frac{1}{B_i} \left\{ \frac{1}{B_i} \left[\frac{R_i}{B_i} \left[\frac{1}{B_i} \varphi_i'(\beta) \right] \right] \right\}' + \frac{1}{B_i} \left[\frac{1}{R_i B_i} \varphi_i'(\beta) \right]', \\
S_1^0 &= \sum_{i=1}^n \left\{ \frac{1}{B_i} \left[\frac{R_i}{B_i} \left[\frac{1}{B_i} \varphi_i'(\beta) \right] \right] \right\}' + \frac{1}{R_i B_i} \varphi_i'(\beta) \left\{ \frac{d}{d\alpha} \left[\frac{a_i(\alpha)}{f_1'(\alpha)} \right] \right\}.
\end{aligned} \tag{1.11}$$

$$\begin{aligned}
T_2^0 &= - \sum_{i=1}^n \frac{R_i}{B_i} \left[\frac{1}{B_i} \varphi_i'(\beta) \right]' \frac{d^2 a_i(\alpha)}{d\alpha^2}, \\
U_2 &= \sum_{i=1}^n \varphi_i(\beta) f_1(\alpha) \cdot \frac{d^2 a_i(\alpha)}{d\alpha^2}.
\end{aligned}$$

By considering the increase of forces ΔT_{1q}^0 and ΔS_{1q}^0 as an external influence, we will find the forces in the structural frames:

$$\begin{aligned}
M_{qim}^0, \\
Q_{qim}^0.
\end{aligned} \tag{1.12}$$

Unknown functions $a_i(\alpha)$ are found by means of solution of a mixed variational problem.

Considering (1.2), we shall write expressions for potential energy of the system:

$$U = \int_0^1 \phi (T_1^0 + T_1^2) \cdot \frac{B d\beta dz}{2E_1} + \int_0^1 \phi |G_2^0|^2 \frac{B d\beta dz}{2E_2^2} + \sum_{i=1}^n U_{qim}. \tag{1.13}$$

Here

$$\begin{aligned}
U_{qim} &= \sum_{i=1}^3 \phi \frac{|M_{qim}^0 + M_{qim}^2|}{2E_i \cdot I_{im}} \cdot f_1(\alpha_i) \cdot B_i d\beta + \\
&+ \sum_{i=1}^3 \phi \frac{|Q_{qim}^0 + Q_{qim}^2|}{2E_i \cdot F_{im}} f_1(\alpha_i) B_i d\beta,
\end{aligned}$$

$E_t I_{tf}$ and $E_t \mu_t F_f$ are the flexural, torsional, longitudinal, and shear rigidities of the frame, respectively.

In expanded form

$$\begin{aligned}
U &= \int_0^1 \frac{f_1(\alpha)}{2E_1} \left\{ \phi T_1^0(\alpha, \beta) B_i d\beta + 2 \sum_{i=1}^n \left[\phi T_1^2(\alpha, \beta) \psi_i(\beta) B_i d\beta \right] \cdot \frac{a_i(\alpha)}{f_1'(\alpha)} + \right. \\
&+ \sum_{i=1}^n \sum_{k=1}^n \left[\phi \psi_i(\beta) \cdot \psi_k(\beta) \cdot B_i d\beta \right] \frac{a_i(\alpha) \cdot a_k(\alpha)}{f_1'(\alpha)} \Big\} d\alpha +
\end{aligned}$$

$$+ \int_0^1 \frac{12f_1^2(z)}{2Ez_1^3} \left\{ \sum_{i=1}^n \sum_{j=1}^n \left[\oint \varphi_i(\beta) \cdot \varphi_j(\beta) B_1 d\beta \right] \frac{d^2 a_i(z)}{dz^2} \cdot \frac{d^2 a_j(z)}{dz^2} \right\} dz + \quad (1.14)$$

$$+ \sum_{m=1}^n U_{q,m} - \int_0^1 F \left[z, \sum_{i=1}^n (a_i, a_i') \right] dz + \sum_{q=1}^m U_{q,m}.$$

The Euler - Poisson equations

$$F_{a_i} - \frac{d}{dz} (F a_i') + \frac{d^2}{dz^2} (F a_i'') = 0$$

for unknown functions $a_1(z)$ will take on the form of

$$\sum_{i=1}^n \frac{d^2}{dz^2} \left[\frac{12f_1^2(z)}{Ez_1^3} \cdot \frac{d^2 a_i(z)}{dz^2} \right] \oint \varphi_i(\beta) \cdot \varphi_k(\beta) B_1 d\beta +$$

$$+ \sum_{i=1}^n \frac{a_i(z)}{Ez_1 f_1^2(z)} \cdot \oint \varphi_i(\beta) \cdot \varphi_k(\beta) B_1 d\beta + \frac{1}{Ez_1 f_1(z)} \cdot \oint T_1^0(z, \beta) \varphi_i(\beta) B_1 d\beta = 0, \quad (1.15)$$

$$i = 2, 3, \dots, n.$$

The sought functions $a_1(z)$ have to satisfy also certain boundary conditions

$$U_m = 1_m, \quad m = 1, 2, \dots, l, \quad (1.16)$$

which are formulated depending upon the conditions of fastening of the shell [1], [2], [6].

With arbitrary selection of functions $\varphi_1(\beta)$, the matrix of system (1.15) is complete, in consequence of which, the solution of boundary value problem (1.15) and (1.16) becomes awkward and very time-consuming even for sharply cut-off series (1.10). Such functions $\varphi_1(\beta)$ can be obtained, however, which reduce the matrix of system (1.15) to diagonal form. In this case the boundary value problem (1.15), (1.16) for shells with arbitrary contour of cross section is solved with the same ease as for shells with circular contour of cross section. The way to do this is prompted by the conditions of conversion into zero of nondiagonal elements of the matrix of system (1.15)

$$\oint \varphi_i(\beta) \cdot \varphi_k(\beta) B_1 d\beta = 0, \quad (1.17)$$

$$\oint \psi_i(\beta) \cdot \psi_k(\beta) B_1 d\beta = 0, \quad i \neq k,$$

where $\psi_1(\beta)$ is determined by formulas (1.11).

It turns out that if we construct a differential operator

$$\frac{1}{B_1} \left\{ \frac{1}{B_1} \left[\frac{R_1}{B_1} \left[\frac{1}{B_1} \varphi_i'(\beta) \right]' \right]' + \frac{1}{B_1} \left[\frac{1}{R_1 B_1} \varphi_i'(\beta) \right]' - \lambda_i \varphi_i(\beta) \right\} = 0, \quad (1.18)$$

$$V_{ij} = \varphi_i^{j-1}(\beta) - \varphi_i^{j-1}(\beta + 2\pi) = 0, \quad i = 1, 2, \dots, n, \quad j = 1, 2, 3, 4,$$

where V_{1j} are the conditions of periodicity of functions $\varphi_1(\beta)$ and their derivatives $\varphi_1^{(j-1)}(\beta)$, we find its solution (eigenfunctions), then they automatically will satisfy the conditions of (1.17).

§ 2. Certain Basic Properties of Solutions of Operator (1.18)

1. Operator (1.18), as an even self-adjoint operator with $D = \theta_C^2 - 4\theta_1 \cdot \theta_{-1} = 0$ ([9], pp. 53-55), generates a denumerable set of characteristic numbers λ_1 , which, starting from the second, are either single or double. To this set there corresponds a complete and orthogonal system of chains of eigenfunctions $\varphi_{1r}(\beta)$ (r is the number of the eigenfunction in the 1-th chain) with weight B_1 . Therefore, with arbitrary r and t

$$\oint \varphi_{1r}(\beta) \cdot \varphi_{1t}(\beta) \cdot B_1 d\beta = 0, \quad i \neq k. \quad (2.1)$$

2. The first chain, which corresponds to $\lambda_1 = 0$, contains three functions (Fig. 2)

$$\begin{aligned} \varphi_{11} &= \theta_1(\beta) \cdot \cos \beta = y(\beta), \\ \varphi_{12} &= \theta_1(\beta) \cdot \sin \beta = z(\beta), \\ \varphi_{13} &= 1, \end{aligned} \quad (2.2)$$

which obviously approximate the elementary state of strain of the shell.

3. The remaining chains starting from the second one, contain either one or two eigenfunctions.

4. Their orthogonalization inside the i -th chain may be performed according to the system

$$\begin{aligned}\bar{\varphi}_n &= \varphi_n(\beta), \\ \bar{\varphi}_n &= v_n \cdot \varphi_n(\beta) + \varphi_n(\beta),\end{aligned}\quad (2.3)$$

where

$$v_n = - \frac{\oint \varphi_n(\beta) \cdot \varphi_n(\beta) B_1 d\beta}{\oint \varphi_n^2(\beta) B_1 d\beta},$$

after which, the following is valid at any i :

$$\oint \bar{\varphi}_n(\beta) \cdot \bar{\varphi}_n(\beta) B_1 d\beta = 0. \quad (2.4)$$

5. $\varphi_{ir}(\beta)$, when all $i \neq 1$ and $r = 1, 2$, satisfy uniform conditions (1.4) which are equivalent to six scalar conditions of self-balance:

$$\oint \varphi_{ir}(\beta) \cdot \varphi_{ir}(\beta) B_1 d\beta = 0, \quad i = 1, 2, 3, \quad (2.5a)$$

$$\begin{aligned}& \oint \left\{ \frac{1}{B_1} \left[\frac{R_1}{B_1} \left[\frac{1}{B_1} \varphi'_{ir}(\beta) \right]' \right] + \frac{1}{R_1 B_1} \varphi'_{ir} \right\} \varphi'_{ir}(\beta) d\beta = \\ &= \left\{ \frac{1}{B_1} \left[\frac{R_1}{B_1} \left[\frac{1}{B_1} \varphi'_{ir}(\beta) \right]' \right] + \frac{1}{R_1 B_1} \varphi'_{ir}(\beta) \right\} \cdot \varphi_{ir}(\beta) \Big|_0^{2\pi} - \\ &- \lambda_i \oint \varphi_{ir}(\beta) \cdot \varphi_{ir}(\beta) B_1 d\beta = 0, \quad i = 1, 2, \quad (2.5b)\end{aligned}$$

$$\begin{aligned}& \oint \left\{ \frac{1}{B_1} \left[\frac{R_1}{B_1} \left[\frac{1}{B_1} \varphi'_{ir}(\beta) \right]' \right] + \frac{1}{R_1 B_1} \varphi'_{ir}(\beta) \right\} \varphi_i^2(\beta) d\beta = \\ &= \oint \left[\lambda_i \int_0^{\beta} \varphi_{ir}(\eta) \cdot B_1(\eta) d\eta + C_i \right] \varphi_i^2(\beta) d\beta = 0 \quad (2.5c)\end{aligned}$$

(conditions (2.5a) and (2.5b) are satisfied in virtue of (2.1) and the periodicity of functions $\varphi_{ir}(\beta)$; conditions (2.5c) are satisfied with the appropriate selection of arbitrary constant C_1).

6. Trigonometric series with arbitrary constants a_1 and b_1

$$f(\beta) = \frac{a_0}{2} + \sum_{n=1}^{\infty} a_n \cos n\beta + \sum_{n=1}^{\infty} b_n \sin n\beta$$

is the solution of operator (1.18) when $R_1 = B_1 = \text{const.}$ Eigenvalues in this case are determined by the formula

$$\lambda_i = \frac{i}{R_1^3} i^2 (i^2 - 1), \quad i = 1, 2, 3, \dots, n, \quad (2.6)$$

whereupon $\lambda_1 = 0$ is a triple root and the other λ_i are double.

7. Due to the orthogonality of the eigenfunctions of operator (1.18), the matrix of system (1.15) become diagonal:

$$\begin{aligned} & \frac{d^2}{dz^2} \left[\frac{f_1^2(z)}{E f_1^3(z)} \cdot \frac{d^2 a_{ir}(z)}{dz^2} \right] + \frac{\lambda_i^2}{E f_1^3(z)} \cdot a_{ir}(z) + \\ & + \frac{\oint \bar{r}_1^0(z, \beta) \cdot \bar{r}_{ir}(z) B_1 d\beta}{\oint \bar{r}_{ir}^2(z) B_1 d\beta} \cdot \frac{\lambda_i}{E f_1(z)} = 0, \quad i = 2, 3, \dots, n, \quad r = 1, 2. \end{aligned} \quad (2.7)$$

§ 3. Algorithm for the Calculation of Eigenfunctions of Operator (1.18)

After the introduction of a new independent variable s (arc of contour of cross section of shell $\alpha = \alpha_1 = \text{const}$) according to formulas

$$ds = B_1 d\beta, \quad s = \int B_1 d\beta, \quad (3.1)$$

operator (1.18) takes on the form of

$$\begin{aligned} & \frac{d^2}{ds^2} \left[R_1(s) \frac{d^2 \varphi_i(s)}{ds^2} \right] + \frac{d}{ds} \left[\frac{1}{R_1(s)} \cdot \frac{d \varphi_i(s)}{ds} \right] - \lambda_i \varphi_i(s) = 0, \\ & V_m = \varphi_i^{(m-1)}(s) - \varphi_i^{(m-1)}(s + 2p) = 0, \\ & i = 1, 2, \dots, n, \quad m = 1, 2, 3, 4. \end{aligned} \quad (3.2)$$

Here $2p$ is the perimeter of cross section of the shell. For determining the eigenfunctions operator (3.2) it is possible to use the method of series approximations [10]. In this case, the calculation of the n -th approximation of λ_{in} and φ_{in} is carried out according to the system.

1. Determination of auxiliary function:

$$f_m(s) = \oint \tilde{r}(s, \xi) \cdot \varphi_{i,m-1}(\xi) d\xi. \quad (3.3)$$

2. Calculation of $\lambda_{1, n}$:

$$\lambda_{1, n} = \left\{ \oint f_{1, n}^2(s) ds - \sum_{k=1}^{i-1} \left[\oint f_{1, n}(s) \cdot \varphi_k(s) ds \right] \right\}^{-1}. \quad (3.4)$$

3. Finding $\varphi_{1, n}(s)$:

$$\varphi_{1, n}(s) = \lambda_{1, n} \left\{ f_{1, n}(s) - \sum_{k=1}^{i-1} \varphi_k(s) \left[\oint f_{1, n}(s) \varphi_k(s) ds \right] \right\}. \quad (3.5)$$

The eigenfunctions obtained will be standardized and mutually orthogonal.

The iterative process, (3.3)-(3.5), starts from the calculation of the second chain of eigenfunctions of operator (3.2), since for the first chain (function (2.2)) they are already known. Function $f_{10}(s)$ is designated in such a way, so that the zero approximation of eigenfunction $\varphi_{10}(s)$, calculated by formula (3.5), is different than identical zero. As $f_{10}(s)$, it is convenient to take $\sin \frac{1s\pi}{p}$ for the first eigenfunction of the i -th chain, and $\cos \frac{1s\pi}{p}$ for the second. In the course of the calculation of λ_1 and $\varphi_1(s)$, all the earlier found $\varphi_k(s)$ ($k \leq i-1$) are used. Transition to the calculation of the following eigenfunction is carried out automatically upon achievement of the given approximation. As a criterion for that, it is convenient to take the inequality

$$\varepsilon_{1, n} = \frac{|\lambda_{1, n-1} - \lambda_{1, n}|}{\lambda_{1, n}} < \varepsilon, \quad (3.6)$$

where ε is a given small number.

The generalized Green function $\tilde{F}(s, \xi)$ of operator (3.2), which is necessary for the calculation of $f_{1n}(s)$, can be constructed by the method given in [10] and [11] in such a manner that

$$\int_0^p \tilde{F}(s, \xi) \cdot \varphi_r(s) ds = 0, \quad r = 1, 2, 3, \quad (3.7)$$

where $\varphi_{1r}(s)$ is equal to $y(s)$, $z(s)$ and 1, respectively.

Therefore, the process (3.3)-(3.5) can be begun directly from the determination of λ_2 and the second chain of the eigenfunctions (§ 2). Let us give the final form of $\tilde{\Gamma}(s, \xi)$, which we constructed for a shell with arbitrary contour of cross sections:

$$\begin{aligned} \tilde{\Gamma}(s, \xi) = & - \sum_{n=1}^4 \sum_{k=2}^4 \frac{(-1)^n}{I_{kk}} [\eta_n(s) \cdot \eta_k(\xi) \cdot \Phi_{k, 5-n}(s) + \eta_n(\xi) \cdot \eta_k(s) \cdot \Phi_{k, 5-n}(\xi)] - \\ & - \eta_1^*(s) + \frac{\eta_1^*(s) \cdot \eta_1^*(\xi)}{[\eta_1(0) - \eta_1(2p)]} + \sum_{l=1}^4 \sum_{k=2}^4 \sum_{n=2}^4 (-1)^l \frac{W_{l, n; k, 5-l}}{I_{nn} \cdot I_{kk}} \cdot \eta_n(s) \cdot \eta_k(\xi) + \\ & + \left\{ - \sum_{l=1}^4 (-1)^l \eta_l(s) \cdot \eta_{5-l}(\xi) \right\} \begin{cases} 0 \leq s \leq \xi, \\ \xi \leq s \leq 2p. \end{cases} \end{aligned} \quad (3.8)$$

Here

$$\begin{aligned} \Phi_{k, q}(s) &= \int_0^s \eta_k(t) \cdot \eta_q(t) dt, \\ I_{kq} &= \oint \eta_k(t) \cdot \eta_q(t) dt, \\ W_{l, n; k, q} &= \oint \eta_l(s) \cdot \eta_n(s) \cdot \Phi_{k, q}(s) ds, \\ \eta_1(s) &= \omega(s), \\ \eta_2(s) &= y(s), \\ \eta_3(s) &= z(s), \\ \eta_4(s) &= 1, \\ d\omega &= [z(s) \cdot y'(s) - y(s) \cdot z'(s)] ds, \\ \eta_1^*(s) &= \eta_1(s) - \sum_{k=2}^4 \frac{I_{1k}}{I_{kk}} \cdot \eta_k(s). \end{aligned} \quad (3.9)$$

YOZ are the main central axes of cross section of the shell.

As can be seen from (3.8) and (3.9), Green's function contains only the functions $y(s)$, $z(s)$, 1, and $\omega(s)$, which are known to the calculator.

§ 4. Realization of Algorithm (3.3)-(3.5)

By algorithm (3.3)-(3.5) we composed and set up a program for the electronic computer (EC) Ural-2 which makes it possible to

calculate λ_1 and $\varphi_1(s)$ for shells with an arbitrary closed contour of cross section, which is given in tables.

We made up tables of λ_1 and $\varphi_1(s)$ for different shells, including one for a wing-type shell (RAF-34, 10% with rear wall 70.5%). The tables contain 128 values of function $\varphi_1(s)$ through equal intervals of $\Delta s = \frac{2\pi}{128}$.

A check showed that the functions $\varphi_1(s)$ are close to orthonormal

$$\oint \varphi_j^2(s) ds = 1 \pm 1 \cdot 10^{-7}, \quad (4.1)$$

$$\left| \oint \varphi_i(s) \varphi_k(s) ds \right| < 0.5 \cdot 10^{-9},$$

and the relative error of calculation of λ_1 does not exceed the magnitude

$$\epsilon_1 < 0.005. \quad (4.2)$$

§ 5. Application of Functions $\varphi_1(s)$ to the Strength Analysis of Shells

Reference literature contains the vast experience of the analysis of semimomentless circular shells [1], [2], and [3], for which a closed solution was obtained in infinite trigonometric series.

Due to the presence of the algorithm for calculating $\varphi_1(s)$ all of this experience is carried over to the calculation of shells with arbitrary contour of cross section, since the trigonometric functions are a particular case of $\varphi_1(s)$. The property of orthogonality of $\varphi_1(s)$ allows us to construct a process for calculating the state of strain of a shell with controlled error ϵ_1 , which is suitable for a computer. This reduces to the consecutive determination of independent i -th states of strain of a shell with subsequent summation. The latter remains on that stage, when the given accuracy $[\epsilon]$ is

attained. A block-diagram of this process is represented in Fig. 3.

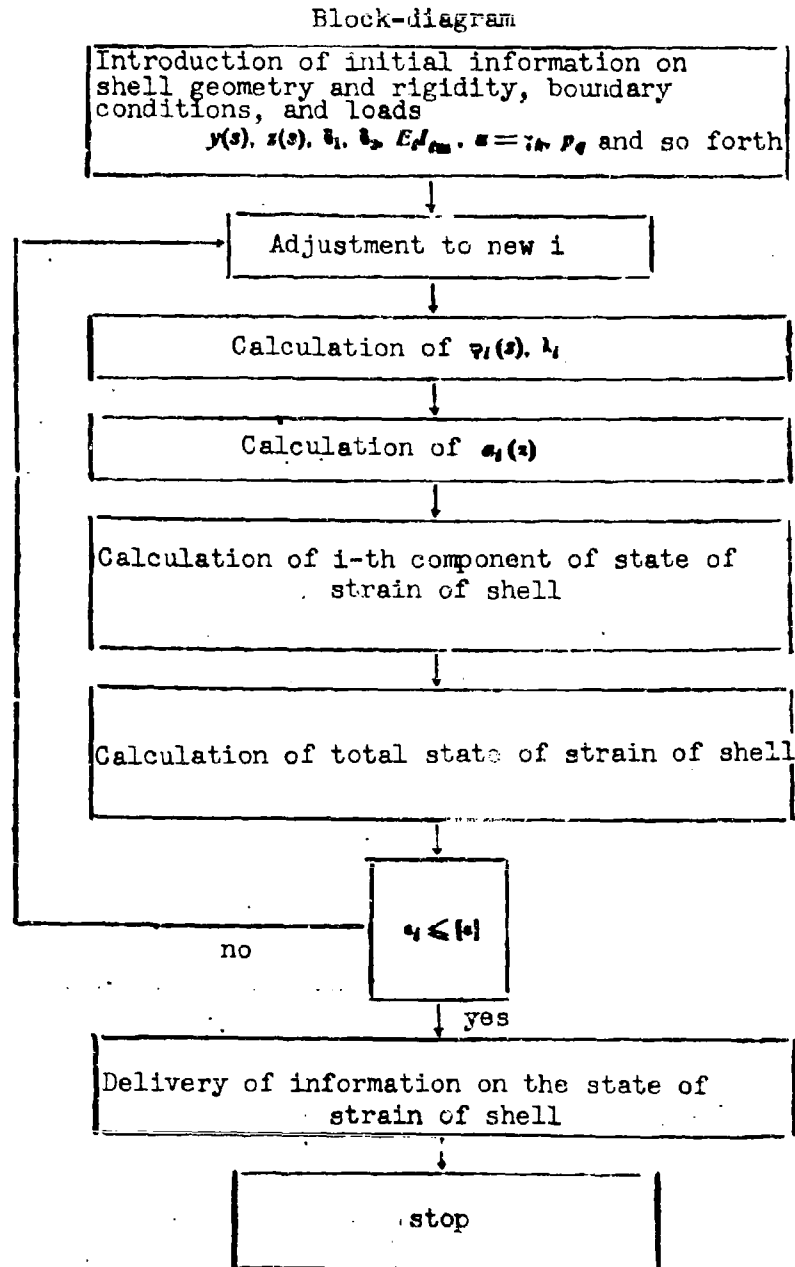


Fig. 3.

Conclusions

1. By means of isolating function $f_1(\alpha)$ (1.6) from the first quadratic shell form, we found a single solution for cylindrical and slightly conical shells.

2. We obtained and investigated a differential operator (1.18) that generates eigenfunctions of a semimomentless closed shell.

3. We constructed a generalized Green function (3.8) which makes it possible to organize an iterative process (3.3)-(3.5) for calculating characteristic numbers λ_1 and functions $\varphi_1(s)$.

4. We composed and set up a program for calculating λ_1 and $\varphi_1(s)$ for any shell whose cross section can be given tabularly.

5. Due to the orthogonality of functions $\varphi_1(s)$, system (1.15) for unknown $a_1(\alpha)$ is divided, which significantly lowers the time and effort of shell strength analysis and simultaneously increases its accuracy.

6. The results allow us effectively to use electronic computers for mechanization and automation of strength analysis of semimomentless shells with arbitrary contour of cross section.

Literature

1. S. N. Kan. Strength of closed and open cylindrical shells. Collection: "Analysis of spatial structures" edited by A. A. Umanskiy, No. 6, Gosstroyizdat, Moscow, 1961.

2. A. G. Immerman. Calculation of an orthotropic circular cylindrical shell under a lateral load. Collection: "Analysis of spatial structures" edited by A. A. Umanskiy, No. 3, Gosstroyizdat, Moscow, 1955.

3. R. A. Malakhovskiy. Calculation of circular orthotropic conical shells. IVUZ, "Aeronautical Engineering," No. 2, 1960.

4. V. Z. Vlasov. General theory shells and its application in engineering. State Press for Technical and Theoretical Literature, Moscow-Leningrad, 1949.

5. A. L. Gol'denveyzer. Theory of thin elastic shells. State Press for Technical and Theoretical Literature, Moscow, 1953.

6. V. V. Novozhilov. Theory of thin shells. Sudpromgiz, Leningrad, 1962.

7. L. A. Malashenko. Investigation of general strain of thin-walled systems on the basis of a simplifying hypothesis. "Theory of plates and shells" (Transactions of II All-Union Conference), Academy

of Sciences Ukrainian SSR, Kiev, 1962.

8. N. A. Shelomov. State of strain of thin-walled systems of variable cross section. "Theory of plates and shells" (Transactions of II All-Union Conference), Academy of Sciences Ukrainian SSR, Kiev, 1962.

9. M. A. Naymark. Linear differential operators. State Press for Technical and Theoretical Literature, Moscow, 1954.

10. E. Kamke. Hand book of ordinary differential equations. Fizmatgiz, Moscow, 1961.

11. R. Kurant and D. Gil'bert. Methods of mathematical physics. Vol. I, State Technical and Theoretical Press, Moscow-Leningrad, 1933.

Submitted
3 January 1964

EXPERIMENTAL INVESTIGATION OF THE PROPAGATION OF FAN AND PAIRED PLANE JETS IN A TRANSVERSE FLOW

Ye. V. Rzhevskiy and V. A. Kosterin

Definitions of Cyrillic Items

III = s = slot

The work indices of combustion chambers of aviation gas-turbine engines are determined not only by the regularities of the chemical reaction of fuel burning, but also to a significant extent by the aerodynamic structure of flow in the chamber. From this point of view the value of the investigations of aerodynamics of combustion chambers of gas-turbine engines can be placed on a level with the investigations of aerodynamics of compressors and turbines.

Of much value for an understanding of the operating process in gas-turbine engine combustion chambers, and also for development of new methods of organization of the process of fuel burning in an air flow, is the investigation of complex jet streams. Such streams include the propagation of fan and paired plane jets in a transverse carrier flow.

Fan and paired plane jets, which form in the exhaust of gas from a peripheral slot or two parallel, oppositely oriented, plane slots (Fig. 1), differ from single jets by their extreme "continuity."

Therefore, in the interaction with a transverse carrier flow they form "shields," behind which, just as behind poorly-streamlined bodies, there appear zones of lowered pressure with intense reverse currents. The reverse currents behind such "gas-dynamic shields" can be effectively used for flame stabilization in the combustion chambers of air-breathing jet engines [1].

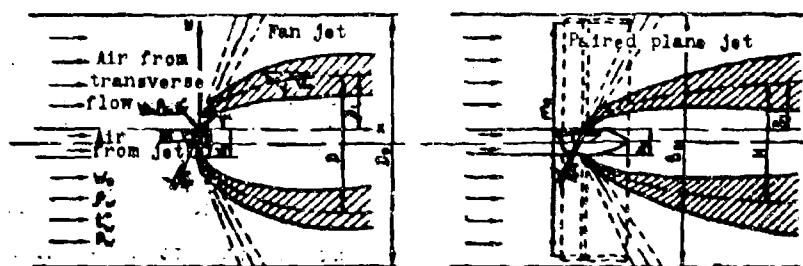


Fig. 1. Diagram of propagation fan and paired plane jets in a transverse flow.

Available experimental and theoretical material on jets that spread in a transverse flow, presented in the works of G. S. Shandorov [2], Yu. V. Ivanov [3], [4], [5], [6], and G. N. Abramovich [7], has been accumulated as a result of the investigation of single jets of different form or their combination, the structure of flow behind which essentially differs from the one under consideration.

In connection with the fact that the theoretical solution of the problem [8] of calculating the trajectories and range of fan and paired plane jets in a transverse flow contains certain, in general unknown, constants which consider the peculiarities of turbulent flow of a viscous gas, the decision was made to conduct an experimental investigation of the propagation of fan and paired plane jets in a transverse flow. This work gives certain regularities of the propagation of fan and paired plane jets in free transverse flows and those limited by walls.

Statement of the Investigation

For construction of a correct program for carrying out tests, it is necessary in the first place to establish what parameters determine the pattern of propagation of fan and paired plane jets in a transverse flow.

During the interaction of viscous gas streams, one of the characteristic criteria is the Re number. With sufficient foundation one may assume that the considered phenomenon is self-similar with respect to Re number, inasmuch as experiments with jets in a transverse flow were conducted in a range of high Re numbers ($1.50-2.33 \cdot 10^4$) which were calculated according to the speed and state of the gas at the slot exit and according to its width.

In [8] we find the theoretical obtainment of an equation for the calculation of trajectories of fan and paired plane jets in free and limited transverse flow.

On the basis of the equations it is possible to establish that the form of the axis of fan and paired plane jets in a transverse flow depends on the hydrodynamic parameter which constitutes the ratio of impact pressures of the jet and the transverse flow (Fig. 1)

$$\bar{q}_0 = \frac{\rho_v V_0^2}{\rho_w W_0^2} \quad (1)$$

where ρ_v is the density of gas of the jet,

V_0 is the jet velocity in mouth,

ρ_w is the density of gas of a transverse undisturbed flow,

W_0 is the average velocity of transverse undisturbed flow with respect to cross section;

and also the geometric characteristics of the installation:

a) width of slot b_0 ,

b) diameter of tube d_0 or height of profile h_0 ,

- c) diameter of pipe D_0 or high of plane channel B_0 ,
- d) angle of incidence of jet α .

Thus, if the geometric characteristics of the installation are given, the form of the jets in transverse flow will depend only on one magnitude, i.e., hydrodynamic parameter \bar{q}_v . In spite of the fact that the theoretical solution of the problem [8] is conducted with a number simplifying assumptions and contains unknown magnitudes, this gave us a basis, in the construction of a test program, to take \bar{q}_v to be decisive.

By means of simple transformations, equality (1) can be reduced to the form of

$$\bar{q}_v = \frac{p_o^*}{p_w} \cdot \frac{\lambda_v^3}{\lambda_w^3} \cdot \kappa(\lambda_v) \cdot \tau(\lambda_w), \quad (2)$$

where p_v^* is the total pressure in front of the slot,

p_w is the static pressure of gas of the transverse flow,

λ_v is the velocity coefficient of the jet at the slot exit,

λ_w is the velocity coefficient of the transverse flow.

Velocity coefficient λ_v depends on the ratio of pressures $\frac{p_v^*}{p_w}$ and the form of the slot channel. This article investigates convergent peripheral and plane slots with compression coefficient 5.0. With a supercritical drop of pressures the gas in the convergent slots is not completely expanded. At the slot exit, the velocity in the jet will be equal to the local speed of sound ($\lambda_v = 1$), and static pressure will be greater than static pressure in the transverse flow ($p_c > p_w$). However, we know that in such cases further expansion of gas in the jet up to $p_c = p_w$ occurs beyond the limits of the nozzle, where the jet velocity becomes supersonic ($\lambda_v > 1$).

A question arises. How do we calculate the hydrodynamic

parameter \bar{q}_v with a supercritical drop of pressures in the convergent slots? Do we calculate it according to the parameters of the not yet expanded gas at the slot exit, or according to the parameters of the completely expanded gas of jets in the flow? Examples show that \bar{q}_v for these two cases of calculation will be different.

For an answer to this question, on an installation, whose diagram and description are given below, we photographed colored fan jets in a free transverse flow, which were obtained at identical values of hydrodynamic parameter \bar{q}_v , but with a different drop of pressures in the slot (and correspondingly different velocity coefficients λ_w). For some jets the pressure drops in the slots were subcritical and for others, supercritical. The external boundaries of the fan jets in dimensionless coordinates $\frac{x}{b_0}$ and $\frac{y}{b_0}$ are represented in Fig. 2.

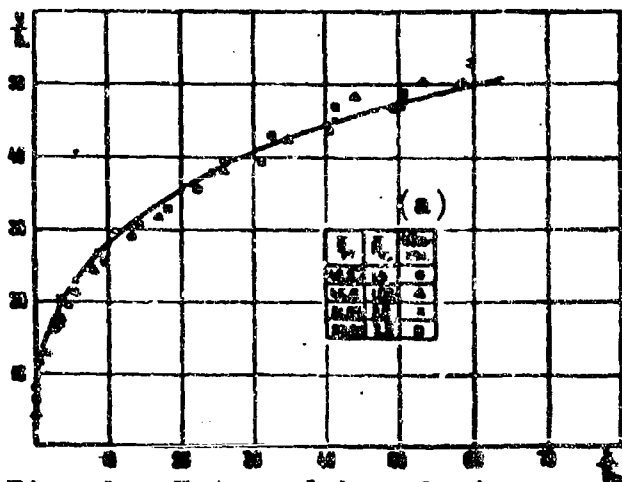


Fig. 2. External boundaries subsonic and supersonic fan jets at identical \bar{q}_v .

KEY: (a) designation.

The jet boundaries completely coincide if \bar{q}_v is calculated according to the parameters of completely expanded gas with any drop of pressures in the slots. The coincidence of jet boundaries gives us a basis to consider that the jet axes also coincide.*

Therefore, subsequently in formula (2) we determined λ_v for magnitude $\frac{p_v^*}{p_w}$ on the assumption

of full adiabatic expansion of gas in the jet:

$$\frac{p_v^*}{p_w} = \left(\frac{p_v}{p_w} \right)^{\frac{\gamma}{\gamma-1}} \quad (3)$$

Additional experiments confirmed that the trajectories of jet axes measured by four-channel rotary tubes at identical \bar{q}_v , but different $\frac{p_v^}{p_w}$, coincide.

Thus, \bar{q}_v is a function of two magnitudes: $\frac{p_v^*}{p_w}(\lambda_v)$ and λ_w .

Investigations were conducted with a change of hydrodynamic parameter \bar{q}_v in a range from 8 to 420.

The basic experiments were set up with values of \bar{q}_v that are the most characteristic for combustion chambers with gas-dynamic flame stabilization (in a range from 14 to 68). The limits of change of the ratios of velocities, temperatures, and pressures in the jet and in the transverse flow were selected taking into account the technical possibilities of the experimental installation:

$$1) \frac{V_0}{W_0} = 3-6 \text{ (in separate experiments up to 13),}$$

$$2) \frac{T_v^*}{T_w^*} = 0.65-1.0,$$

$$3) \frac{p_v^*}{p_w} = 1.2-3.1.$$

The absolute values of velocities varied within the following limits: $V_0 = 124-406$ m/sec, $W_0 = 60$ m/sec. The angle of incidence of jets was assumed to be constant and equal to 90° .

Description of Experimental Installation and Method of Measurements

A diagram of the experimental installation is shown in Fig. 3. The installation consists of two ducts — high and low pressure — and the nozzle to be investigated with slot 6. Air as low pressure, which forms the transverse carrier flow, was moved by compressor 1 through heat exchanger 2, in which it was heated by gases after combustion chamber 5. The flow rate of air through the low-pressure duct was measured by standard nozzle 18. Change of flow rate of air and correspondingly, the velocity of the transverse flow, was attained

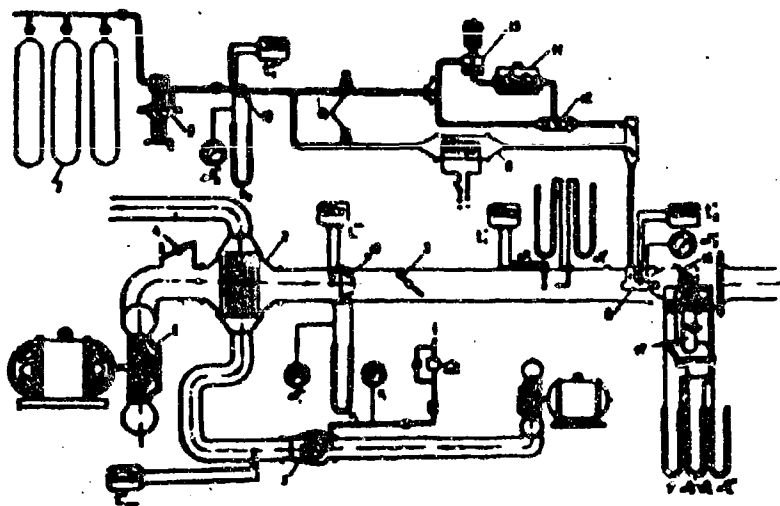


Fig. 3. Diagram of experimental installation.

by flaps 3 and 4. Air of high pressure, which forms the investigated jet, proceeded to the nozzle from receiver 7 through reducer 9 and throttle cock 10. The flow rate air was measured by diaphragm 19. Heating of the high-pressure air was

carried out in electric heater 8. Air pressure through the ducts high and low pressure was measured by piezometers and manometers. Air temperature was determined with the help of thermocouples. Measurement of velocities and pressures in the zone of interaction of jets with transverse flow was produced by a four-channel rotary tube 16 with a diameter of 3.8 mm and fixed on coordinator 17.

Temperature of gas in the zone of interaction was measured by a chromel-drop thermocouple attached to the tube in such a way that the joint of the thermocouple was near the tube spout. Thickness of wire of the thermocouple was 0.4 mm and diameter of the joint was 0.8 mm. For coloring the jet during the photographing there was a device, consisting of an atomizer 11, ejector 12, and pneumatic cutoff valve 13. Coloring of jets was produced by aluminum dust. The jets were photographed on the background of the sieve-like shield which made it possible to obtain a quantitative dependence between coordinates of the jet boundaries.

We investigated two types of slots, i.e., peripheral convergent

slots having a width of $b_0 = 0.6, 0.8,$ and 1.12 mm which were made on tubes with diameters of $d_0 = 21$ and 30 mm, and paired plane slots with a width of $b_0 = 0.5$ mm which were made on a streamlined profile with a height of $h_0 = 9$ mm. For decreasing air leakage, on the ends of the plane nozzle we placed limiting washers. During tests in a limited transverse flow, the nozzle with a peripheral slot was placed in a cylindrical pipe with a diameter of 200 mm. Correspondingly, the plane nozzle was placed in a 175×178 mm rectangular pipe. The walls of the pipes had windows for introduction of the measuring instrument. For photographing the colored jets in the limited flow we made a set of pipes with transparent walls.

Results of Experiments

Trajectories of jets. One of the basic problems of this investigation was finding experimental equations of the trajectories of fan and paired plane jets in free and limited transverse flows. As the jet trajectories we conditionally selected the geometric places of points of maximum velocities in the jets. In Figures 4 and 5, in dimensionless coordinates, we have constructed the trajectories of fan and paired plane jets in a free transverse flow with different values of hydrodynamic parameter \bar{q}_v . Introduction of dimensionless coordinates allowed us to generalize, at constant \bar{q}_v , the trajectories of the jets flowing from slots of different width b_0 (curves 4.5). On the other hand, from the curves it is clear that bending of the axis of the jets essentially depends on \bar{q}_v . The smaller \bar{q}_v is, the greater the bending of the jets.

However, the same magnitude of \bar{q}_v may be obtained at different temperatures of the jet and transverse flow. In order to compare

the propagation of hot and cold jets in the free transverse flow, we photographed the external boundaries of fan jets with different ratios of $\frac{T_V^*}{T_W^*}$ (Fig. 6).

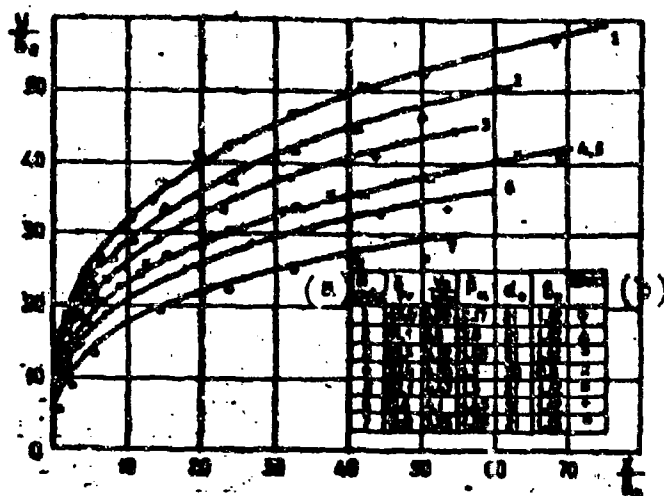


Fig. 4. Trajectories of fan jets when $\alpha = 90^\circ$. Solid lines signify the trajectories obtained with equation (4).
KEY: (a) curve number; (b) designation.

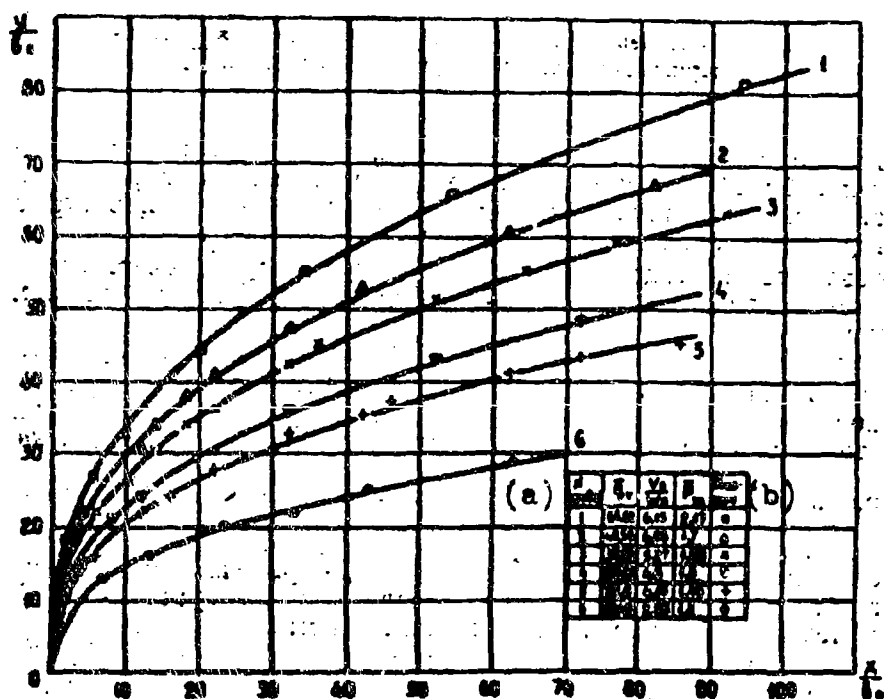


Fig. 5. Trajectories of paired plane jets when $\alpha = 90^\circ$. Solid lines signify the trajectories obtained with equation (5).
KEY: (a) curve number; (b) designation.

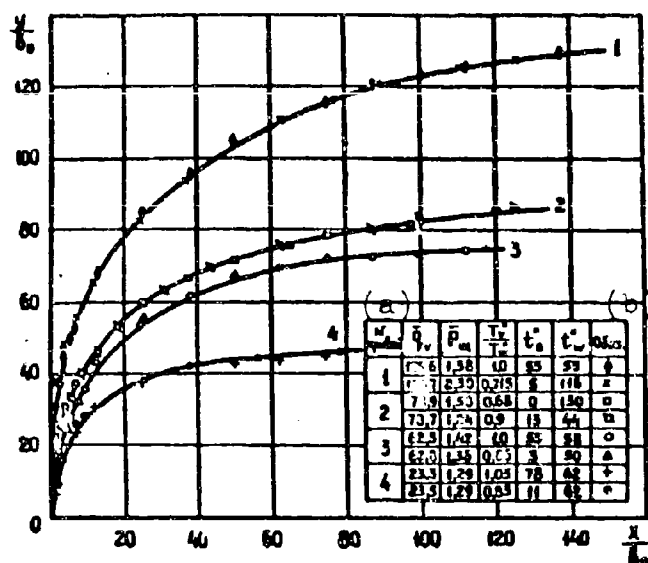


Fig. 6. Comparison of external boundaries of isothermal and non-isothermal fan jets at identical \bar{q}_v . KEY: (a) curve number; (b) designation.

range of change of temperatures. They established that bending of the axis of the jets does not depend on the temperatures of the gas in the jet and in the flow if treatment of the results of experiments is produced according to hydrodynamic parameter \bar{q}_v which considers the change in density of the gas of the jet and flow depending upon temperature.

Earlier it was shown (Fig. 2) that the boundaries and trajectories of the jets also coincide at identical \bar{q}_v calculated with respect to parameters of a completely adiabatically expanded gas in a jet, independently of the actual conditions of expansion of the gas in the slot and on the fact that at any pressure ratios $\frac{p_v^*}{p_w}$ and velocity coefficients λ_w , this magnitude of \bar{q}_v is obtained.

Consequently, the basic parameter that determines the form of the axis of the fan and paired plane jets in free transverse flows and those limited by walls with the given geometric characteristics of the installation is hydrodynamic parameter \bar{q}_v .

From the curves of Fig. 6, it is clear that the external boundaries, and consequently also the axes of the fan jets, plotted at different $\frac{T_v^*}{T_w}$, but at constant \bar{q}_v , coincide. Yu. V. Ivanov [3], [6] and G. S. Shandrov [2] conducted a similar experiment on single circular and plane jets in a wider

As a result of treatment of experimental data, in logarithmic coordinates we obtained the following experimental equation of trajectories of fan jets spreading in a free transverse flow at an angle of attack $\alpha = 90^\circ$ in the range of change of $\bar{q}_v = 14-65$:

$$\frac{x}{b_0} = 0.024 \left(\frac{y}{b_0} \right)^{2.3} \cdot \frac{1}{\bar{q}_v^{1.3}}. \quad (4)$$

Correspondingly, the trajectory equation of paired plane jets developed in a free transverse flow at $\alpha = 90^\circ$ and with a change of $\bar{q}_v = 10.5-66$ has the form of

$$\frac{x}{b_0} = 0.192 \left(\frac{y}{b_0} \right)^{2.6} \cdot \frac{1}{\bar{q}_v^{1.5}}. \quad (5)$$

Analysis of the trajectories of fan and paired plane jets in a limited transverse flow, constructed in dimensionless coordinates $\frac{x}{b_0}$ and $\frac{y}{b_0}$, shows that the form of the jet axis, just as in a free transverse flow, essentially depends on the magnitude of \bar{q}_v .

A comparison of the trajectories of jets at identical values of determining parameter \bar{q}_v in free and limited flows shows that bending of jets in flows limited by walls is greater (Fig. 7). The distinction in jet trajectories is explained by the fact that fan and paired plane jets in a limited transverse flow, in forming a "shield," they cover part of the passage section of the channel. As a result, the velocity of the carrier flow in this place is increased. In turn the increase of velocity, and consequently also impact pressure, increases bending of the fan or paired plane jet in the transverse flow. From Fig. 7 it is also clear that the distinction in trajectories of fan jets decreases with the decrease of \bar{q}_v , which can be explained by the decrease of the degree of covering the channel by the "dome" of the fan jet. With the degree of covering the channel $\delta = 0.18$ the distinction in trajectories of fan jets in free

and limited flow ceases to be noticeable. Here and subsequently the degree of covering δ is calculated as the ratio of the area occupied by the jet in the channel in transverse direction and taken on the center line of the jet to the entire area of cross section of the channel.

Experiments with fan jets in a limited transverse flow were conducted with a change of the degree of covering of the channel from

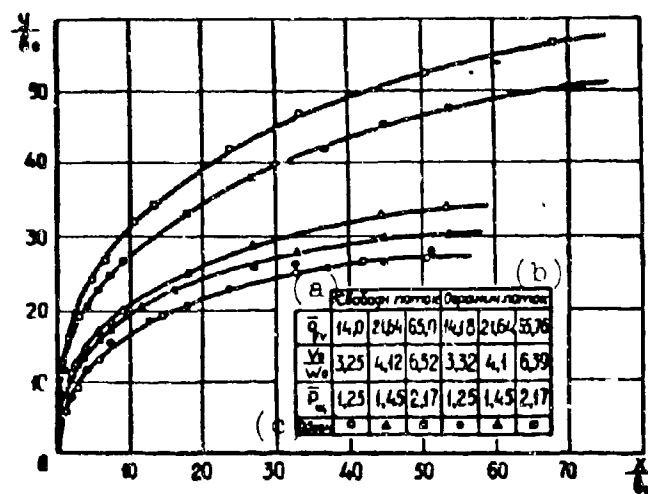


Fig. 7. Comparison of trajectories of fan jets in free and limited flows.
KEY: (a) free flow; (b) limited flow; (c) designations.

0.18 to 0.70 (in the range of $\bar{q}_v = 14.6-103.6$) and with paired plane jets from 0.22 to 0.56 (with $\bar{q}_v = 14.3-109.6$).

As a result of treatment of experimental data we obtained an equation for calculation of the trajectories of fan jets in a limited flow when $\alpha = 90^\circ$:

$$\frac{x}{b_0} = 0,02 \left(\frac{y}{b_0} \right)^{1,3} \cdot \frac{1}{\bar{q}_v^{1,16}}. \quad (6)$$

For paired plane jets in a limited transverse flow the trajectory equation has the form of:

$$\frac{x}{b_0} = 0,16 \left(\frac{y}{b_0} \right)^{2,8} \cdot \frac{1}{\bar{q}_v^{1,35}}. \quad (7)$$

Range of jets. We shall introduce, for estimating the range of a fan jet in a transverse, the concept of the hydraulic dome diameter, i.e., D (Fig. 1) which may be expressed as

$$D = d_0 + 2D_1$$

or in relative magnitudes

$$\bar{D} = \bar{d}_0 + 2\bar{D}_1. \quad (8)$$

$\bar{d}_0 = \frac{d_0}{b_0}$ is the relative diameter of the tube on which a peripheral slot is made,

$\bar{D}_1 = \frac{D_1}{b_0}$ is the range of a branch of the fan jet, referred to the width of the slot b_0 .

The range of a branch of the fan jet D_1 is defined as the distance from the mouth of the jet in the direction of axis y to a point on the axis in which the projection of the axial velocity on axis y ($V_m \cos \varphi$) is equal to zero, i.e., when the jet axis becomes parallel to axis x .

Figure 8 gives graphs of the change of the projection of axial velocity of the fan jet in a free transverse flow on axis y depending upon relative coordinate $\frac{y}{b_0}$ at different values of determining parameter \bar{q}_v . After treatment of experimental data taken from the graph, in logarithmic coordinates, and substitution in (8), we obtain the following equation for determination of the hydraulic dome diameter of the fan jet in a free transverse flow when $\alpha = 90^\circ$:

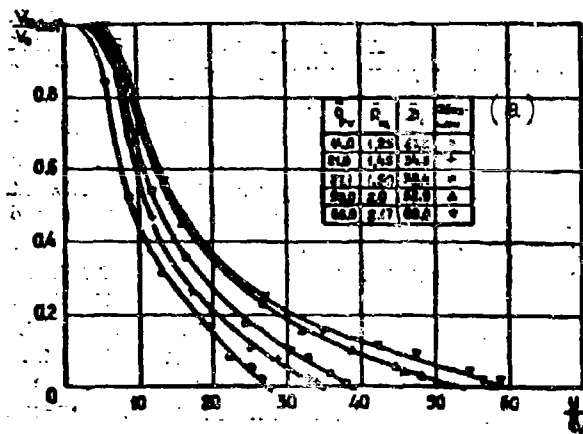


Fig. 8. Change of projections of axial velocities of fan jets in a free transverse flow.
KEY: (a) designations.

$$\bar{D} = \bar{d}_0 + 14.0 \cdot \bar{q}_v^{0.53} \quad (9)$$

We analogously obtain an equation for calculation of hydraulic dome diameter of a fan jet in a limited flow in a range from 0.18 to 0.50 (with $\bar{q}_v = 14.2-65.8$) in the form of:

$$\bar{D} = \bar{d}_0 + 18.7 \bar{q}_v^{0.42} \quad (10)$$

The range of paired plane jets in a transverse flow will be condi-

tionally estimated as the "height of the hydraulic profile" $H = n_0 + 2D_1$ (Fig. 1) or in relative magnitudes

$$\bar{H} = \bar{h}_0 + 2\bar{D}_1 \quad (11)$$

where $\bar{h}_0 = \frac{h_0}{b_0}$ is the relative height of the profile on which plane slots are made,

$\bar{D}_1 = \frac{D_1}{b_0}$ is the relative range of one branch of a paired plane jet, counted off from the mouth of the slot in the direction of axis y to a point on the axis in which the jet is parallel to axis x. Magnitudes \bar{D}_1 were measured on the graph in Fig. 9 as segments on the axis of abscissas. Treatment of the results obtained in logarithmic coordinates depending upon \bar{q}_v and substitution in (11) led to the following equation for calculation of the height of the hydraulic profile of a paired plane jet in a free transverse flow when $\alpha = 90^\circ$:

$$\bar{H} = \bar{h}_0 + 24,8 \cdot \bar{q}_v^{0,48}. \quad (12)$$

We analogously obtain an equation for calculation of \bar{H} of a paired plane jet in a limited transverse flow in the range of $\delta = 0.27-0.43$ (when $\bar{q}_v = 22-65.6$)

$$\bar{H} = \bar{h}_0 + 20,8 \bar{q}_v^{0,5}. \quad (13)$$

It is simple to establish (for instance with Fig. 7) that the range of fan and paired plane jets in a limited flow is less than in a free flow. The difference in ranges increases with the increase of the degree of covering of the channel δ .

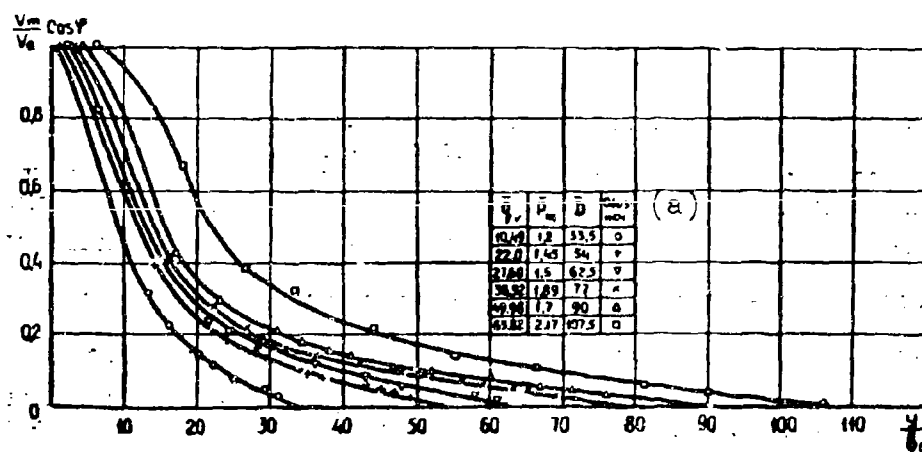


Fig. 9. Change of projections of axial velocities of paired plane jets in a free transverse flow.
KEY: (a) designation.

Change of axial velocity. Thus, just as for circular and rectangular jets in a transverse flow [6], the change of maximum axial velocities of fan and paired plane jets in a transverse flow depends on the relation of velocities (or relation of impact pressures) of the jet and flow. Figure 10 represents a graph of the change of $\frac{V_m}{V_0}$ along the axis of a fan jet in a free flow.

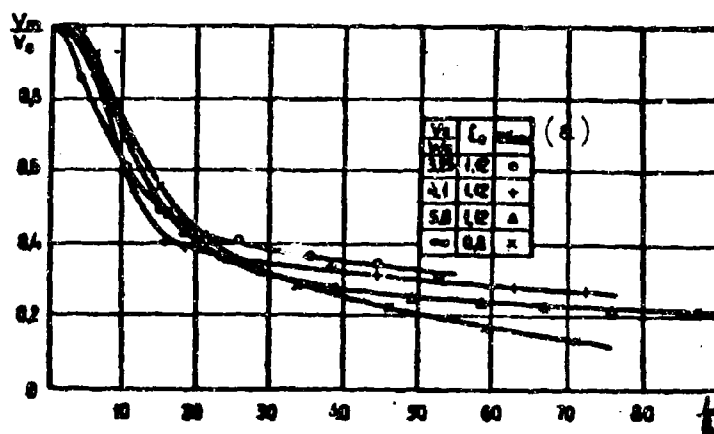


Fig. 10. Change of relative velocity along the axis of fan jets in a free transverse flow.
KEY: (a) designation.

Here V_m is the maximum jet velocity in a given section,

V_0 is the jet velocity at the slot exit.

Analogous curves are obtained for paired plane jets. From the graph it is clear that a change in axial velocity occurs faster the smaller the ratio of velocities $\frac{V_0}{W_0}$ (i.e., the greater the relative velocity of the carrier flow $\frac{W_0}{V_0}$). With larger $\frac{W_0}{V_0}$ there occurs more intense washout and ablation of gas from the external boundaries of the fan jet due to the turbulent pulsations of the transverse flow, which also leads to a more intense drop in gas velocity on the axis of the jet. Each of the curves on the graph tends to a definite limit which is equal to $\frac{W_0}{V_0}$.

Analysis of Results and Comparison with Results of Works by Other Authors

As already noted, fan and paired plane jets in a transverse flow differ from single circular and plane jets by the fact that behind them there will form a zone of rarefaction with intense reverse currents. Furthermore, during expiration of jets into a flow limited by walls, as a result of covering the channel we observe acceleration of the external flow. Along with the relation of impact pressures and geometric characteristics of the installation, the rarefaction and reverse currents behind the jets, and also the local acceleration of the external flow, render an additional influence on the trajectories and ranges of fan and paired plane jets in a transverse flow. Therefore, it is of practical interest to establish the distinction of trajectories of fan and plane jets from the trajectories, for instance, of single plane jets, which was investigated in detail by Yu. V. Ivanov [5], [6].

As a result of treatment of experiments with subsonic plane jets in a subsonic transverse flow in the range of $\bar{q}_v = 12.5-400.0$, Yu. V. Ivanov recommends the following equation for calculation of the trajectory of plane jets at $\alpha = 90^\circ$:

$$\frac{x}{b_0} = 1.9 \left(\frac{x}{b_0} \right)^{2.5} \cdot \frac{1}{\bar{q}_v}.$$

With the mean value of the coefficient of the jet structure $\alpha = 0.10$ we will obtain:

$$\frac{x}{b_0} = 0.03 \left(\frac{x}{b_0} \right)^{2.5} \cdot \frac{1}{\bar{q}_v}.$$

Fig. 11 compares the trajectories of fan, paired, and single plane jets in a free transverse flow at identical \bar{q}_v . From the graph it is clear that the trajectory of the fan jet is more distorted and the trajectory of the single plane jet, less than the others. The

large distortion of the fan jet may be explained by the large degree of rarefaction behind the jet and by the corresponding large drop in pressures acting on the elements of the jet. From what has been said it follows that the relative range (range referred to width of slot) of fan jets will be less than the range of paired plane jets and all the more so of single plane jets.

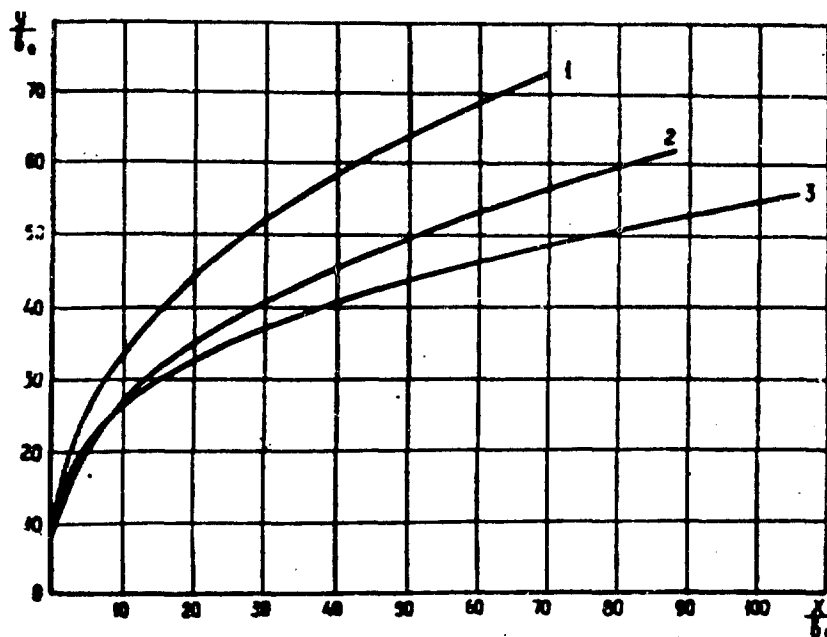


Fig. 11. Comparison of trajectories of fan, paired, and single plane jets in a free transverse flow at identical values of determining parameter $\overline{q}_v = 39.0$. Curve 1 is constructed according to Yu. V. Ivanov's equation for single plane jets. Curve 2 is the paired plane jet. Curve 3 is the fan jet.

Conclusions

1. This work experimentally proves that the trajectories and ranges of both subsonic and supersonic fan and paired plane jets in a subsonic transverse flow with given geometric characteristics of the installation are completely determined by the hydrodynamic parameter

$$\overline{q}_v = \frac{\rho_v V_0^2}{\rho_w W_0^2}, \text{ which is calculated according to the parameters of a}$$

completed expanded gas of high pressure.

2. It was determined that for jets flowing at an angle of 90° to the transverse flow with a small supercritical drop in pressures in the slot (up to $\frac{p_v^*}{p_w} = 3.1$) it is not necessary that the gas be completely expanded in the slot (that is, it is possible to limit ourselves to a convergent peripheral or plane slot). Additional expansion of gas beyond the limits of the slot will increase the breakthrough ability of the jet in a transverse flow to a magnitude that is close to the rated valve with full adiabatic expansion.

2. [3 sic] experimental equations (4), (5), (6), and (7) were obtained for calculation of trajectories of fan and paired plane isothermal and nonisothermal turbulent jets spreading in free and limited transverse flows.

3. [4 sic] for calculation of the jet range, experimental equations (9), (10), (12), and (13) are recommended.

Literature

1. Yu. K. Zastela, V. A. Kosterin, E. A. Petrov, Ye. V. Rzhnevskiy, A. Ya. Khismatullin, A. A. Bulavkin, A. G. Yevtyugin, V. P. Smirnov, A. V. Shipulina and L. G. Miropol'skaya. Methods of stabilizing the zone of burning in combustion chambers of air-breathing jet engines. Bulletin of Inventions, No. 16, 1960.

2. G. S. Shandorov. Flow from a channel into a motionless and moving medium. ZhTF, Vol. XXVII, No. 1, 1957.

3. Yu. V. Ivanov. Certain regularities of a free circular jet developed in an external transverse flow. News of the Academy of Sciences USSR, OTN, No. 8, 1954.

4. Yu. V. Ivanov. Investigation of trajectories of circular turbulent jets developed in a limited transverse flow. News of the Academy of Sciences USSR, OTN, No. 3, 1957.

5. Yu. V. Ivanov. A plane jet in an external transverse flow. News of the Academy of Sciences of the Estonian SSR, Vol. II, No. 2, 1953.

6. Yu. V. Ivanov. Effective burning substratum combustible gases in furnaces. EGI, 1958.

7. G. N. Abramovich. Theory of turbulent jets. Fizmatgiz, 1960.

8. V. A. Kosterin and Ye. V. Rzhevskiy. The calculation of trajectory and range of fan and paired plane jets in a limited transverse flow. IVUZ, "Aeronautical Engineering," No. 1, 1964.

Submitted
20 August 1963

METHOD OF SUPERSONIC ANALOGY FOR CALCULATION OF ONE-DIMENSIONAL NON-STATIONARY GAS FLOWS

A. P. Pudoveyev

Definitions of Cyrillic Items

$\pi = p$ = piston

$\kappa p = \text{crit}$ = critical

Designations

x, x_0, x_k — coordinates of points of flow,

x_p, x_{pt} — piston coordinates,

y — coordinate,

t, t_0, t_1 — time,

v, v_{\max} — velocity of flow,

v_p, v_{pt} — velocity of piston,

c, c_0, c_{crit} — local speeds of sound,

\bar{c} — speed scale,

p, p_0 — pressure in flow and stagnation pressure,

k — isentropic index,

n — exponent,

f — designation of function,

T, T_0 — temperature in flow and stagnation temperature,

X, X_p — dimensionless coordinates of points of flow and piston,
 U, U_p — dimensionless velocities of points of flow and piston,
 δ — angle of revolution of supersonic flow,
 $\theta, \theta_{crit}, \theta_{max}$ — angles tangent to the graph of piston trajectory,
 λ — velocity coefficient,
 ξ — variable,
 ρ, ρ_0 — density in flow and stagnation density,
 φ — angle of inclination of characteristic in supersonic flow,
 $\psi, \psi_0, \psi_k, \psi_{crit}, \psi_{max}$ — angles of inclination of characteristic in non-stationary flow,
 π — π number,
 a — coefficient.

The general solution for a one-dimensional transient flow of an ideal gas [1] contains an arbitrary function of velocity $f(v)$ which can be comparatively easily determined only for simple boundary and initial conditions. Here we shall consider the methods of solving the boundary value problem with the use of a supersonic analogy which makes it possible to conduct calculations of non-stationary flows under more complicated boundary conditions than permitted by the known methods, and also a generalized form of the solution in dimensionless magnitudes.

The analogy between transient flow in a plane x, t (time coordinate) and supersonic flow in a physical plane x, y consists in that the potential equations for these two forms of motion are equations of the hyperbolic type [2] and consequently, both flows have characteristics.

This analogy recently has been frequently used for a qualitative analysis and graphic representation of various cases of interaction of waves (both shock and rarefaction waves) [3].

But on this analogy there may also be based the determination of the quantitative aspects, and also the development of a method for calculation of non-stationary flows.

We shall compare a simple case of transient motion — self-similar — the so-called centered flow with a supersonic flow around the

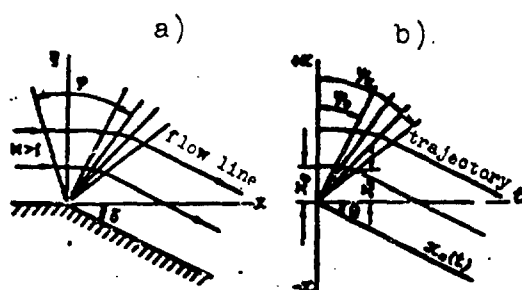


Fig. 1. a) Supersonic flow around a corner; b) centered flow.

exterior of a corner (Prandtl-Meyer flow) (Fig. 1).

In the Prandtl-Meyer flow a change in the state of the gas occurs on the expansion fan. The parameters of the gas on each of the fan characteristics depend on the angle of its inclination φ , in

particular, and the velocity coefficient λ is determined by the relationship:

$$\lambda^2 = \left(\frac{v}{c_{sp}} \right)^2 = 1 + \frac{2}{k-1} \sin^2 \left(\sqrt{\frac{k-1}{k+1}} \varphi \right).$$

The parameters of the gas can be determined with the help of gas-dynamic functions:

$$\begin{aligned} \frac{T}{T_0} &= 1 - \frac{k-1}{k+1} \lambda^2, \\ \frac{\rho}{\rho_0} &= \left(1 - \frac{k-1}{k+1} \lambda^2 \right)^{\frac{1}{k-1}}, \\ \frac{p}{p_0} &= \left(1 - \frac{k-1}{k+1} \lambda^2 \right)^{\frac{k}{k-1}}. \end{aligned}$$

The angle of inclination of characteristic φ is simply connected with the local flow angle of rotation δ .

The centered flow [4] constitutes a wave of rarefaction which appears in the gas during motion of a piston with constant velocity $v^p = \text{const}$. On each of the characteristic lines $\xi = \frac{x}{t} = \text{const}$ the parameters of the gas are constant. The basic relationships for a self-similar flow are

$$v = t - c, \quad (1)$$

$$v = \frac{2}{k-1}(c - c_0), \quad (2)$$

where c_0 is the speed of sound for a motionless gas.

By analogy with the Prandtl-Meyer flow we will establish a connection for the centered flow between the angle of inclination of characteristic ψ and the parameters of the state of the gas on it.

For determination of angle ψ we will introduce into consideration the distance, which proportional to time, while the proportionality factor — speed \bar{c} — remains indefinite. Then (Fig. 1)

$$\tan \psi = \frac{\bar{c}t}{x} = \frac{\bar{c}}{\xi}, \quad (3)$$

whence, $\xi = \frac{\bar{c}}{\tan \psi}$ and from (1)

$$c = t - v = \frac{\bar{c}}{\tan \psi} - v.$$

Placing the obtained expression of c in (2), after transformations we have:

$$v = \frac{2}{k+1}c_0\left(\frac{\bar{c}}{c_0 \tan \psi} - 1\right).$$

Selecting

$$\bar{c} = c_0, \quad (4)$$

we will finally obtain the expression of velocity:

$$v = \frac{2}{k+1}c_0\left(\frac{1}{\tan \psi} - 1\right). \quad (5)$$

The limits of change of angle ψ :

- 1) $v = 0$, $\operatorname{tg} \psi_0 = 1$, $\psi_0 = \frac{\pi}{4}$,
- 2) $v = c_{\text{cr}} = -\frac{2}{k+1} c_0$, $\operatorname{tg} \psi_{\text{cr}} = \infty$, $\psi_{\text{cr}} = \frac{\pi}{2}$,
- 3) $v = v_{\text{max}} = -\frac{2}{k-1} c_0$, $\operatorname{tg} \psi_{\text{max}} = -\frac{k-1}{2}$.

Using (5) and the expression for critical speed, we shall establish a relationship between the velocity coefficient λ and the angle of inclination of the characteristic ψ :

$$\lambda = \frac{v}{c_{\text{cr}}} = 1 - \frac{1}{\operatorname{tg} \psi}. \quad (6)$$

Converting dependence (2) and using the isentropic relationship, we will obtain the expressions of gas-dynamic functions for calculation of non-stationary gas flows:

$$\frac{r}{r_0} = \left(1 - \frac{k-1}{k+1} \lambda\right)^2, \quad \frac{p}{p_0} = \left(1 - \frac{k-1}{k+1} \lambda\right)^{\frac{2}{k-1}}, \quad \frac{\rho}{\rho_0} = \left(1 - \frac{k-1}{k+1} \lambda\right)^{\frac{2k}{k-1}}. \quad (7)$$

Relationship (5) is a differential equation of the trajectories of particles of flow in plane x, t

$$\frac{dx}{dt} = v = \frac{2}{k+1} c_0 \left(\frac{1}{\operatorname{tg} \psi} - 1 \right) = \frac{2}{k+1} c_0 \left(\frac{x}{c_0 t} - 1 \right),$$

by integrating which, we will obtain

$$x = \frac{k+1}{k-1} x_0 \left(\frac{t}{t_0} \right)^{\frac{2}{k+1}} \left[1 - \frac{2}{k+1} \left(\frac{t}{t_0} \right)^{\frac{k-1}{k+1}} \right] \text{ for } t > t_0,$$

where x_0 is the coordinate of a particle in undisturbed gas,

$t_0 = \frac{x_0}{c_0}$ is the moment of the beginning of its motion.

Considering that $\tan \psi_0 = 1$, we have

$$\frac{t}{t_0} = \frac{x}{x_0} \operatorname{tg} \psi,$$

then

$$x = x_0 \frac{1}{\operatorname{tg} \psi} \left[\frac{k-1}{k+1} \left(\frac{2}{k-1} + \frac{1}{\operatorname{tg} \psi} \right) \right]^{-\frac{k+1}{k-1}}. \quad (8)$$

The equation of trajectories (8) also determines the position of a particle in the moment of passage of the rear boundary of the front of the rarefaction wave. The particle in this moment attains a velocity equal to the velocity of the piston $v = v_p$; then from (5):

and

$$\frac{1}{\lg \psi_x} = 1 + \frac{k+1}{2} \cdot \frac{v_n}{c_0}$$

$$x_x = x_0 \left(1 + \frac{k+1}{2} \cdot \frac{v_n}{c_0} \right) \left(1 + \frac{k-1}{2} \cdot \frac{v_n}{c_0} \right)^{-\frac{k+1}{k-1}} \quad (9)$$

Expressions (5) and (6) constitute the general solution. The boundary conditions are given the law of motion of the piston $x_p(t)$ or, the very same, by angle θ which is the analog of the angle of rotation of supersonic flow in the Prandtl-Meyer flow.

We shall establish a connection between angle θ and the angle of inclination of characteristic ψ .

From Fig. 1, as earlier, we have

$$\lg \theta = \frac{x_n}{ct} = \frac{v_n}{c},$$

or, considering (4),

$$\lg \theta = \frac{v_n}{c_0}. \quad (10)$$

The limits of change of angle θ :

- 1) $v_n = 0$, $\lg \theta = 0$, $\theta = 0$,
- 2) $v_n = c_{xp}$, $\lg \theta_{xp} = -\frac{2}{k+1}$,
- 3) $v_n = v_{max}$, $\lg \theta_{max} = -\frac{2}{k-1}$.

Inasmuch as the velocity on the final characteristic is equal to the velocity of the piston ($v = v_p$), by using dependence (5) we will obtain the sought relationship:

$$\frac{1}{\lg \psi} = 1 + \frac{k+1}{2} \lg \theta, \quad (11)$$

The coefficient of velocity λ can be directly expressed through

$$\lambda = -\frac{k+1}{2} \operatorname{tg} \theta. \quad (12)$$

Let us note that with the selected reference system angle θ and $\tan \theta$ are negative magnitudes.

These relationships at a constant velocity of piston motion ($\theta = \text{const}$) make it possible to determine the parameters of gas flow as functions of the magnitude of the angle of inclination of the characteristic in plane x, t , and in particular, to determine the distribution of parameters on the wave of rarefaction ($\psi_0 < \psi \leq \psi_K$) in an arbitrary moment of time t_1 . The position of the point of flow which has definite values of parameters ($\psi = \text{const}$) in this moment of time is determined by the following dependence:

$$x = \frac{c_0^2 t_1}{\operatorname{tg} \psi}. \quad (13)$$

The analogy between a flat supersonic flow around a convex wall and the pattern of non-stationary motion of a gas with the accelerated law of motion of a piston (Fig. 2) allows us to use the relationships obtained for determination of gas parameters under arbitrary boundary conditions up to the appearance of a shock wave in the flow (during deceleration of the piston).

Every point of curve $x_p(t)$ generates a characteristic whose angle of inclination is determined by the value of the piston velocity in the corresponding moment of time:

$$\operatorname{tg} \psi = \frac{1}{1 + \frac{k+1}{2} \cdot \frac{v_p}{c_0}}.$$

On each of the characteristics the values of the parameters of flow are determined by dependences (5), (6), and (7).

A practically important problem is the determination of the distribution parameters along the length of flow in the considered general case. This makes it necessary to know through what point

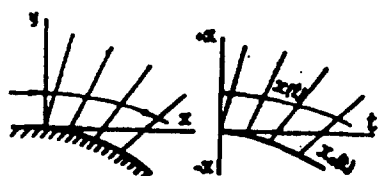


Fig. 2.

of flow in a given moment of time t_1 passes that or another characteristic which carries definite values of parameters.

From Fig. 3 it follows:

$$x = \frac{c_0(t_1 - t)}{\tan \psi} + x_{pt}. \quad (14)$$

Here x_{pt} and ψ correspond to an arbitrary moment in time $0 \leq t \leq t_1$, where x_p is negative.

Thus, in the arbitrary law of piston motion the determination of distribution of parameters along the length of flow is produced in the following order:

1) for consecutive moments t we determine v_{pt} , x_{pt} , and the corresponding values of the angle of inclination of the characteristic ψ ,

2) in the needed moment of time t_1 , according to (14) we find the coordinate of the point of flow which has a velocity v_{pt} , and

we determine the regularity of $v =$
 $= f(x)_{t_1} = \text{const},$

3) with the help of (6) and (7) we find the regularities of distribution of the remaining parameters.

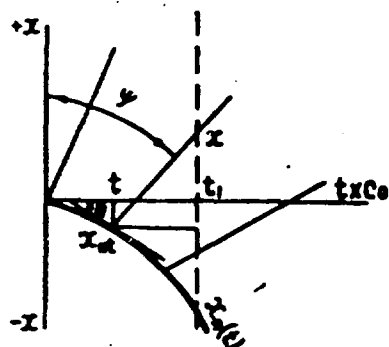


Fig. 3.

The relationship between the coordinate

of an element of flow, its velocity, and

time may be obtained in clear form. From (5) and (14) we have:

$$\frac{1}{\tan \psi} = 1 + \frac{k+1}{2} \cdot \frac{v_{pt}}{c_0},$$

$$\frac{1}{\tan \psi} = \frac{x - x_{pt}}{c_0(t_1 - t)}.$$

Equating the right sides, we will obtain:

$$1 + \frac{k+1}{2} \cdot \frac{v_{st}}{c_0} = \frac{x - x_{st}}{c_0(t_1 - t)}.$$

Thus, the solution may be represented by a system of equations [1]:

$$\begin{aligned} x &= x_{st} + (t_1 - t) \left(c_0 + \frac{k+1}{2} v_{st} \right), \\ v &= v_{st}. \end{aligned} \quad (15)$$

We shall convert the system of equations (15) to dimensionless form:

$$\begin{aligned} x &= x_{st} + c_0 t_1 \left(1 - \frac{t}{t_1} \right) \left(1 + \frac{k+1}{2} \cdot \frac{v}{c_0} \right), \\ \frac{x}{c_0 t_1} &= \frac{x_{st}}{c_0 t_1} + \left(1 - \frac{t}{t_1} \right) \left(1 + \frac{k+1}{2} \cdot \frac{v}{c_0} \right). \end{aligned}$$

Here $c_0 t_1$ is the distance passed by the forward boundary of the wave front during the time t_1 .

We shall designate

$$\frac{x}{c_0 t_1} = X, \quad \frac{v}{c_0} = U, \quad (16)$$

then

$$X = X_{st} + \left(1 - \frac{t}{t_1} \right) \left(1 + \frac{k+1}{2} U \right). \quad (17)$$

In the analytic assignment of the law of piston motion from dependence (17) we may exclude time, and the solution obtains the most generalized form.

Let us assume, for instance, that the piston velocity may be represented by an exponential function

$$v_n = -a t^n,$$

then

$$x_n = -\frac{a}{n+1} t^{n+1} = v_n \frac{t}{n+1}$$

or in dimensionless magnitudes:

$$X_n = \frac{1}{n+1} \cdot \frac{v_n}{c_0} \cdot \frac{t}{t_1} = \frac{U}{n+1} \cdot \frac{t}{t_1}.$$

We shall place the obtained expression in (17):

$$X = 1 + \frac{k+1}{2} U - \left\{ 1 - \frac{U}{n+1} \left[1 - \frac{(k+1)(n+1)}{2} \right] \right\} \frac{t}{t_1}.$$

Considering that

$$\frac{t}{t_1} = \sqrt{\frac{u}{u_1}}.$$

we will finally obtain:

$$X = 1 + \frac{k+1}{2} U - \sqrt{\frac{U}{U_1}} \left(1 - \frac{U}{U_1} \left[1 - \frac{(k+1)(n+1)}{2} \right] \right). \quad (18)$$

The form of solution which is represented by dependence (18) is very convenient, since for obtaining a dimensionless law of velocity distribution through the flow it is sufficient to assign only the dimensionless value of piston velocity.

Figure 4 represents the results of calculations ($k = 1.4$) of velocity distribution through a flow under different laws for accelerating the piston up to a velocity of v_{\max} , i.e., until separation of flow from the piston. Direction and speed of the wave are considered positive.

Inasmuch as in most cases $v_p < c_0$, this part of the graph is represented in Fig. 5 in a bigger scale.

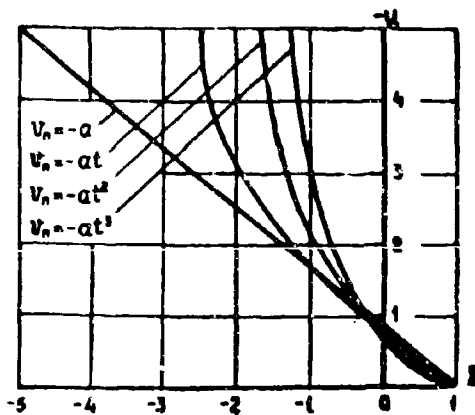


Fig. 4.

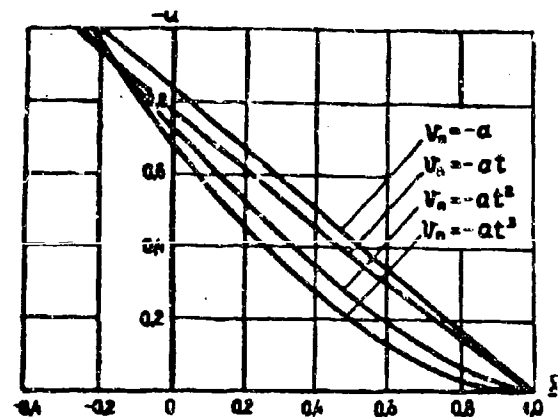


Fig. 5.

Literature

1. L. D. Landau and Ye. M. Lifshits. Mechanics of continuous media. State Press for Technical and Theoretical Literature, Moscow, 1954.
2. R. Sauer. Flows of a compressible fluid. IL, Moscow, 1954.
3. G. V. Lipman and A. Roshko. Elements of gas dynamics. IL, Moscow, 1960.
4. Ya. B. Zel'dovich. Theory of shock waves and an introduction to gas dynamics. Academy of Sciences USSR, Moscow-Leningrad, 1946.

Submitted
14 December 1963

OPTIMUM COMPRESSION IN THE COMPRESSOR OF A DUCTED-FAN
TURBOJET ENGINE WITH AN AFTERBURNER

Ye. D. Sten'kin

Definitions of Cyrillic Items

ДТРДФ = DTJEA = Ducted-Fan Turbojet Engine with Afterburner.

сн = dh = dynamic head.

с = n = nozzle.

к = с = compressor.

БЭВ = ees = effect of exhaust system.

л = л' = flight.

н = е = external medium.

ВХ = in = inlet.

т = t = turbine.

КС = сс = combustion chamber.

ф = af = afterburner.

см = mix = mixing.

в = а = air.

г = g = gas.

м = m = mechanical.

тп = fu = fuel.

гг = bound = boundary.

ЗТ = bt = behind the turbine.

ПЛ = com = complete.

НП = incom = incomplete.

ОХЛ = cool = cooling.

СУЖ = conv = convergent.

ТРД(Ф) : ТУЕА = Turbojet Engine with Afterburner.

Designations

DTUEA — ducted-fan turbojet engine with additional heat feed (with afterburner),

π — degree of increase in pressure in compressor or degree of decrease in pressure in turbine (depending upon lower index),

γ — degree of double flow: ratio of flow rate of air through external duct to flow rate through main duct,

ϵ — coefficient of recovery of full pressure,

α_{dh} — degree of isentropic increase of pressure from dynamic head,

η — efficiency,

k — adiabatic index,

i — enthalpy, $\frac{j}{kg}$,

H_u — lowest calorific value of fuel, $\frac{j}{kg}$,

G — mass flow rate of air or gas, $\frac{H}{sec}$,

T — temperature, $^{\circ}K$,

P — pressure, $\frac{H}{m^2}$

\dot{q} — specific output pulse per second, $\frac{H}{kg/sec}$,

λ — reduced speed,

φ_n — velocity coefficient of jet nozzle,

R — gas constant, $\frac{j}{kg \cdot deg}$,

$$G_{r1} = G_{s1} + G_{m1}, \quad \lambda_r = \frac{G_{r1}}{G_{s1}} \lambda_{m1}, \quad \lambda = \frac{1}{\lambda_r} \frac{\lambda_s}{\lambda_s - 1} \frac{\lambda_r - 1}{\lambda_r}.$$

$$\eta_1 = \eta_{s1}^* \eta_{r1}^* \eta_{m1}, \quad \eta_{II} = \eta_{sII}^* \eta_{rII}^* \eta_{m1}, \quad \eta_m = \frac{G_m}{G_s}.$$

$$\epsilon_1 = \epsilon_{s1}^* \frac{\lambda_s - 1}{\lambda_s}, \quad \epsilon_{II} = \epsilon_{sII}^* \frac{\lambda_s - 1}{\lambda_s}.$$

$C_1 = 1.075$ (see formulas (21) and (25)),

Σ_{II} — parameter of influence of external duct on π_{cIopt}^* is determined by formula (18),

B — parameter, determined by formulas (31) and (32),

S — parameter determined by one of formulas (depending upon exhaust system) (36), (37), or (38),

Σ_{ees} — parameter of effect of exhaust system on π_{cIopt}^* is determined by formula (40),

M_f — flight Mach number,

Indices

Subscripts:

e — external medium,

in — inlet,

I — main duct (where this subscript is obviously omitted),

II — external duct,

c — compressor,

t — turbine,

cc — combustion chamber,

z — coefficient of completeness of fuel combustion,

af — afterburner,

1, 2, 3, 4, 5 — sections through gas-air duct (Fig. 1),

mix — mixing parameter,

a — air,

g — gas,

Σ — total,
 m — mechanical,
 fu — fuel,
 bound — boundary,
 bt — diffuser behind turbine,
 com — complete expansion in jet nozzle,
 incom — incomplete expansion in jet nozzle (in main
 or external, indicated by second index),
 cool — cooling,
 opt — optimum,
 ees — effect of exhaust system,
 conv — parameter with convergent jet nozzle.

Superscript:

* — parameter of isentropic stagnation.

Introduction

In the designing of a ducted-fan turbojet engine with afterburner (DTJEA), of essential value is the degree of increase of pressure in the main duct π_{cI}^* which determines its effectiveness to a significant extent. Presently, the optimum values of π_{cI}^* are found by means of conducting a number of thermodynamic calculations with different π_{cI}^* whose analysis, from the point of view of the influence of π_{cI}^* on the main engine parameters, leads to π_{cI}^* . This method is awkward; therefore it is desirable to have analytic dependences of π_{cI}^* on parameters of the DTJEA cycle similar to the ones that a TJEA has ([1], p. 181), for example.

Here, of course, one should remember that the selection of optimum parameters of a specific engine will demand a number of calculations with π_{cI}^* near π_{cI}^* , on the basis of which, π_{cI}^*

is definitized. The selection of π_{cIopt}^* is also influenced by the weight requirements for the engine in unrated conditions. At the same time, analytic values of π_{cIopt}^* allow us to conduct the most effective comparison of different types of engines. π_{cIopt}^* will be determined in accordance with the DTJEA diagram shown in Fig. 1. The distinction between this diagram and the possible structural DTJEA diagrams is not essential from the point of view of the determination of π_{cIopt}^* .

As it is known, DTJEA's are possible with mixing and without mixing of gas flows inside the engine.

In accordance with this division, π_{cIopt}^* will be determined below. Let us assume that the adiabatic exponent is constant and equal to:

- a) in the process of compression — k_a ,
- b) in the process of expansion — k_b .

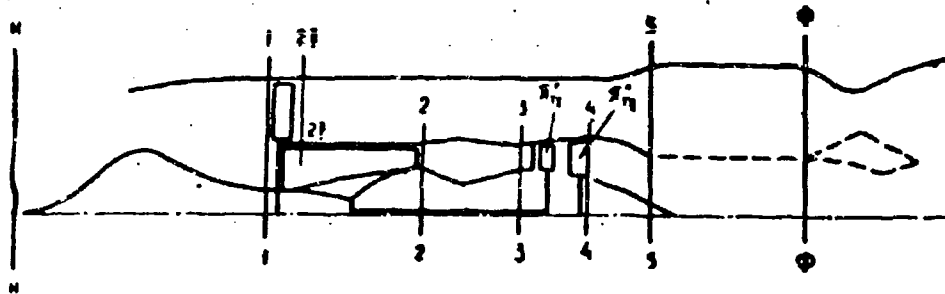


Fig. 1.

DTJEA with Mixing of Flows

We shall show that π_{cIopt}^* , which correspond to maximum specific thrust and minimum specific expenditure of fuel, practically coincide. We shall consider the formula for determination of total fuel consumption $G_{fu\Sigma}$.

In accordance with [1] (pp. 116-121) and [2] (formula (1.35)) we have, for $G_{fu\Sigma}$, the expression

$$G_{m\Sigma} = \frac{G_{ac} (i_1^* - i_2^*)}{H_a \eta_{r1}} + \frac{G_{rz} (i_\phi^* - i_{cu}^*)}{H_a \eta_{r\phi}}, \quad (1)$$

where

$$G_{ac} = G_{a1} + G_{m1} - G_{a2},$$

$$G_{rz} = G_{a1} + G_{a11} + G_{a2}.$$

We shall make assumptions that are close to reality:

$$G_{ac} = G_{a1},$$

$$G_{rz} = G_{a1} + G_{a11} = G_{a\Sigma},$$

$$\eta_{r1} = \eta_{r\phi} = \eta_r, \quad (2)$$

$$\eta_a = 1.$$

Taking into account the assumptions, we have these expressions:

for enthalpy of mixture —

$$i_{cu}^* = \frac{G_{a1} i_1^* + G_{a11} i_{211}^*}{G_{a1} + G_{a11}}, \quad (3)$$

for power balance of turbocompressor —

$$i_3^* - i_1^* = i_2^* - i_1^* + \frac{G_{a11}}{G_{a1}} (i_{211}^* - i_1^*). \quad (4)$$

Determining the difference $i_3^* - i_2^*$ from (4) and putting it, and also i_{mix}^* , from (3) into (1), we obtain:

$$G_{m\Sigma} = \frac{G_{a\Sigma} (i_\phi^* - i_1^*)}{H_a \eta_r}. \quad (5)$$

This formula shows that $G_{fu\Sigma}$ is determined by $G_{a\Sigma}$, temperatures T_1^* and T_{af}^* , and practically, in connection with the fact that in the conclusion we made assumptions (2), does not depend on the parameters of the main duct, π_{cII}^* and y .

Thus, for given T_{af}^* in the determination of optimum parameters of the cycle, including π_{cIopt}^* , $G_{fu\Sigma}$ will remain practically constant, and consequently, to maximum specific thrust will correspond minimum specific fuel consumption.

For determination of π_{cIopt}^* we shall consider known expressions of specific pulse output per second.

a) with complete expansion in jet nozzle [1]—

$$j = (1 + q_{reg}) \epsilon_c \sqrt{\frac{2k_\phi}{k_\phi - 1} R_\phi T_\phi^* \left[1 - \left(\frac{p_{af}}{p_\phi^*} \right)^{\frac{k_\phi - 1}{k_\phi}} \right]}. \quad (6.1)$$

b) with convergent jet nozzle (if output section has a critical regime) [5]—

$$j_{crg} = (1 + q_{reg}) \epsilon_c \sqrt{\frac{2k_\phi}{k_\phi - 1} R_\phi T_\phi^* \left\{ 1 + \frac{1}{k_\phi} \left[1 - \left(\frac{k_\phi + 1}{2} \right)^{\frac{k_\phi}{k_\phi - 1}} \frac{p_{af}}{p_\phi^*} \right] \right\}}. \quad (6.2)$$

From (6.1) and (6.2) it follows that with given T_{af}^* the minimum value of $\frac{p_e}{p_{af}^*}$ corresponds to the maximum value of j . Under the given conditions of flight, the j -maxima and specific thrust coincide, and maximum pressure p_{af}^* will correspond to them. Pressure p_{af}^* depends on the pressures in the miscible gas flux and on the degree of preheating in the afterburner or the afterburner-mixing chamber.

At given T_1^* and T_{af}^* , p_{af}^* does not depend very much on the degree of preheating and we shall disregard this dependence. We shall also consider that the losses in pressures, which are connected with the heat feed, are limited.

In [2] it is shown that mixing is the most effective with close magnitudes of full pressures of initial flows. In accordance with this conclusion we shall assume that in § 5 (Fig. 1) we have an equality:

$$p_i = p_{ii} = p^*. \quad (7)$$

Pressure p_{af}^* can be expressed through p^* in the following manner:

$$p_{af}^* = \sigma_{mix} p^*. \quad (8)$$

On the inlet to the afterburner-mixing chambers, as generally in afterburners, the λ numbers are usually small ($\lambda = 0.2-0.3$), which will determine small losses of pressure due to mixing, the change of which in the determination of π_{cIopt}^* can be completely disregarded. Thus, when $T_{af}^* = \text{const}$ we will also have $\sigma_{mix af} = \text{const}$. Consequently, instead of the maximum of p_{af}^* it is possible to consider the maximum of p^* , which is more convenient. For p^* we obtain an expression through the parameters of the main duct:

$$p^* = p_1^* \pi_{xI}^* \sigma_{xI} \frac{1}{\pi_{rI}^* \pi_{rII}^*} \sigma_{rI}. \quad (9)$$

From (9) it follows that for the determination of π_{cIopt}^* it is necessary to consider the extreme values of function

$$\Phi = \frac{\pi_{xI}^*}{\pi_{rI}^* \pi_{rII}^*}. \quad (10)$$

We shall differentiate Φ with respect to π_{cI}^* ; we shall equate the result to zero, and after transformations, by considering the limitation of π_{tI}^* and π_{tII}^* , we will obtain a differential equation:

$$1 - \pi_{xI}^* \frac{\partial (\ln \pi_{rI}^* \pi_{rII}^*)}{\partial \pi_{xI}^*} = 0. \quad (11)$$

From the condition of equality of effective performance of compressor and turbine I, and also fan and turbine II, after transformations, we obtain formulas for π_{tI}^* and π_{tII}^*

$$\pi_{rI}^* = \frac{1}{\left[1 - \frac{m}{\eta_I} \frac{T_1^*}{T_3^*} (e_1 - 1) \right]^{\frac{\lambda_r}{\lambda_r - 1}}}, \quad (12)$$

$$\pi_{rII}^* = \left[\frac{1 - \frac{m}{\eta_I} \frac{T_1^*}{T_3^*} (e_1 - 1)}{1 - \frac{m}{\eta_I} \frac{T_1^*}{T_3^*} (e_1 - 1) - \frac{1}{\eta_{rII}} \frac{\Delta T_{rII}^*}{T_3^*}} \right]^{\frac{\lambda_r}{\lambda_r - 1}}, \quad (13)$$

where

$$\frac{1}{\gamma_{II}} \frac{\partial \gamma_{II}}{\partial \gamma_2} = \frac{m}{\gamma_{II}} y \frac{\gamma_1}{\gamma_2} (e_{II} - 1). \quad (14)$$

Proceeding from (7) and (9), for $\pi_{c II}^*$ we obtain:

$$\pi_{c II}^* = \frac{e_{ac} e_{ar}}{e_{II}} \frac{\pi_{c I}^*}{\pi_{c I}^* \pi_{c II}^*}. \quad (15)$$

We shall determine derivative $\frac{\partial(\Delta T_{c II}^*)}{\partial \pi_{c I}^*}$ which will be demanded subsequently. On the basis of (14), (15), and also (10) and (11), we have:

$$\left[\frac{\partial(\Delta T_{c II}^*)}{\partial \pi_{c I}^*} \right]_{\pi_{c I}^* \text{ opt}} = 0. \quad (16)$$

We shall convert (11), using (12) and (13), and considering (16),

$$\pi_{c I \text{ opt}}^* = \left[\frac{m + \frac{\gamma_2}{\gamma_1} \gamma_1}{m + \frac{1}{\gamma_1} (1 + \Sigma_{II})} \right]^{\frac{h_2}{h_2 - 1}}. \quad (17)$$

where

$$\Sigma_{II} = \frac{\gamma_1}{\gamma_{II}} \frac{\Delta \gamma_{II}}{\gamma_2} \times \frac{1 - \frac{m}{\gamma_1} \frac{\gamma_1}{\gamma_2} (e_{I \text{ opt}} - 1)}{\left[1 - \frac{m}{\gamma_1} \frac{\gamma_1}{\gamma_2} \frac{\gamma_1}{\gamma_2} (e_{I \text{ opt}} - 1) \right] \left[1 - \frac{m}{\gamma_1} \frac{\gamma_1}{\gamma_2} \frac{\gamma_1}{\gamma_2} (e_{I \text{ opt}} - 1) - \frac{1}{\gamma_{II}} \frac{\Delta \gamma_{II}}{\gamma_2} \right]}. \quad (18)$$

In accordance with the structure of formula (18) Σ_{II} should be called the parameter of the influence of the external duct on $\pi_{c I \text{ opt}}^*$.

When $y = 0$, we have $\Sigma_{II} = 0$ (this follows from (14) and (18): in this case formula (17) determines $\pi_{c \text{ opt}}^*$ for TJEA).

If we additionally take

$$m = 1, \quad \eta_u = 1, \quad g_t = 1, \quad (19)$$

Then (17) coincides with the known expression in [1] (page 181, (6.17)) for $\pi_{c \text{ opt}}^*$ in TJEA. Thus, even for TJEA, formula (17) is more general than the one existing for determination of $\pi_{c \text{ opt}}^*$ since it makes it possible to calculate the distinction of k in processes of compression and expansion.

For contemporary turbojet engines (single-and double-flow), and also for engines now being developed, the following magnitudes are characteristic:

$$\begin{aligned} \frac{T_1^*}{T_3^*} &= 0.2 - 0.5, \quad m = 0.85 - 1.0, \quad \eta_l = 0.7 - 0.75, \\ g_t &= 0.97 - 1.0, \quad \eta_{t1}^* = 0.88 - 0.91. \end{aligned} \quad (20)$$

We shall show, by considering (20), that the magnitude of Σ_{II} is significantly less than the denominator of formula (17). This will prove the validity of the transformation of the formula for determination of $\pi_{c \text{ I opt}}^*$ to the form of (17). For that it is necessary to determine $\pi_{c \text{ II}}^*$. In DTJEA with mixing, as follows from (15), $\pi_{c \text{ II}}^*$ and $\pi_{c \text{ I}}^*$ are interconnected. We shall find the expression for $\pi_{c \text{ II opt}}^*$ by using (12)-(15) and introducing the following designation:

$$C_1 = \left(\frac{\pi_{II}}{\pi_{uc} \pi_{3T}} \right)^{\frac{k_u - 1}{k_u}} \frac{1 - \frac{m}{\eta_l} \frac{T_1^*}{T_3^*} (e_1 - 1)}{1 - \frac{m}{\eta_l} \frac{T_1^*}{T_3^*} (e_1 - 1)} \frac{\frac{k_u - 1}{k_u} - \frac{k_t - 1}{k_t}}{(\pi_{t1}^* \pi_{tII}^*)}. \quad (21)$$

After transformations, we obtain:

$$\pi_{c \text{ II opt}}^* = \left[\frac{1 + y \frac{m}{\eta_{II}} \frac{T_1^*}{T_3^*} - \frac{m}{\eta_{II}} \frac{T_1^*}{T_3^*} (e_{1 \text{ opt}} - 1)}{C_1 + y \frac{m}{\eta_{II}} \frac{T_1^*}{T_3^*} e_{1 \text{ opt}}} \right]^{\frac{k_u}{k_u - 1}} \pi_{c \text{ I opt}}^* \quad (22)$$

Analysis shows that C_1 changes insignificantly, i.e., for conditions (20) and when

$$\begin{aligned} k_s = 1.4, \quad k_r = 1.33, \quad y = 0.5 - 6.0, \quad \eta_{II} = 0.7 - 0.75, \\ \eta_{rII} = 0.85 - 0.9, \quad \alpha_{II} = 0.97 - 0.99, \quad \alpha_{ec} = 0.92 - 0.97, \\ \alpha_{sc} = 0.98 - 1.0, \end{aligned} \quad (23)$$

we have:

$$C_1 = 1.05 - 1.10. \quad (24)$$

Proceeding from the structure of formula (22), it is possible to take parameter C_1 as being constant (with maximum error of determination of $\pi_{c II opt}^*$ less than 3%) and equal to

$$C_1 = 1.075. \quad (25)$$

We shall determine Σ_{II} by proceeding from (14), (17), (18), and (25) for conditions (20) and (23). After the calculations, we obtain;

$$\Sigma_{II} = 0 - 0.2. \quad (26)$$

Thus, Σ_{II} comprises less than 8% of the denominator of formula (17) and consequently, this proves the validity of conversion of the formula for $\pi_{c I opt}^*$ to the form of (17).

We simultaneously arrive at this important conclusion. With identical corresponding parameters of cycles, the $\pi_{c I opt}^*$ of DTJEA with mixing is always smaller than the $\pi_{c opt}^*$ of TJEA.

DTJEA Without Mixing of Flows (with Forcing in External Duct)

Let us consider the formula for total fuel consumption $G_{fu\Sigma}$. In accordance with (1), considering (4), and also that secondary heat feed is carried out only in the external duct, and making assumptions (2), we obtain the formula for $G_{fu\Sigma}$:

$$G_{fu\Sigma} = \frac{Q_{u\Sigma}}{1+y} \frac{i_4 - i_1 + y(i_4^* - i_1^*)}{H_{u\Sigma}}. \quad (27)$$

From (27) it follows that at $T_{af}^* = \text{const}$ and $T_3^* = \text{const}$, a change in π_{cI}^* will lead to a change in $G_{fu\Sigma}$ due to the dependence of i_4^* on π_{cI}^* .

Consequently, if we consider optimum π_{cI}^* at $T_3^* = \text{const}$ and $T_{af}^* = \text{const}$, which correspond to maximum specific thrust and minimum specific fuel expenditure, then they will not coincide. At the same time, the condition of $T_{af}^* = \text{const}$ for cruising conditions, in which one should determine the optimum parameters, is not determining since under these conditions there is limitation with respect to T_{af}^* , and consequently, a change in T_{af}^* is allowed. It is necessary also to consider that DTJEA's without mixing correspond to high y ; therefore the influence of π_{cI}^* on $G_{fu\Sigma}$ (at $T_{af}^* = \text{const}$) or on T_{af}^* (when $G_{fu\Sigma} = \text{const}$) will be insignificant.

These considerations allow us to more fully satisfy the requirements presented to parameters of the working process of the jet engine, i.e., the thermal machine and propelling agent of a flight vehicle.

Optimum parameters, including π_{cI}^* opt, should ensure;

- 1) maximum possible thrust with the given fuel consumption,
- 2) minimum possible fuel consumption for obtaining the given thrust.

It is not difficult to be convinced that in both cases π_{cI}^* opt is determined by the following system of equations:

$$\begin{aligned} \frac{\partial j}{\partial \pi_{cI}^*} &= 0, \\ \frac{\partial G_{fu\Sigma}}{\partial \pi_{cI}^*} &= 0. \end{aligned} \quad (28)$$

Under condition (28) the optimum π_{cI}^* for specific thrust and specific fuel consumption will coincide.

Let us consider the expressions of specific pulse output per second:

a) with complete expansion in the jet nozzle, in accordance with (6.1), we have:

$$j = \frac{1+q_m}{1+y} q_c \sqrt{\frac{2k_r}{k_r-1} R_r} \left\{ \sqrt{T_i \left[1 - \left(\frac{p_2}{p_1} \right)^{\frac{k_r-1}{k_r}} \right] + B \sqrt{T}} \right\}. \quad (29.1)$$

b) with a convergent jet nozzle in the main duct (if in the outlet section there is a critical regime) in accordance with (6.2) we have:

$$j_{c, \text{jet}} = \frac{1+q_m}{1+y} q_c \sqrt{\frac{2k_r}{k_r-1} R_r} \left\{ \sqrt{\frac{k_r-1}{k_r+1} T_i} \times \right. \\ \left. \times \left[1 + \frac{1}{k_r} \left[1 - \left(\frac{k_r+1}{2} \right)^{\frac{k_r-1}{k_r}} \frac{p_2}{p_1} \right] \right] + y B \sqrt{T_i} \right\}. \quad (29.2)$$

Expressions (29.1) and (29.2) are obtained under assumptions for cruising augmented ratings which are close to reality:

$$\begin{aligned} k_0 &= k_{r1} = k_r, \\ \frac{q_{m1}}{q_{s1}} &= \frac{q_{m2}}{q_{s2}} = q_m, \\ q_{c1} &= q_{c2} = q_c. \end{aligned} \quad (30)$$

We introduce a designation:

$$\sqrt{1 - \left(\frac{p_2}{p_1} \right)^{\frac{k_r-1}{k_r}}} = B. \quad (31)$$

Expressions (29.1) and (29.2) are applicable for typical DTJEA systems without mixing of flows.

The DTJEA system with convergent jet nozzle in both ducts for the given analysis is described by formula (29.2) in which magnitude B will enter in the form of

$$B = \sqrt{\frac{k_r-1}{k_r+1}} \left\{ 1 + \frac{1}{k_r} \left[1 - \left(\frac{k_r+1}{2} \right)^{\frac{k_r-1}{k_r}} \frac{p_2}{p_1} \right] \right\}. \quad (32)$$

Subsequent analysis will be conducted with $\pi_{c\ II}^* = \text{const}$, in distinction from the preceding variant in which from the point of view of optimumness of mixing $\pi_{c\ II}^*$ changed according to (15). The condition of $\pi_{c\ II}^* = \text{const}$ does not disturb the community of analysis and is in full conformity with the methods of analysis of functions of many variables. Magnitude B, when $\pi_{c\ II}^* = \text{const}$, practically will not change due to the weak dependence of T_{a1}^* on $\pi_{c\ I}^*$ (when $G_{fu\Sigma} = \text{const}$) and consequently, a small change in the thermal losses of full pressure in the afterburner (it is also necessary to consider the small magnitude of λ numbers at the chamber inlet). Let us consider dependences T_4^* and p_4^* , which are necessary for further analysis, through the initial parameters of the cycle. Proceeding from (9) (rejecting σ_{3t}), (12), and (13), as a result of transformations we obtain:

$$\frac{T_4^*}{T_3^*} = 1 - \frac{\pi}{\eta_1} \eta_{r1} \frac{T_1^*}{T_3^*} (e_1 - 1) - \frac{\Delta T_{rII}^*}{T_3^*}, \quad (33)$$

$$\frac{p_4^*}{p_a} = \sigma_{cc} \sigma_{\Sigma} \sigma_{cc} \pi_{c1}^* \times \\ \times \left\{ \frac{\left[1 - \frac{\pi}{\eta_1} \frac{T_1^*}{T_3^*} (e_1 - 1) \right] \left[1 - \frac{\pi}{\eta_1} \eta_{r1} \frac{T_1^*}{T_3^*} (e_1 - 1) - \frac{1}{\eta_{rII}} \frac{\Delta T_{rII}^*}{T_3^*} \right]}{1 - \frac{\pi}{\eta_1} \eta_{r1} \frac{T_1^*}{T_3^*} (e_1 - 1)} \right\}^{\frac{k_r}{k_r - 1}}. \quad (34)$$

Differentiating (29.1) and (29.2) with respect to $\pi_{c\ I}^*$, and equating the result to zero, after transformations, by considering condition $G_{fu\Sigma} = \text{const}$ we obtain one (instead of two) generalized differential equation

$$\frac{k_r}{k_r - 1} S \frac{\partial(\ln T_4^*)}{\partial \pi_{c1}^*} + \frac{\partial(\ln p_4^*)}{\partial \pi_{c1}^*} = 0, \quad (35)$$

where

a) with complete expansion in jet nozzles -

$$S - S_{\infty} = \left[\left(\frac{p_i^*}{p_n} \right)^{\frac{k_r - 1}{k_r}} - 1 \right] \left[1 - \sqrt{\frac{\frac{r_i^*}{r_\phi^*} \left(1 - \left(\frac{p_n}{p_\phi^*} \right)^{\frac{k_r - 1}{k_r}} \right)}{1 - \left(\frac{p_n}{p_i^*} \right)^{\frac{k_r - 1}{k_r}}}} \right]. \quad (36)$$

b) with convergent nozzle in the main duct -

$$S - S_{im} = \frac{k_r - 1}{2} \left(\frac{2}{k_r + 1} \right)^{\frac{k_r}{k_r - 1}} \left\{ \frac{p_i^*}{p_n} + \frac{1}{k_r} \left[\frac{p_i^*}{p_n} - \left(\frac{k_r + 1}{2} \right)^{\frac{k_r}{k_r - 1}} \right] \right\} \left\{ 1 - \sqrt{\frac{\frac{k_r + 1}{k_r - 1} \frac{r_i^*}{r_\phi^*} \frac{V}{1 - \left(\frac{p_n}{p_\phi^*} \right)^{\frac{k_r - 1}{k_r}}}}{1 + \frac{1}{k_r} \left[1 - \left(\frac{k_r + 1}{2} \right)^{\frac{k_r}{k_r - 1}} \frac{p_n}{p_i^*} \right]}} \right\}. \quad (37)$$

c) with convergent nozzle in both ducts (it is possible to trace by using (32) that equation (35) is also valid for this case) -

$$S - S_{(1+11)m} = \frac{k_r - 1}{2} \left(\frac{2}{k_r + 1} \right)^{\frac{k_r}{k_r - 1}} \left\{ \frac{p_i^*}{p_n} + \frac{1}{k_r} \left[\frac{p_i^*}{p_n} - \left(\frac{k_r + 1}{2} \right)^{\frac{k_r}{k_r - 1}} \right] \right\} \left\{ 1 - \sqrt{\frac{\frac{r_i^*}{r_\phi^*} \left[1 + \frac{1}{k_r} \left[1 - \left(\frac{k_r + 1}{2} \right)^{\frac{k_r}{k_r - 1}} \frac{p_n}{p_\phi^*} \right] \right]}{1 + \frac{1}{k_r} \left[1 - \left(\frac{k_r + 1}{2} \right)^{\frac{k_r}{k_r - 1}} \frac{p_n}{p_i^*} \right]}} \right\}. \quad (38)$$

Proceeding from (35), using (33) and (34), as a result of transformations we have the formula for $\pi_{c \text{ I opt}}^*$

$$\pi_{c \text{ I opt}}^* = \left[\frac{m + \frac{r_3^*}{r_1^*} \eta_1}{m + \frac{1}{g_1} (1 + \Sigma_{II} + \Sigma_{mcs})} \right]^{\frac{k_0}{k_0 - 1}}. \quad (39)$$

where

$$\Sigma_{ees} = \frac{1 - \frac{\pi}{\eta_1} \frac{T_1^*}{T_3^*} (\epsilon_{1opt} - 1)}{1 - \frac{\pi}{\eta_1} \frac{T_1^*}{T_3^*} (\epsilon_{1opt} - 1) - \frac{\Delta T_{r, II}}{T_3^*}} \eta_{11}^* S. \quad (40)$$

Parameter Σ_{ees} considers the effect of the type of exhaust system and therefore it is naturally called the parameter of the exhaust system effect. In DTJEA with mixing of flows $S = 0$, and consequently, $\Sigma_{ees} = 0$. Thus, (39) is a generalized formula that includes, as a particular case, formula (17) and the formula for the determination of $\pi_{c opt}^*$ in TJEA.

Further we shall consider the order of magnitudes Σ_{ees} and Σ_{II} to prove the validity of conversion of the formula for $\pi_{c I opt}^*$ to the form of (39). Σ_{ees} contains parameter S . Figures 2-4 give graphs of S for different types of exhaust systems. The order of magnitude S can be determined according to the following considerations. For augmented cruising conditions, which correspond to supersonic flight, the following magnitudes are characteristic (see also [4]):

$$\begin{aligned} \frac{T_4^*}{T_1^*} &= 1 - 1.5, \\ \frac{P_4^*}{P_1^*} &= 1.5 - 2.0. \end{aligned} \quad (41)$$

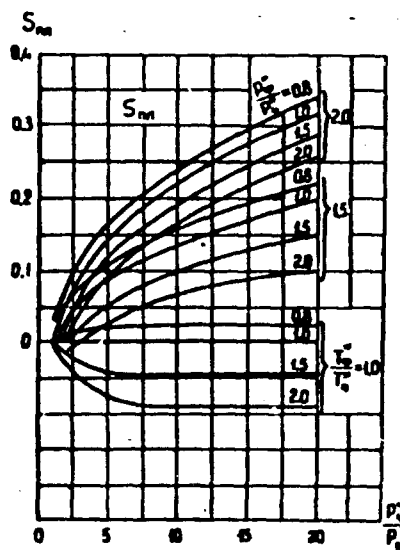


Fig. 2.

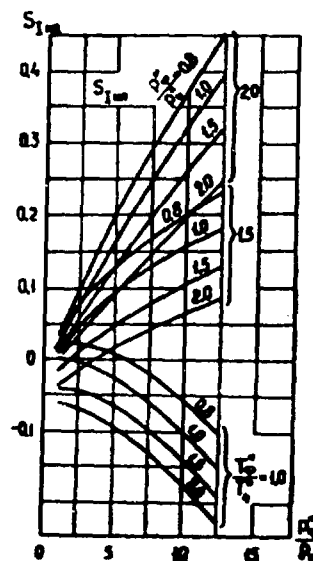


Fig. 3.

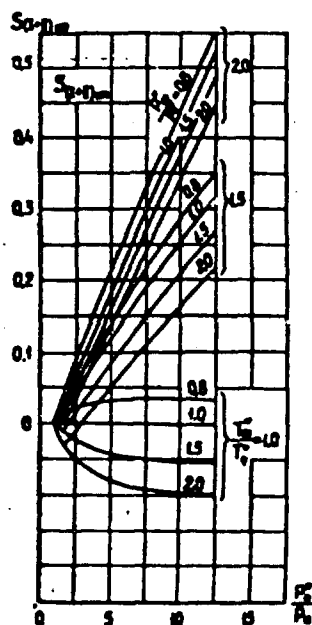


Fig. 4.

Ratios of $\frac{p_{af}^*}{p_4^*}$ are given for DTJEA without mixing. Usually in (41), larger T_{af}^*/T_4^* correspond to larger p_{af}^*/p_4^* . For DTJEA, just as for other types of turbojet engines, the turbocompressor leads to an essential improvement in the main engine parameters and at the contemporary level of gas temperature in front of the turbine up to Mach flight numbers equal to $M = 2.5-3.0$ [4]. In this case, originating from (34) and (39), we obtain:

$$\frac{p_i}{p_n} < 20. \quad (42)$$

Convergent jet nozzles usually are applied up to magnitudes of the pressure ratio:

$$\frac{p_i}{p_n} < 5. \quad (43)$$

Thus, proceeding from Figures 2-4, and also from formulas (41)-(43), we obtain the range of change of S :

$$S = -0.05 - 0.10. \quad (44)$$

For the purpose of obtaining a small specific gravity of DTJEA, the fan is usually made no more than three-stage (see, for instance, [4] and [5]), i.e., we have:

$$\pi_{cII} = 1.5 - 3.0. \quad (45)$$

The degrees of two-flow ability vary within the limits [5] of

$$y = 0.5 - 2.0. \quad (46)$$

Here, a larger y corresponds to a smaller π_{cII}^* , and conversely.

Thus, we can determine the magnitude of Σ_{ees} . Proceeding from (39), (40), and (44), we obtain:

$$\Sigma_{ees} = -0.07 - 0.15. \quad (47)$$

In a similar manner, using (18) and (15), we can determine Σ_{II} :

$$\Sigma_{II} = 0.10 - 0.20. \quad (48)$$

Thus, the sum of $\frac{1}{g_t}(\Sigma_{II} + \Sigma_{ees})$ can constitute from 5 to 15% of the denominator of formula (39). This percent is small, and consequently, formula (39) will be valid for determination of $\pi_{c I opt}^*$. From a comparison of (17) and (39), considering (26), (47), and (48), there follows a conclusion.

With identical parameters of the main duct the optimum value of the degree of increase in pressure in the main duct of a DTJEA with mixing of flows is always greater than in a DTJEA without mixing of flows. The difference can reach up to 20% (for high supersonic speeds of flight).

Figures 5 and 6 give graphs of $\pi_{c I opt}^*$ and $\pi_{c II opt}^*$ for the most characteristic magnitudes of efficiency and adiabatic exponents. From these figures it follows that the double-flow parameters render an essential influence on $\pi_{c I opt}^*$. For example, when $\frac{T_3^*}{T_1^*} = 3.8$

(corresponds flight with $T_3^* = 1500^\circ$ abs. in conditions of $H \geq 11$ km, $M_\infty = 2$) the TJEA has $\pi_{c opt}^* = 11.1$; when $y = 1$ the DTJEA with mixing of gas flows has $\pi_{c I opt}^* = 9.5$ ($\pi_{c II opt}^* = 1.95$), and the DTJEA forced in the external duct $\pi_{c II}^* = 2.3$ and $S = 0.1$ (this magnitude corresponds to high degrees of forcing) has $\pi_{c I opt}^* = 7.6$. Figure 6 shows the influence of parameter S , which considers the degree of forcing, and the exhaust diagram. It is clear that an increase of S (for instance, an increase of the degree of forcing) leads to a decrease of $\pi_{c I opt}^*$.

When $\frac{T_3^*}{T_1^*} = 3.8$ and $\frac{\Delta T_{t II}^*}{T_3^*} = 0.075$, with an increase of S from $S = 0$

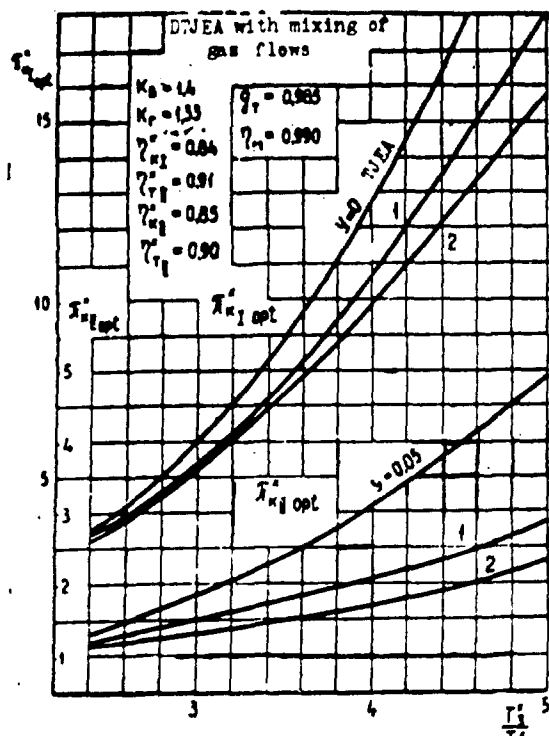


Fig. 5.

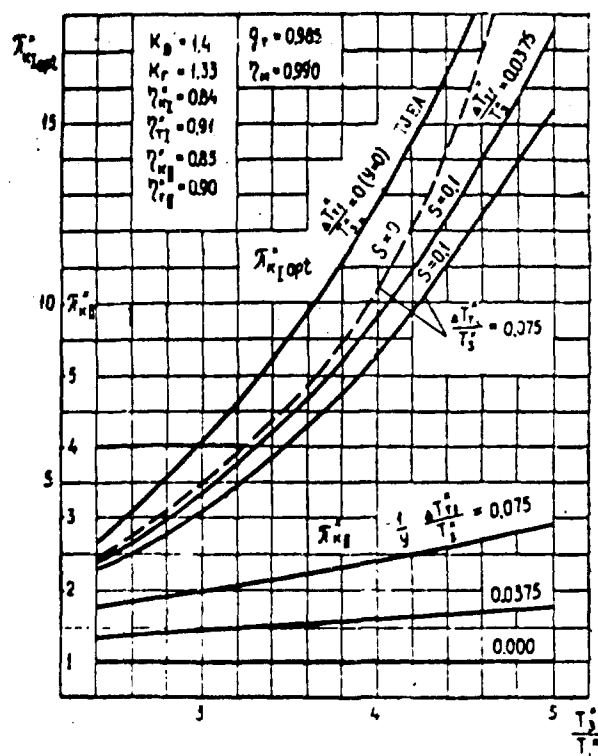


Fig. 6. DTJEA forced in external duct.

to $S = 0.1$, we have a decrease of π_{cI}^* from $\pi_{cI}^* = 9$ to $\pi_{cI}^* = 7.6$.

Conclusions

1. Formulas are obtained for determining π_{cI}^* of DTJEA with mixing and DTJEA without mixing of flows. For DTJEA with mixing, the formula for determining π_{cII}^* is simultaneously obtained. The formulas can be used in the selection of optimum DTJEA parameters especially if this selection is produced with an electronic computer, since the presence of formulas for determining π_{cI}^* sharply reduces the necessary number of variants, and consequently subsequent analysis of results of calculation.

2. The formula for determining π_{cI}^* of a DTJEA without

mixing has a universal character and includes, as particular cases, the formulas for $\pi_{c I \text{ opt}}^*$ of a DTJEA with mixing and for $\pi_{c \text{ opt}}^*$ of a TJEA.

3. Analysis shows that with identical corresponding parameters of cycle $\pi_{c \text{ opt}}^*$ are arranged by magnitude in decreasing order in the following way: $\pi_{c \text{ opt}}^*$ of TJEA, $\pi_{c I \text{ opt}}^*$ of DTJEA with mixing, and then $\pi_{c I \text{ opt}}^*$ of DTJEA without mixing of flows.

The difference between $\pi_{c \text{ opt}}^*$ of a TJEA and $\pi_{c I \text{ opt}}^*$ of a DTJEA with mixing can reach up to 25%. The difference between $\pi_{c I \text{ opt}}^*$ of a DTJEA with mixing and $\pi_{c I \text{ opt}}^*$ of a DTJEA without mixing can reach up to 20%. For instance, in conditions of flight $H \geq 11$ km, $M_f = 2$ with $T_2^* = 1500^\circ$ abs, a TJEA has $\pi_{c \text{ opt}}^* = 11.1$, and when $y = 1$ the DTJEA with mixing of gas flows has $\pi_{c I \text{ opt}}^* = 9.5$ ($\pi_{c II \text{ opt}}^* = 1.95$), and the DTJEA forced in the external duct, with $\pi_{c II}^* = 2.3$, depending upon the degree of augmentation, has $\pi_{c I \text{ opt}}^* = 7.6-9$ (with an increase in the degree of augmentation, $\pi_{c I \text{ opt}}^*$ decreases).

4. In a DTJEA with mixing, the effect of the external duct on $\pi_{c I \text{ opt}}^*$ leads to a change of $\pi_{c I \text{ opt}}^*$ within the limits of 25%.

5. In a DTJEA without mixing of flows, $\pi_{c I \text{ opt}}^*$ will be affected both by the external duct (this influence changes $\pi_{c I \text{ opt}}^*$ within the limits of 20%) and also the exhaust system, which can lead to a change of $\pi_{c I \text{ opt}}^*$ within the limits of 15%.

Literature

1. E. S. Stechkin, P. K. Kazandzhan, L. P. Alekseyev, A. N. Gerasimov, N. Ye. Kononov, Yu. N. Nechayev, and R. M. Fedorov. Theory of Jet Engines. Part II, Oborongiz, Moscow, 1958.

2. K. V. Kholshchevnikov. Certain questions of the theory and design of turbojet engines. Oborongiz, Moscow, 1960.

3. N. V. Inozemtsev. Aviation gas-turbine engines. Oborongiz, Moscow, 1955.

4. R. R. Jemison and R. J. Lane. Engines for supersonic airlines. Journal of the Royal Aeronautical Society, September, 1960.

5. I. S. Butz. Fan Burner dominates supersonic Designs. Aviation Week, 73, No. 2, 1960.

Submitted
6 January 1964

AN APPROXIMATE METHOD OF ESTIMATING GAS-DYNAMIC INFLUENCE ON A SUPERSONIC FLOW

Z. G. Shaykhutdinov

Definitions of Cyrillic Items

KP = crit = critical

np = nor = normal

BM = unidentified designation

In analyzing the available experimental works on questions of gas-dynamic influence on a supersonic flow [1], [2], it may be concluded that a secondary gas blast will form an obstacle on the surface of an airfoil or nozzle wall in its main flow. At its flowing around, as in the case of the flow around solid obstacles, in the main flow there appears a complicated system of shock waves in front of the blast and behind it. The complicated configuration of the system of shocks in front of a slot is explained by separation of the boundary layer. This depends on the relationship of the effective height of the obstacle and the thickness of the boundary layer.

For the purpose of simplification of the problem we shall consider perfect gases and disregard the boundary layer effect. As

from a slot of infinite length. The slot may be convergent or divergent and the direction of the blast may be perpendicular to the main flow or close to perpendicular. Then it is possible to present such a model of the interaction of flows (Fig. 1).

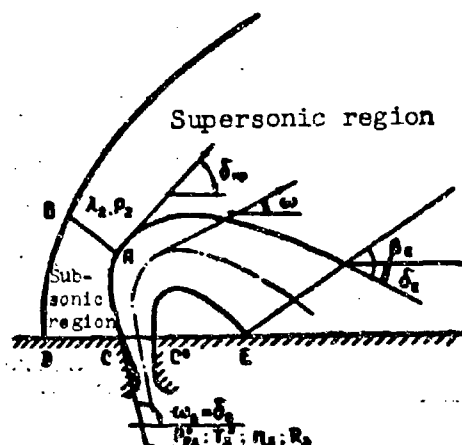


Fig. 1.

Fig. 1.

The gas blast will form an obstacle of rather complicated profile: at first the secondary stream is separated from the wall, and in this zone there is significant rarefaction; further, downwards through the flow it turns around and again "adheres" to the wall.

Around this airfoil in the main flow in front of the blast site there will form a detached curved shock wave, and at the point of adhesion, a completing shock wave.

Behind the leading shock wave at the wall the flow is subsonic and its parameters are calculated from the usual gas-dynamic relationships for a normal shock. The intensity of the wave upon removal from the wall weakens, and in a certain point B the flow behind it already becomes sonic. By using the assumptions presented in the work of B. S. Vinogradov and this author [4] it is possible to draw the line of transition through the speed of sound BA. Point A corresponds to such a revolution of the secondary stream in which

the angle of inclination of the tangent to its profile in this point is equal to the critical angle of flow deviation:

$$\delta_{sp} = \arctg \frac{M_1^2 \sin^2 \alpha_{sp} - 1}{\left[M_1^2 \left(\frac{k+1}{2} - \sin^2 \alpha_{sp} \right) + 1 \right] \frac{\sin \alpha_{sp}}{\sqrt{1 - \sin^2 \alpha_{sp}}}} \quad (1)$$

Here M_1 is the Mach number of forward flow,

α_{crit} is the angle of the wave front, behind which the speed of flow becomes equal to the speed of sound,

k is the adiabatic exponent,

$$\alpha_{sp} = \arcsin \sqrt{\frac{1}{kM_1^2} \left[\frac{k+1}{4} M_1^2 - \frac{3-k}{4} + \sqrt{(k+1) \left(\frac{9+k}{16} - \frac{3-k}{8} M_1^2 + \frac{k+1}{16} M_1^4 \right)} \right]} \quad (2)$$

Subsequently, the region lying before line BA will be called "subsonic," and the region behind it, "supersonic," inasmuch as around the profile of the stream obstacle the main flow in this place again obtains supersonic speed.

Thus, we can consider that the pressure at point D is equal to the static pressure behind a normal shock $P_{2 \text{ nor}}$, and at point C, to stagnation pressure $P_{2 \text{ nor}}^*$. The pressure in the interval between points D and C may be assumed variable according to linear law, which is confirmed by experiments [2].

For the adopted model the pressure on the leading boundary of the secondary stream in the "subsonic" region will vary from $P_{2 \text{ nor}}^*$ to $P_{2 \text{ M=1}}$, whereupon

$$P_{2 \text{ M=1}} = \left(\frac{2}{k+1} \right)^{\frac{k}{k-1}} \cdot P_{2 \text{ nor}}^* \quad (3)$$

As the experiments show, at blast angles δ_0 which do not differ much from 90° , the leading boundary of the profile of the secondary stream on the initial section is close to the circumference.

Therefore, it is possible to use the law of change of pressure in the interval between A and C the same as in the transverse flow around a cylinder, the experimental data for which [2], [6], up to $\theta = \theta_{crit}$ (Fig. 2), are well approximated by the dependence

$$P_2 = P_{2cr} - (P_{2cr}^* - P_{2M-1}) \cdot \frac{\lg \theta}{\lg \theta_{cr}} \quad (4)$$

where θ is the polar angle of the current point on the surface of the cylinder (Fig. 1, 2) and θ_{crit} is the polar angle of point A.

Expression (4) is valid for the case of $\delta_0 = \frac{\pi}{2}$; however, during a blast with angles that do not differ much from normal, it is obviously possible to use a similar relationship. Angle θ is

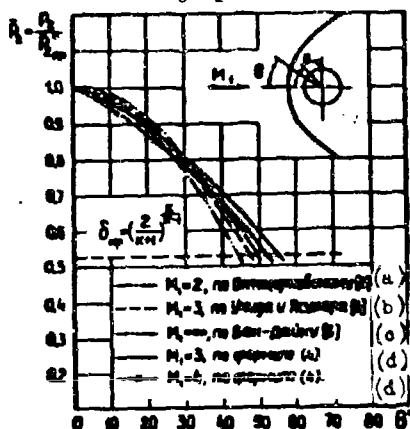


Fig. 2.
KEY: (a) according to Belotserkovskiy; (b) according to Uchida and Yasukhara; (c) according to VanDyke; (d) according to formula.

conveniently expressed through the characteristic parameter of the secondary stream, i.e., the angle of inclination of the tangent to its leading boundary, δ :

$$\frac{\lg \theta}{\lg \theta_{cr}} = \frac{\cos \delta - \cos \delta_0}{\cos \delta_{cr} - \cos \delta_0} \cdot \frac{\sin \delta_{cr}}{\sin \delta} \quad (5)$$

The last relationship, which was

derived taking into account the possible distinction of δ_0 from $\frac{\pi}{2}$, is found from analysis of Fig. 3. It is absolutely clear that here δ_0 in no case should be less than δ_{crit} . When $\delta_0 < \delta_{crit}$ the entire flow

changes, inasmuch as the shock in this case is oblique and attached.

Considering what has been said, we obtain for the subsonic region:

$$P_2 = P_{2cr} - (P_{2cr}^* - P_{2M-1}) \cdot \frac{\cos \delta - \cos \delta_0}{\cos \delta_{cr} - \cos \delta_0} \cdot \frac{\sin \delta_{cr}}{\sin \delta} \quad (6)$$

[illegible]

the relationships for the supersonic flow around a curved wall. In first approximation it is possible to take the relationships for the flow around an external obtuse angle, namely:

Here λ_2 is the coefficient of speed, which is equal to the relation of true speed to critical, is found on the appropriate table or is determined by the solution of the known equation

where $\Delta\delta'$ is the angle of rotation of flow from its direction in the zone of transition through the sonic line to the current line. It is defined as

The rear boundary of the secondary stream is acted upon by static pressure \overline{P}_4 which is equal to the pressure in the separation zone. Its value is calculated by the empirical relationship

which is obtained on the basis of analysis of experimental data of this author, and also the data in [1]. Here λ_{03}' is the coefficient of speed which may be attained during isentropic expansion of the secondary stream to a certain average pressure on the slot cutoff;

$$P_4' = \frac{2}{3} P_{2m}' \quad (9)$$

Pressure P_{03}' is an approximation to average pressure in an isobaric section of the secondary stream

$$P_4 = \frac{2P_{2m}' + P_1}{3}, \quad (10)$$

which is obtained from the condition of parabolic change of static pressure in the secondary stream.

As can be seen from Fig. 4, the points corresponding to values of \bar{P}_4 for different blast conditions lie quite well on one curve that is constructed depending upon λ_{03}' , which allows us to describe the law of its change with a simple empirical equation (8).

Knowing the dependences that determine P_2 and P_4 , and considering the average speed in the secondary stream to be constant in length,

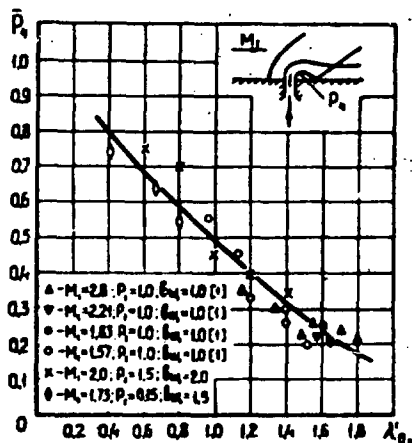


Fig. 4.

we can obtain relationships that determine its profile. Let us note that, in virtue of the selected law distribution of static pressures through a section of the stream, its parameters with the known equation of the leading boundary are obtained in the following way: distance to axis of stream in current section —

$$b_2' = b_1 \cdot \frac{2P_2 + P_1}{3P_4}, \quad (11)$$

and from axis of rear boundary —

$$b'' = b_1 \cdot \frac{4P_2 - P_1}{3P_4}. \quad (12)$$

Width of stream in initial isobaric section is determined from conditions of conservation of mass and pulse by the relationship

$$b_{a_3} = b_{a_2} \cdot \frac{P_{a_2}}{P_{a_3}}, \quad (13)$$

where b_{a_3} is the width of the lateral nozzle on its cutoff,

P_{a_3} is the static pressure on the lateral nozzle cutoff.

The current value of the width of the secondary stream is

$$b_3 = b_{a_3} \cdot \frac{P_{a_3}}{P_3}, \quad (14)$$

where P_3 is the average static pressure in the stream which is analogous to (10):

$$P_3 = \frac{2P_2 + P_1}{3}. \quad (15)$$

For obtaining the form of the leading boundary of the secondary stream (Fig. 5) we shall use the expression for determination of the reaction of a fluid flowing in a curved channel [7] between sections 1 - 1 and 1. Disregarding magnitudes of the second order of smallness, we will have:

$$\begin{aligned} & -m'_3 w_{1-1} \sin(\delta_1 - \omega_{1-1}) + \\ & + m'_3 \cdot w_1 \cdot \sin(\delta_1 - \omega_1) = P_2 \Delta l + \\ & + P_4 \Delta l_1 - P_3 b \Delta \omega_1. \end{aligned} \quad (16)$$

Here

$$\omega_1 \approx \delta_1 - \arctg \frac{b'_1 - b'_{1-1}}{\Delta l} \approx \delta_1 - \frac{b'_1 - b'_{1-1}}{\Delta l}, \quad (17)$$

m'_3 is the mass flow rate through a slot of unit length,

w_1 is the average-mass speed of the secondary stream in current section.

Considering that

$$\Delta l_1 = R_1 \Delta \delta_1, \quad w = \text{const}, \quad P_2 = \frac{P_{21} + P_{22-1}}{2},$$

taking

$$\Delta l_1 = \Delta l - \frac{b_1 + b_{1-1}}{2} \Delta \omega_1,$$

and also taking into account the smallness of $\Delta \delta$ in the numerical solution of the problem

$$\sin(\omega_1 - \delta_1) \approx \omega_1 - \delta_1,$$

after simple transformations we find the expression for radius of curvature in the 1-th section:

$$R_1 = \frac{2\pi_1' - (b_1 + b_{1-1})P_1 + (P_M + P_{M-1})b_1}{P_M + P_{M-1} - 2P_1} \cdot \frac{\Delta\omega_1}{\Delta\delta_1} = \Phi(\delta_1). \quad (18)$$

The solution of equation (18) in final form is difficult, and it is simpler to solve it numerically, for instance by Euler's method. Considering that

$$R_1 = \frac{dl_1}{d\delta_1} \text{ or } R_1 = \frac{\Delta l_1}{\Delta\delta_1} \text{ when } \Delta\delta_1 \rightarrow 0, \quad (19)$$

where Δl_1 is an element of the arc of the leading boundary of the secondary stream,

$\Delta\delta_1$ is the angle of elementary revolution of the stream which corresponds to arc Δl_1 ,

we have for the 1-th section of the stream

$$\Delta l_1 = \Phi(\delta_1) \Delta\delta_1, \quad (20)$$

$\Delta\delta_1$ is the integration step which will be designated according to the necessary accuracy of calculations. For the "subsonic" section, $\Delta\delta$ is conveniently assigned in the following way:

$$\Delta\delta = \frac{\delta_1 - \delta_{12}}{n}. \quad (21)$$

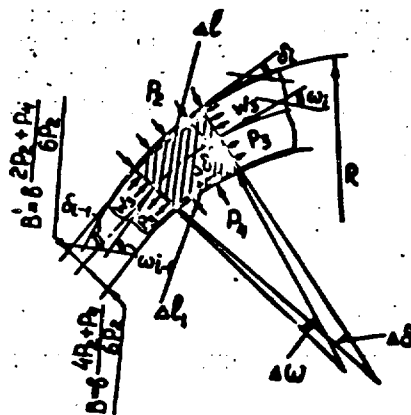


Fig. 5.

Here n is the number of partitions of the "subsonic" part.

As the calculations show, sufficiently good results can be obtained already when $n = 10$.

With known Δl_1 we shall determine:

$$\delta_1 = \delta_{1-1} - \Delta\delta_1, \quad (22)$$

$$x_1 = x_{1-1} + \Delta l_1 \cdot \cos \delta_1, \quad (23)$$

$$y_1 = y_{1-1} + \Delta l_1 \cdot \sin \delta_1, \quad (24)$$

etc.

In the supersonic region the integration step is arbitrarily selected and calculation is conducted up to the adhesion points.

After obtaining the profile of the secondary stream it is possible to construct the pattern of its main flow: calculation of the position and form of the leading shock wave is produced according to the

method presented in [4] and calculation of the terminating oblique shock at the known angle of rotation of flow presents no difficulties.

In the presence of parameters of shock waves, according to the usual gas-dynamic relationships we determine pressure and speed, and consequently, the entire pattern of interaction of flows becomes known.

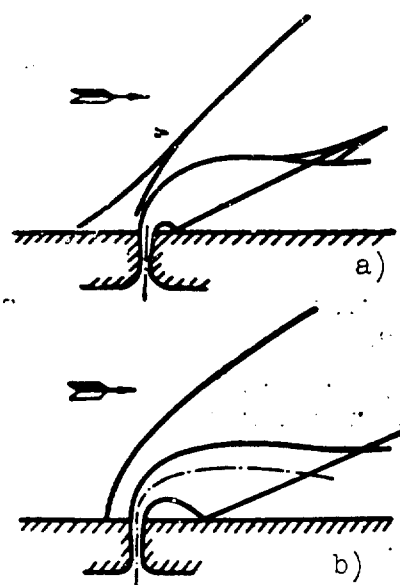


Fig. 6.

The experimental and calculating pattern of flows shown in Fig. 6a and 6b agree well qualitatively. For checking the quantitative coincidence of results of calculation with experiment, calculations were conducted for determining the effectiveness of a blast of secondary gas in a supersonic flow under conditions of the experiments of [1]. With the help of the derived relationships we calculated the pattern of flow and found the corresponding distribution of pressures throughout wall. The total effect was estimated by the magnitude of transverse force appearing on the wall during the blast

$$N_s = N_j + N_R,$$

where N_j is the jet force taking place on a slot of unit length of stream blast, which was calculated as

$$N_j = m'_3 \cdot w_3 + (P_a - P_0) \cdot b_a,$$

N_R is force appearing on a wall of unit length as a result of reconstruction of the pressure profile. The latter, taking into account the fact that the pressure below point E is close to the pressure in an undisturbed flow, was calculated as

$$N_R = (P_{2,p}^* - P_1) \cdot \overline{DC} + (P_4 - P_1) \overline{CE}.$$

Figure 7 shows the relative magnitude

$$k = \frac{N_I + N_R}{N_0},$$

which was constructed depending upon blast pressure (consequently, with constant b_{a_3} and on flow rate m_3^1). It shows how many times the force appearing during the blast on the wall exceeds the jet force of the secondary stream N_V during its flow into a vacuum. As can be seen, coordination with the experiment in this case is also sufficiently good.

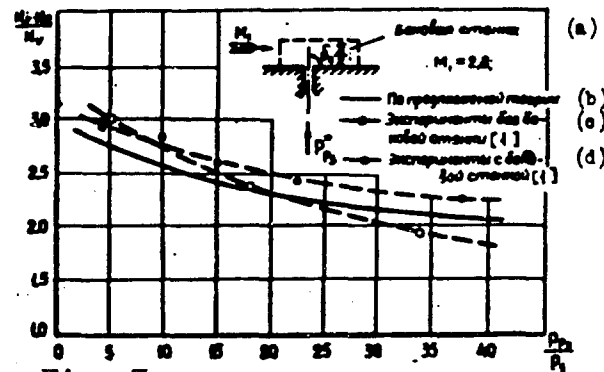


Fig. 7.

KEY: (a) Lateral wall; (b) According to the proposed theory; (c) Experiments without lateral wall [1]; (d) Experiments with lateral wall [1].

Hence, it may be concluded that the proposed method of approximation of theoretical estimation of the gas-dynamic influence on a supersonic flow, although it is based on rather rough assumptions and proposals, nevertheless gives an accuracy sufficient for practical calculations.

Literature

1. A. Heuser and F. Maurer. Experimentelle Untersuchungen an festen Spoilern und Strahlspoilern bei Machschen Zahlen von 0.6 bis 2.8. Z. Flugwiss, 10 (1962), Heft 4/5.
2. W. Seibold. Theoretische Abschätzung der Spoilerwirkung im Ubershallbereich. Jahrbuch 1955 der DWL.
3. G. Dupuichs. C. R. Acad. sci., 1960, 251, No. 2.
4. B. S. Vinogradov and Z. G. Shaykhutdinov. Method of approximation of the calculation of a detached bow wave in a supersonic flow around blunt bodies. IVUZ, "Aeronautical Engineering," No. 2, 1963.
5. L. G. Loytsyanskiy. Mechanics of fluids and gas. State Press for Technical and Theoretical Literature, Moscow, 1957.
6. V. D. Heiss and R. F. Probstine. Theory of hypersonic flows. IIL, 1962.
7. A. I. Borisenko. Gas dynamics of engines. Oborongiz, 1960.

Submitted
14 December 1963

THE INFLUENCE OF A SEQUENTIAL DECREASE IN THICKNESS
OF A METAL ON THE CURVATURE OF SHAPED COMPONENTS

M. N. Lysov and Yu. P. Katayev

Definitions of Cyrillic Items

$p = h$ = height

$H = cv$ = concave

$B = cx$ = convex

$\Gamma = g$ = geometric

In the design contemporary flight vehicles we find the wide application cylindrical skins with variable outline thickness of the guide and wafer type.

Obtainment of such skins from sheets of variable of thickness can be complicated due to the unequal strength of the blank: it is impossible to apply bending with extension, while the processes of bending and rolling and free bending become difficult to control. Therefore, in a number of cases it is expedient to prepare such components from sheets of constant thickness with a sequential change of it by the method of chemical etching (chemical milling).

As it is known [1], [2], [3], in a shaped component there are residual stresses that are variable with respect to height of cross section, in magnitude, and in sign (Fig. 1c). With the stable form

of a component these residual stresses are mutually balanced and their moment with respect to the axis of rigidity of cross section is equal to zero.

If we subject such components to chemical etching, as a result of which a layer of metal of definite magnitude will be removed, and the thickness of the material will decrease, the equilibrium of the residual stresses will be disturbed. Their resultant P_z gives a moment M_x with respect to the axis of rigidity of cross section. A new equilibrium state of residual stresses is attained as a result of the change in shape of the component.

Determination of the magnitude of change and the final form of the component, in which the residual stresses change in cross section, arrive in equilibrium state which is necessary in the designing of structures and equipment that ensure the given accuracy of manufacture of components.

Obtaining Components with Variable Thickness along the Guide Outline

The section of a component which remains after chemical milling, depending upon the relationship of removed layers with convex and concave sides, can consist of the following combination of deformations created during shaping of elastic and plastic zones:

- 1) the elastic zone and sections of plastic zones asymmetric in magnitude and located with convex and concave sides of component (Fig. 1, h_1),
- 2) the elastic zone located on the convex side and the plastic located on the concave side of the component (Fig. 1, h_2),
- 3) the elastic zone located on the concave side and the plastic located on the convex side (Fig. 1, h_3),

4) the plastic zone on the concave side of the original component shape (Fig. 1, h_4),

5) the plastic zone on the convex side of the original component shape (Fig. 1, h_5).

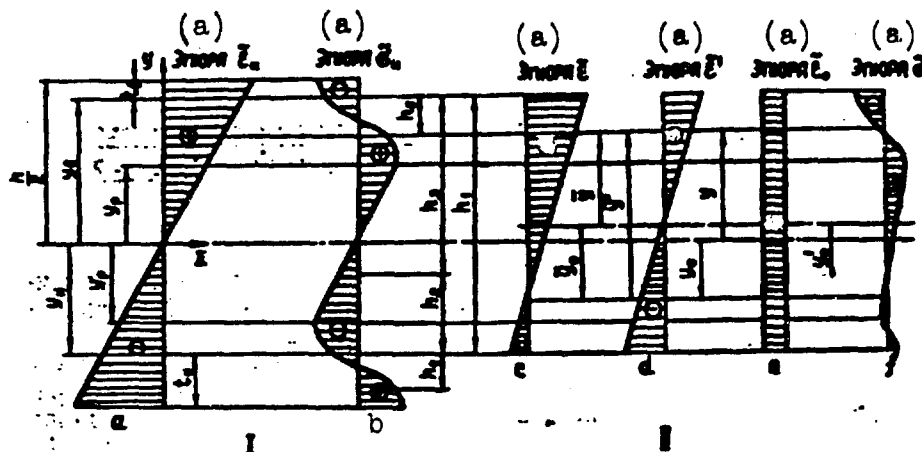


Fig. 1. Diagram of percentage elongations and residual stresses. I) in original component; II) in component after chemical milling.
KEY: (a) Diagram.

The diagram of plastic unit strain in a cross section of a component after chemical milling will be linear (hypothesis of flat sections). It is possible to divide it into components from pure bending $\tilde{\epsilon}'$ and from extension or compression $\tilde{\epsilon}_0$ (Fig. 1c, d, e).

Expressing component $\tilde{\epsilon}'$ from pure bending through curvature $\tilde{\kappa}^x$ of a layer that is neutral during pure bending, we will have

$$\tilde{\epsilon} = \tilde{\kappa}^x \tilde{y} + \tilde{\epsilon}_0 - \tilde{\kappa}^x \tilde{y}_0, \quad (1)$$

where

$$\tilde{y} = \tilde{y} - \tilde{y}_0, \quad \tilde{y}_0 = -\frac{\tilde{\epsilon}_0}{\tilde{\kappa}^x}.$$

\tilde{y} is the distance of the fiber from neutral during pure bending of a layer that has curvature $\tilde{\kappa}^x$,

\tilde{y}_0 is the distance between the neutral layer of the complete diagram of permanent deformations and the neutral layer during pure bending.

Taking the middle layer of a component before chemical milling, as the beginning of reading of ordinates of fibers with respect to height of cross section, we have the following expression for percentage elongation

$$\tilde{\epsilon} = \tilde{x}'y - \tilde{x}'y_0, \quad (2)$$

where

$$y_0 = \tilde{y}_0 - y'_0. \quad (3)$$

y is the distance of the fiber from the middle layer of the component before chemical milling,

y'_0 is the distance between the middle layer of the initial section and the layer of the section after chemical milling which is neutral during pure bending.

In the active stage of shaping, the stresses in the elastic and plastic zones are expressed accordingly as linear $\sigma = E \cdot \epsilon$ and exponential $\sigma = K\epsilon^n$ dependences [2]. The residual stresses will be: in the elastic zone —

$$\tilde{\sigma} = E\tilde{\epsilon}, \quad (4)$$

in the plastic zone —

$$\tilde{\sigma}_1 = K\tilde{\epsilon}^n + E(\tilde{\epsilon} - \epsilon), \quad (5)$$

where K , n are constants of the strain hardening curve [2],

E is the elastic modulus,

ϵ and $\tilde{\epsilon}$ are the unit elongations of the fiber correspondingly in the active stage of bending and remaining in the component after chemical etching.

Putting the value of $\tilde{\epsilon}$ from (2) and $\epsilon = xy$ in equations (4) and (5), we obtain

$$\tilde{\sigma} = E\tilde{x}'y - E\tilde{x}'y_0, \quad (6)$$

$$\tilde{\sigma}_1 = Kx^ny^2 - E(x - \tilde{x}')y - E\tilde{x}'y_0, \quad (7)$$

where x is the curvature of the middle layer of the component before chemical milling in the active stage of bending.

Conditions of equilibrium of internal forces in a section of the component after chemical milling are determined by the following equations:

$$\Sigma Z - p, \Sigma M_x = 0. \quad (8)$$

We shall expand these equations for Case 1, when the remaining section of the component after chemical milling consists of an elastic zone and sections of plastic zones that are asymmetric in magnitude

$$\Sigma Z = \int_{-y_h}^{y_h} \tilde{\sigma}_1 dy + \int_{-y_{cv}}^{y_h} \tilde{\sigma} dy + \int_{y_h}^{y_{cx}} \tilde{\sigma}_1 dy = 0, \quad (9)$$

$$\Sigma M_x = \int_{-y_h}^{y_h} \tilde{\sigma}_1 y dy + \int_{-y_{cv}}^{y_h} \tilde{\sigma} y dy + \int_{y_h}^{y_{cx}} \tilde{\sigma}_1 y dy = 0, \quad (10)$$

where y_h is the ordinate of the boundary of zones of elastic and plastic flow with respect to height of cross section,

y_{cv} , y_{cx} are correspondingly the ordinates of boundaries of removed layers with concave and convex surfaces, counted off from the middle layer of the component before chemical milling.

Putting in the values of $\tilde{\sigma}$ and $\tilde{\sigma}_1$ from (6) and (7) equations (9) and (10) we have:

$$\begin{aligned} \Sigma Z = & \int_{-y_h}^{y_h} Kx^2 y^2 dy - \int_{-y_h}^{y_h} E(z - \tilde{x}^2) y dy - \int_{-y_h}^{y_h} E\tilde{x}^2 y_0 dy + \int_{y_h}^{y_{cx}} E\tilde{x}^2 y dy - \\ & - \int_{y_h}^{y_{cv}} E\tilde{x}^2 y_0 dy + \int_{y_h}^{y_{cx}} Kx^2 y^2 dy - \int_{y_h}^{y_{cx}} E(z - \tilde{x}^2) y dy - \int_{y_h}^{y_{cx}} E\tilde{x}^2 y_0 dy = 0, \end{aligned}$$

$$\begin{aligned} \Sigma M_x = & \int_{-y_h}^{y_h} Kx^2 y^{2+1} dy - \int_{-y_h}^{y_h} E(z - \tilde{x}^2) y^2 dy - \int_{-y_h}^{y_h} E\tilde{x}^2 y_0 y dy + \\ & + \int_{y_h}^{y_{cx}} E\tilde{x}^2 y^2 dy - \int_{y_h}^{y_{cv}} E\tilde{x}^2 y_0 y dy + \int_{y_h}^{y_{cx}} Kx^2 y^{2+1} dy - \\ & - \int_{y_h}^{y_{cx}} E(z - \tilde{x}^2) y^2 dy - \int_{y_h}^{y_{cx}} E\tilde{x}^2 y_0 y dy = 0. \end{aligned}$$

After solving this system we find:
from the first equilibrium equation -

$$\bar{y}_0 = \frac{2^{1-n} K}{E(n+1)} \cdot \frac{\bar{\xi}^x}{\bar{\xi}^n} \cdot \frac{\bar{y}_n^{n+1} - \bar{y}_n^{n+1}}{\bar{y}_n + \bar{y}_0} - \left(\frac{\bar{\xi}^x}{\bar{\xi}} - 1 \right) \frac{\bar{y}_n - \bar{y}_0}{2}, \quad (11)$$

from the second equilibrium equation -

$$\begin{aligned} \frac{2^{1-n} K}{E(n+2) \bar{\xi}^n} (\bar{y}_n^{n+2} + \bar{y}_n^{n+2}) - \frac{\bar{y}_n^3 + \bar{y}_0^3}{3 \bar{\xi}} - \left[\frac{2^{1-n} K (2\epsilon_p)^{n+2}}{E(n+2)} - \frac{2(2\epsilon_p)^3}{3} \right] \bar{\xi}^2 + \\ + \frac{\bar{y}_n^3 + \bar{y}_0^3}{3 \bar{\xi}^x} - \frac{\bar{y}_0}{2 \bar{\xi}^x} (\bar{y}_n^2 - \bar{y}_0^2) = 0, \end{aligned} \quad (12)$$

$$\text{where } \bar{y}_0 = \frac{y_0}{h}, \quad p = \frac{1}{2}, \quad \bar{\xi} = \frac{p}{h}, \quad \bar{p}^x = \frac{1}{\bar{\xi}^x}, \quad \bar{\xi}^x = \frac{\bar{p}^x}{h},$$

h is the thickness of the component before chemical milling,
 ϵ_p is the conditional limit of proportionality (approximated point of transition of linear dependence $\sigma - \epsilon$ to exponential), according to [3]

$$\epsilon_p = \left(\frac{K}{E} \right)^{\frac{1}{1-n}}.$$

By solving equations (11) and (12), after corresponding transformations we finally obtain the basic formula for determination of radius of curvature of the bent component after chemical milling:

$$\bar{\xi}^x = \frac{\gamma_2 \bar{\xi}}{\gamma_2 - \gamma_1 \bar{\xi}^{1-n} + c_1 \bar{\xi}^2}. \quad (13)$$

Constants c_1 , γ_1 , γ_2 depend on the mechanical properties of the material and the magnitudes of layers removed during chemical milling and are determined by the following expressions:

$$\begin{aligned} c_1 &= \frac{2^{1-n} K}{E(n+2)} (2\epsilon_p)^{n+2} - \frac{2}{3} (2\epsilon_p)^3, \\ \gamma_1 &= \frac{2^{1-n} K}{E} \left[\frac{\bar{y}_n^{n+2} + \bar{y}_0^{n+2}}{n+2} - \frac{(\bar{y}_n - \bar{y}_0)(\bar{y}_n^{n+1} - \bar{y}_0^{n+1})}{2(n+1)} \right], \\ \gamma_2 &= \frac{\bar{y}_n^3 + \bar{y}_0^3}{3} - \frac{(\bar{y}_n + \bar{y}_0)(\bar{y}_n - \bar{y}_0)^2}{4}. \end{aligned} \quad (14)$$

For finding the position of the layer of the component after chemical milling, which is neutral during pure bending, we will use

equations (1) and (3) which are written in relative magnitudes:

$$\begin{aligned}\bar{y}_0 &= -2\bar{x}_0\bar{t}^2, \\ \bar{y}_0 &= \bar{y}_0 - \bar{y}_1.\end{aligned}$$

By solving this system we obtain the expression for determination of the ordinate of the indicated layer:

$$\bar{y}_0 = -2\bar{x}_0\bar{t}^2 - \bar{y}_0. \quad (15)$$

$\bar{\epsilon}_0$ depends on component tensile force P_z

$$\bar{\epsilon}_0 = \frac{P_z}{EF}, \quad (a)$$

where F is the area of cross section of the component after chemical milling.

As shown in [2], the residual stresses in the component after unloading can be determined by the formulas

$$\bar{\sigma} = E\bar{x}y, \quad (b)$$

$$\bar{\sigma}_1 = Kx^2y' - E(x - \bar{x})y, \quad (c)$$

where \bar{x} is the remaining curvature of the middle layer after unloading.

According to Fig. 1, the vector of resultant force of internal stresses will be written as

$$P_z = - \int_{-y_0}^{y_0} \bar{\sigma}_1 \cdot l \cdot dy - \int_{-y_0}^{y_0} \bar{\sigma} \cdot l \cdot dy - \int_{-y_0}^{y_0} \bar{\sigma}_1 \cdot l \cdot dy. \quad (d)$$

Jointly solving equations (a) and (d), taking into account (b) and (c), after a number of transformations we finally obtain the formula for determination of the magnitude sought:

$$\bar{\epsilon}_0 = \frac{K}{2E(n+1)t^2} \cdot \frac{\bar{y}_0^{n+1} - \bar{y}_1^{n+1}}{\bar{y}_0 + \bar{y}_1} - \left(\frac{1}{t} - \frac{1}{t}\right) \frac{\bar{y}_0 - \bar{y}_1}{4}. \quad (16)$$

Considering a particular case of bilateral uniform chemical milling, i.e., considering $\bar{y}_{cv} = \bar{y}_{cx} = \bar{y}^x$, equation (13) will be written in the form of

$$\bar{\epsilon}^x = \frac{1}{1 - \frac{y^x}{y^2} - \left(1 - \frac{y^{n+2}}{y^2}\right) \frac{n^{1-n}}{y^{1-n}}}.$$

where $\nu = \frac{y_h}{\frac{h}{2}}$ is the relative ordinate of the boundary of zones of elastic and plastic strains with respect to height of section. Expressing all relative magnitudes in this equation through component thickness after chemical milling, equal to $2y^x$, we have:

$$\tilde{\xi} = \frac{t}{1 - [\nu^2 + \beta(1 - \nu^{n+2})\xi^{1-n}]},$$

i.e., we have obtained the known formula that determines the residual radius of curvature in components obtained by the method of elastic-plastic bending [2]. Consequently, the residual radius of curvature of the component depends on the curvature created in the active stage of deformation and does not depend when the bilateral uniform decrease of thickness took place, i.e., before or after shaping.

Thus, for the given case we have found analytic dependences for determining the basic geometric parameters of a component after chemical milling.

The solution of the questions under consideration for other cases of chemical milling in principle is similar to the one presented. Therefore, we shall give final formulas that determine the relative radius of curvature ξ^x of a layer that is neutral during pure bending, which remains after chemical milling, and parameters \bar{y}_0 and $\tilde{\epsilon}_0$ which characterize its position.

Case 2 (section after chemical milling consists of part of the elastic zone which located on the convex side, and part of the plastic zone which is located on the concave side of the component):

$$\begin{aligned} \tilde{\xi}^x &= \frac{y_0^x}{y_2 - y_1 \xi^{1-n} - y_0 \xi^n + \frac{1}{2} \epsilon_0 \xi^n}, \\ \bar{y}_0 &= \frac{2^{1-n} K}{E(n+1) \xi^n} \cdot \frac{y_2^{n+1} - y_1^{n+1}}{y_2 \pm y_1} - \frac{\tilde{\xi}^x}{\xi} \cdot \frac{y_2^2 - y_1^{n+2}}{2(y_2 \pm y_1)} - \frac{y_2 \mp y_1}{2}, \\ \tilde{\epsilon}_0 &= \frac{K}{2^2 E(n+1) \xi^n} \cdot \frac{y_2^{n+1} - y_1^{n+1}}{y_2 \pm y_1} - \frac{1}{4\xi} \cdot \frac{y_2^2 - y_1^2}{y_2 \pm y_1} + \frac{1}{4\xi} (y_2 \mp y_1). \end{aligned} \quad (17)$$

$$\begin{aligned}
\text{where } c_2 &= \frac{2^{1-n} K (2a_p)^{n+1}}{E(n+1)} - (2a_p)^2, \\
\gamma_0 &= \frac{\bar{y}_{\max} \mp \bar{y}_{\min}}{4}, \\
\gamma_1 &= \frac{2^{1-n} K}{E} \left(\frac{\bar{y}_{\max}^{n+1}}{n+2} - \frac{\bar{y}_{\min}^{n+1}}{n+1} \cdot \frac{\bar{y}_{\max} \mp \bar{y}_{\min}}{2} \right), \\
\gamma_2 &= \frac{\bar{y}_{\max}}{3} - \frac{\bar{y}_{\max}^2 (\bar{y}_{\max} \mp \bar{y}_{\min})}{4}, \\
\gamma_3 &= \frac{\bar{y}_{\max} \pm \bar{y}_{\min}}{3} - \frac{(\bar{y}_{\max} \mp \bar{y}_{\min})(\bar{y}_{\max} - \bar{y}_{\min})}{4},
\end{aligned} \tag{18}$$

\bar{y}_{\max} and \bar{y}_{\min} correspondingly are the maximum and minimum ordinates of boundaries of removed layers.

In the system of equations (17) and (18) the upper sign pertains to the case when \bar{y}_{\max} and \bar{y}_{\min} are divided by the middle line of cross section of the component before chemical milling, and the lower sign, when \bar{y}_{\max} and \bar{y}_{\min} are located on one side of the middle line of cross section of the component before chemical milling.

Case 3 (section after chemical milling consists of part of the elastic zone which is located on the concave side, and part of the plastic zone which is located on the convex side):

$$\begin{aligned}
\tilde{\xi} &= \frac{\gamma_3^2}{\gamma_2 - \gamma_1 \xi^{1-n} - \gamma_0 c_2^2 + \frac{1}{2} c_1^2}, \\
\bar{y}_0 &= \frac{2^{1-n} K \tilde{\xi}}{E(n+1) \xi^n} \cdot \frac{\bar{y}_s^{n+1} - \bar{y}_a^{n+1}}{\bar{y}_s \pm \bar{y}_a} - \frac{\tilde{\xi}}{\xi} \cdot \frac{\bar{y}_s^2 - \bar{y}_a^2}{2(\bar{y}_s \pm \bar{y}_a)} + \frac{\bar{y}_s \mp \bar{y}_a}{2}, \\
\bar{c}_0 &= -\frac{K}{2^n E(n+1) \xi^n} \cdot \frac{\bar{y}_s^{n+1} - \bar{y}_a^{n+1}}{\bar{y}_s \pm \bar{y}_a} + \frac{1}{4\xi} \cdot \frac{\bar{y}_s^2 - \bar{y}_a^2}{\bar{y}_s \pm \bar{y}_a} - \frac{1}{4\xi} (\bar{y}_s \mp \bar{y}_a).
\end{aligned} \tag{19}$$

With respect to the double signs the above-mentioned remark is valid.

Case 4 (section after chemical milling consists of part of the plastic zone which is located on the concave side of the original component shape):

$$\begin{aligned}\tilde{\xi}^n &= \frac{\gamma_2 \xi}{\gamma_2 - \gamma_1 \xi^{1-n}}, \\ \bar{y}_0 &= \frac{2^{1-n} K \tilde{\xi}^n}{E(n+1) \xi^n} \cdot \frac{\bar{y}_n^{n+1} - \bar{y}_n^{n+1}}{\bar{y}_n - \bar{y}_n} + \frac{\tilde{\xi}^n}{\xi} \cdot \frac{\bar{y}_n + \bar{y}_n}{2} - \frac{\bar{y}_n + \bar{y}_n}{2}, \\ \bar{s}_0 &= - \frac{K}{2^n E(n+1) \xi^n} \cdot \frac{\bar{y}_n^{n+1} - \bar{y}_n^{n+1}}{\bar{y}_n - \bar{y}_n} - \frac{1}{2} \left(\frac{1}{\xi} - \frac{1}{\tilde{\xi}} \right) \cdot \frac{\bar{y}_n + \bar{y}_n}{2},\end{aligned}\quad (20)$$

where

$$\begin{aligned}\gamma_1 &= \frac{2^{1-n} K}{E} \left[\frac{\bar{y}_{\max}^{n+2} - \bar{y}_{\min}^{n+2}}{n+2} - \frac{(\bar{y}_{\max} + \bar{y}_{\min})(\bar{y}_{\max}^{n+1} - \bar{y}_{\min}^{n+1})}{2(n+1)} \right], \\ \gamma_2 &= \frac{\bar{y}_{\max}^3 - \bar{y}_{\min}^3}{3} - \frac{(\bar{y}_{\max} + \bar{y}_{\min})(\bar{y}_{\max}^2 - \bar{y}_{\min}^2)}{4}.\end{aligned}\quad (21)$$

Case 5 (section after chemical milling consists of part of the plastic zone which is located on the convex side of the original component shape):

$$\begin{aligned}\tilde{\xi}^n &= \frac{\gamma_2 \xi}{\gamma_2 - \gamma_1 \xi^{1-n}}, \\ \bar{y}_0 &= \frac{2^{1-n} K \tilde{\xi}^n}{E(n+1) \xi^n} \cdot \frac{\bar{y}_n^{n+1} - \bar{y}_n^{n+1}}{\bar{y}_n - \bar{y}_n} - \frac{\tilde{\xi}^n}{\xi} \cdot \frac{\bar{y}_n + \bar{y}_n}{2} + \frac{\bar{y}_n + \bar{y}_n}{2}, \\ \bar{s}_0 &= - \frac{K}{2^n E(n+1) \xi^n} \cdot \frac{\bar{y}_n^{n+1} - \bar{y}_n^{n+1}}{\bar{y}_n - \bar{y}_n} + \frac{1}{2} \left(\frac{1}{\xi} - \frac{1}{\tilde{\xi}} \right) \cdot \frac{\bar{y}_n + \bar{y}_n}{2}.\end{aligned}\quad (22)$$

Thus, formulas are derived which make it possible to determine the remaining curvature of neutral layer during pure bending and its position after chemical milling for components with variable thickness along the guide outline.

In these formulas, constants γ_2 , γ_2' , γ_2'' , γ_3 , which depend only on the magnitude of the removed layer for the case of one-sided chemical milling, can be determined on graphs (Fig. 4, 6, 8). Constants γ_1 , γ_1' , γ_1'' , besides the geometry of the remaining section, also depend on the mechanical properties of the material. For case of one-sided chemical milling they can be determined on the graphs shown in Fig. 3, 5, 7.

On the graphs of Fig. 3 - 8 and 10, along the axis of abscissas the relative thickness of the removed layer $\bar{t} = \frac{t}{h}$ is plotted.

Obtaining Components of the Wafer Type

Chemical etching for obtaining components of the wafer type is basically produced only on its concave surface, wherein the thickness of the runner along the length of the guide remains constant.

The runner of the component after chemical milling can consist of different combinations of elastic and plastic zones of deformations:

- 1) plastic zone located on convex side of component, elastic zone, and part of plastic zone,
- 2) plastic zone located on convex side of component and part of elastic zone,
- 3) part of plastic zone located on convex side of component.

Equations of equilibrium of forces (8) for case 1 of wafer-type components will be written (Fig. 2) as

$$\sum Z = \bar{l}_1 \int_{-\frac{A}{2}}^{\frac{A}{2}} \tilde{\sigma}_1 \cdot dy + \bar{l}_2 \int_{-\frac{A}{2}}^{\frac{A}{2}} \tilde{\sigma}_1 \cdot dy + \int_{\frac{A}{2}}^{\frac{A}{2}} \tilde{\sigma} \cdot dy + \int_{\frac{A}{2}}^{\frac{A}{2}} \tilde{\sigma}_1 \cdot dy = 0,$$

$$\sum M_z = \bar{l}_1 \int_{-\frac{A}{2}}^{\frac{A}{2}} \tilde{\sigma}_1 \cdot y \cdot dy + \bar{l}_2 \int_{-\frac{A}{2}}^{\frac{A}{2}} \tilde{\sigma}_1 \cdot y \cdot dy + \int_{\frac{A}{2}}^{\frac{A}{2}} \tilde{\sigma} \cdot y \cdot dy + \int_{\frac{A}{2}}^{\frac{A}{2}} \tilde{\sigma}_1 \cdot y \cdot dy = 0,$$

where $\bar{l}_1 = \frac{l_1}{l}$, $\bar{l}_2 = \frac{l_2}{l}$, $l_1 = \sum l_{1i}$, $l_2 = \sum l_{2i}$.

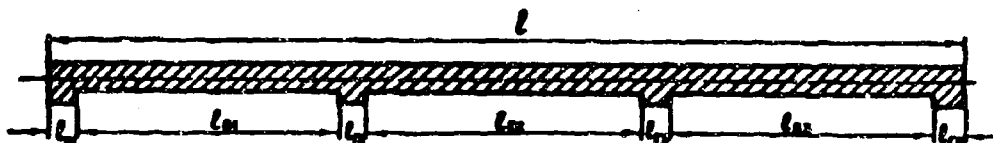


Fig. 2. Geometric parameters of wafer-type component.

Putting the values of $\tilde{\sigma}$ and $\tilde{\sigma}_1$ from (6) and (7) in these equations and calculating the integrals, we obtain:

$$\begin{aligned}
& \sum Z = \bar{I}_r \left[Kx^n \frac{y_p^{n+1} - \left(\frac{h}{2}\right)^{n+1}}{n+1} - E(x - \tilde{x}^x) \frac{y_p^2 - \left(\frac{h}{2}\right)^2}{2} - \right. \\
& \quad \left. - E\tilde{x}^x y_0 \left(\frac{h}{2} - y_p\right) \right] + \\
& + \bar{I}_s \left[Kx^n \frac{y_p^{n+1} - y^{n+1}}{n+1} - E(x - \tilde{x}^x) \frac{y_p^2 - y^2}{2} - E\tilde{x}^x y_0 (y^x - y_p) \right] - \\
& - 2E\tilde{x}^x y_0 y_p + Kx^n \frac{\left(\frac{h}{2}\right)^{n+1} - y_p^{n+1}}{n+1} - E(x - \tilde{x}^x) \frac{\left(\frac{h}{2}\right)^2 - y_p^2}{2} - \\
& - E\tilde{x}^x y_0 \left(\frac{h}{2} - y_p\right) = 0, \\
& \sum M_x = Kx^n \frac{\left(\frac{h}{2}\right)^{n+2} - y_p^{n+2}}{n+2} - E(x - \tilde{x}^x) \frac{\left(\frac{h}{2}\right)^3 - y_p^3}{3} - E\tilde{x}^x y_0 \frac{y_p^2 - \left(\frac{h}{2}\right)^2}{2} - \\
& - Kx^n \frac{\left(\frac{h}{2}\right)^{n+2} - y_p^{n+2}}{n+2} \bar{I}_s + E(x - \tilde{x}^x) \frac{\left(\frac{h}{2}\right)^3 - y_p^3}{3} \bar{I}_s + \\
& + E\tilde{x}^x y_0 \frac{y_p^2 - \left(\frac{h}{2}\right)^2}{2} \bar{I}_s + Kx^n \frac{y_p^{n+2} - y^{n+2}}{n+2} \bar{I}_s - E(x - \tilde{x}^x) \frac{y_p^2 - y^2}{3} \bar{I}_s - \\
& - E\tilde{x}^x y_0 \frac{y_p^2 - y^2}{2} \bar{I}_s + \frac{2}{3} E\tilde{x}^x y_p^3 + Kx^n \frac{\left(\frac{h}{2}\right)^{n+2} - y_p^{n+2}}{n+2} - \\
& - E(x - \tilde{x}^x) \frac{\left(\frac{h}{2}\right)^3 - y_p^3}{3} - E\tilde{x}^x y_0 \frac{\left(\frac{h}{2}\right)^2 - y_p^2}{2} = 0.
\end{aligned}$$

After a series of transformations the equations are reduced to the form of

$$\bar{y}_0 = \frac{2^{1-n} K \bar{I}_s \bar{I}_r}{E(n+1) \xi^n} \cdot \frac{1 - \bar{y}^{n+1}}{2 - \bar{I}_s (1 - \bar{y}^n)} - \frac{\bar{I}_s}{2} \left(\frac{\xi^x}{\xi} - 1 \right) \frac{1 - \bar{y}^2}{2 - \bar{I}_s (1 - \bar{y}^n)}, \quad (23)$$

$$\begin{aligned}
& - \frac{2^{1-n} K}{E(n+2) \xi^n} [2 - \bar{I}_s (1 - \bar{y}^{n+2})] - \frac{1}{3\xi} [2 - \bar{I}_s (1 - \bar{y}^3)] - \\
& - \left[\frac{2^{2-n} K}{E(n+2)} (2y_p)^{n+2} - \frac{2}{3} (2y_p)^3 \right] \xi^2 + \frac{1}{3\xi^2} [2 - \bar{I}_s (1 - \bar{y}^3)] - \\
& - \frac{\bar{I}_s}{2\xi^2} (1 - \bar{y}^2) \bar{y}_0 = 0, \quad (24)
\end{aligned}$$

where ξ is the relative radius of curvature of the middle layer of the component before chemical milling,

ξ^x is the relative radius of curvature of the layer that is neutral during pure bending after chemical milling.

By solving the system of equations (23) and (24) with respect to $\tilde{\xi}^x$, after the corresponding transformations we will finally obtain the formula for determination of the remaining curvature of the component after chemical milling:

$$\tilde{\xi}^x = \frac{\gamma_1^x}{\gamma_1^x \tilde{\xi}^{1-x} + c_1 \tilde{\xi}} \quad (25)$$

Constants γ_1 and γ_2 are determined by expressions

$$\gamma_1 = \frac{2^{1-\alpha} K}{E} \left\{ \frac{2 - \bar{L}_0 (1 - \bar{y}^{2\alpha+1})}{\alpha + 2} - \frac{\bar{L}_0 (1 - \bar{y}^2) (1 - \bar{y}^{2\alpha+1})}{2(\alpha + 1) [2 - \bar{L}_0 (1 - \bar{y})]} \right\},$$

$$\gamma_2 = \frac{2 - \bar{L}_0 (1 - \bar{y}^2)}{3} - \frac{\bar{L}_0 (1 - \bar{y}^2)^2}{4[2 - \bar{L}_0 (1 - \bar{y})]} \quad (26)$$

and constant c_1 is determined by corresponding equation (14).

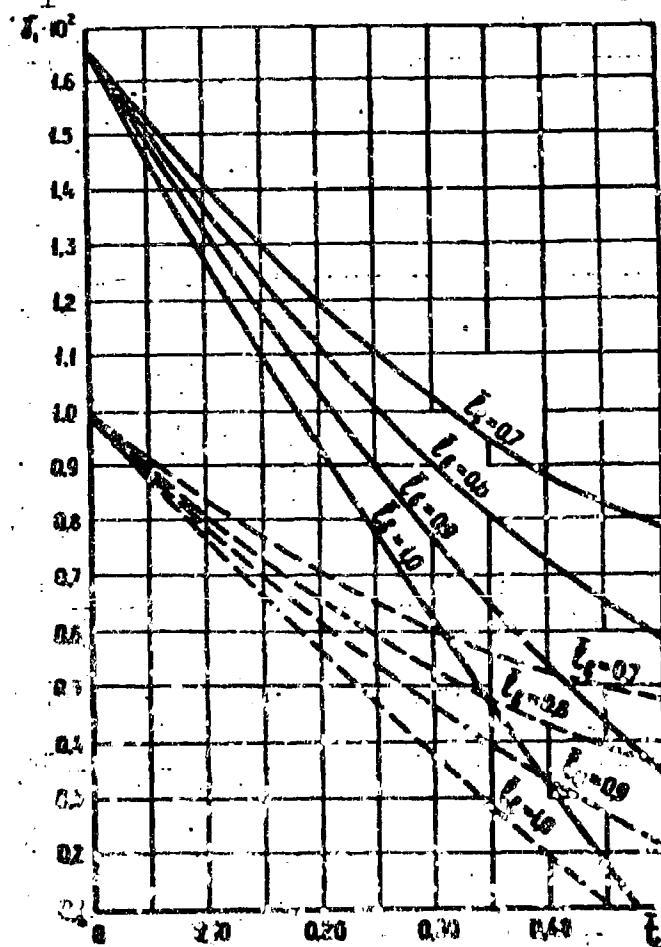


Fig. 3. Graphs of the function $\gamma_1 = f(\bar{L}, \bar{L}_0)$ for materials D16AM (---) and D16Al (—).

The position of the layer that is neutral during pure bending of the component after chemical milling, with respect to the middle layer of the component before chemical milling, will be determined by equation (15); the magnitude of $\tilde{\epsilon}_0$ for the case under consideration is found with the expression

$$\tilde{\epsilon}_0 = \bar{l}_s \left[\frac{K}{2 \cdot (n+1) E \bar{l}_s} \cdot \frac{\bar{y}^{n+1} - 1}{2 - \bar{l}_s (1 - \bar{y}^2)} - \frac{1}{4} \left(\frac{1}{\bar{\epsilon}} - \frac{1}{\tilde{\epsilon}} \right) \frac{\bar{y}^2 - 1}{2 - \bar{l}_s (1 - \bar{y}^2)} \right]. \quad (27)$$

For other cases of chemical milling of wafer-type components, the solutions in principle are analogous. By omitting a detailed description of the solution, we shall give the final results.

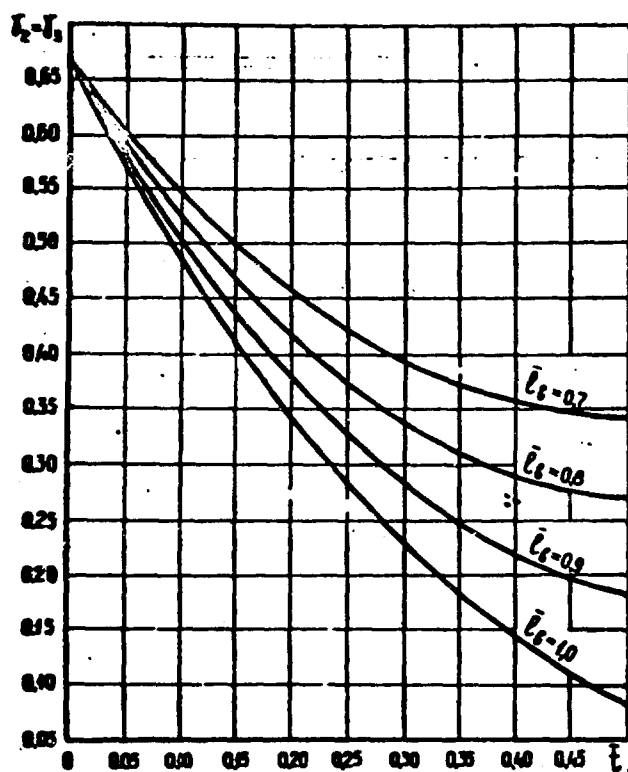


Fig. 4. Graphs of function $\gamma_2 = \gamma_3 = f(\bar{t}, \bar{l}_{cx})$.

Case 2 (section of runner consists of plastic zone located on convex side of component, and part of elastic zone)

$$\begin{aligned}
\bar{\epsilon}^2 &= \frac{2\bar{\epsilon}^2}{\bar{\epsilon}_2 - \bar{\epsilon}_1 \bar{\epsilon}^{1-\alpha} - c_1 \bar{\epsilon}_0^2 + \frac{3}{2} c_1^2 c_1 \bar{\epsilon}^2}, \\
\bar{y}_0 &= \frac{2^{1-\alpha} K \bar{\epsilon}_0^2}{E(\alpha+1) \bar{\epsilon}^2} \cdot \frac{1 - \bar{\epsilon}^{\alpha+1}}{2 - \bar{\epsilon}_0 (1 \mp \bar{y}^2)} - \frac{\bar{\epsilon}_0 \bar{\epsilon}_0^2}{2\bar{\epsilon}} \cdot \frac{1 - \bar{\epsilon}^2}{2 - \bar{\epsilon}_0 (1 \mp \bar{y}^2)} + \\
&\quad + \frac{\bar{\epsilon}_0}{2} \frac{1 - \bar{y}^2}{2 - \bar{\epsilon}_0 (1 \mp \bar{y}^2)}, \\
\bar{u}_0 &= \bar{\epsilon}_0 \left[\frac{K}{2^{\alpha} E(\alpha+1) \bar{\epsilon}^2} \cdot \frac{\bar{\epsilon}^{\alpha+1} - 1}{2 - \bar{\epsilon}_0 (1 \mp \bar{y}^2)} - \frac{1}{4\bar{\epsilon}} \cdot \frac{\bar{\epsilon}^2 - 1}{2 - \bar{\epsilon}_0 (1 \mp \bar{y}^2)} + \right. \\
&\quad \left. + \frac{1}{4\bar{\epsilon}} \cdot \frac{\bar{y}^2 - 1}{2 - \bar{\epsilon}_0 (1 \mp \bar{y}^2)} \right],
\end{aligned} \tag{28}$$

where $c_1 = \frac{2 - \bar{\epsilon}_0}{3}$.

$$\begin{aligned}
\bar{\epsilon}_1 &= \frac{2^{1-\alpha} K}{E} \left(\frac{2 - \bar{\epsilon}_0}{\alpha + 2} - \frac{\bar{\epsilon}_0^2 (1 - \bar{y}^2)}{2(\alpha + 1)(2 - \bar{\epsilon}_0 (1 \mp \bar{y}^2))} \right), \\
\bar{\epsilon}_2 &= \frac{2 - \bar{\epsilon}_0}{3} - \frac{\bar{\epsilon}_0^2 (1 - \bar{y}^2)}{4(2 - \bar{\epsilon}_0 (1 \mp \bar{y}^2))}, \\
\bar{\epsilon}_0 &= \frac{2 - \bar{\epsilon}_0 (1 \mp \bar{y}^2)}{3} - \frac{\bar{\epsilon}_0^2 (1 - \bar{y}^2)^2}{4(2 - \bar{\epsilon}_0 (1 \mp \bar{y}^2))}, \\
\bar{\epsilon}_0 &= c_1 - \bar{\epsilon}_2.
\end{aligned} \tag{29}$$

Constant c_2 is determined by corresponding equation (18).

The upper sign in equations of system (28) and (29) pertains to the case when the thickness of the runner is more than half of the thickness of the component before chemical milling and the lower sign, when the thickness of the runner is less than half of the thickness of the component before chemical milling.

Case 3 (section of runner consists of part of plastic zone located on convex side of component)

$$\begin{aligned}\bar{\xi}^* &= \frac{\bar{\tau}_2^* \bar{\xi}}{\bar{\tau}_2^* - \bar{\tau}_1^* \bar{\xi}^{1-n} + \frac{3}{2} c_2^* c_1 \bar{\xi}}, \\ \ddot{y}_0 &= \frac{2^{1-n} K \bar{\xi}^* \bar{\tau}_0}{E(n+1) \bar{\xi}^n} \cdot \frac{1 - \bar{y}^{n+1}}{2 - \bar{\tau}_0(1 + \bar{y}^n)} - \frac{\bar{\xi}^* \bar{\tau}_0}{2\bar{\xi}} \cdot \frac{1 - \bar{y}^{n+1}}{2 - \bar{\tau}_0(1 + \bar{y}^n)} + \\ &\quad + \frac{\bar{\tau}_0}{2} \frac{1 - \bar{y}^{n+1}}{2 - \bar{\tau}_0(1 + \bar{y}^n)}, \\ \bar{c}_0 &= \bar{\tau}_0 \left[\frac{K}{2^n E(n+1) \bar{\xi}^n} \cdot \frac{\bar{y}^{n+1} - 1}{2 - \bar{\tau}_0(1 + \bar{y}^n)} + \frac{1}{4} \left(\frac{1}{\bar{\xi}} - \frac{1}{\bar{\xi}^*} \right) \frac{1 - \bar{y}^{n+1}}{2 - \bar{\tau}_0(1 + \bar{y}^n)} \right],\end{aligned}\quad (30)$$

where $c_2^* = \frac{2}{3}(1 - \bar{\tau}_0)$,

$$\begin{aligned}\bar{\tau}_1^* &= \frac{2^{1-n} K}{E} \left\{ \frac{2 - \bar{\tau}_0(1 + \bar{y}^{n+1})}{n+2} - \frac{\bar{\tau}_0^2(1 - \bar{y}^{n+1})(1 - \bar{y}^{n+1})}{2(n+1)(2 - \bar{\tau}_0(1 + \bar{y}^n))} \right\}, \\ \bar{\tau}_2^* &= \frac{2 - \bar{\tau}_0(1 + \bar{y}^{n+1})}{3} - \frac{\bar{\tau}_0^2(1 - \bar{y}^{n+1})^2}{4(2 - \bar{\tau}_0(1 + \bar{y}^n))}.\end{aligned}\quad (31)$$

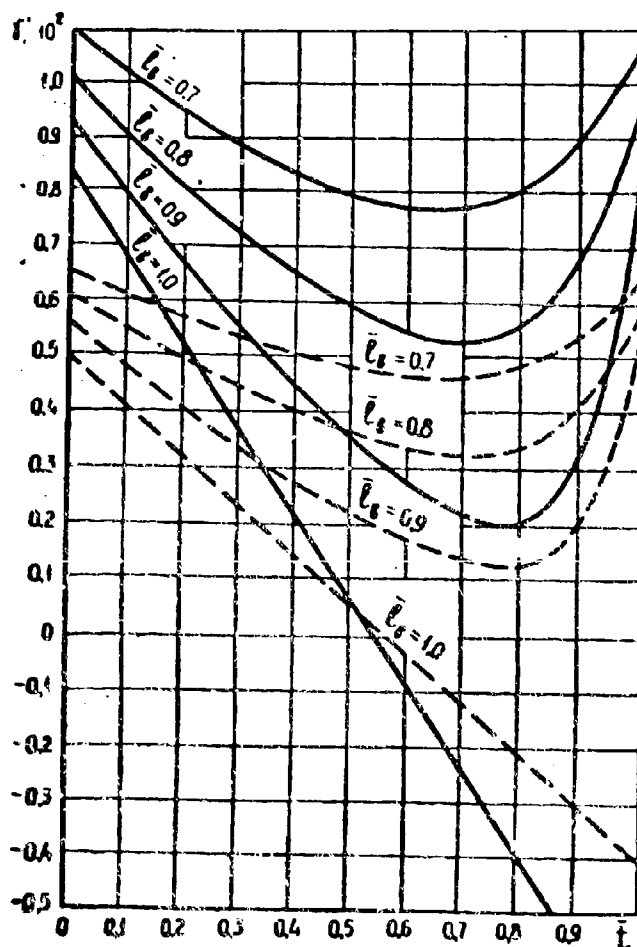


Fig. 5. Graphs of function $\gamma'_1 = \gamma(\bar{\tau}, \bar{\tau}_0)$ for materials D16AM (—) and D16AT (---).

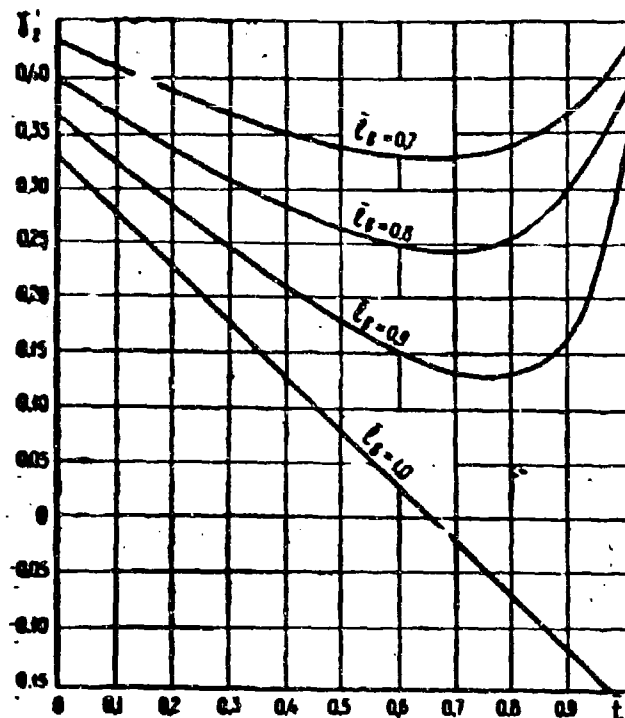


Fig. 6. Graphs of function $\gamma_2' = f(\bar{\tau}, \bar{\tau}_{cx})$.

Thus, for different forms of wafer-type components we found analytical dependences which make it possible to determine their basic geometric parameters after chemical milling.

Constants γ_2 , γ_2' , γ_2'' , γ_3 , which depend only on the magnitude of the removed layer, can be found on the graphs shown in Fig. 4, 6, 8, and constants γ_1 , γ_1' , γ_1'' , which depend, besides the geometry of the remaining section, on the mechanical properties of the materials, are found on the graphs of Fig. 3, 5, 7.

In the determination of the curvature which must be given to the component in the active stage of bending, in order to obtain the given curvature after unloading and subsequent chemical milling, it is necessary that the dependence $\frac{1}{\bar{\xi}} = f(\bar{\tau}, \bar{\tau}_{cx}, \frac{1}{\bar{\xi}})$ for different materials be presented in the form of graphs similar to the ones shown in Fig. 9 for material D16AT.

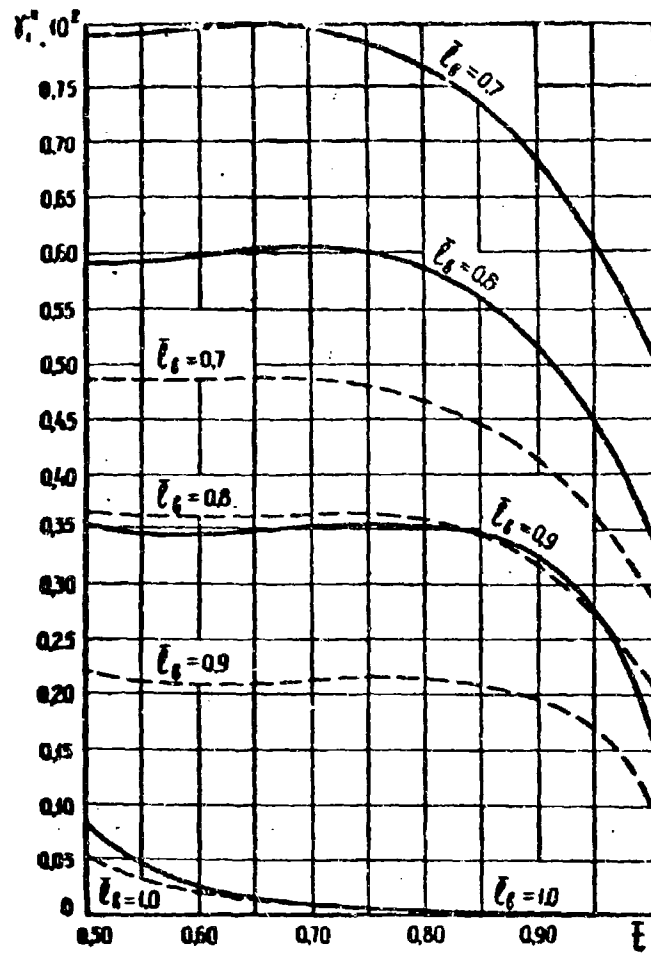


Fig. 7. Graphs of function $\gamma_1'' = f(\bar{t}, \bar{t}_{cx})$ for materials D16AM (---) and D16AT (—).

Residual stresses in components after chemical milling are determined by equations (6) and (7) which in dimensionless form have the appearance:

$$\tilde{\sigma} = \frac{E}{2\tilde{\xi}^x} \cdot - \frac{E}{2\tilde{\xi}^x} \cdot \bar{y}_0 - \text{in the elastic zone,}$$

$$\tilde{\sigma}_1 = \frac{K}{2n\tilde{\xi}n} \bar{y}^n - \frac{1}{2}E \left(\frac{1}{\tilde{\xi}} - \frac{1}{\tilde{\xi}^x} \right) \bar{y} - \frac{E}{2\tilde{\xi}^x} \cdot \bar{y}_0 - \text{in the elastic-plastic zone.}$$

The diagram residual stresses which depicts these equations is shown in Fig. 1f.

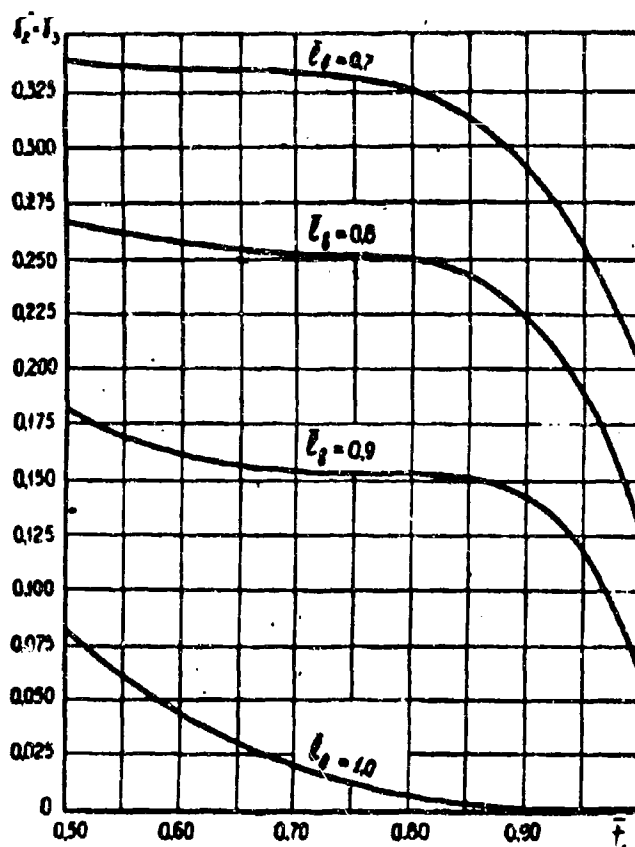


Fig. 8. Graphs of function $\gamma_2'' = \gamma_3'' = f(\bar{t}, \bar{t}_{cx})$.

As already was indicated, with the decrease of thickness of material the instability of internal stresses with respect to moment causes a change in curvature of the shaped component. Let us consider the change of this moment during chemical milling of the concave surface of a component.

With the removal of a layer within the limits of the extended zone of the diagram of residual stresses (Fig. 1b), a moment is created which decreases the curvature. Upon further increase of the removed layer the magnitude of additional unloading moment will decrease.

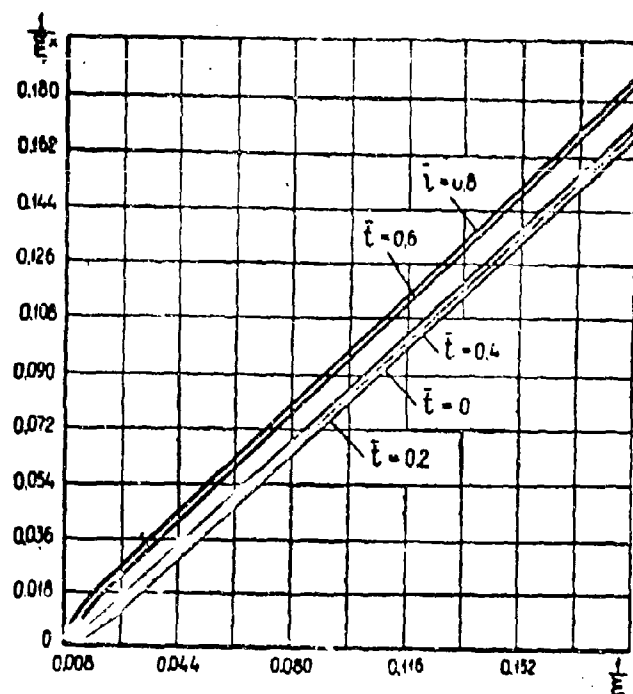


Fig. 9. Graphs of function $\frac{1}{\xi X} = r(\bar{t}, \frac{1}{\xi})$ for material D16AT during one-sided chemical milling.

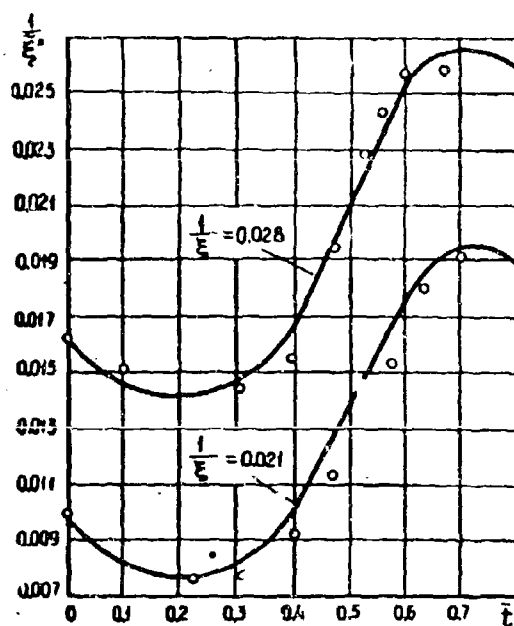


Fig. 10. Theoretical and experimental values (depicted by points) of function $\frac{1}{\xi X} = r(\bar{t}, \frac{1}{\xi})$ for material D16AT during one-sided chemical milling.

At a specific thickness of removed layer a moment is created which increases the initial curvature whose maximum value at the thickness of the removed layer will be equal to half of the thickness of the component before chemical milling. A further increase in thickness of the removed layer leads to a decrease of this moment.

This pattern of change of moment is confirmed by experimental check of the change of curvature which was conducted for material D16AT with a thickness of 1.5 and 2.5 mm (Fig. 10, 11, 12).



Fig. 11. Photograph of samples made from D16AT after chemical milling of the entire concave surface at a different magnitude ($t_1 < t_2 < t_3$, $\rho_3 < \rho_1 < \rho_2$).

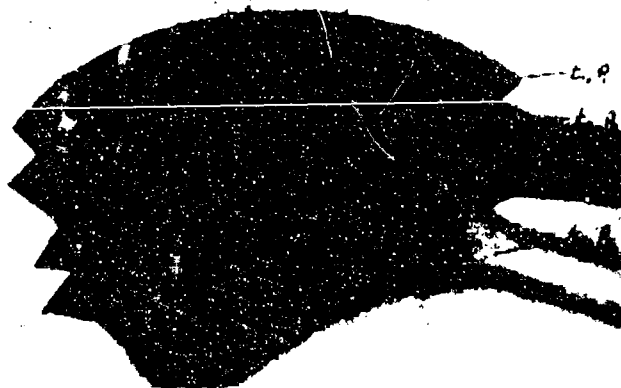


Fig. 12. Photograph of samples of the wafer type made from D16AT after chemical milling of the concave surface at a different magnitude ($t_1 < t_2 < t_3 < t_4$, $\rho_4 < \rho_1 = \rho_3 < \rho_2$).

Literature

1. A. A. Il'yushin. Plasticity. Part 1, State Technical Press, 1948.
2. M. I. Lysov. Investigation of the process of bending components made from sheet metal. KAI Transactions, No. 31, 1956.
3. M. I. Lysov. The question of determination of parameters of elasticity and residual stresses during plastic bending. KAI Transactions, No. 37, 1957.

Submitted
10 July 1963

TECHNICAL NOTES

APPROXIMATE CALCULATION OF SPEED OF FLIGHT IN A SLANTED DIVE AND DETERMINATION OF LOSS IN ALTITUDE AND RANGE ON THE DIVE ENTRY SECTION ON A PROGRAM FOR A PILOTLESS AIRCRAFT WITH TURBOJET ENGINE (TJE)

Ye. A. Kuklev

Definitions of Cyrillic Items

np = rect = rectilinear

MKGCC = MKGFS = Meter -- Kilogram -- Force -- Second

BKJ = inc = inclusion

BX = en = entry

The method of calculating the speed of an aircraft with TJE on a section of slanted and rectilinear diving on the assumption of constancy of air density and drag coefficient, and disregard of engine thrust, is given in [1]. In the same place there are investigations of motion of an aircraft during dive entry and pullout with constant overloads $n_y = \text{const}$ and $n_x = \text{const}$.

In this article we obtain a precise expression for calculating the speed of flight in a slanted dive with large thrust weight ratios: I. V. Ostoslavskiy's formula considers engine thrust as a constant.

Furthermore, the article gives expressions for determination loss of altitude and flying range in the dive entry of a pilotless aircraft based on one of the two proposed automatic pilot programs, and gives recommendation on the selection of these programs under the condition that the speed of flight can be considered constant. The concept of overload n_y is introduced here as the designation of a certain limit of maneuverability or strength which should not be exceeded in the process of motion of the aircraft, but whose assignment is a basic criterion in the selection of a permissible program. Inasmuch as programmed motions of the aircraft which are investigated in the article are not flight conditions with $n_y = \text{const}$, the results obtained can be assessed as a certain supplement to that which is already known in literature about programmed motions [2], and have an independent interest in this sense.

1. Determination of Speed During a Slanted Dive Taking into Account Engine Thrust as a Constant

Equations of motion of an aircraft with TJE during a slanted dive on the assumption of constancy of mass (m), thrust (P), and drag coefficient (c_x), which are equal to certain mean values for a given small drop in altitudes, can be written as

$$\begin{aligned} m \frac{dV}{dt} &= m \dot{V} = P - c_x \frac{\rho S V^2}{2} - G \sin \theta_0, \\ \dot{y} &= V \sin \theta_0, \quad \dot{x} = V \cos \theta_0, \quad \theta_0 = \text{const}. \end{aligned} \quad (1.1)$$

Following the designations of [1], we will take

$$\dot{V} = \frac{dV}{dv} \frac{v}{dt} = \frac{dV}{dy} V \sin \theta_0 = \frac{1}{2} \frac{dV^2}{dy} \sin \theta_0, \quad (1.2)$$

$$V_{sp}^2 = - \frac{16 G \sin \theta_0}{c_x \cdot \Delta \cdot S}, \quad (1.3)$$

$$n_1 = - \frac{P}{G \sin \theta_0}, \quad (1.4)$$

where P and G are in newtons, m in kg, n_1 is conditionally considered as the thrust weight ratio of an aircraft with TJE in a dive, and θ_0 is the dive angle.

We shall place (1.2)-(1.4) in the first equation of (1.1); then for determination of speed we will obtain a differential equation with dividing variables:

$$\frac{dV^2}{dy} = -2 \frac{G}{m} (1 + n_1) \left[1 - \frac{V^2}{V_{sp}^2 (1 + n_1)} \right]. \quad (1.5)$$

Dividing the variables in (1.5) and integrating in given limits from V_0^2 to V^2 and from y_0 to y , we will finally find

$$V^2 = V_{sp}^2 (1 + n_1) \left\{ 1 - \left[1 - \frac{V_0^2}{V_{sp}^2 (1 + n_1)} \right] \cdot \exp \left(-2 \frac{G}{m} \frac{y - y_0}{V_{sp}^2} \right) \right\}, \quad (1.6)$$

where V_0 and y_0 are the values of speed and altitude of flight in the moment of the beginning of a rectilinear slanted dive. If we put $n_1 = 0$ and $\frac{G}{m} = g$ in (1.6) for a check in the MKGFS system, we will obtain exactly the same formula as in [1].

Calculations show that the values of speed which were calculated for a small drop in altitudes (< 10 km) according to the precise formula (1.6), almost completely coincide with the results of numerical integration.

2. Determination of Loss in Altitude and Horizontal Range on the Section of Entry of an Aircraft with TJE into a Slanted Dive According to a Program

Among the possible programs for entry of an aircraft into a slanted dive we shall consider those which transfer the aircraft from horizontal flight into conditions of a slanted dive in a longitudinal plane with constant pitch angle. A dive with constant pitch angle

may be easily carried out by means of shifting the initial conditions of stabilization of horizontal flight to slanted conditions by feeding a constant programmed signal to the pitch control track. It is obvious that from considerations for the guarantee of stability and limitation of normal overload, a signal that is proportional to the pitch angle during diving cannot be fed to the control track immediately and suddenly but should be sent out gradually with a certain regularity, i.e., according to a program. The program of dive entry with constant pitch angle may be either proportional to the sweep of the control signal in time with a limitation upon achievement of a specific value which is carried out by a time mechanism, or by a gradual influence, quantized in level and supplied by a relay system (Fig. 1a, b).

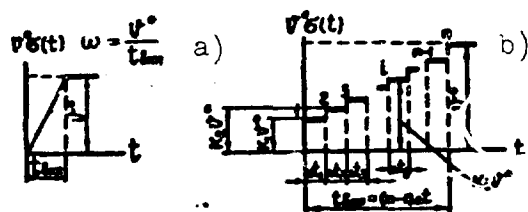


Fig. 1.

It is required to determine the losses in altitude and horizontal range for the considered programmed motions and to find correspondingly the permissible angular velocity of rotation of the programmer ω or magnitude k_1 and the duration Δt_1 of pulses under the conditions that are assigned by the pitch angle during diving (programmed signal ψ^*) and the limiting permissible normal overload $n_y \text{ max}$.

For a solution to the problem on hand we shall use the system of equations of motion of an aircraft in a longitudinal plane in variations with respect to horizontal flight [1], [2]. We shall assume that at small angles of inclination of trajectory ($< 45^\circ$) the speed of flight on the dive entry section changes insignificantly, i.e., $V = V_0 = \text{const}$, the mass of the aircraft is constant, and $\cos \theta \cong \cos \theta_0 \cong 1$, $\sin \theta \cong \theta$. Furthermore, we shall assume that the

automatic pilot is ideal and the motion of the aircraft with respect to the center of gravity will be considered only as a balancing relationship, taking the angular pitch velocity to be approximately equal to the angular turn velocity of the aircraft on the trajectory, i.e.,

$$m_x^a \cdot \alpha + m_x^b \cdot \beta + m_x^v \cdot \dot{\alpha} \approx m_x^a \cdot \alpha + m_x^b \cdot \beta + m_x^v \cdot \dot{\theta} = 0.$$

Where by, in the automatic pilot equation it is possible to take

$$i_{\omega_z} \omega_{z1} \approx i_{\omega_z} \cdot \dot{\theta}.$$

As calculations show, these assumptions are fully acceptable. For instance, an increase in speed, found with relationships [1] for the case of dive entry with $n_y = \text{const}$, does not exceed 10%. The short-periodic motion of the aircraft with respect to angle of attack, in comparison with the slowly changing program of dive entry, attenuates extraordinarily quickly and almost does not render an influence on the trajectory.

Taking into account the remarks made, the initial system of equations of motions may be written as

$$\begin{aligned} \dot{\theta} &= a_1 \alpha, & \dot{\alpha} &= -\theta + \alpha, \\ \ddot{\alpha} &= -\frac{a_1^2}{\pi_x^2} \alpha - \frac{a_1^2}{\pi_x^2} \dot{\theta}, & \dot{y} &\approx V_0 \dot{\theta}, \\ \ddot{\theta} &= i_0 \ddot{\alpha} + i_{\omega_z} \ddot{\theta} + i_{\sigma} \ddot{\sigma}(t), & \dot{x} &\approx V_0. \end{aligned} \quad (2.1)$$

where i_0, i_{ω_z} are the transmission numbers of the automatic pilot for the pitch channel,

$\sigma(t)$ is the dimensionless program of dive entry which varies from 0 to 1,

$a_1 = \frac{Y^a + P}{mV_0}$ is the dynamic coefficient.

We shall find an equation for the determination of angle θ , by excluding α , $\dot{\alpha}$, and $\ddot{\alpha}$ from the first four equations of [2.1]

$$\pi \ddot{\theta} + \theta = -i_{\sigma} \ddot{\sigma}(t), \quad (2.2)$$

where $T = \left[\frac{1 + \frac{\pi_{x_1}^2}{\pi_{x_2}^2} \frac{1}{l_0}}{\frac{\pi_{x_1}^2}{\pi_{x_2}^2}} + \frac{l_{02} + \frac{\pi_{x_2}^2}{\pi_{x_1}^2}}{l_0} \right] \approx \left[\frac{1 + \frac{\pi_{x_1}^2}{\pi_{x_2}^2} \frac{1}{l_0}}{\frac{\pi_{x_1}^2}{\pi_{x_2}^2}} + \frac{l_{02}}{l_0} \right]$ is the time constant

of the dynamic system "aircraft-automatic pilot." If we consider the initial conditions as zero (horizontal flight), the solution in expressions according to [3] will be

$$\theta(p) = -\theta^* \frac{\sigma(p)}{(T^2 + 1)}; \quad (2.3)$$

where p is the transformation parameter in a Laplace integral.

The sought solution in originals is found for every program separately.

A. Program for Diving is Worked Out with Constant Angular Velocity (Fig. 1a)

Since in this case the representation for $\sigma(p)$ according to [3] is equal to

$$\sigma(p) = \frac{1}{l_{\text{max}}} \frac{1 - e^{-p l_{\text{max}}}}{p}, \quad (2.4)$$

then in (2.3) going on to variable t by means of inverse Laplace transformation, we will obtain the following expressions for determination of angle θ :

$$\theta(t) = -\frac{\theta^*}{k} \left[\frac{t}{T} + (e^{-\frac{t}{T}} - 1) \right], \quad (2.5)$$

if the current time is less than the time of work of the programmer, i.e.,

$$t < t_{\text{max}} \text{ and } \theta(t) = -\frac{\theta^*}{k} \left[k + e^{-\frac{t}{T}} (e^k - 1) \right] \quad (2.6)$$

for any moment of time after programmer stops, i.e., for $t \geq t_{\text{inc}}$.

Here $k = \frac{t_{\text{inc}}}{T}$ and $\Delta t = t - t_{\text{inc}}$ is the current time counted off from the moment of achievement of limitation of the program.

For determination of the loss in altitude on the dive entry section it is necessary to integrate the equation for vertical velocity taking into account (2.5) and (2.6), and as a result, when $t < t_{inc}$,

$$\Delta y = y - y_0 = -\frac{g}{k} TV_0 \left[\frac{t^2}{2T^2} - \frac{t}{T} - (e^{-\frac{t}{T}} - 1) \right], \quad (2.7)$$

when $t > t_{inc}$,

$$\begin{aligned} \Delta y = & -\frac{g}{k} TV_0 \left[\frac{k^2}{2} - k - (e^{-k} - 1) \right] - \\ & -\frac{g}{k} TV_0 [k\Delta t - T(e^{-k} - 1)(1 - e^{-\frac{\Delta t}{T}})]. \end{aligned} \quad (2.8)$$

As can be seen from (2.5) and (2.6), angle θ asymptotically tends to its own limit, i.e., the programmed pitch signal ϑ^* . Therefore, for determining the moment of termination of dive entry of an aircraft it is necessary to have some specific values of this angle which are less than limiting. Let us assume that the angle of trajectory inclination at moment $\Delta t = \Delta t_\xi$ after stop of the programmer must be equal to:

$$\theta_\xi = -\xi \vartheta^*. \quad (2.9)$$

We shall place (2.9) in (2.6), and then we will see that

$$\Delta t_\xi = -T \ln \left[\frac{k(\xi - 1)}{(1 - e^{-k})} \right], \quad (2.10)$$

and the total time of dive entry of the aircraft is

$$t_{\Sigma} = t_{\Sigma 1} + \Delta t_\xi. \quad (2.11)$$

The horizontal range of the maneuver is also found here:

$$\Delta x = x - x_0 \cong V_0 t_{\Sigma}. \quad (2.12)$$

Now we shall determine the permissible angular velocity of rotation of the programmer $\omega = \frac{\vartheta^*}{t_{inc}}$ and the "time of inclusion" $k = \frac{t_{inc}}{T}$

at the given pitch angle of the dive and limitation on normal overload.

Let us note that when an aircraft follows a program for dive entry the maximum angular velocity for a turn by angle θ is attained at the moment the programming stops, i.e., when $t = t_{inc}$, after which the angular turn velocity will only attenuate. Therefore, by differentiating (2.5) and putting $t = t_{inc}$, we will find that

$$\dot{\theta}_{max} = \frac{\dot{\theta}^*}{kT}(1 - e^{-k}), \quad (2.13)$$

and from the condition of the limitation of permissible overload

$$\dot{\theta}_{max} \leq \frac{G}{m} \frac{(n_y - 1)}{V_0}. \quad (2.14)$$

If we now place (2.14) in (2.13), then there will be obtained an equation for determination of permissible values of k depending upon $\dot{\theta}^*$, n_y , V_0 , T , G , m

$$e^{-k} \leq 1 - bk, \quad (2.15)$$

where $b = -\frac{G}{m} \frac{(n_y - 1)T}{\dot{\theta}^* V_0}$ is positive in virtue of the negativity of the overload during dive entry of the aircraft. Equation (2.15) was solved graphically; a dependence of the form $k = k(b)$ is represented

in Fig. 2.

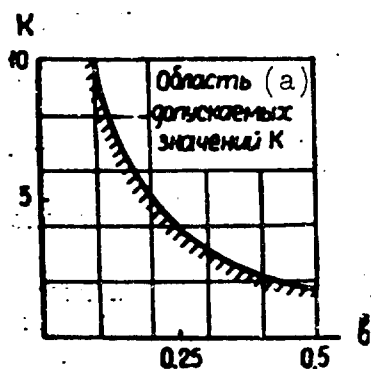


Fig. 2.

KEY: (a) region of permissible values of k .

Thus, by finding k with respect to b , we will always be able to determine the angular velocity of rotation of the programmer, and according to (2.5)-(2.12) we can find the change of the angle of inclination of the trajectory and the loss in altitude and range at any moment of time.

B. Step Program (Fig. 1b)

In the assignment of an automatic pilot program in the form of a certain step curve it is necessary to know how to calculate, on the

basis of the given criteria the permissible magnitude and duration of steps, and also the trajectory elements of the programmed motion. We shall first find the elements of the trajectory. As earlier, we shall start from the determination of angle θ . Considering the program depicted in Fig. 1b as a step influence composed of a series of equal-duration Δt pulses, of magnitude $k_1 \delta^*$, and fed consecutively in moments of time $i\Delta t$, and a single influence applied in moment of time $t = t_{inc} = (n-1)\Delta t$, for a representation of the influence according to the superposition principle [4] we will be able to write the following expression:

$$\sigma(p) = k_1 \frac{1 - e^{-\Delta t p}}{p} + k_2 \frac{e^{-\Delta t p} - e^{-2\Delta t p}}{p} + \dots + k_i \frac{e^{-(i-1)\Delta t p} - e^{-i\Delta t p}}{p} + \dots + \frac{e^{-(n-1)\Delta t p}}{p}. \quad (2.16)$$

Further, by making an inverse Laplace transform of expression (2.3), with the help of Tables [3], where (2.16) is placed instead of $\sigma(p)$, we will obtain a dependence for angle θ :

$$\theta(t) = -\theta^* \sum_{\zeta=1}^i k_{\zeta} \left[\left(1 - e^{-\frac{t-\zeta\Delta t}{T}} \right) - \left(1 - e^{-\frac{t-\zeta\Delta t}{T}} \right) \right], \quad (2.17)$$

where $i = 1, 2, \dots, n$ and when $t < i\Delta t$ $t - \zeta\Delta t = 0$ for all $\zeta = 1, \dots, n$.

The expression for calculation of the loss in altitude during dive entry will be found after integration of the equation for vertical velocity in the calculation of (2.17)

$$\Delta y = y - y_0 = -\theta^* V_0 \sum_{\zeta=1}^i k_{\zeta} \left[\left(t - (\zeta-1)\Delta t \right) - \frac{1}{T} \left(1 - e^{-\frac{t-\zeta\Delta t}{T}} \right) - \left(t - \zeta\Delta t \right) - \frac{1}{T} \left(1 - e^{-\frac{t-\zeta\Delta t}{T}} \right) \right], \quad (2.18)$$

where $i = 1, 2, \dots, n$ and when $t < i\Delta t$ $t - \zeta\Delta t = 0$ for all $\zeta = 1, \dots, n$.

The horizontal range can then be calculated by analogy with (2.12).

The magnitudes of pulses, their duration, and quantity will be found from the condition that at the moment of supply of each control pulse the maximum angular velocity of turn of a pilotless aircraft with respect to angle of trajectory inclination must not exceed the permissible value determined depending upon the available overload, i.e., from the condition of

$$\dot{\theta}_i(t) \leq \theta_{\max} \text{ (permissible)}, \quad (2.19)$$

where the right side is determined according to (2.14).

The expression for angular velocity of turn of an aircraft in any moment of time will be obtained if we differentiate (2.17), i.e.,

$$\dot{\theta}_i(t) = -\frac{\pi}{T} \sum_{\zeta=1}^i (k_{\zeta} - k_{\zeta-1}) e^{-\frac{(t-\zeta)\Delta t}{T}}, \quad (2.20)$$

where $i = 1, 2, \dots, n$ and when $t < i\Delta t$ $t - \zeta\Delta t = 0$ for all $\zeta = 1, \dots, n$, and for maximum angular velocity, if in (2.20) we place the value of current time $t = i\Delta t$ at the moment of supply of the next pulse

$$\dot{\theta}_i(t) = -\frac{\pi}{T} \sum_{\zeta=1}^i (k_{\zeta} - k_{\zeta-1}) e^{-\frac{\Delta t}{T}(i-\zeta)}, \quad (2.21)$$

where $i = 1, 2, \dots, n$ and when $t < i\Delta t$ $t - \zeta\Delta t = 0$ for all $\zeta = 1, \dots, n$.

In the calculation of (2.21) from (2.19) there follows a relationship that connects the limitations on each of the pulses with the magnitudes of all preceding pulses

$$\sum_{\zeta=1}^i (k_{\zeta} - k_{\zeta-1}) e^{-\frac{\Delta t}{T}(i-\zeta)} < b, \quad (2.22)$$

where $\zeta = 1, 2, \dots, n$, $\Delta t = 0$ when $i = 1$, and b is found according to (2.19).

On the basis of (2.22) the magnitude of any pulse may be found as a function of only its number, duration and parameter b ; namely,

$$k_1 \leq b, \\ k_1 \leq b \left[i - (i - 1)e^{-\frac{\Delta t}{T}} \right]. \quad (2.23)$$

The quantity of pulses required for the automatic pilot to gradually process a given programmed pitch signal Φ^* , is simply connected with pulse duration and may be easily found from (2.23) if we consider that the last signal of the program is characterized by the value of $k_n = 1$.

We will then be able to write

$$1 = b \left[n - (n - 1)e^{-\frac{\Delta t}{T}} \right], \quad (2.24)$$

whence it follows that permissible n should satisfy the relationship

$$n > \frac{1 - e^{-\frac{\Delta t}{T}}}{b(1 - e^{-\frac{\Delta t}{T}})} > \frac{1}{b} \quad (2.25)$$

and, conversely, on the basis of given n from (2.25) we will be able to determine the permissible pulse duration:

$$\Delta t \geq T \ln \frac{bn - 1}{b(n - 1)}. \quad (2.26)$$

It is obvious that due to the arbitrariness in the assignment of one of the magnitudes Δt or n the time of processing of the program $t_{inc} = (n - 1)\Delta t$, which is necessary for the achievement of the same value of the programmed signal, will be different. However, as one may see in (2.25) and (2.26), with the increase of quantity of pulses it will decrease and asymptotically approximate its own limit according to logarithmic law. By using this property it is possible to find, in a certain sense, an optimum (with respect to high-speed operation) program by selecting n and Δt which respond to t_{inc} , close

to limiting. For that it is possible to assign a gradient of decrease in operating time of the program depending upon the amount of pulses

$$\frac{\partial \bar{t}_{inc}}{\partial n} = \frac{\partial}{\partial n} \left[(n-1) \ln \frac{bn-1}{b(n-1)} \right] = \bar{c} \quad (2.27)$$

(where $\bar{t}_{inc} = \frac{t_{inc}}{T}$, $\Delta \bar{t} = \frac{\Delta t}{T}$ are the dimensionless time of inclusion and pulse duration, $\bar{c} = \frac{c}{T}$ is the gradient), and either, by solving (2.27), to determine optimum $n = n(b, c)$, or on the graphs of $\bar{t}_{inc} = \bar{t}_{inc}(n, b)$ to find $n = n(b)$, for given \bar{c} . Practically, when $c = 0.05-0.1 \bar{t}_{inc}$ will be limiting. Optimum $n = n(b, c)$, which is found by the second method, is given in Fig. 3. The method of evaluating a programmed maneuver entry may be the following: depending upon b , on the graphs in Fig. 3 we find the optimum (with respect to time of inclusion) $n = n(b, c)$, then with (2.26) we calculate the pulse duration Δt ; according to (2.23) we construct the program itself $k_i = k_i(b, \Delta t n)$; finally, with (2.18) and (2.12) we calculate the losses in altitude and range.

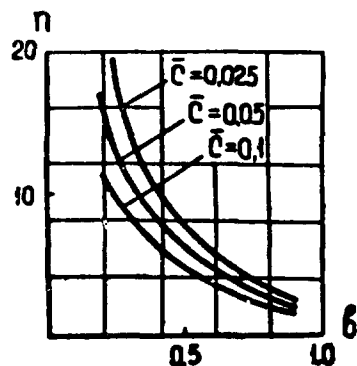


Fig. 3.

Further correction of programs constructed according to the proposed system as first approximations should consist mainly in the selection of automatic pilot transmission ratios, that ensure the given quality of stability of short-periodic motion, and can be carried out with the help of known methods.

Literature

1. I. V. Ostoslavskiy. Aerodynamics of an aircraft. Oborongiz, 1955.
2. A. A. Lebedev and L. S. Chernobrovkin. Flight dynamics of pilotless vehicles. Oborongiz, 1962.

3. Dech Gustav. Guide to the practical use of operational calculus on the basis of the Laplace transformation. Gosfizmatizdat, 1958.

4. Fundamentals of automatic control. Edited by Professor V. V. Solodovnikov, Mashgiz, 1954.

Submitted
14 November 1963

SPEED OF PROPAGATION OF A FLAME IN AN OPEN AND LIMITED FLOW OF UNIFORM MIXTURE

V. M. Yermolayev and A. V. Talantov

Definitions of Cyrillic Items

T = fl = flame

H = n = normal

$$\frac{M}{\text{сек}} = \frac{m}{\text{sec}}$$

The process of burning in engine combustion chambers occurs in a flow limited by the walls. The majority of experimental research in burning till now was carried out in an open flow. The question of the possibility of using the results of an experiment which were obtained in an open flow, in examining the processes of burning in a flow limited by walls, has not been considered by anyone.

This work analyzes this question and gives the results of a specially set up experiment.

Burning in a free flow attracts attention by the simplicity of the conditions of the experiment. The torch is open; therefore, it is possible to observe it and to easily fix the position of the flame front and the burning zone. However, the possibilities of studying burning in a free flow are restricted by the limits in which the flow

preserves its characteristics and composition. Usually these limits constitute several gauges of burner pipe. The advantages of studying burning in a flow that is limited by walls, with the extreme complexity of the experiment, are the invariability of composition of mixtures, the unlimited possibilities of studying the process through the length of a pipe, and the proximity of the experiment to conditions of the process in chambers.

Burning in an open and a limited flow has certain inherent gas-dynamic peculiarities. In the case of an open flow the gases have the possibility of expanding in transverse direction, since they are not limited by walls. There is no drop in pressure in the direction of flow in the surrounding space; therefore, the speeds of the combustion products and the fresh mixture in axial direction are kept practically unchanged and equal.

The presence of limiting walls in a closed flow excludes the possibility of expansion of gases in transverse direction. Due to the continuous feed of heat there occurs expansion of gases, a drop in pressure along the length of the chamber, and an increase in the rate of flow of combustion products and the fresh mixture.

These peculiarities of flow can render an influence on the process of burning.

First, the change of the rate of flow in the course of burning in a limited flow may cause a change in the form of the flame front and the entire torch, as compared to a torch in an open flow, even with the preservation of constancy of the speed of flame propagation. However, the dimensions of the surface of the flame front, in accordance with Michelson's law, will then remain constant. Actually, the volume flow rate of mixture (V) is the product of the speed of flame propagation (u_{fl}) on the surface of the flame front (F):

$$V = u_n \cdot F. \quad (1)$$

With the equality of flow rates and the speed of flame propagation for both cases $F = \text{const}$ is inevitable.

In Fig. 1 the solid line depicts the position of the flame for a flat torch in an open flow with ignition on the periphery; the dotted line indicates position of the flame in a limited flow in a channel of constant size. The point of closing of flame fronts shifts due to the change in form of the generator (front), with its constant length. As calculations showed [1], the shift is usually insignificant ($< 5\%$). Consequently, even for a turbulent chamber that is variable in length, such a shift will render no perceptible influence on the speed of flame propagation.

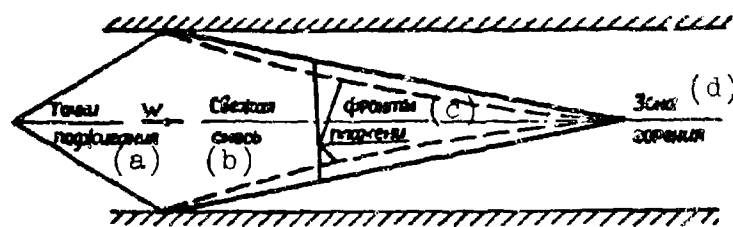


Fig. 1. Position of flame in an open flow (—) and in a chamber (---).
KEY: (a) ignition points; (b) fresh mixture; (c) flame fronts; (d) burning zone.

Secondly, a change in the rate of flow can render a direct influence on the speed of flame propagation.

In general, the speed of flame propagation in a turbulent flow of uniform mixture is a function of the pulsational rate of flow (w'), the normal speed of flame propagation (u_n), and the degree of expansion (\bar{v}):

$$u_t = f(w', u_n, \bar{v}). \quad (2)$$

The normal speed and the expansion ratio are physical-chemical characteristics of the mixture and upon transition from an open flow to a

closed one with other parameters being constant do not change. Thus, the single parameter that determines the speed of flame propagation and can be changed depending upon the conditions of expansion is the pulsational speed.

In a flow that is limited by walls the speed of the mixture increases with burning out. If we consider that the pulsational speed follows the change of the rate of flow, then various sections of the flame front will correspond to different magnitudes of pulsational speed and the considered section is located even further away from the ignition point. The biggest increase can be expected in the section that is close to the point of closing of the flame front. In this section, burning out for the most commonly used parameters of flow and mixture constitutes 0.05-0.1. The increase in the rate of flow of fresh mixture will be equal to 0.1-0.2. If the pulsational speed also increases by this magnitude, then the speed of flame propagation at the point of encounter of fronts will constitute 1.1-1.16 of the initial speed, since $u_{f1} \sim (w')^{0.8}$ [2]. The average (with respect to the torch) velocity of flame propagation increases even less and will constitute ~ 1.08 of the initial velocity, since burning out and growth of the rate of flow along the length of the chamber occur in an S-shaped curve. In reality, the pulsational speed in a convergent flow will lag behind the change of the rate of flow. This, in particular is confirmed by experiments with geometric compression of flow. Consequently, the change in the pulsational rate of flow and the rate of propagation of the flame will constitute an even smaller magnitude.

For a comparison of the magnitudes and dependences of the rates of flame propagation in an open and a closed flow we set up special experiments with a uniform gasoline-air mixture. The set up is

GRAPHS NOT
REPRODUCIBLE

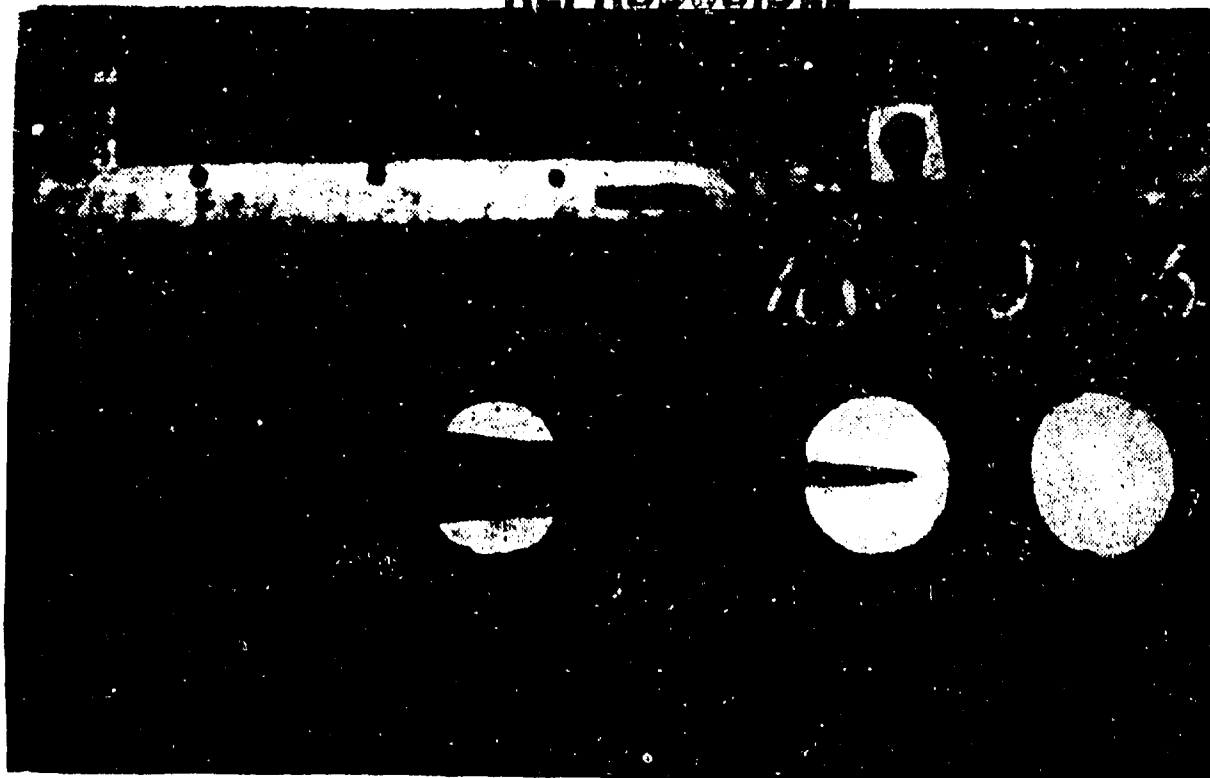


Fig. 2. Photograph of flame position in chamber.

similar to the one we described in [1]. The combustion chamber in which the experiment was conducted in a closed flow could be disassembled immediately behind the lowest flow holders. Owing to this it was possible to determine the rate of propagation of the flame also in an open flow — with removed combustion chamber — in absolutely identical conditions.

The combustion chamber had a constant square section along its entire length $a \times a$ mm; on the inlet, at a distance of half the diameter of the chamber, we placed a turbulization grid. The removable part of the combustion chamber was cooled on three sides. On one side we assembled quartz windows for registration of the position of the flame front (Fig. 2) which was fixed photographically by means of a miniature camera on film of high sensitivity. The exposure was

selected in such a manner that a further increase of it did not change the recorded position of the flame. Consequently, in the experiment we determined the front boundary of the burning zone — the flame front — the ignition front. With the dimensions of the flame surface and volume flow rate known from processing of the photorecordings, with a relationship similar to (1), we determined the rate of flame propagation.

The experiment was conducted at atmospheric pressure and temperature of the mixture 423° abs, and the composition of the mixture varied from $\alpha = 1.0$ to $\alpha = 1.5$, while the rate of flow varied from 20 to 80 m/sec (see Fig. 3 for results).

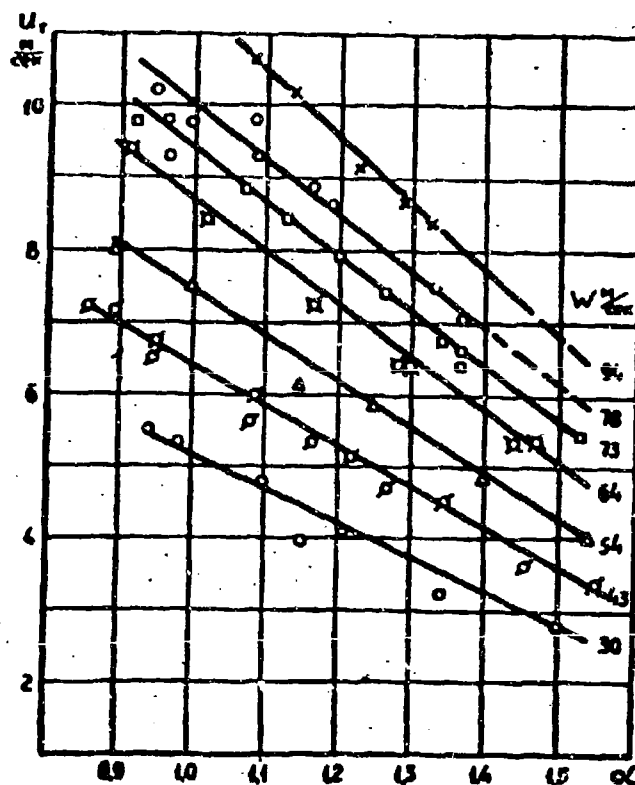


Fig. 3. Dependence of rate of flame propagation in an open turbulent flow on mixture composition for different rates of flow.

On the graphs in Figures 4 and 5 we have plotted the values of the rate of flame propagation in a turbulent flow as a function of

mixture composition: the points depict the values of u_{fl} which were obtained in an experiment with an open flow with removed combustion chamber; the curves - according to the results of experiments in a flow limited by walls - in a combustion chamber.

From a consideration of the graphs a conclusion can be made about the insignificant distinction of the magnitudes of rate of flame propagation in an open and limited flow (< 5%). The character of the dependences of speed u_{fl} on different parameters for a chamber and a free flow is absolutely identical. As should have been expected, the rate of flame propagation in the chamber is somewhat greater than in an open flow. However, this distinction is less than on the assumption of the proportionality of the pulsation rate and the rate of flow. Consequently, the pulsation rate in an accelerated flow changes slower than the rate of flow.

An indirect judgement about the insignificant change in the rate of flame propagation by means of acceleration of flow in a chamber may be also made from an analysis of the results of the experiment of V. P. Solntsev [3]. In [3] Solntsev investigated the process of combustion of a uniform gasoline-air mixture behind linear stabilizers in conditions of a closed flow. The investigation was produced in 200×175 at normal pressure and temperature of 400° abs. The rate of flame propagation was determined by the angle between the surface of the flame front and the direction of flow in a number of points on the cone length. It was determined that the local speed of flame propagation on the length of the chamber changes in proportion to the pulsational speed determined in a cold flow before burning. This means that the process of burning does not cause a noticeable change of pulsational speed of the forward flow on the cone length of the closed flame fronts.

The dependences of speed of flame propagation in a free turbulent flow were experimentally studied in the works of L. S. Kozachenko [4], A. V. Talantov [5], and other authors.

The results of the experiment of [5] for a wide range of initial conditions during burning in an open flow can be described by the dependence

$$\frac{u_{fl}}{u_n} = A(1 - 1)^{0.75} \left(\frac{u'}{u_n} \right)^{0.75},$$

where $A = 1$.

As a result of treatment of experiments of our work [2], for a chamber we obtained the dependence

$$\frac{u_{fl}}{u_n} = A(1 - 1)^{0.75} \left(\frac{u'}{u_n} \right)^{0.75},$$

where $A = 1$.

The distinction in dependences was very small.

For a comparison of the results of the experiment in a closed and open flow the data of different authors are depicted in coordinates of the form $\frac{u_{fl}}{u_n} - \theta = f \left(\frac{u'}{u_n} \right)$ (Fig. 6). These coordinates ensue from the theory of burning in a turbulent flow. It is not difficult to see that all data are grouped in one region, practically near one curve.

Thus, on the basis of a consideration of the peculiarities of the process of burning in an open and limited flow of uniform mixture and an analysis of the results of experiments described in literature and specially set up by us, the following conclusions can be made.

The magnitudes and the character of the dependences of rate of flame propagation in a free and limited flow of uniform mixture differ insignificantly; in first approximation this distinction can be disregarded. Consequently, in calculations of combustion chambers of the

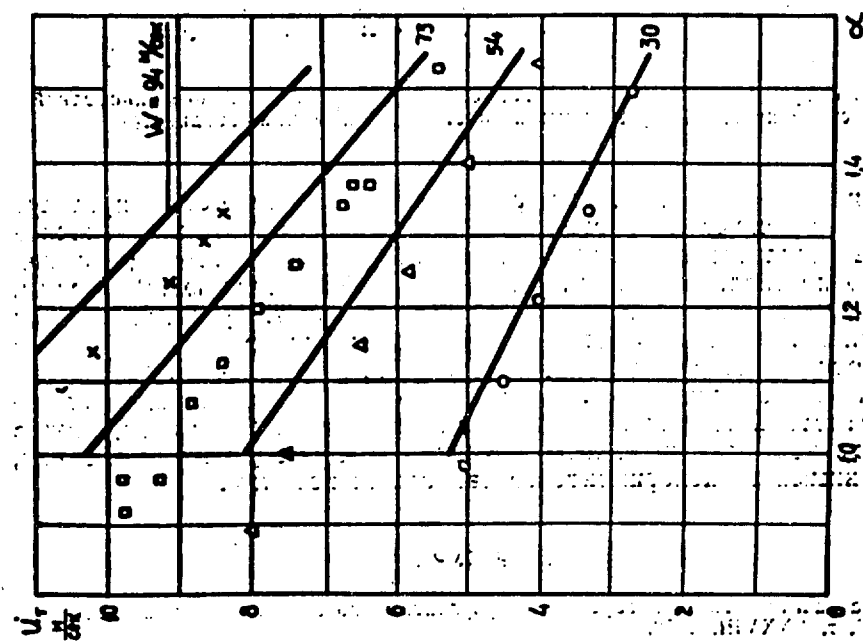


Fig. 4. Rate of flame propagation for an open and closed flow depending upon composition of the mixture; points — open flow, lines — chamber.

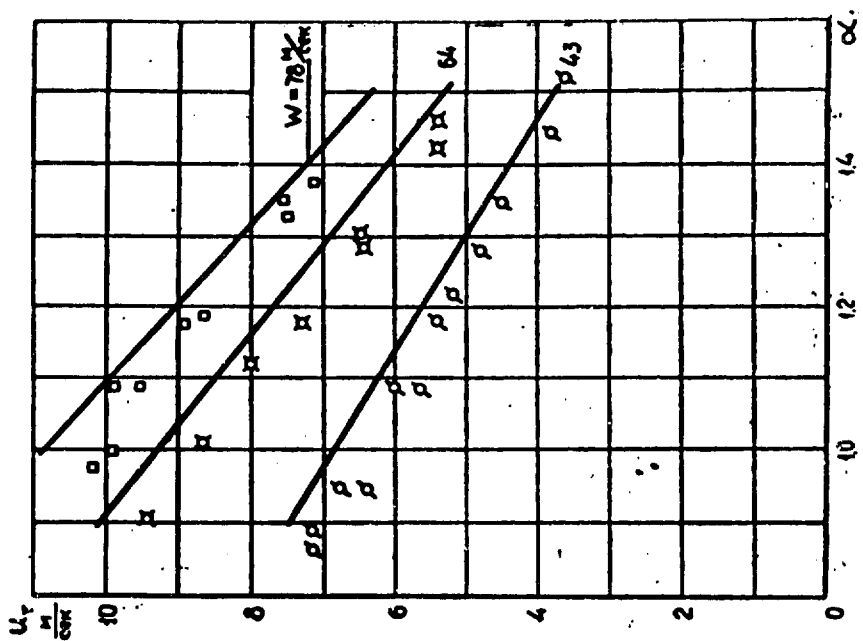


Fig. 5. Rate of flame propagation for an open and closed flow depending upon composition of the mixture; points — open flow, lines — chamber.

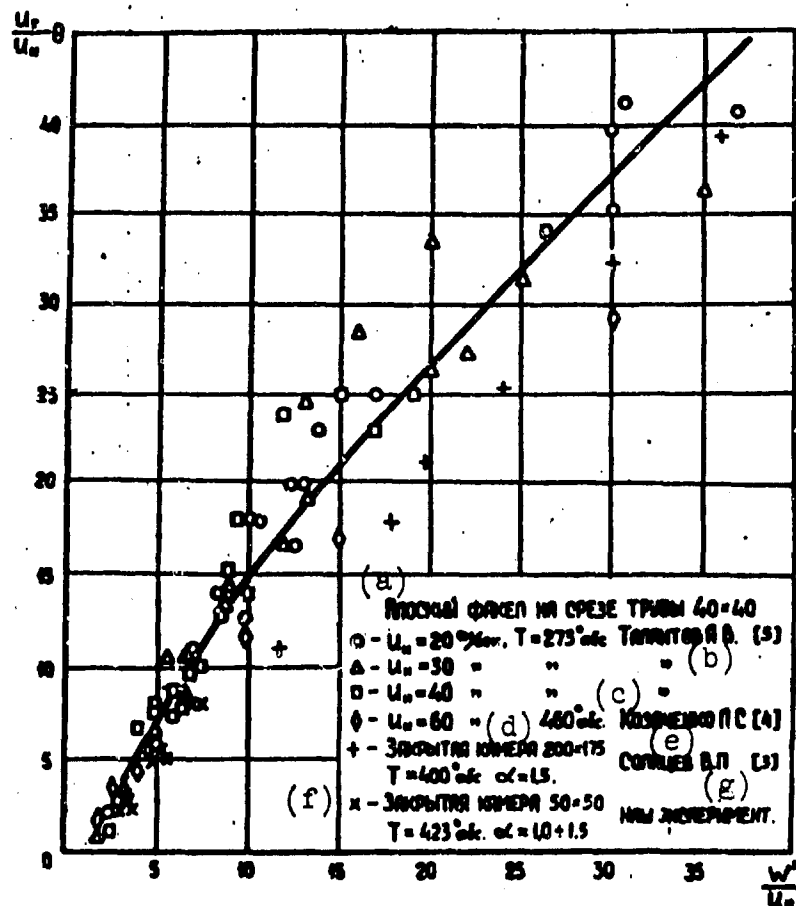


Fig. 6. Rate of flame propagation in a turbulent flow of uniform mixture according to various authors in dimensionless coordinates.

KEY: (a) plane jet on pipe cutoff; (b) A. V. Talantov [5]; (c) L. S. Kozachenko [4]; (d) closed chamber; (e) V. P. Solntsev [3]; (f) closed chamber; (g) our experiment.

straight-through flow type, which operate on a uniform mixture, it is possible to use the dependences of rate flame propagation which were obtained in the experiment with a free flow.

Literature

1. A. V. Talantov. Burning in a turbulent flow limited by walls. KAI Transactions, Vol. XXXVIII, 1958.
2. V. M. Yermolaye and A. V. Talantov. Investigation of the effect of pressure on the rate of flame propagation in a turbulent

flow of uniform mixture. IVYZ, "Aeronautical Engineering," No. 4, 1961.

3. V. P. Solntsev. The influence of turbulence parameters on the process of combustion of a uniform gasoline-air mixture behind a stabilizer in conditions of a closed flow. Collection: "Flame stabilization and development of the process of combustion in a turbulent flow," Oborongiz, 1961.

4. L. S. Kozachenko. Burning of gasoline-air mixtures in a turbulent flow. News of the Academy of Sciences USSR, Division of Chemical Sciences, No. 1, 1960.

5. A. V. Talantov. Investigation of burning in a turbulent flow of a uniform gas mixture. Oborongiz, 1955.

Submitted
11 October 1963

INVESTIGATION OF AN ULTRASONIC GENERATOR OF A LIQUID FUEL

N. S. Lamekin

Definitions of Cyrillic Items

ст = j = jet

p = r = resonator

c = n = nozzle

град = deg = degree

пс = cs = constant section

вт = w = watt

кгц = kc = kilocycles

тек = cur = current

макс = max = maximum

References [1], [2], and [3] give descriptions, theoretical prerequisites, and results of an investigation of an ultrasonic burner.

The energy source of this burner for splitting the liquid into drops is an annular gas-current generator mounted in body 3 (Fig. 1)

and differing from the usual type by the fact that the resonator cavity has a round rod 7 around which an annular cavity 5 is formed. The nozzle works with excess pressure in a jet equal to $0.43 \cdot 10^4 \frac{\Pi}{m^2}$, the degree of noncalculation $n = \frac{p_j}{p_a} = 4$ and $M = 1$. Under the action of ultrasonic oscillations that appear in resonator 5, the jet of liquid at the radial clearance outlet 4 is broken up into drops. In distinction from the generators of Bergman [4] and V. P. Kurkin, the investigated generator is significantly less in weight and is noiseless, which excludes the necessity of protective means.

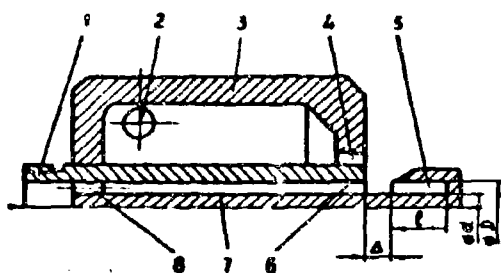


Fig. 1. Diagram of burner with generator. 1 - body, 2 - entry of liquid into burner chamber, 3 - body of burner, 4 - radial clearance for outlet of liquid, 5 - generator chamber, 6 - annular nozzle of generator, 7 - generator rod, 8 - inlet channels for air.

Up to now the physical nature of oscillations excited by an annular generator has not been studied and there are no theories and methods for calculating the parameters of constructions. Assuming that displacement of air particles from the position of equilibrium ζ is proportional to $\cos (nt + \epsilon)$, it is possible on the basis of the theory of plane waves [5] to write the differential oscillation equation in the form of

$$\frac{\partial^2 \zeta}{\partial x^2} + \frac{\omega^2}{a^2} \zeta = 0, \quad (1)$$

where a is the speed of sound.

The solution of equation (1), taking into account forced oscillations of given frequency $\omega/2\pi$, when the axis of the resonator at point $x = 0$ supports an oscillation of $\zeta = A (\cos \omega t + \epsilon)$, and the opposite end of this resonator at a distance of $x = l$ is closed, will have the following form:

$$\zeta = \frac{A}{\sin \frac{\omega l}{a}} \cdot \sin \frac{\omega (l-x)}{a} \cdot \cos (\omega t + \epsilon). \quad (2)$$

However, equation (1) does not consider the losses in the resonator, which are connected with radiation of spherical waves at the open end. Therefore, it follows to find the section ψ , where the transition from plane wave to spherical is carried out. On the section before this transition we shall write the velocity potential

$$\varphi = A \cos k(l - x), \quad (3)$$

where k is the wave number $\left(k = \frac{2\pi}{aT} = \frac{\omega}{a}\right)$.

Using an electrical analogy we shall find the magnitude of flow as the product of the rate of flow and the inlet area of the resonator

$$q = \frac{\partial \varphi}{\partial x} \cdot F, \quad (4)$$

the velocity potential at the point where $x = 0$, will be

$$\varphi = A \cos kl. \quad (5)$$

Then

$$A \cos kl = \frac{q}{F} \cdot k \cdot FA \sin kl.$$

Finally we have:

$$\operatorname{ctg} kl = \psi k. \quad (6)$$

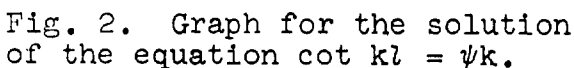
The transcendental equation (6) is solved graphically (Fig. 2).

The points of intersection of lines $y = x = \psi k$ with the curve $y = \cot x = \cot kl$ will give the roots of equation (6). Considering that ψk is small, we shall obtain a second solution of equation (6)

$$k(l + \psi) = m + \frac{1}{2} \pi, \quad (7)$$

where m is an integer.

The solutions of equation (6) and (7) allowed us to calculate the length of the resonator l_r . The resonator is designed in such a manner so that it is possible to change its length in accordance with



(a) ПТЧЕВАЯ УСТАНОВКА ТЕ-21

(b) МОДЕЛЬ ГЕНЕРАТОРА, 3

(c) ОТСЕК Т-2

$V = 446 \text{ м}^3$
 $P = 0,15 \text{ атм.}$

(d) К ВОЗДУХУ

KEY: (a) shadow installation TE-21; (b) model of generator, 3; (c) T-2 section; (d) to vacuum pump.

An investigation of a generator model, and then a generator, was conducted on an installation whose diagram is shown in Fig. 3.

We obtained the dependence $\theta =$
 $= f(p)$, i.e., we found the deflec-

GRAPHIC NOT
REPRODUCIBLE

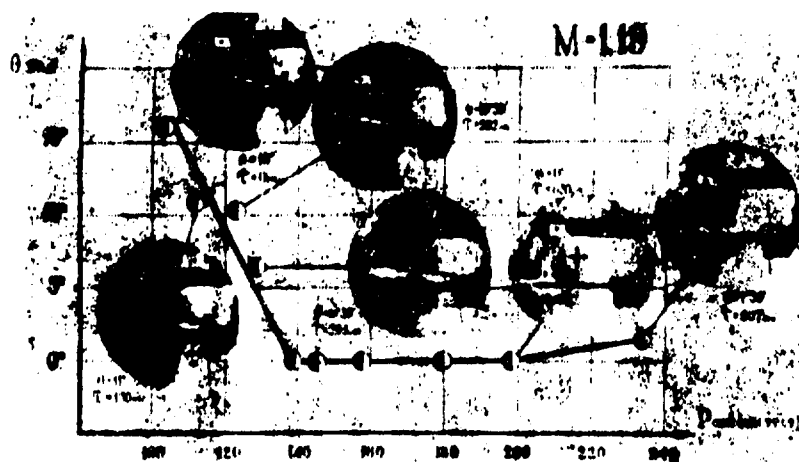


Fig. 4. Deflection of gas jet flowing from nozzle of generator model depending upon pressure in pipe $\theta = f(p)$.

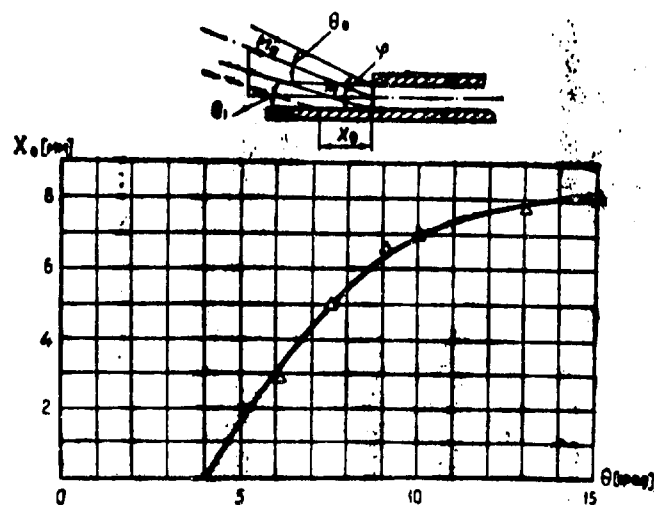


Fig. 5. Separation of boundary layer depending upon deflection of gas jet $x_0 = f(\theta)$.

boundary layer occurs at length x_0 from the nozzle cutoff. A picture of the process is represented in Fig. 4.

Figure 5 shows the dependence $x_0 = f(\theta)$. On the basis of the obtained results, the diameter of the resonator can be recommended

within the limits of $1 \leq \frac{d_r}{d_n} \leq 1.2$. The experiment established that the power and frequency of the generator with the change of wedge angle γ remain constant.

Investigation of the generator was conducted on an installation whose diagram is given in Fig. 6. Before beginning the test the generator was assembled in body 4 so that its clearance Δ was established in the focus of parabolic reflector 6. The generator was fastened to housing 6 and was joined to the compressor through filter 1 and receiver 3 by a hose.

In the section that housed the mechanical drive of piezoelectric transducer 11, we secured a paralon 9 for absorption of ultrasonic waves from the parabolic reflector. This removes interference of the face and lateral surfaces of housing 7.

The piezoelectric transducer was placed on frame 12. Its movement along the radius was carried out by an electric motor 8 through a transmission system which allowed us to fix the uniformity of the sound field from periphery to center. Electric motor 10 ensured rotation of frame 12 and, if necessary, moved it along guides A and C. In one turn of frame 12 the piezoelectric transducer moved 10 mm along the radius, thus exhibiting the uniformity of the sound field around the circumference.

The experiment used the following equipment: amplifier, millivoltmeter, frequency-spectrum analyzer, and sonic pressure recorder. Air pressure in the generator was controlled by manometer 5.

In the process of testing we investigated the influence of the length of the resonator l_r and its distance from the nozzle cutoff Δ on the acoustic characteristics of the generator. We obtained the

dependences $W = f(\Delta)$ and $\nu = f(\Delta)$ when $l_r = \text{const}$, and also $W = f(l_r)$, $\nu = f(l_r)$ when $\Delta = \text{const}$, as represented in Fig. 7 and 8. As can be seen from Fig. 7, maximum power is obtained for the generator with $l_r = 2.5$ and $\Delta = 2.5$ mm, and maximum frequency, for the one with $l_r = 5.0$ and $\Delta = 3$ mm. From the graph it is clear that minimum power is registered for the resonator with chamber $l_r = 7$ mm, and frequency, $l_r = 9$ mm. The generator that operates with $\Delta = 1.5$ mm and different chamber lengths gave the lowest power, while the lowest frequencies were given by the generator with $\Delta = 4$ mm.

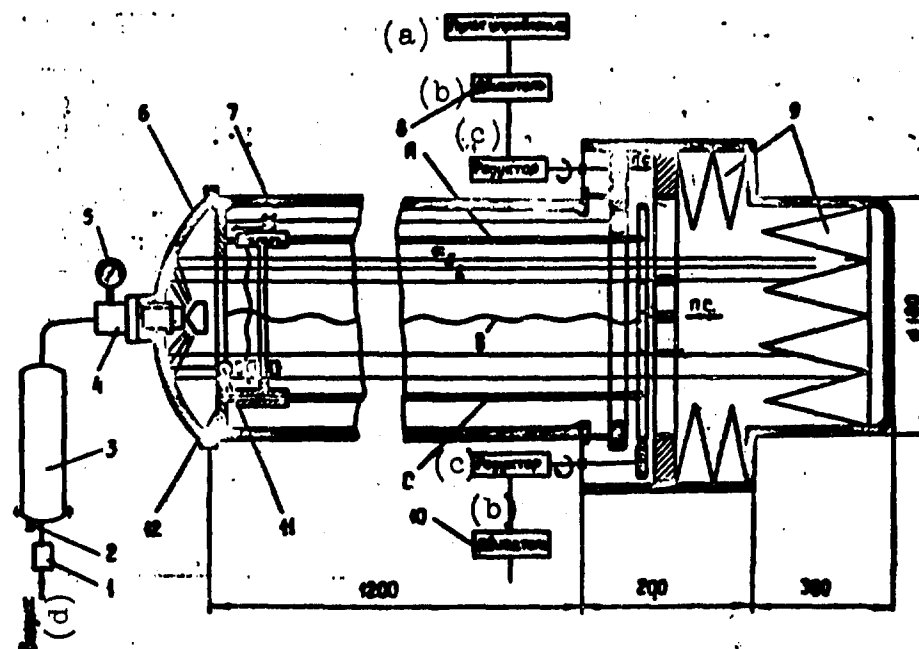


Fig. 6. Diagram of installation for removal of the acoustical characteristics of a generator.
KEY: (a) control panel; (b) motor; (c) reducer; (d) air.

The measured frequencies with different l_r differ from the theoretical ones by no more than on 5% (see table). Coincidence of data of the experiment with theory is obtained when the resonator is located from the nozzle cutoff at a distance not less than ψ (6) and (7).

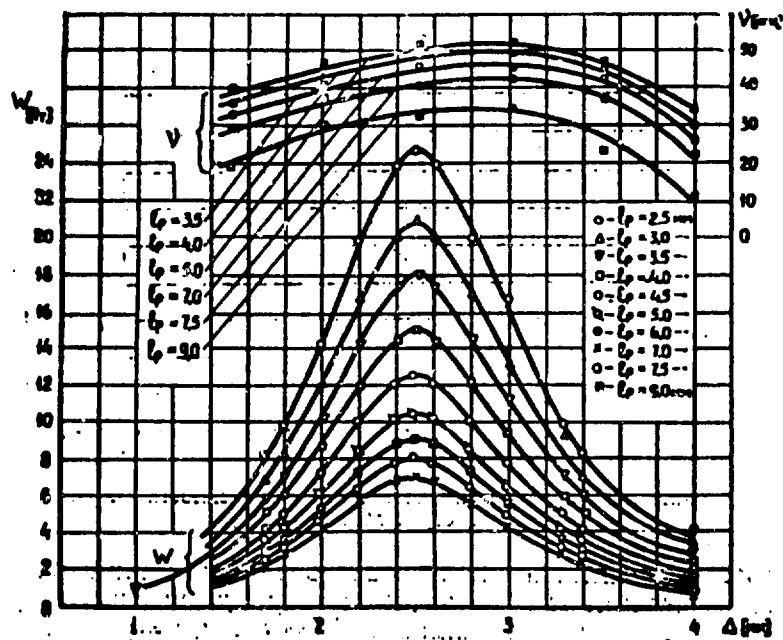


Fig. 7. Dependence of generator power and frequency on the change of clearance $\Delta W = f(\Delta)$, $\nu = f(\Delta)$ with constant length of resonator chamber $l_r = \text{const.}$

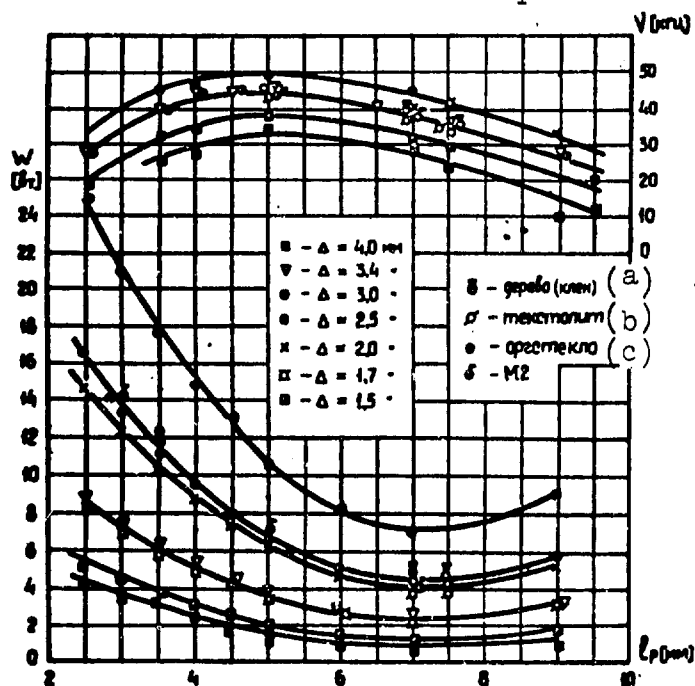


Fig. 8. Dependence of generator power and frequency on the change of chamber length $W = f(l_r)$, $\nu = f(l_r)$ with constant resonator clearance $\Delta = \text{const.}$
KEY: (a) wood (maple); (b) textolite; (c) organic glass.

Table

Δ mm	l_r cm	ν_{ex} cps	$\nu_{fl} = m \frac{a}{2l_r}$ cps	$\nu_p = \frac{a}{2(l_r + \psi)}$ cps	$\delta\%$
2	0.8	33000	39100	31500	4.6
2	0.9	28000	34800	29400	4.6
2	1.0	19000	31300	18200	4.2

By reconstructing the set of curves $W = f(\Delta)$ in dimensionless coordinates, we can obtain a curve that is approximated by the equation

$$y = Ae^{-nx^2} \quad (8)$$

with coefficients $A = 1$ and $n = 0.02$.

By assigning the generator power, we find dimensionless parameter $\bar{W} = y = \frac{W_{cur}}{W_{max}}$. Maximum power is selected for the corresponding l_r .

The generator ensured reliable work with a frequency from 10 to 50 kilocycles, and also a uniform sound field both around the radius and also around the circumference. Its efficiency was 6%. The acoustic characteristics of resonators made from copper, textolite, organic glass, and wood are analogous to the characteristics of resonators, made of steel. We have experimentally established that high-frequency oscillations of the generator originate from oscillations of a column of air in the annular cavity of the resonator.

Literature

1. N. S. Lamekin. Cavitation as a means of atomization of a liquid. Transactions of A. F. Mozhayskiy LKVVIA, No. 296, 1959.
2. N. S. Lamekin. Fundamentals of the burner theory for liquid fuel with a gas generator. IVUZ, "Machine Building," No. 11, 1960.
3. N. S. Lamekin. Method of calculating the clearance of a liquid-fuel burner generator. IVUZ, "Machine Building," No. 10, 1961.

4. L. Bergman. Der Ultraschall. Zuruck, 1954.
5. S. N. Rzhevkin. Course of lectures on the theory of sound. Moscow State University Press, 1960.

Submitted
15 November 1963

INVESTIGATION OF A PARTIAL TURBINE

V. N. Zanadvorova and V. A. Podgornov

Definitions of Cyrillic Items

cp = av = average

geom = geom = geometric

ад = ad = adiabatic

опт = opt = optimum

в = w = windage

макс = max = maximum

In the designing of turbines with low gas flow rates there appears the necessity of employing fractional or partial gas feed to the rotor wheels.

The characteristics of turbines with partial feed have a number of peculiarities which are explained by the forming of additional losses of energy which are known in literature under the name of windage losses and knock-out losses.

This classification of losses in a partial turbine, which is formal to a certain extent, does not exclude the complexity of the gas-dynamic phenomena that accompany the gas flow in it. Thus, upon introduction of partiality the internal turbine performance η_1 is

lowered due to

1) the fan action of the moving blades that do not receive a jet of working gas at a given moment,

2) the friction of surfaces of nonworking cascade parts against the gas,

3) the irregularities of gas parameters along the active arc of feed which causes the phenomenon of instability,

4) suction and leakage of gas from the active feed arc to the inactive,

5) discontinuity of gas entry into the partial wheel, as a result of which, in the extreme channels the gas on one side of the feed arc is accelerated, and is braked on the other.

Total lowering of η_i is not caused by the influence of each of these factors separately, but by their interconnection.

For turbines with different geometric and regime parameters the influence of partial feed on the characteristics is unequal. The existing methods of estimating energy losses from partial feed are based on an experiment with one or several types of turbines (stages) and do not consider all factors that affect the losses; therefore, the use of recommendations of different authors for calculation gives a noncoincident result.

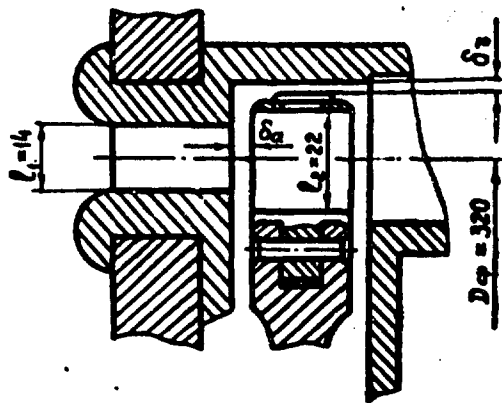


Fig. 1. Diagram of turbine blading.

For accumulation of experimental data that characterizes losses with partial gas feed, we conducted an investigation with a single-stage turbine.

We tested an active turbine, whose blading diagram is represented in Fig. 1. From the nozzles the air

flow emerged at an angle of $\alpha_1 = 24^\circ$.

Moving blades of symmetric profile ($\beta_{1 \text{ geom}} = \beta_{2 \text{ geom}} = 27^\circ$) were equipped with a tape band.

In the process of testing we changed the degree of partiality from $\varepsilon = 0.1$ to $\varepsilon = 0.5$ by covering a group of nozzle channels from the inlet and outlet sides.

The characteristics of the turbine were taken at a constant drop that corresponds to $\lambda_{ad} = 0.81$. The degree of reactance on the average diameter was equal to zero. The change in parameter u/c_{ad} was carried out by changing the turbine speed by means of changing the shaft load.

Tests were conducted with different combinations of the magnitude of axial δ_a and radial δ_r clearances.

As a result of the tests we obtained curves of change of effective performance η_e from $\frac{u}{c_{ad}}$, ε , δ_a , δ_r (Figs. 2, 3, and 4).

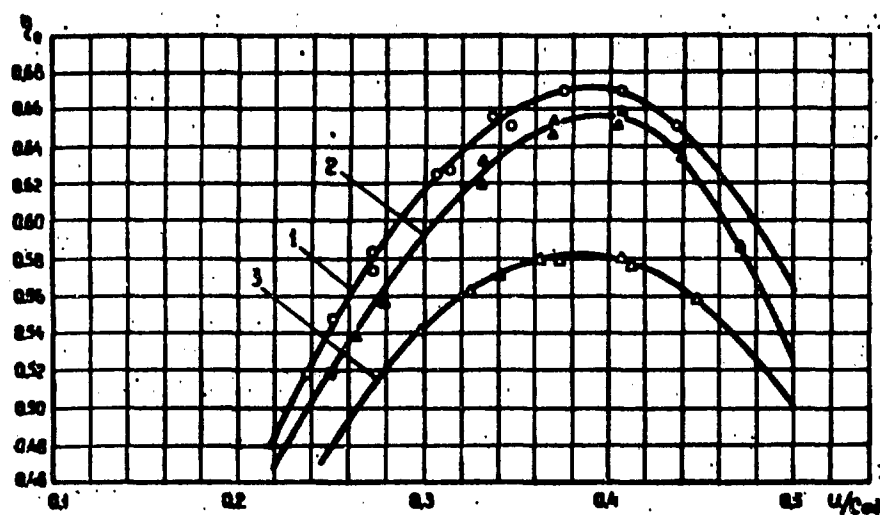


Fig. 2. Turbine characteristics when $\varepsilon = 0.5$.
1) $\delta_r = 1.2$, $\delta_a = 4$, 2) $\delta_r = 3$, $\delta_a = 4$, 3) $\delta_r = 1.2$, $\delta_a = 10$.*

*Here and in the following notations under the figures the clearance values are given in mm.

The given characteristics show that a decrease in the degree of partiality lowers the maximum value of η_e and leads to a decrease in $\left(\frac{u}{c_{ad}}\right)_{opt}$ that corresponds to it. An increase of both the radial, and axial clearances significantly lowers η_e at all values of the degree of partiality. In this case, the greatest lowering in performance is observed under optimum conditions.

Inasmuch as axial and radial clearances render such a significant influence on the characteristics of a partial turbine, it is important to estimate the lowering of its performance with one of these clearance sizes.

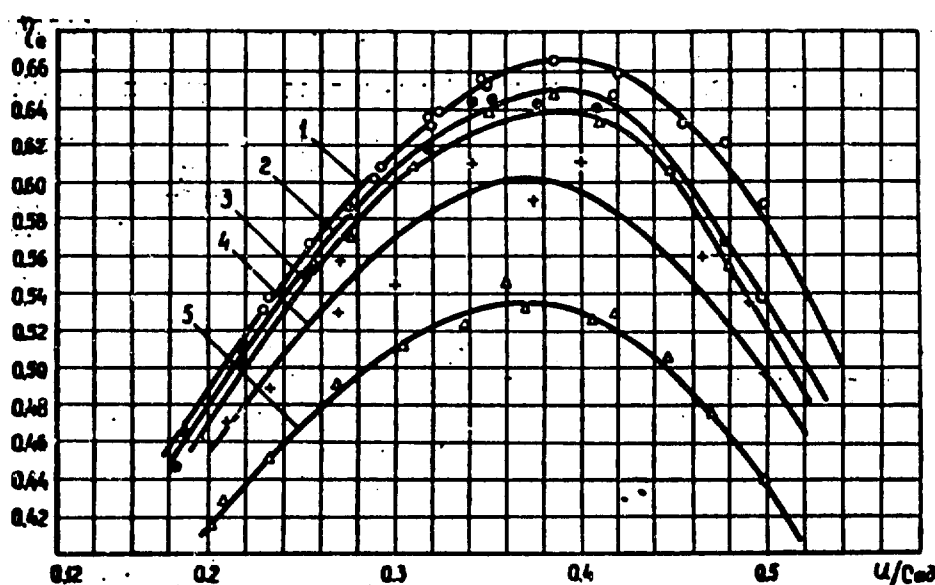


Fig. 3. Turbine characteristics when $\epsilon = 0.3$.
 1) $\delta_r = 1.2$, $\delta_a = 4$ mm, 2) $\delta_r = 2$, $\delta_a = 4$ mm,
 3) $\delta_r = 3$, $\delta_a = 4$ mm, 4) $\delta_r = 1.2$, $\delta_a = 7$,
 5) $\delta_r = 1.2$, $\delta_a = 10$.

Under optimum conditions the performance of a partial turbine is

$$\eta_e = \eta_e^* - \epsilon_r - \epsilon_a - \epsilon_p,$$

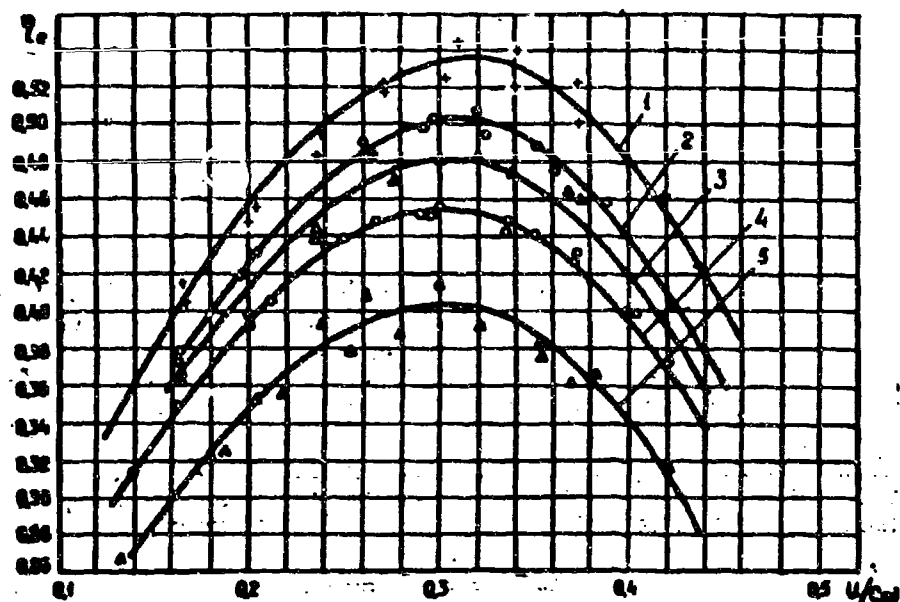


Fig. 4. Turbine characteristics when $\varepsilon = 0.1$.
 1) $\delta_r = 1.2$, $\delta_a = 4$, 2) $\delta_r = 2$, $\delta_a = 4$, 3) $\delta_r = 3$, $\delta_a = 4$, 4) $\delta_r = 1.2$, $\delta_a = 7$, 5) $\delta_r = 1.2$, $\delta_a = 10$.

where $\eta_e^\varepsilon = 1$ is the effective performance of this turbine at full gas feed,

ξ_w is the coefficient of windage losses of the partial turbine with $\delta_r = 0$ and $\delta_a = 0$,

ξ_a , ξ_r are the loss factors, caused by the presence of correspondingly axial δ_a and radial δ_r clearances.

This classification of losses in a partial turbine is conditional, but from our point of view it is a convenience. Unconditionally, each of the three loss factors in turn depends on many factors, geometric and regime, including the degree of partiality ε .

Figure 5 shows the trend of curves $\eta_{e \max}$ (η_e under optimum conditions) with a change in the degree of partiality at different axial and radial clearances. Here the dotted line shows curves $\eta_{e \max} = f(\varepsilon)$ when $\delta_a = 0$ and $\delta_r = 0$, which were obtained conditionally by means of linear extrapolation of experimental curves

$$\eta_{e \max} = f(\delta_a, \epsilon) \text{ and } \eta_{e \max} = f(\delta_r, \epsilon).$$

The dependences shown in Fig. 5 make it possible to quantitatively estimate the influence of axial and radial clearances on η_e of the test turbine. For every value of the degree of partiality ϵ

$$\xi_a = \frac{\eta_{e \max}^i - \eta_{e \max}^0}{\eta_{e \max}^0},$$

$$\xi_r = \frac{\eta_{e \max}^i - \eta_{e \max}^0}{\eta_{e \max}^0},$$

where index i corresponds to the value of the axial and radial clearances that take place in the experiment. A change in the degree of partiality, as already indicated, causes a change in ξ_a and ξ_r . These dependences are shown graphically in Fig. 6, and from their consideration it is clear that with a decrease in ϵ the influence of clearances, especially the radial, increases.

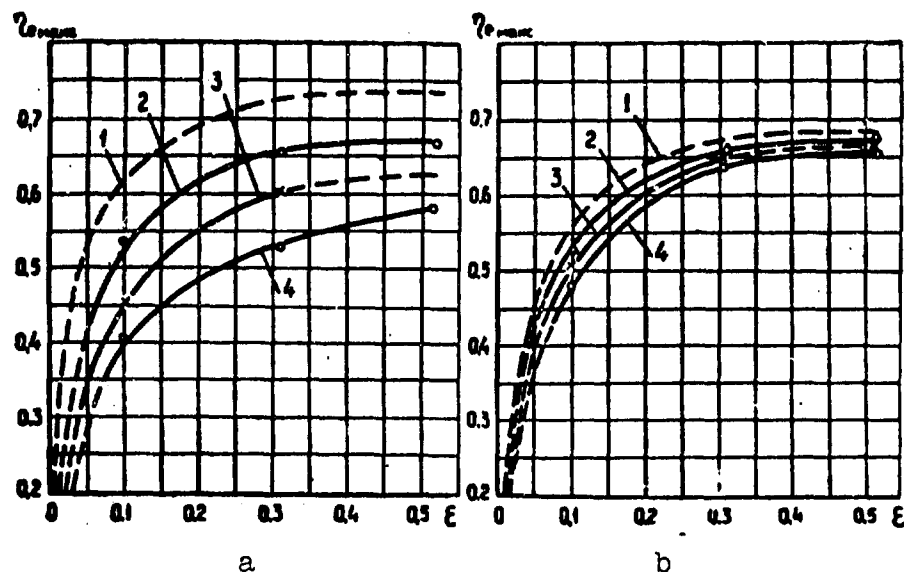


Fig. 5. Effective performance under optimum conditions for different ϵ .

$$a) \delta_r = 1.2 \begin{cases} 1) \epsilon = 0, \\ 2) \epsilon = 1.2, \\ 3) \epsilon = 2, \\ 4) \epsilon = 3. \end{cases} \quad b) \delta_a = 4 \begin{cases} 1) \epsilon = 0, \\ 2) \epsilon = 1.2, \\ 3) \epsilon = 2, \\ 4) \epsilon = 3. \end{cases}$$

In order to obtain the values of ξ_w it is necessary to know $\eta_{e \max}$ when $\epsilon = 1$. Because of its design, the test turbine did not

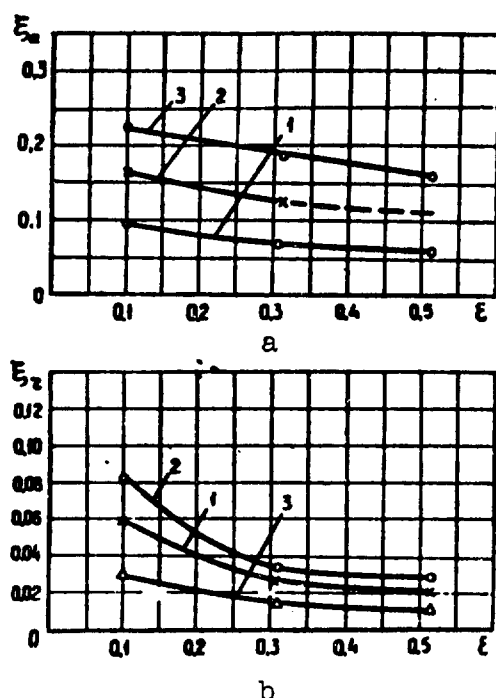


Fig. 6. Values of coefficients ξ_a and ξ_r for different ϵ .

- a) 1) $\delta_a = 4$,
 2) $\delta_a = 7$,
 3) $\delta_a = 10$,
 b) 1) $\delta_r = 2$,
 2) $\delta_r = 3$,
 3) $\delta_r = 1.2$.

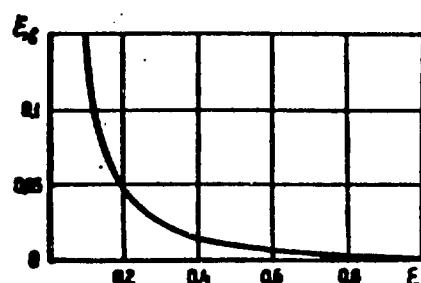


Fig. 7. Values of coefficients ξ_w for different ϵ .

allow us to carry out full gas feed. On the basis of available reference material it is possible with an accuracy that is sufficient for practical purposes to consider that in the range of $0.3 < \epsilon < 1$ the turbine performance under optimum conditions changes in proportion to ϵ . If, by taking into account this assumption, we extrapolate curve $\eta_{e \max} = f(\epsilon)$ to the value of $\epsilon = 1$, then

$$\xi_w = \eta_{e \max} - \eta_{e \max+1}.$$

Such extrapolation of the experimental curve of $\eta_{e \max}$ was performed for $\delta_a = 4$ mm and $\delta_r = 1.2$ mm, and Fig. 7 shows the dependence of ξ_w on ϵ .

It is interesting to compare the results obtained in the experiment with the calculation data.

Calculation with the formulas given in different works was produced by taking into account the actual

value of $\left(\frac{u}{c_{ad}}\right)_{\text{opt}}$ for every degree

of partiality. Figure 8 graphically shows the results of the calculation. Here, for comparison, our empirical curve $\xi_w = f(\epsilon)$, is plotted; the curve corresponds to performance loss when $\delta_r = 0$ and

$\delta_a = 0$. Unfortunately, most of the investigators whose recommendations we used did not calculate the influence of clearances. Let us assume that in the experiments that were proposed on the basis of recommendations, the axial clearance, just as the radial, was reduced to minimum.

Comparison of results shows that in the range of $0.3 < \epsilon < 0.5$ the recommendations of Stodola [7], Traupel [8], and Kerton [5] give values of ξ_w , which practically coincide with the ones obtained by us. When $\epsilon < 0.3$ the computed values lie lower than the experimental ones. With calculation by the formulas of Terent'yev [3], Mezheritskiy [2], Linnecken [6], and Chupirev [4] the values are 2-5 times lower than ours and hardly differ from one another.

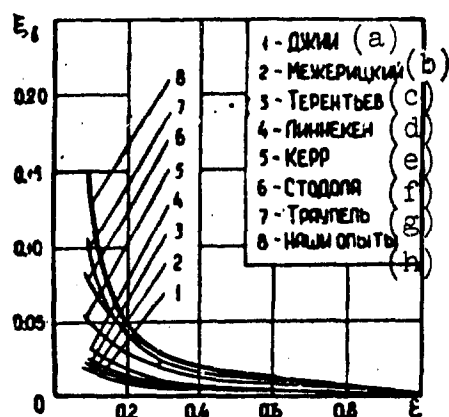


Fig. 8. Dependence of ξ_w on ϵ (according to different authors).

KEY: (a) Chupirev; (b) Mezheritskiy; (c) Terent'yev; (d) Linnecken; (e) Kerton; (f) Stodola; (g) Traupel; (h) our experiments.

The calculation of windage losses, on the recommendation MEI (Moscow Institute of Energetics) [1], gives a result, that exceeds the experimental data shown in Fig. 8. If we assume that in the MEI experiments the axial clearance constituted a magnitude of the order of 5 mm, then the result of calculation by the MEI formula will agree well with them in a range of $0.1 < \epsilon < 0.5$.

In the process of carrying out the experiments we measured the static pressures on the disk diameter that passes

through the middle of the active and inactive arcs both on the gas inlet side, and also on the gas outlet side. The experiments showed that at all values of ϵ the pressure on the inlet side is less than on the outlet side. This can obviously be explained by the ejecting action of the active jet which sucks gas from the cavity between the body

and the disk. The larger the active arc, the bigger the mass of flowing gas, and the more significant the evacuation on the inlet side of the disk.

On the basis of distribution of static pressures we calculated the axial force, which is increased in proportion to ϵ and is directed opposite the main flow.

The turbine flow coefficient, which usually, means the relation of the actual flow rate to the theoretical, practically remained constant.

Conclusions

Investigation of a partial active turbine showed that

1) the performance of a partial turbine depends not only on the degree of partiality, but also on the magnitude of the axial and radial clearances, which agrees with the indications of A. D. Mezheritskiy;

2) the maximum value of performance of $\eta_{e \max}$ at δ_a and δ_r is lowered with the decrease of ϵ in the beginning slowly; then, starting with $\epsilon = 0.3$, quite rapidly;

3) the optimum value of $\left(\frac{u}{c_{ad}}\right)_{\text{opt}}$ decreases with the decrease in the degree of partiality;

4) the turbine flow coefficient with the change in the degree of partiality practically does not change;

5) a comparison of the coefficient of windage losses found by us with the magnitudes determined by formulas known from literature shows that our experiments most of all correspond to the formulas of Stodola, Traupel, and (in the region of $\epsilon \geq 0.3$) Kerton. Other formulas give underestimated values of the loss coefficient, especially with small ϵ .

Obviously, the magnitude of the coefficient of windage losses is influenced by a number of factors that are not considered by certain formulas.

Literature

1. M. Ye. Deych, G. A. Filippov, and V. I. Abramov. Investigation of single-rim stages with partial steam feed. "Heat Power Engineering," No. 7, 1963.
2. A. D. Mezheritskiy. Windage losses in a turbine stage. "Power Equipment Construction," No. 6, 1962.
3. I. K. Terent'yev. Investigation of active stages with partial feed of working medium. "Power Equipment Construction," No. 4, 1960.
4. D. A. Chupirev. Designing and thermal calculations of stationary steam turbines. Mashgiz, 1953.
5. W. Kerton. Steam Turbine Theory and Practice, 6 Edition, Pitman, London, 1951.
6. H. Linnecken. Der Radreibungsverlust, insbesondere bei Turbomaschinen. AEG-Mitteilungen, No. 1/2, 1957.
7. A. Stodola. Dampf-und Gasturbinen 6 Aufl. Springer, 1924.
8. W. Traupel. Thermische Turbomaschinen, Band 1. Springer, Berlin, 1958.

Submitted
27 November 1963

HEATING OF A LIMITED VOLUME OF LIQUID THROUGH PLATES

M. D. Mikhaylov

Designations

δ - thickness of insulation,

$x, \xi = \frac{x}{\delta}$ - current and dimensionless coordinate, respectively,

a - coefficient of thermal diffusivity,

τ - time,

$F = \frac{a\tau}{\delta^2}$ - Fourier number,

$t(x, \tau)$ - temperature at point with coordinate x for a moment of time,

t_a - adiabatic stagnation temperature,

t_0 - initial temperature of thermal insulation and fuel,

t_f - temperature of fuel,

$\theta = \frac{t - t_0}{t_a - t_0}$ - dimensionless temperature,

$\theta_f = \frac{t_1 - t_0}{t_a - t_0}$ - dimensionless temperature of fuel,

$\lambda, \alpha_1, \alpha_2$ - coefficient of thermal conductivity, heat exchange between fuel and insulation, and between insulation and boundary layer,

$$B_1 = \frac{\alpha_1 \delta}{\lambda}, \quad B_2 = \frac{\alpha_2 \delta}{\lambda} - \text{Biot numbers,}$$

c, c_f - specific heat capacities of insulation and fuel,

γ, γ_f - specific gravity of insulation and fuel,

S - surface of insulation,

V_f - fuel volume,

$$K = \frac{c\gamma}{c_f \gamma_f} \frac{S\delta}{V_f} - \text{criterion.}$$

During motion of aircraft with high speeds, as a result of the sharp compression of air and the friction between the skin and the air, a large quantity of heat is released. If flight continues for several hours, the temperature of the fuel can become too high. Then it is necessary to heat-insulate the fuel tanks which leads to an increase in the dry weight of the vehicle. A question of determining the relative thickness of insulation arises during the designing of aircraft that are designed for a maximum flying range.

In connection with this we shall consider the problem of heating of fuel through an insulation with thickness δ . (Thermal resistance of the skin can be disregarded.) Thermal insulation is taken as an unlimited plate. On one side of the plate when $x = 0$ there is a limited volume of fuel V_f . The initial temperature of thermal insulation and fuel is identical and $t_0 = \text{const}$. At the initial moment of time $\tau = 0$ the temperature of adiabatic stagnation in the boundary layer is taken as $t_a = \text{const}$.

The temperature field of the plate is described by the equation

$$\frac{\partial^2 (t, F)}{\partial F^2} = \frac{\partial^2 (t, F)}{\partial \xi^2} \quad (F > 0, 0 < \xi < 1) \quad (1)$$

under the conditions

$$\theta(\xi, 0) = 0, \quad (2)$$

$$-\frac{\partial \theta(1, F)}{\partial \xi} + B_2[\theta(1, F) - 1] = 0, \quad (3)$$

$$-\frac{\partial \theta(0, F)}{\partial \xi} + B_1[\theta(0, F) - \theta_f(F)] = 0, \quad (4)$$

Equation (4) is obtained from heat balance under the condition that the temperature of the fuel is identical everywhere.

Here ξ is a dimensionless coordinate that is the relation of the current coordinate to the plate thickness,

$$\theta = \frac{t - t_0}{t_a - t_0} \quad \text{is the dimensionless temperature,}$$

F is the Fourier number,

B_1 and B_2 are Biot numbers,

θ_f is the temperature of the fuel,

$$K = \frac{c\gamma}{c_f \gamma_f} \frac{S\delta}{V_f} \quad \text{is a criterion that is the relation between the accumulation ability of the insulation and the accumulation ability of the fuel,}$$

c and c_f is the specific heat capacity of the insulation and the fuel,

γ and γ_f is the specific gravity of the insulation and the fuel,

S is the insulation surface.

For a solution to the problem we shall use a Laplace transformation with respect to variable F . The solution of equation (1) can be represented in the form of

$$\bar{\theta}(\xi, s) = C_1 \operatorname{ch} \sqrt{s} \xi + C_2 \operatorname{sh} \sqrt{s} \xi. \quad (5)$$

The boundary conditions (2), (3), and (4) can be written in the following way:

$$\bar{\theta}(1, s) + B_2 \left[\bar{\theta}(1, s) - \frac{1}{s} \right] = 0, \quad (6)$$

$$-\bar{\theta}(0, s) + B_1 [\bar{\theta}(0, s) - \bar{\theta}_f(s)] = 0, \quad (7)$$

$$-K \bar{\theta}(0, s) + s \bar{\theta}_f(s) = 0. \quad (8)$$

By substituting $\bar{\theta}_f(s)$ from (7) into (8), we have:

$$-\left(\frac{s}{B_1} + K\right) \bar{\theta}'(0, s) + s \bar{\theta}(0, s) = 0. \quad (9)$$

After determining constants C_1 and C_2 from (6) and (9) we place the obtained expressions in (5):

$$\bar{\theta}(\xi, s) = \frac{(KB_1 + s) \operatorname{ch} \xi \sqrt{s} + B_1 \sqrt{s} \operatorname{sh} \xi \sqrt{s}}{s \left[\left(\left(1 + \frac{B_1}{B_2}\right) s + KB_1 \right) \operatorname{ch} \sqrt{s} + \left(\left(1 + \frac{K}{B_2}\right) B_1 + \frac{s}{B_2} \right) \sqrt{s} \operatorname{sh} \sqrt{s} \right]}. \quad (10)$$

Applying the expansion theorem, we find

$$\theta(\xi, F) = 1 - \sum_{n=1}^{\infty} A_n \left\{ \left(1 - \frac{KB_1}{\mu_n^2}\right) \cos \mu_n \xi + \frac{B_1}{\mu_n} \sin \mu_n \xi \right\} \exp(-\mu_n^2 F), \quad (11)$$

where

$$A_n = \frac{1}{\left(1 + \frac{B_1}{B_2} - \frac{KB_1}{\mu_n^2}\right) \frac{\sin \mu_n \cos \mu_n + \mu_n}{2 \sin \mu_n} + \frac{\mu_n}{B_2} \sin \mu_n - \left(1 + \frac{B_1}{B_2}\right) \cos \mu_n}. \quad (12)$$

μ_n is an infinite number of roots of the characteristic equation:

$$\cotg \mu = \frac{\frac{\mu}{B_2} - \left(1 + \frac{K}{B_2}\right) \frac{B_1}{\mu}}{1 + \frac{B_1}{B_2} - \frac{KB_1}{\mu^2}}. \quad (13)$$

The expression for fuel temperature is obtained from (8):

$$\bar{\theta}_f(s) = C_2 \frac{K}{\sqrt{s}}. \quad (14)$$

Putting C_2 in (14)

$$\bar{\theta}_f(s) = \frac{KB_1}{s \left[\left(\left(1 + \frac{B_1}{B_2}\right) s + KB_1 \right) \operatorname{ch} \sqrt{s} + \left(\left(1 + \frac{K}{B_2}\right) B_1 + \frac{s}{B_2} \right) \sqrt{s} \operatorname{sh} \sqrt{s} \right]}. \quad (15)$$

with the help of the expansion theorem we will find

$$\theta_f(F) = 1 + \sum_{n=1}^{\infty} A_n \frac{KB_1}{\mu_n^2} \exp(-\mu_n^2 F), \quad (16)$$

where A_n and μ_n are determined from (12) and (13).

Submitted
10 June 1963

APPLICATION OF THE PRINCIPLE OF MINIMUM
DISSIPATION OF MECHANICAL ENERGY TO
THE EQUALIZING ACTION OF LATTICES

Yu. V. Stepanov

Definitions of Cyrillic Items

p = lat = lattice

cp = av = average

A single solution to the problem of steady-state motion of a viscous fluid in a certain volume is possible only with known boundary conditions on the surface that is limiting the given volume. Inasmuch as the boundary conditions are stipulated by the actual form of motion, the problem loses its definiteness. In a number of cases the boundary conditions are incompletely given. Then inside the considered volume of fluid an infinite number of mathematically equal forms of motion can be realized. For an approximation to an actually existing form of motion it is necessary to either make additional assumptions, or apply some criteria, which would allow us to select from all the mathematically possible forms of motion one form that could be observed and actually realized.

As criteria, for selecting the possible form of motion, in the solution of certain problems variation principles of maximum flow

rate, maximum flow of mechanical energy, minimum dissipation, etc. are applied. During the last few years we have conducted work on the use of variation criteria of stability in application to turbomachines [1]. We have proved the principle of maximum flow of mechanical energy. Its application, and also the use of a particular case, i.e., minimum dissipation of mechanical energy, make possible a new approach to the investigation of motion in the flow-through part of turbomachines in all operating conditions (including unstable conditions). However, the value of these principles is more general. Many problems of aeromechanics require the introduction of additional, in most cases not always evident, assumptions. The application of stability criteria instead of these assumptions can give more reliable solutions.

As an example we shall consider the possibility of application of the principle of minimum dissipation of mechanical energy to the solution of a problem about the equalizing action of a lattice that is placed in a flow with regular nonuniformity.

The question of the equalizing action of a lattice was examined by G. I. Taganov and is discussed in [2].

In the solution (Fig. 1) it was assumed that there are no tangential stresses between the streams and between the streams and the walls during the motion of a fluid in a pipe with different speeds. The following constants were taken:

- a) static pressures in sections of the pipe which are located far in front of and behind the lattice,
- b) the axial speeds on a section of every flow tube in view of the small initial nonuniformity and smallness of transverse speeds as compared to axial speeds,

- c) the resistance factor of the lattice $\zeta_{\text{lat}} = \frac{\Delta H}{\rho \frac{c_{\text{lat}}^2}{2}}$ through a

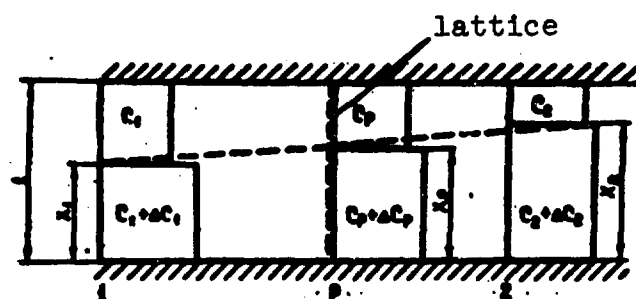


Fig. 1. Schematic picture of spreading of flow in front of a lattice and behind it.

section of the pipe. (It is also taken that the dimensions of the lattice cells are extremely small as compared to a section of the flow tube.)

By jointly solving a Bernoulli equation and equations of discontinuity and momentum, G. I. Taganov obtained, with the adopted assumptions, the magnitude of speeds in two flow pipes at a distance behind the lattice, thus determining the quantitative influence of the net on nonuniformity of flow.

It is necessary, however, to indicate that with the application of the momentum equation additional assumptions are introduced. Thus, the force of the influence of the lattice on the flow is determined from this expression:

$$X = x_1 \zeta_1 \frac{(c_1 + \Delta c_1)^2}{2} + (1 - x_1) \zeta_2 \frac{c_2^2}{2}. \quad (1)$$

This means that the influence of elementary lattice sites on the flow over an entire section of the flow tube is equal and the difference of static pressures on both sides of the lattice is constant for each of the flow tubes.

The actual picture of flow, from all appearances, differs from the accepted diagram. The rearrangement of the flow in front of the lattice and the changes in the area of each flow tube and speeds with

respect to magnitude and direction lead to a different force interaction of every elementary lattice site with the flow. Consequently, the total force of action of the lattice on the flow depends on the sought form of motion and cannot be described by equation (1).

Application of the principle of minimum dissipation of mechanical energy will lead to the following solution of this problem.

Dissipation of mechanical energy on section 1-lat may be written in the following form:

$$D = \rho \left[c_p (1 - x_p) h c_p \frac{c_p^2}{2} + (c_p + \Delta c_p) x_p h c_p \frac{(c_p + \Delta c_p)^2}{2} \right] + \int D' dx.$$

Here D' is the dissipation of mechanical energy per unit of volume in a unit of time on a section of flow rearrangement.

As an assumption, in the future we will disregard the dissipation of mechanical energy behind the lattice (section lat-2).

In the case of the flow of an incompressible medium

$$D' = \nu' \left[2 \left(\frac{\partial c_x}{\partial x} \right)^2 + 2 \left(\frac{\partial c_y}{\partial y} \right)^2 + 2 \left(\frac{\partial c_z}{\partial z} \right)^2 + \left(\frac{\partial c_y}{\partial z} + \frac{\partial c_z}{\partial y} \right)^2 + \left(\frac{\partial c_x}{\partial z} + \frac{\partial c_z}{\partial x} \right)^2 + \left(\frac{\partial c_x}{\partial y} + \frac{\partial c_y}{\partial x} \right)^2 \right].$$

where ν' is the coefficient of apparent kinematic viscosity (as an assumption we take $\nu' = \text{const}$).

By considering the speeds of perturbation c_x to be small and by solving the problem in the plane $xy(hl)$ ($c_z = 0$ and $\frac{\partial \dots}{\partial z} = 0$), we will obtain:

$$D' = \nu' \left[2 \left(\frac{\partial c}{\partial x} \right)^2 + \left(\frac{\partial c}{\partial y} \right)^2 \right].$$

By averaging the values of the derivatives for each of these volumes, we will approximately consider:

$$\left(\frac{\partial c}{\partial x} \right)_{cp} \approx \frac{\Delta c}{l} \quad \text{and} \quad \left(\frac{\partial c}{\partial y} \right)_{cp} \approx \frac{\Delta c}{h}.$$

Then

$$\int D' dx \approx \nu' \left[2 \frac{(c_p - c_1)^2}{\rho} (1 - x_p) hl + \right. \\ \left. + 2 \frac{(c_p + \Delta c_p - c_1 - \Delta c_1)^2}{\rho} x_p hl + \frac{(\Delta c_p + \Delta c_1)^2}{8h^3} hl \right].$$

Considering the flow rate equation,

$$c_1(1 - x_1) = c_p(1 - x_p) = c_2(1 - x_2), \quad (2)$$

$$(c_1 + \Delta c_1)x_1 = (c_p + \Delta c_p)x_p = (c_2 + \Delta c_2)x_2, \quad (3)$$

after certain transformations we will obtain

$$D = \frac{\rho}{2} K_p c_1^2 \left[\frac{(1 - x_1)^2}{(1 - x_p)^2} + \left(1 + \frac{\Delta c_1}{c_1} \right)^2 \frac{x_1^2}{x_p^2} + \right. \\ \left. + \frac{4}{\zeta_p Re} \frac{\nu}{j} \left[\frac{(x_p - x_1)^2}{1 - x_p} + \left(1 + \frac{\Delta c_1}{c_1} \right) \frac{(x_1 - x_p)^2}{x_p} \right] + \right. \\ \left. + \frac{1}{2} \frac{1}{\zeta_p Re} \frac{\nu}{h} \left[\frac{(x_1 - x_p) + \frac{\Delta c_1}{c_1} (1 - x_p)(x_1 + x_p)}{x_p(1 - x_p)} \right] \right], \quad (4)$$

where

$$Re = \frac{c_1 h}{\nu}.$$

With the help of equation (4) it is not difficult, for the given values of $\frac{\Delta c_1}{c_1}$, x_1 and ζ_{lat} , to find x_{lat} , which corresponds to minimum dissipation (D_{min}).

Then by applying the Bernoulli equation for both flow tubes and considering the constancy of static pressures in sections 1-1 and 2-2, we will have:

$$\frac{c_1^2}{2} - \frac{c_2^2}{2} - \zeta_p \frac{c_p^2}{2} - D_1 = \frac{(c_1 + \Delta c_1)^2}{2} - \frac{(c_2 + \Delta c_2)^2}{2} - \\ - \zeta_p \frac{(c_p + \Delta c_p)^2}{2} - D_{1\Delta}. \quad (5)$$

Here D_1 and $D_{1\Delta}$ are dissipations of mechanical energy during rearrangement of flow in every flow tube, expressed the following dependences:

$$D_1 \approx \nu' \left[2 \frac{(c_p - c_1)^2}{\rho} (1 - x_p) hl + \frac{(\Delta c_p + \Delta c_1)^2}{8h^3} hl \right], \\ D_{1\Delta} \approx \nu' \left[2 \frac{(c_p + \Delta c_p - c_1 - \Delta c_1)^2}{\rho} x_p hl + \frac{(\Delta c_p + \Delta c_1)^2}{8h^3} hl \right].$$

By solving equation (5) jointly with the flow rate equations (2) and (3), we find c_2 , Δc_2 , and x_2 , i.e., we determine the form of motion in section 2-2.

Application of the obtained relationships for a particular case of flow in a pipe with given regular initial nonuniformity and with different resistance factors of lattices ζ_{lat} (see the experimental data of I. Ye. Idel'chik [2]) indicates a fully satisfactory convergence of calculation with experiment (Fig. 2). The equalizing action of the lattice when $\zeta_{lat} \approx 2$ is clear in this instance.

In the solution of the indicated example we took:

$$\frac{1}{Re} \frac{v'}{v} = 1 \text{ and } \frac{l}{h} = 0.35.$$

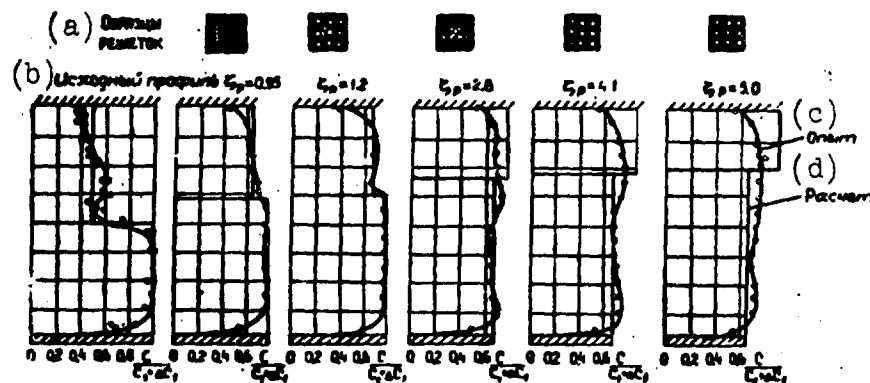


Fig. 2. Comparison of experimental and calculated distribution of speeds behind a lattice. KEY: (a) samples of lattices; (b) initial profile; (c) experiment; (d) calculation.

It should be noted that the question of selecting $\frac{v'}{v}$ and $\frac{l}{h}$ requires a special investigation and in the confines of this article it is not considered. Preliminary calculations from the condition of minimum dissipation show, however, that basically rearrangement of flow in front of a lattice is carried out at a relative length of $\frac{l}{h} \approx 0.35$.

Nevertheless, the results testify to the expediency of application of the principle of minimum dissipation of mechanical energy to flows

of similar kind and they can be proposed on the basis of further investigations in this direction.

Literature

1. V. N. Yershov. Variational principle of maximum flow of mechanical energy and its application to the design of axial turbomachines. IVUZ, "Aeronautical Engineering," No. 1, 1959.

2. I. Ye. Idel'chik. Hydraulic resistances. Gosenergoizdat, 1954.

Submitted
9 December 1963